

8th German Pharm-Tox Summit 2023

Abstracts

of the

89. Jahrestagung der Deutschen Gesellschaft für Experimentelle und Klinische
Pharmakologie und Toxikologie (DGPT) in Zusammenarbeit mit der AGAH

6–9 March 2023 | Ulm

This supplement was not sponsored by outside commercial interests. It was funded entirely by the publisher.

Short talks: Food Toxicology

1

Mercapturic Acids of Acrylamide (AAMA) and Glycidamide (GAMA) in Urine Samples from Vegans, Omnivores and Strict Raw Food Eaters

B. Monien¹, N. Bergau¹, C. Weikert¹, K. Abraham¹

¹Bundesinstitut für Risikobewertung, Lebensmittelsicherheit, Berlin, Germany

Introduction: The mercapturic acids *N*-acetyl-S-(2-carbamoyl)ethyl-L-cysteine (AAMA) and *N*-acetyl-S-(2-carbamoyl-2-hydroxyethyl)-L-cysteine (GAMA) are formed from glutathione conjugation of acrylamide and its metabolite glycidamide, respectively, and are well established urinary short-term biomarkers of exposure. However, AAMA and GAMA are not necessarily specific for the dietary uptake.

Objectives: In order to determine the ratio between dietary and non-dietary exposure of acrylamide, we compared the urinary excretion of AAMA/GAMA in strict raw food eaters, who did not consume any food heated to higher temperatures than 42 °C for at least 4 months, with non-smoking vegans and omnivores.

Methods: AAMA and GAMA in human 24-h urine samples of vegans (n = 32), omnivores (n = 28) and strict raw food eaters (n = 16) were quantified following a dilute-and-shoot protocol and isotope-dilution UHPLC-MS/MS.

Results: The median levels of AAMA excretion were 49.4 (IQR: 33.7 – 65.5) µg/d for omnivores and 66.7 (IQR: 48.3 – 91.8) µg/d for vegans (p for difference = 0.009). The urinary excretion of GAMA was 8.4 (IQR: 6.0 – 10.9) µg/d for omnivores and 10.0 (IQR: 8.5 – 12.8) µg/d for vegans (p for difference = 0.01). The median values for AAMA and GAMA excretion in the group of strict raw food eaters were 20.6 (IQR: 11.1 – 29.7) µg/d and 5.6 (IQR: 4.6 – 6.7) µg/d, respectively. These values were significantly lower compared to the excretion of AAMA and GAMA observed in vegans and omnivores (p = 0.006 or less).

Conclusions: The data on AAMA and GAMA excretion in vegans and omnivores is in line with a previous study showing a slightly elevated acrylamide intake in vegans in comparison to omnivores. This was attributed to the relatively high consumption of pan-fried vegetables, meat surrogates like tofu or seitan and bread-based products (Goerke et al. 2019, Arch. Tox., 93, 987). The observation of AAMA and GAMA in urine samples of raw food eaters supports previous notions that these metabolites may be formed by other substances than acrylamide or that there is a source of acrylamide independent from the dietary exposure contributing substantially to the overall exposure. As a consequence, calculations of acrylamide exposure from the urinary excretion of AAMA leads to overestimations.

2

Micro- and nanoplastics: A closer look on the impact of size and surface

H. Sieg¹, M. Paul¹, A. Braeuning¹

¹German Federal Institute for Risk Assessment, Food Safety, Berlin, Germany

Micro- and nanoplastics is a research field of increasing importance for environmental and consumer protection. With a recent advance in analytical method development and scientific understanding, a closer look on the interrelations between particle parameters, such as size, surface chemistry and functionalization is becoming necessary. Especially the essential differences between microplastics and particles below the micrometer range deserves special attention.

In our studies, we investigated food-relevant polymer particles of different materials (polylactic acid, melamin resin, polymethyl-methacrylate and polystyrene) in the micrometer, submicrometer and nanometer range. We applied human intestinal *in vitro* barrier models and differentiated intestinal and liver cell models to study cellular uptake and toxicological impact. A special focus was put on the different effects and subcellular distributions of particles with regard to their surface chemistry.

We observed significant differences in the behavior of microparticles and particles in the size range below 1 µm but also strong influences of the surface properties, especially the hydrophobicity of the materials on the cellular uptake and subcellular distribution.

Taken together, this implies the need of an attentive view on the material characteristics, especially particle size and hydrophobicity in the investigation of micro- and nanoplastics.

3

Pre- and postnatal dioxin exposure and semen quality in young adulthood.

D. Kurz¹, J. Lehner², K. Hancke², R. Peter¹, C. Weikert³, K. Penczynski³, J. Genuneit⁴, M. Wabitsch⁵, S. Brandt⁶, H. Brenner^{6,7}, D. Rothenbacher¹, K. Abraham¹

¹University of Ulm, Institut of Epidemiology and Medical Biometry, Ulm, Germany

²University of Ulm, Department of Gynecology and Obstetrics, Ulm, Germany

³German Federal Institute for Risk Assessment, Department of Food Safety, Berlin, Germany

⁴Leipzig University, Pediatric Epidemiology, Leipzig, Germany

⁵University of Ulm, Department of Pediatrics and Adolescent Medicine, Division of Paediatric Endocrinology and Diabetes, Ulm, Germany

⁶University of Heidelberg, Heidelberg, Germany

⁷German Cancer Research Center (DKFZ), Division of Clinical Epidemiology & Aging Research, Heidelberg, Germany

Introduction: Dioxins, i.e. polychlorinated dibenzo-p-dioxins (PCDDs) and dibenzofurans (PCDFs), are environmental contaminants with high persistence in the human body leading to a distinct background accumulation especially in breast-fed infants. While chloracne is the hallmark of high dioxin exposure in humans, possible other effects in populations exposed to dioxin background levels are under discussion. In 2018, the European Food Safety Authority (EFSA) derived a new tolerable weekly intake (TWI), based on a study reporting inverse associations between internal dioxin levels in 9-year-old Russian boys and their semen quality in young adulthood. However, these findings in the background range have currently not been confirmed by other studies.

Objectives: To expand the data basis on possible associations between early dioxin exposure and semen quality in young adulthood.

Materials and methods: The Ulm Birth Cohort Study (UBCS) is a population based longitudinal birth-cohort study recruited in Ulm from 11/2000 to 11/2001. Breast milk was collected from breastfeeding mothers 6 weeks after delivery and stored at -80 °C. Levels of PCDDs, PCDFs und PCBs were measured by GC-MS/MS (Eurofins GfA Lab Service GmbH, Hamburg). Participating boys were invited in 2021/22 to provide semen samples which were analyzed at the reproductive center Ulm, Department of Gynecology and Obstetrics according to the 2010 WHO manual. Multivariable regression methods are used to analyze the associations between dioxin exposure and semen quality after adjustment for covariates.

Results: Semen was available from n=98 males (age 20.4 ± 0.4 yrs., 84% provided two samples, mean 6.5 weeks apart); 86% of them were breastfed at 6 weeks. Median WHO2005-TEQ concentrations in breast milk (n=77) were 0.321 pg/g milk for PCDD/Fs and 0.198 pg/g milk for PCBs, roughly corresponding to 8.0 and 5.0 pg/g fat (assuming an average fat content of 4%). Regarding possible associations with semen quality, the analysis is based on two separate measures of early exposure: the concentrations in breast milk (mainly reflecting prenatal exposure), and the cumulative breastfeeding dose (concentration x duration of breastfeeding, mainly reflecting the exposure in infancy). Statistical evaluation is currently on the way.

Conclusion: The approach described will provide further insights on the question whether early dioxin exposure in the background range can have an impact on semen quality in young adulthood.

4

Exposure to the Mycotoxin Citrinin in Germany: Urine Biomarker Analysis in Children and Adults

G. H. Degen¹, J. Reinders¹, M. Kraft², W. Völkel³, F. Gerull⁴, R. Burghardt⁴, S. Sievering², J. Engelmann², J. G. Hengstler¹, H. Fromme⁵

¹Leibniz Research Centre for Working Environment and Human Factors, Systox, Dortmund, Germany

²LANUV NRW, Essen, Germany

³Bayerisches Landesamt für Gesundheit und Lebensmittelsicherheit, München, Germany

⁴Landeslabor Berlin-Brandenburg, Berlin, Germany

⁵Ludwig-Maximilians-Universität, München, Germany

Introduction: Citrinin (CIT), a mycotoxin known to exert nephrotoxicity, is a contaminant in food and feed. Since CIT contamination is not regularly analyzed, data on its occurrence and levels in food commodities are insufficient for conducting a conventional exposure assessment. Yet, human biomonitoring, i.e. analysis of CIT and its metabolite dihydrocitrinone (DH-CIT) in biological samples allows to estimate an exposure [Ali & Degen, doi: 10.1007/s00204-019-02570-y]. Objectives: To investigate CIT exposure in young (2-14 years) and adult (24-61 years) residents of three federal states in Germany.

Materials and methods: A total of 175 urine samples from children and 138 from adults were collected and analysed by a targeted LC-MS/MS based method for presence of CIT and DH-CIT.

Results: At least one of the biomarkers was detected and quantified in all urines which indicates a widespread dietary exposure to the mycotoxin in Germany. Interestingly, biomarker concentrations of CITtotal (sum of CIT and DH-CIT) were higher in children urines (range 0.03–7.62 ng/mL; median 0.54 ng/mL) than in urines from adults (range 0.03–3.50 ng/mL; median 0.30 ng/mL). The biomarker levels (CITtotal) measured in individual urines served to calculate their probable daily CIT intake, and compare it to a value of 0.2 µg/kg bw/day defined as "level of no concern for nephrotoxicity" by the European Food Safety Authority. Median exposure of German adults was 0.013 µg/kg bw, with only one urine donor exceeding this provisional tolerable daily intake (PTDI) for CIT. Median exposure of children was 0.05 µg/kg bw per day (i.e. 25% of the PTDI); however, CIT exposure in twelve individuals (6.3% of our study group) exceeded the limit value, with a maximum daily intake of 0.46 µg/kg bw.

Conclusions: As these results show evidence of non-negligible exposure to CIT in some individuals in Germany, mainly in children, further biomonitoring studies and also investigations aimed to identify the major sources of CIT exposure in food commodities are required.

Short talks: Toxins I

5

Insights into the causes and consequences of Ochratoxin A mediated replication stress

C. Klotz¹, L. Lutz¹, J. Borchers¹, J. Brode¹, A. Mally¹

¹University of Würzburg, Department of Toxicology, Würzburg, Germany

The mycotoxin and renal carcinogen Ochratoxin A (OTA) is weakly genotoxic in mammalian cells, yet neither DNA adducts nor oxidative DNA damage appear to play a role. Based on the hypothesis that the genetic effects of OTA may derive from unresolved replication stress, we recently observed a small albeit significant delay in replication fork progression in human kidney (HK-2) cells exposed to OTA. Moreover, visualization of γH2AX along newly replicated chromatin fibers revealed a concentration-dependent increase in γH2AX, suggesting a replication-coupled mechanism of OTA induced DNA damage. As the available evidence points towards a key role of replication stress in OTA genotoxicity, the present study aims to further understand the causes and consequences of replication stress induced by OTA. Specifically, we were interested to analyse whether changes in chromatin environment as a result of OTA mediated loss of histone acetylation may be responsible for replication fork slowing induced by OTA. Therefore, we employed isolation of proteins on nascent DNA (iPOND) and immunostaining along individual chromatin fibers to identify effects of OTA on proteins at the replication fork and on chromatin following DNA replication. Furthermore, we aimed to characterize the cellular response to OTA mediated replication stress by western blot analysis of the ATR-Chk1 and ATM-Chk2 DNA damage response (DDR) pathway. iPOND methodology coupled with immunoblotting revealed a significant reduction of histone H3 acetylation (H3K9ac) on chromatin following DNA replication in response to 1h treatment with OTA. Consistent with iPOND, visualization of H3K9ac using the extended chromatin fiber assay demonstrated a clear OTA-related reduction of H3K9ac along replicative chromatin fibers, thus supporting a mechanistic link between hypoacetylation of histones and perturbation of DNA replication induced by OTA. Western blot analysis revealed a slight induction of the ATM-Chk2 DDR by OTA, but no apparent effect on ATR-Chk1 signaling. Taken together, results from this study suggest altered histone acetylation as an early key event linked to replication stress induced by OTA. Based on western blot analysis, it appears that the mild levels of replication stress induced by OTA may be not sufficient to effectively activate checkpoint signaling, which may allow cells with under-replicated DNA to enter mitosis, which may promote genomic instability.

6

Toxin profiling for marine algae and seafood: an applied approach for ciguatera poisoning outbreaks and algal cultures.

C. Loeffler^{1,2,3}, A. Spielmeier¹, L. Tartaglione^{2,4}, V. Miele², F. Varriale², M. Varra², D. Bodi¹, M. Monti³, A. Varone³, S. Capellacci³, A. Penna⁵, C. Dell'Aversano^{2,4}, O. Kappenstein¹

¹BfR, Department of Safety in the Food Chain, Berlin, Germany

²University of Napoli Federico II, Naples, Italy

³National Research Council, Institute for Endocrinology and Experimental Oncology "G. Salvatore", Naples, Italy

⁴Italian Interuniversity Consortium on Marine Sciences, Rome, Italy

⁵University of Urbino, Department of Biomolecular Sciences, Urbino, Italy

Marine biotoxins can be a hazard for human health and constraint to the utilization of seafood resources. The most commonly reported non-bacterial seafood related illness worldwide is ciguatera poisoning (CP), caused by the ingestion of seafood products containing ciguatoxins (CTXs). *Gambierdiscus* and *Fukuyoa* are two genera of microalgae known to produce a suite of biologically active natural marine products, including CTXs, maitotoxins, gambierol, gambieroxide, gambieric acids, gambierone, sulfogambierones, and 44-methylgambierone. CTXs are a class of toxic polycyclic polyethers with a strong interaction on mammalian sodium channels and potent toxic activity at sub ppb levels. Seafood and algae generally represent complex matrices, requiring extensive clean-up procedures to investigate CTXs at human health relevant concentrations. Herein, a dereplication procedure was used as a key screening process for profiling crude fish and algae extracts to be investigated for biological activity. The dereplication approach was applied using the methods of liquid chromatography high-resolution mass spectrometry (LC-HRMS), *in vitro* cell based bioassay (N2a), and a combined bioassay guided micro-fractionation to help identify biologically active peaks with toxic effects in fish and algae extracts. This investigative approach was critical to the identification of regionally novel CTX3C-group compounds present in fish products implicated in two outbreaks of CP in the EU as well as a novel description of a putative CTX in a *Gambierdiscus* algal culture isolated from the marine environment. This approach will ensure that laboratories investigating CTXs or responding to outbreaks of CP will have a method process capable of identifying CTXs and other bioactive compounds.

7

Okadaic acid modulates JAK/STAT signalling and subsequent CYP expression in HepaRG cells

L. Würger¹, F. Kudiabor¹, H. Sieg¹, A. Braeuning¹

¹German Federal Institute for Risk Assessment, Food Safety, Berlin, Germany

Introduction: The marine Biotoxin Okadaic acid (OA) is produced by dinoflagellates. As a lipophilic toxin, it accumulates in the fatty tissue of filter-feeding shellfish, which can then lead to human exposure after consumption of contaminated shellfish. After consumption, it can cause diarrhetic shellfish poisoning (DSP). Symptoms include severe gastrointestinal disorders, like diarrhea, stomach pain and vomiting. OA also disrupts tight junctions in the intestine and therefore the mechanical barrier function in the intestine. Furthermore, it also disrupts the metabolic barrier in the liver by downregulating several xenobiotic-metabolizing enzymes.

Objectives: In this study, we analyzed the mechanism behind the downregulation of CYP enzymes by OA. Therefore, we investigated the influence on the JAK/STAT pathway as a possible target of OA.

Materials and methods: Differentiated HepaRG cells were incubated with OA and inhibitors for NF-κB activation, interleukin-6 activation, interleukin-8 activation and JAK activation. The proteins and RNA of these cells were isolated and analyzed using qPCR and Western blotting. Furthermore, STAT3 activation was visualized using confocal microscopy.

Results: Obtained data demonstrate activation of STAT3 in HepaRG hepatocarcinoma cells upon OA exposure. Interleukin-1α, -1α, -6, -8 and -12, TNFα and SOCS3 expression is upregulated after contact with OA. Furthermore, representative CYP enzymes were downregulated in HepaRG cells after exposure to OA. Stepwise inhibition at several points of this proposed activation pathway antagonized the effects of OA.

Conclusion: In conclusion, our data suggests an activation of the JAK/STAT signaling pathway through activation of NF-κB in HepaRG cells. This pathway is furthermore connected to the expression of CYP enzymes.

Short talks: Cardiac pharmacology and treatment

9

microRNA-21 inhibition prevents adverse cardiac remodeling and dysfunction following myocardial infarction, an effect driven by macrophages.

I. Duran Fernandez¹, D. P. Ramanujam¹, C. Beck¹, P. Vaccarello¹, S. Engelhardt¹

¹Institute of Pharmacology and Toxicology, Technical University of Munich, Munich, Germany

Fibrosis is the default response to myocardial injury, where a fibrotic scar replaces the infarct tissue and later progress into heart failure. MicroRNA-21 (miR-21) has been previously reported as a key regulator of myocardial fibrosis. Small-RNA sequencing of the major cardiac cell fractions showed that miR-21 is upregulated in murine cardiac cells seven days after myocardial infarction (MI). Previous studies with small and large animal models of heart failure revealed that miR-21 inhibition prevented cardiac dysfunction and myocardial fibrosis. Here, we aim to identify the target cell population through which miR-21 inhibition treatment prevents cardiac disease.

Myocardial infarction was induced in wild-type mice, and anti-miR-21 or control was injected for three consecutive days starting seven days after the injury. The first group of hearts was harvested two days after the last injection (day 11) to assess miR-21 activity through its targetome deregulation in macrophages and fibroblasts using Argonaute2-ribonucleoprotein immunoprecipitation (AGO-RIP). The second group of hearts was harvested on day 21 to evaluate molecular changes associated with the treatment at the border zone and infarct region. Cardiac function was measured by echocardiography throughout the study.

Unlike controls, mice treated with anti-miR-21 showed improved cardiac function both shortly after treatment and on day 21. Bioinformatic analysis of the transcriptome and the corresponding targetome revealed a strong de-enrichment (AGO2-RIP) and de-repression (input) of miR-21 targets in macrophages after treatment. Additionally, gene ontology analysis indicated downregulation of genes associated with inflammation and fibrosis. For the hearts harvested on day 21, a stronger effect of anti-miR-21 was observed at the border zone than at the infarct region. Moreover, an anti-fibrotic phenotype was found for the significant-deregulated-abundant genes of the border zone, indicating conservation of the phenotype observed on day 11 in fibroblasts.

Altogether, our data suggest that macrophages from the border zone are the main target cell population of anti-miR-21 treatment, promoting an anti-fibrotic phenotype that translates into an immediate and sustained improvement in heart function.

10

Characterization of molecular and ventricle-specific events in cardiac hypertrophy and subsequent failure using RNAseq and smRNA FISH in an animal model of slowly progressing disease

L. Jurida¹, S. Werner¹, F. Knapp², O. Dittrich-Breiholz³, S. Rohrbach², M. Kracht¹

¹Justus-Liebig-Universität Giessen, Rudolf-Buchheim-Institut für Pharmakologie, Gießen, Germany

²Justus-Liebig-Universität Giessen, Institut für Physiologie, Giessen, Germany

³Medizinische Hochschule Hannover, RCU Transcriptomics, Hannover, Germany

Introduction: Heart failure is a leading cause of death worldwide and it has shown that treatment options for left ventricular failure often prove ineffective in right ventricular disease. The right ventricle (RV) differs developmentally, anatomically and functionally from the left ventricle (LV), which limits direct application of the substantial knowledge concerning LV failure for improving RV function. Therefore, a deeper understanding of the molecular, right ventricle-specific events in cardiac hypertrophy and subsequent failure is urgently needed.

Objectives: Therefore, we pursued the objective to unravel right heart specific mechanisms of disease by identifying transcriptomic changes and differences between left and right ventricle in specific stages of disease. It is known that ventricular failure

progresses through a hypertrophic compensatory phase followed by failure of the ventricle function through rapid decompensation, but the underlying molecular mechanisms and the key factors involved have not been defined yet.

Materials and methods: To address these questions, we have established an animal model based on weaning rats, which develop two clearly distinguishable, slowly forming stages of disease (compensated and decompensated) in response to aortic or pulmonary artery banding (AOB, PAB). The parallel analysis of heart tissue and isolated cardiomyocytes from this model allowed the direct and systematic comparison of functional and transcriptomic changes by RNAseq, as well as the visualization of gene expression at spatial and single cell resolution by adapting smRNA FISH.

Results: Our data show that the transcriptomic changes differ substantially between left and right ventricle and additionally depend on the stage and disease type. Protein interaction analyses based on the transcriptomic data reveal ventricle-specific protein networks, which are assembled of co-regulated factors. Single molecule RNA FISH analysis does not only confirm RNAseq results, but also reveals specific expression patterns of disease-associated RNAs across individual cells and heart regions.

Conclusion: Taken together, these data obtained in a rat model which closely resembles the course of human disease, allowed the characterization of molecular, particular right ventricle-specific changes during the transition from cardiac hypertrophy to subsequent failure.

11

The Ca²⁺ re-uptake inhibitor PLN^{R9C} perturbs cardiac excitation/contraction coupling with implication on mitochondria and SR/ER

T. Brand¹, B. T. Baumgarten², S. Denzinger¹, Y. Reinders², M. Kleindl², F. Funk^{3,4}, N. Gedlik⁵, P. Kleinbongard⁵, E. Tolstik², A. Sickmann², J. P. Schmitt^{3,4}, K. Lorenz^{2,1}

¹Institute of Pharmacology and Toxicology, Würzburg, Germany

²Leibniz-Institut für Analytische Wissenschaften -ISAS- e.V., Dortmund, Germany

³Institute of Pharmacology and Clinical Pharmacology, Düsseldorf, Germany

⁴Cardiovascular Research Institute Düsseldorf (CARID), Düsseldorf, Germany

⁵Institute for Pathophysiology, West German Heart and Vascular Center, Essen, Germany

Introduction: Dysregulated Ca²⁺ cycling impairs cardiac contractility and is a feature of heart failure. A mutation (R9C) in the Ca²⁺ regulatory protein phospholamban (PLN^{R9C}) causes a severe dilative cardiomyopathy in patients characterized by decreased contractile function and premature death.

Objectives: Here, we investigate the impact of PLN^{R9C} on Ca²⁺-sensitive cellular functions such as contraction/excitation coupling and organelles, e.g. mitochondria or sarcoplasmic reticulum (SR/ER) and analyze the benefits of early correction of mislead Ca²⁺ handling on disease progression.

Material and methods: PLN^{R9C}-transgenic mice were used that mimic the human dilative cardiomyopathy phenotype, mice with cardiac overexpression of the Raf kinase inhibitor protein (RKIP-tg) that accelerate Ca²⁺ cycling and respective double transgenic mice (PLN^{R9C}/RKIP-tg). Ca²⁺ cycling in cardiomyocytes was analyzed using the Ca²⁺ indicator Fura-2, contractile function was assessed by echocardiography, mitochondrial function by a Clarke electrode and the mitochondrial membrane potential by tetramethylrhodamine staining, expression level of proteins involved in SR/ER stress response by mass spectrometry and Western blots and cardiac remodeling by Sirius red and H&E staining.

Results: The analysis of the mitochondrial function revealed that the PLN^{R9C} mutation causes profound alterations in murine hearts that go beyond a slowed Ca²⁺ re-uptake in diastole and a decline in contractile function but extend to a massive decrease in mitochondrial function reflected by a collapse in mitochondrial membrane potential, reduced respiration and in the initiation of the SR/ER stress response reflected by enhanced protein expression of e.g. calreticulin. Overexpression of RKIP improved Ca²⁺ cycling and in line with this attenuated most of these cellular malfunctions, i.e. mitochondrial dysfunction and SR/ER stress. In addition, cardiac interstitial fibrosis as well as premature death of PLN^{R9C}-tg were significantly reduced by RKIP.

Conclusion: Our study suggests that the altered Ca²⁺ cycling in PLN^{R9C}-tg triggers an impairment of further Ca²⁺ sensitive cellular organelles such as mitochondria and SR/ER. The normalization of Ca²⁺ cycling by RKIP and the subsequent rescue of the respective organelle functions underscores the central role of Ca²⁺ dysregulation for disease progression.

12

NO-induced cGMP generated in fibroblasts increases cardiac cAMP and phospholamban phosphorylation.

L. Menges¹, J. Giesen¹, K. Yilmaz¹, A. Fuchtbauer², E. M. Fuchtbauer², D. Koesling¹, M. Russwurm¹

¹Ruhr-Universität Bochum, Pharmakologie und Toxikologie, Bochum, Germany

²Aarhus University, Molecular Biology and Genetics, Aarhus, Denmark

The signaling molecule cGMP with an important role in the cardiovascular system is formed by NO-sensitive guanylyl cyclases (NO-GCs) in response to stimulation by nitric oxide (NO). Novel activators and stimulators activating NO-GCs have been developed and are approved e.g. for treatment of heart failure.

Using a FRET-based cGMP indicator (cGi500), cGMP increases in response to NO were detectable in isolated cardiac fibroblasts whereas cultured myocytes were devoid of those signals. Yet in a co-culture model, NO-induced cGMP formed in cardiac fibroblasts was shown to enter cardiac myocytes via gap junctions. It was the aim of the present study to show the existence of the gap junction-mediated transfer of cGMP in native cardiac tissue.

For the detection of cGMP-signals in cardiac myocytes in native tissue, a mouse line (MHC- α -cGi500) with a myocyte-specific expression of the cGMP indicator was generated. Indeed, NO-induced cGMP-signals were successfully measured in cardiac slices from MHC- α -cGi500-mice. The signals were abolished by different gap junction inhibitors (carbenoxolone, gap26 peptide, gap27 peptide). Furthermore, NO-induced cGMP signals were found to be degraded by the "cAMP-degrading, cGMP-inhibited" PDE3.

Accordingly, we asked whether NO-induced cGMP affects cAMP levels in cardiomyocytes via PDE3 and found Isoprenaline (Iso)-induced cAMP to be increased by the NO-GC stimulator Bay41-2272 in heart slices as measured in radioimmuno-assays. Similarly, phospholamban phosphorylation induced by Iso was augmented by the NO-GC stimulator as studied in Western blots. Both of the NO-GC/cGMP-mediated effects were abolished by gap junction inhibitors compatible with the assumption that NO-induced cGMP is formed in fibroblasts and reaches cardiac myocytes via gap junctions.

In sum, by measuring cGMP signals in cardiac slices we demonstrate the occurrence of NO-induced cGMP in cardiac myocytes and show the dependency of the signal on gap junctions. In cardiomyocytes, we find cGMP to increase Iso-induced cAMP most likely by the inhibition of PDE3 and II) to augment Iso-induced phospholamban phosphorylation. Both cGMP effects are expected to cause positive inotropic and lusitropic effects.

13

Differential regulation of MMPs, apoptosis and cell proliferation by the cannabinoid receptors CB1 and CB2 in vascular smooth muscle cells and cardiac myocytes

B. Greiner¹, M. Sommerfeld¹, U. Kintscher¹, T. Unger², K. Kappert³, E. Kaschina¹

¹Charité University, Institute of Pharmacology, Berlin, Germany

²Maastricht University, CARIMSchool for Cardiovascular Diseases, Maastricht, Netherlands

³Charité University, Institute of Diagnostic Laboratory Medicine, Berlin, Germany

Cannabinoids (CB) are implicated in cardiovascular diseases via the two main receptor subtypes CB1R and the CB2R. The role of CB receptors in proteolytic processes by extracellular matrix turnover in the heart and blood vessels have been poorly investigated.

This study aimed to explore whether cannabinoids regulate the activity of matrix metalloproteases (MMP-2, MMP-9) in vascular smooth muscle cells (VSMCs) and in cells of cardiac origin (H9c2 cell line). The influence of CB1- and CB2 receptor stimulation or inhibition on the regulation of cell proliferation, apoptosis and glucose uptake was also evaluated. We used four synthetic compounds, which activate or block CB receptors: arachidonyl-2-chloroethylamide (ACEA) – CB1R agonist, rimonabant - CB1R antagonist; John W. Huffman (JWH133) - CB2R agonist, and CB2R antagonist - 6-iodopravadoline (AM630). Treatment of cells with the CB2R agonist JWH133 decreased cytokine activated secretion of proMMP-2, MMP-2 (27.6%; p<0.05) and MMP-9 (30%; p<0.0001), reduced Fas ligand and caspase-3 mediated apoptosis (2-fold), normalized the expression of TGF-beta1 and prevented cytokine-induced increase of glucose uptake into the cell. CB1R inhibition with Rimonabant showed similar protective properties as the CB2R agonist JWH133, but to a lesser extent.

In conclusion, CB1R and CB2R exert opposite effects on the regulation of cell glucose uptake, proteolysis and apoptosis in both VSMCs and cardiac H9c2 cells. The CB2R agonist JWH133 demonstrated highest protective properties. These findings may pave the way to new medications for the treatment of cardiovascular diseases especially those associated with extracellular matrix degradation, such as aneurysm formation.

14

ADAM10 is upregulated in human heart failure and its pharmacological as well genetic inhibition abolishes CX3CL1-dependent leucocyte infiltration and improves survival and cardiac function after infarction

E. Klapproth¹, P. Klöse¹, J. Wiedemann¹, A. Witt², S. Künzel¹, S. Weber¹, K. Guan¹, I. Kopallani², P. Mirtschink³, P. Saftig⁴, K. Lorenz^{2,6}, A. El-Armouche¹

¹Technische Universität Dresden, Institut für Pharmakologie und Toxikologie, Dresden, Germany

²Technische Universität Dresden, Institute of Physiology, Faculty of Medicine Carl Gustav Carus, Dresden, Germany

³Technische Universität Dresden, Institute for Clinical Chemistry and Laboratory Medicine, Faculty of Medicine Carl Gustav Carus, Dresden, Germany

⁴Christian-Albrechts-Universität Kiel, Biochemical Institute, Kiel, Germany

⁵Julius-Maximilians-University of Würzburg, Institute of Pharmacology and Toxicology, Würzburg, Germany

⁶Leibniz-Institut für Analytische Wissenschaften -ISAS- e.V., Dortmund, Germany

Background and purpose: The membrane sheddase ADAM10 has been implicated in immune regulatory processes, upregulated in response to specific heart pathologies e.g. ischemic heart failure and elevated serum levels of the ADAM10 substrates CX3CL1 and CXCL16 have been reported following MI. The causal role of ADAM10 in cardiovascular diseases, however, has not been known yet.

Methods and results: Our study uses human tissue biopsies, a cardiomyocyte-specific ADAM10 knockout mouse model (ADAM10 KO) and pharmacological ADAM10 inhibitors.

We show that ADAM10 protein levels are elevated in patients with ischemic cardiomyopathy (2-fold) and ADAM10 mRNA expression correlates with expression of atrial (ANP) and brain natriuretic peptide (BNP) mRNA. Upon MI, cardiomyocyte-specific ADAM10 KO and ADAM10 inhibited mice (GI254023X) show significantly improved overall survival and preserved cardiac function. ADAM10 inhibition significantly reduces IL-1 beta-driven inflammation and leucocyte infiltration as evidenced by mRNA sequencing and FACS analysis. Upon hypoxia, cardiomyocyte CX3CL1 is upregulated and its coprecipitation with ADAM10 is enhanced, which is resolved by ADAM10 inhibition. Moreover, we identify this novel cardiomyocyte-specific ADAM10/CX3CL1 signaling axis to regulate leucocyte migration following hypoxia.

Conclusion: Our data show that pharmacological and genetic targeting of ADAM10 is highly efficient for improving post-infarction cardiac function and survival. Due to its role in regulation of the post-MI immune response and leucocyte infiltration, upregulated ADAM10 could be a potential molecular target to be blocked in patients after MI.

Fig. 1

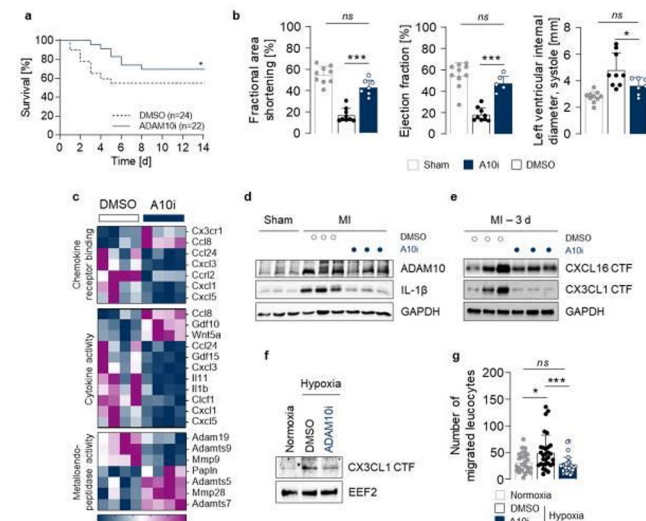


Fig. 1. ADAM10 inhibition improves post-infarction cardiac function via inhibition of the CX3CL1-driven leucocyte migration. (a) Kaplan-Meier survival curves and (b) echocardiographic determination of contractile function (ejection fraction, fractional area shortening) and left ventricular dilation (left ventricular internal diameter, systole) of DMSO and ADAM10 inhibitor (A10i) 28 d following MI or Sham-operated controls (ns; mean \pm SEM; two-way ANOVA). (c) mRNA sequencing and (d and e) western blot analysis of DMSO and A10i-treated mouse hearts 3 d following MI. (f) CX3CL1 c-terminal fragment (CTF) protein expression in HL-1 cells upon 3h of hypoxia. (g) Transwell migration of RAW264.7 macrophages using the supernatants of HL-1 cells upon 3h of

Short talks: Immunopharmacology and inflammation

15

Individuals with weaker humoral response after second booster vaccination are prone to SARS-CoV-2 Omicron BA.5 infections

B. Möhlendick¹, I. Ciucilkaite¹, C. Elsner², B. Wagner³, U. Dittmer², W. Siffert¹

¹University Hospital Essen, Institute of Pharmacogenetics, Essen, Germany

²University Hospital Essen, Institute for Virology, Essen, Germany

³University Hospital Essen, Department of Clinical Chemistry and Laboratory Medicine, Essen, Germany

Introduction: Despite the high level of protection against severe COVID-19 provided by the currently available vaccines some breakthrough infections occur. In a previous study we found an association of a weaker humoral immune response with a higher breakthrough infection risk after the third vaccination against COVID-19. Until now, there is no information whether a potential risk of a breakthrough infection can be inferred from the level of antibodies after second booster vaccination as well.

Objectives: In this study we measured antibody titers after COVID-19 vaccination but prior SARS-CoV-2 Omicron BA.5 infection to analyze the association between antibody level and infection risk.

Study participants and methods: Levels of binding antibodies after the first, one and six month after the second and the third (booster) as well as one month after the fourth (second booster) vaccination against COVID-19 were measured in serum samples from 228 healthcare workers at the University Hospital Essen. Demographics, vaccination scheme and pre-infection antibody titers were compared between individuals with (N=37) and without (N=191) Omicron BA.5 infections.

Results: On average, infections occurred after 74 days after the second booster vaccination. All infections were described as a mild to moderate "cold-like" illness which lasted for eight days. The risk of developing an Omicron BA.5 infection was independent of vaccination scheme, sex, body mass index, smoking status or pre-existing conditions. Pre-infection anti-spike antibodies one month after the second booster vaccination but prior SARS-CoV-2 breakthrough infection were significantly lower in individuals who later

on were infected with SARS-CoV-2 Omicron BA.5 ($P=0.03$, 3391.0 BAU/ml vs. 4787.0 BAU/ml). Currently, we investigate the influence of neutralizing antibodies as well as T-cell response against SARS-CoV-2 Omicron BA.5 after the second booster vaccination on infection risk. To elucidate differences in humoral as well as cellular immune response genetic factors will also be evaluated.

Conclusion: Routine testing of anti-SARS-CoV-2 IgG antibodies can quantify vaccine-induced humoral immune response and may help to identify subjects who are at risk for a breakthrough infection. The establishment of thresholds for SARS-CoV-2 IgG antibody levels identifying "non"- or "low"-responders may be used as an indication for re-vaccination.

17

PD-L1 upregulation by proximal complement activation – a mechanistic model with various clinical implications

S. Hafner¹, M. Anliker², D. Drees³, L. Loacker², A. Griesmacher², G. Hoermann², V. Fux², H. Schennach⁴, P. Hörtnagl⁴, A. Dopler¹, S. Schmidt⁵, R. Bellmann-Weiler⁶, G. Weiss⁵, J. Kimpel⁷, Z. Bánki⁷, A. Marx-Hofmann⁷, S. Körper², B. Höchsmann³, H. Schrezenmeier³, C. Q. Schmidt¹

¹Institute of Experimental and Clinical Pharmacology, Toxicology and Pharmacology of Natural Products, University Hospital Ulm, Ulm, Germany

²Central Institute for Medical and Chemical Laboratory Diagnosis, University Hospital Innsbruck, Innsbruck, Austria

³Institute of Transfusion Medicine, University of Ulm, Ulm, Germany, and Institute of Clinical Transfusion Medicine and Immunogenetics Ulm, German Red Cross Blood Transfusion Service and University Hospital Ulm, Ulm, Germany

⁴Central Institute of Blood Transfusion and Immunology, University Hospital Innsbruck, Innsbruck, Austria

⁵Department of Internal Medicine V, Medical University of Innsbruck, Innsbruck, Austria

⁶Department of Internal Medicine II, Innsbruck Medical University, Innsbruck, Austria

⁷Institute of Virology, Innsbruck Medical University, Innsbruck, Austria

Introduction: The immune checkpoint ligand *programmed cell death 1 ligand 1* (PD-L1) is expressed by many host cells and tissues. Interaction between PD-L1 and PD-1 on T cells is thought to prevent autoimmunity and maintain self-tolerance under inflammatory conditions. The complement system is a key humoral messenger with the alternative complement pathway (AP) distinguishing self from non-self by complement regulatory proteins. We hypothesized that exuberant complement activity results in enhanced immune checkpoint interactions.

Materials and methods: For mechanistic studies a diluted whole blood assay was developed in which PD-L1 expression on leukocytes was measured by flow cytometry following defined complement activation stimuli. Upregulation of PD-L1 gene expression was determined by quantifying the mRNA levels of PD-L1 via qPCR. Paroxysmal nocturnal hemoglobinuria (PNH) is a complement-dependent disease. In peripheral blood from PNH patients, PD-L1 surface expression and soluble PD-L1 (sPD-L1) were analysed by flow cytometry and ELISA, respectively. In another study, PD-L1 in peripheral blood was determined in healthy volunteers after SARS-CoV2 vaccination. To further explore T cell response upon PD-L1 upregulation, IFN- γ release assays were conducted to measure T cell stimulation.

Results: We found increased expression levels of PD-L1 in peripheral blood of PNH patients, i.e. cell surface-expressed on granulocytes and monocytes as well as in soluble form. Mechanistically, we demonstrate that complement activation increased PD-L1 expression on neutrophils and monocytes as shown for different *in vitro* whole blood assays of classical or AP activation. We further establish *in vitro* that complement inhibition at the level of C3, but not C5, inhibited the AP mediated upregulation of PD-L1. In healthy volunteers after vaccination, PD-L1 on peripheral granulocytes and monocytes increased with levels correlating inversely with mitogen-induced T-cell stimulatory in the IFN- γ release assay.

Conclusions: Our study indicates a molecular cross-talk between proximal complement activation and PD-L1 expression on granulocytes and monocytes. PD-L1 surface levels correlate inversely with T-cell stimulatory pointing to a functional role of the identified mechanism. These data may have implications for various immune mediated diseases and conditions with an involvement of complement and beyond (e.g. cancer and vaccination).

18

3D lung-organoid reporter platform for testing of pharmaceutical compounds via high-throughput screening

M. Guedes¹, M. Brandt², R. Müller³, R. Bals², C. Beisswenger², D. Yildiz née Dreymueller¹

¹Saarland University, Experimental and Clinical Pharmacology and Toxicology, PZMS, Homburg, Germany

²Saarland University, University Hospital, Internal Medicine V, Homburg, Germany

³Helmutz Institute for Pharmaceutical Science, Saarbrücken, Germany

Chronic obstructive pulmonary disease (COPD) and cystic fibrosis are characterized by excessive mucus production, disturbed ciliary clearance, and reduced epithelial regeneration due to senescence. Current treatment strategies are mostly symptomatic (e.g. eradication of secondary infection, bronchodilation) rather than causal or curative (e.g. gene therapy). Therefore, respiratory epithelial cells are an important and new target for therapeutic interventions. For testing potential pharmaceutical compounds with regard to cell toxicity, differentiation, inflammation, mucus production, and senescence, we designed a 3D lung-organoid-reporter platform based on lung organoids. The system uses fluorescent markers under control of cell-specific promoters (differentiation, inflammation, mucus) enabling for online and end-point measurements in combination with fluorometric assays (cell toxicity, senescence). Defined quality criteria allows to test compounds such as senolytic drugs under standardized conditions. The use of human cells enables an accurate pre-selection of substances in the development of novel drugs. By its use in both basic research and preclinical drug development as well as its high flexibility, the platform

will strongly reduce the need for animal studies. Furthermore, the applicability to patient samples will allow a personalized identification of active substances.

19

Myeloid-derived suppressor cells dampen airway inflammation through prostaglandin E2 receptor 4

C. van Geffen^{1,2}, A. Deißler², S. Beer-Hammer², B. Nürnberg², R. Handgretinger³, H. Renz¹, D. Hartl⁴, S. Kolahian^{1,2}

¹Philipps University of Marburg - Medical Faculty, Institute of Laboratory Medicine and Pathobiochemistry, Molecular Diagnostics, Marburg, Germany

²University Hospital Tübingen, Department of Experimental and Clinical Pharmacology and Pharmacogenomics, Tübingen, Germany

³Eberhard Karls University of Tübingen, Children's University Hospital, Tübingen, Germany

⁴Eberhard Karls University of Tübingen, Department of Pediatrics I, Tübingen, Germany

Emerging evidence suggests a mechanistic role for myeloid-derived suppressor cells (MDSCs) in lung diseases like asthma. Previously, we showed that adoptive transfer of MDSCs dampens lung inflammation in murine models of asthma through cyclooxygenase-2 and arginase-1 pathways. Here, we further dissected this mechanism by studying the role and therapeutic relevance of the downstream mediator prostaglandin E2 receptor 4 (EP4) in a murine model of asthma. We adoptively transferred MDSCs generated using an EP4 agonist in a murine model of asthma and studied the consequences on airway inflammation. Furthermore, pegylated human arginase-1 was used to model MDSC effector activities. We demonstrate that the selective EP4 agonist L-902,688 increased the number and suppressive activity of MDSCs through arginase-1 and nitric oxide synthase-2. These results showed that adoptive transfer of EP4-primed MDSCs, EP4 agonism alone or arginase-1 administration ameliorated lung inflammatory responses and histopathological changes in asthmatic mice. Collectively, our results provide evidence that MDSCs dampen airway inflammation in murine asthma through a mechanism involving EP4/Arg1.

Short talks: Drug transport, metabolism and pharmacogenomics

20

Bupropion Ameliorates Acetic Acid-Induced Colitis in Rat: The Involvement of the TLR4/NF-κB Signaling Pathway

A. Rashidian^{1,2}, P. Dejbani^{1,2}, K. Karamifard³, A. Abdollahi⁴, C. Mohseni⁵, D. Ahmadrza^{1,2}, A. Hasanvand⁶

¹Tehran University of Medical Sciences, Department of Pharmacology, School of Medicine, Tehran, Iran

²Tehran University of Medical Sciences, Experimental Medicine Research Center, Tehran, Iran

³Lorestan University of Medical Sciences, Department of Pharmacology, School of Pharmacy, Khorramabad, Lorestan, Iran

⁴Tehran University of Medical Sciences, Department of Pathology, School of Medicine, Tehran, Iran

⁵AJA University of Medical Sciences, Department of Pharmacology, School of Medicine, Tehran, Iran

⁶Lorestan University of Medical Sciences, Department of Pharmacology, School of Medicine, Khorramabad, Lorestan, Iran

*Contributed equally

Inflammatory bowel disease composed of ulcerative colitis and Crohn's disease is a disorder that may involve entire gastrointestinal tract. Its pathogenesis is mainly an immune-mediated inflammation. Recently, it has been indicated that bupropion possesses anti-inflammatory properties; hence, the objective of this experiment is the investigation of the anti-inflammatory influence of bupropion on colonic lesions that emerged following the intrarectal administration of acetic acid. Thirty-six male Wistar rats were allocated randomly into six groups, including control, acetic acid, dexamethasone (2 mg/kg), and bupropion (40, 80, and 160 mg/kg). Colitis was induced by intrarectal administration of acetic acid in all study groups except control group, and animals were treated by oral administration of dexamethasone and bupropion. While macroscopic and microscopic lesions were observed after colitis induction, administration of dexamethasone and bupropion 160 mg/kg led to the remarkable improvement in lesions. In addition, the expression of TLR4 and NF-κB was decreased after colitis induction; however, treatment with dexamethasone (2 mg/kg) and bupropion (160 mg/kg) resulted in a significant decrease in their expression. Regarding biochemical factors, following colitis induction, TNF-α level and MPO activity were increased; nevertheless, dexamethasone (2 mg/kg) and bupropion (160 mg/kg) decreased the TNF-α and MPO activity. In conclusion, bupropion exerts anti-inflammatory influence through suppressing the TLR4 and NF-κB expression in the rat model of acute colitis.

Keywords: TLR4/NF-κB signaling pathway; acetic acid; bupropion; inflammatory bowel disease.

21

P-glycoprotein inhibition by rifabutin distinguishes it from rifampicin and partly explains the unequal drug interaction risk

J. Nilles^{1,2}, J. Weiss¹, W. E. Haefeli¹, G. Mikus¹, T. Ebner², S. Ruez², D. Theile¹

¹Heidelberg University Hospital, Clinical Pharmacology and Pharmacoepidemiology, Heidelberg, Germany

²Boehringer Ingelheim Pharma GmbH & Co. KG, Biberach, Germany

Introduction: It remains largely unknown why rifampicin exhibits the greater risk for interactions with P-glycoprotein (Pgp) substrates (e.g. dabigatran etexilate, sofosbuvir) than rifabutin.

Objectives: To compare the pharmacodynamics of mRNA/efflux activity induction and Pgp inhibition of rifampicin vs. rifabutin.

Materials and methods: *ABCB1* mRNA induction after 24, 96, or 144 h exposure of LS180 cells to 0.1-50 μM of the two rifamycins was assessed using quantitative real time-polymerase chain reaction. Pgp efflux activity after 144 h exposure to 0.01-10 μM was determined by calcein extrusion assay using fluorescence-activated cell sorting. The murine leukemia cell line (P388), its *mdr1a/b* (Pgp)-overexpressing counterpart (P388/dx), the porcine kidney epithelial cell (LLC-PK1), and its human *ABCB1*-transduced sub-cell line (L-MDR1) were used in separate experiments to monitor Pgp inhibition by recording calcein accumulation.

Results: While there were no potency differences, rifampicin resulted in higher maximum induction of *ABCB1* mRNA at all time points (e.g. Emax at 144 h: 7.4-fold of control for rifampicin, 4.5-fold for rifabutin; P = 0.003). The resulting Pgp activity levels did not differ (rifampicin (mean ± SD): EC50 0.99 ± 0.001 μM, Emax 3.2-fold ± 0.4 of control; rifabutin: EC50 1.1 ± 0.2 μM, Emax 2.8-fold ± 0.5 of control). Using the P388/dx model, rifabutin surprisingly exhibited potent Pgp inhibition (EC50 0.2 ± 0.03 μM) compared to rifampicin (EC50: 8.15 ± 0.52 μM, P = 0.0003). The L-MDR1 model confirmed the presence (rifabutin) and absence (rifampicin) of Pgp inhibition.

Conclusion: While both drugs can efficiently induce *ABCB1* expression and Pgp activity, rifabutin concurrently inhibits Pgp. This strong Pgp inhibition appears to counterbalance Pgp induction, which may partly explain the markedly different *in vivo* perpetrator effects of rifabutin.

22

Metabolomic profiling and *in silico* ligand screening enable identification of novel drug transporter substrates

A. Nies^{1,2,3}, J. König⁴, P. Leuthold^{1,2}, K. Damme^{1,2}, S. Winter^{1,2}, M. Haag^{1,2}, S. Masuda^{5,6}, S. Kruck⁷, H. Daniel⁸, B. Spanier⁸, M. Fromm⁴, J. Bedke⁷, K. I. Inui⁹, M. Schwab^{1,2,3,10}, E. Schaeffeler^{1,2,3}

¹Dr. Margarete Fischer-Bosch Institute of Clinical Pharmacology, Stuttgart, Germany

²University of Tuebingen, Tuebingen, Germany

³University of Tuebingen, Cluster of Excellence IFIT (EXC 2180) "Image-Guided and Functionally Instructed Tumor Therapies", Tuebingen, Germany

⁴Friedrich-Alexander-Universität Erlangen-Nürnberg, Institute of Experimental and Clinical Pharmacology and Toxicology, Erlangen, Germany

⁵Graduate School of Pharmaceutical Sciences, Kyushu University, Department of Clinical Pharmacology & Biopharmaceutics, Fukuoka, Japan

⁶Himeji Dokkyo University, Department of Clinical Pharmaceutics, Faculty of Pharmaceutical Sciences, Himeji, Japan

⁷University Hospital Tuebingen, Department of Urology, Tuebingen, Germany

⁸Technical University of Munich, TUM School of Life Sciences Weihenstephan, Freising, Germany

⁹Kyoto Pharmaceutical University, Kyoto, Japan

¹⁰University of Tuebingen, Departments of Clinical Pharmacology, Pharmacy and Biochemistry, Tuebingen, Germany

Introduction: Solute carrier (SLC) membrane transport proteins play crucial roles in disease susceptibility and control the response to drugs. The function of many SLC transporters is still unknown.

Objectives: We describe the proof-of-concept of a novel strategy to identify SLC transporter substrates. The two renal transporters multidrug and toxin extrusion 1 (MATE1/SLC47A1) and proton-coupled peptide transporter 2 (PEPT2/SLC15A2), important for drug excretion and reabsorption, respectively, were used exemplarily.

Methods: Non-targeted metabolomic profiling (Leuthold et al. 2017, J Proteome Res 16, 933) of kidneys of *Slc47a1*^{-/-} and *Slc15a2*^{-/-} mice was conducted. Monolayers of polarized Madin-Darby canine kidney cells expressing simultaneously apically localized human MATE1 and basolaterally localized OCT2 or human embryonic kidney cells expressing human PEPT2 were used for transport assays. Test compounds were analyzed by mass spectrometry. Similarity-based *in silico* ligand screening of two databases was applied using similarity score cut-offs of 0.7. Drugs identified by *in silico* screening were tested in transport assays.

Results: Metabolomic profiling identified 57 increased features in kidneys of *Slc47a1*^{-/-} vs. wild-type mice, 18 of which were assigned to metabolites representing 14 novel MATE1 candidates. Transcellular transport assays of candidates from different substance classes confirmed cytosine, 5-methylcytidine, 3-guanidino-propanoate, 4-guanidino-butanoate, acylcarnitine 4:0 as novel MATE1 substrates. In kidneys of *Slc15a2*^{-/-} mice, only asnerine was lower than in wild-type and confirmed as novel PEPT2 substrate. In urine samples of *Slc15a2*^{-/-} mice, 29 features were increased and 20 assigned as dipeptides, known substrates of PEPT2. By *in silico* screening, cytosine-like and 5-methylcytidine-like drugs were identified as potential MATE1 substrates and confirmed by

transcellular transport assays. No drugs related to guanidino acids, acylcarnitine 4:0 or anserine were identified.

Conclusion: By combining metabolomic profiling of mice with genetically-disrupted transporters, *in silico* screening and *in vitro* transport studies for experimental validation, we identify nucleobases and nucleoside-derived anticancer and antiviral agents as new substrates of MATE1 and confirm the narrow substrate spectrum of PEPT2. Beyond the broad applicability of this new approach for identifying substrates for SLC transporters, it may prove particularly relevant in drug research.

23

Influence of single nucleotide polymorphism c.825C>T in *GNB3* on humoral and cellular immune response after vaccination with mRNA-1273 vaccine

I. Ciuciulkaite*

*Essen University Hospital, Institute of Pharmacogenetics, Essen, Germany

Introduction: Immune response and waning of immunity after the vaccination against COVID-19 with different vaccines varies within the population. Genetic host factors are likely to contribute to this variability. To the best of our knowledge, no other study investigated the association between polymorphisms in G-proteins and immune response after the vaccination against COVID-19.

Objectives: The aim of this study was to evaluate immune response after two vaccinations with mRNA-1273 vaccine and to determine whether *GNB3* c.825C>T polymorphism influences the immune response after the vaccination.

Materials and methods: Antibodies against SARS-CoV-2 spike protein and T-cell responses against SARS-CoV-2 spike peptide pools were measured one and six months after the second vaccination with mRNA-1273 in the main study group of 204 participants. Additionally, antibodies against SARS-CoV-2 spike protein were measured in a group of 943 participants one and six months after the second vaccination with mRNA-1273. Genotypes of *GNB3* c.825C>T were determined in all participants.

Results: The median antibody titre against the SARS-CoV-2 spike protein in both study groups and median values of spots increment in the SARS-CoV-2 IFN- γ ELISpot assay in the main study group significantly decreased from month 1 to month 6 ($P < 0.001$). Genotypes of *GNB3* c.825C>T had no influence on the humoral immune response in both study groups. At month 1, CC genotype carriers had significantly increased T-cell responses against S1 domain compared to CT ($P = 0.02$) or TT ($P = 0.05$) genotypes. CC and CT genotype carriers had about 6.5-fold increased probability compared to TT genotype carriers to mount a SARS-CoV-2-specific antibody titre above the median value ($P = 0.01$ and $P = 0.02$, respectively). CC genotype carriers had almost 6-fold increased probability compared to TT genotype carriers to mount a SARS-CoV-2-specific T-cell response against S1 domain above the median value ($P = 0.01$). In addition, compared with CT genotype carriers, CC genotype carriers were about 2.6-fold more likely to have a T-cell response against predicted immunodominant domains above the median value ($P = 0.04$).

Conclusion: CC genotype carriers of the *GNB3* c.825C>T polymorphism have an increased T-cell immune response, which may indicate a better T-cell-mediated protection against COVID-19 after vaccination with mRNA-1273. Role of *GNB3* c.825C>T on the humoral immune response remains elusive and needs to be investigated further.

24

Pharmacogenetics in uncoupling susceptibility of CYP2B6 mediated substrate oxidation

S. Yamoune^{1,2}, J. Müller¹, I. M. Langmia¹, C. Scholl², J. C. Stingl¹

¹Institute for Clinical Pharmacology at the university clinic RWTH Aachen, Aachen, Germany

²Federal Institute for drugs and Medical Devices, Bonn, Germany

Introduction: CYP450 reaction uncoupling describes an unproductive cycle, resulting in a lack of substrate oxidation and increased ROS formation. The susceptibility towards uncoupling varies between CYP450 enzymes, but the role of pharmacogenetic variability in these mechanistic enzymatic effects is yet to be understood. This work includes the *CYP2B6*6* and *CYP2B6*34* alleles. Specifically the allele *CYP2B6*6* is of high functional relevance. *CYP2B6*34* is a variant that contains one further SNP at the C terminus and predominantly occurs in African populations.

Objective: The aim of this study was to compare CYP2B6 pharmacogenetic variant enzymes with SNPs outside the binding pocket on substrate metabolism and H₂O₂ production and substrate oxidation *in vitro*.

Materials and methods: Variant plasmids were produced by quickchange PCR and transformed into *E. coli*

Recombinant enzyme functionality was determined by quantification of bupropione (bpr), efavirenz (efa) and ketamine (keta) biotransformation using HPLC-MS/MS. Determination of extracellular H₂O₂ levels was performed by the amplex red/ horseradish peroxidase assay. Intracellular oxidative stress was quantified via CellRox reagent and microscopy.

Result: Increased extracellular levels of H₂O₂ were detected in *CYP2B6*6* (mean \pm SD: 26 μ M \pm 1.5) and *CYP2B6*34* (mean \pm SD: 65 μ M \pm 7.9) variants compared to 19 μ M \pm 2.8 in *CYP2B6*1*. Addition of the three substrates showed a significant ROS decrease by bpr (mean \pm SD: 18 μ M \pm 1.5) and keta (mean \pm SD: 18 μ M \pm 3.0) but not by efa (mean \pm SD: 24 μ M \pm 1.7) in *CYP2B6*6*. *CYP2B6*34* H₂O₂ levels were not affected by any substrate (bpr mean \pm SD: 50 μ M \pm 5; efa mean \pm SD: 44.7 μ M \pm 12; keta mean \pm SD: 49 μ M \pm 9).

Conclusion: ROS levels were specifically reduced in bpr and keta in *CYP2B6*6* while in *CYP2B6*34*, substrate addition had no effect. Though the mutations encoding *CYP2B6*6* were shown to be inactivating, catalytic analyses of *CYP2B6*1* and *CYP2B6*6* revealed higher KM values (97 μ M bpr, 129 μ M efa and 105 μ M keta) in *CYP2B6*6* compared to *CYP2B6*1* (31 μ M bpr, 23 μ M efa and 72 μ M keta). In contrast, the kcat was increased in *CYP2B6*6* (8 min⁻¹), compared to the wildtype (0.4 min⁻¹), which indicates an unknown rescue mechanism for the substrate oxidation in addition to the reaction uncoupling. Catalytic *CYP2B6*34* characterization and analyses of additional variants (*5 and *37) are ongoing and will allow further understanding of the mechanisms causing uncoupling of CYP2B6 substrate oxidation.

25

Voriconazole clearance can be predicted by CYP3A and CYP2C19 activity using microdosed probe drugs

A. Muhareb¹, A. Blank¹, A. Meid¹, K. Foerster¹, J. Burhenne¹, W. E. Haefeli¹, G. Mikus¹

¹Heidelberg University Hospital, Dept. of Clinical Pharmacology, Heidelberg, Germany

Voriconazole is an important broad-spectrum anti-fungal drug with nonlinear pharmacokinetics. In this single centre, fixed-sequence, open label drug-drug interaction trial with healthy participants (N = 17), we aimed to determine whether voriconazole clearance could be estimated or even predicted when microdosed probe drugs for CYP3A and CYP2C19 were used. On the first trial day, participants were given a single oral microdose of midazolam and omeprazole and plasma drug concentrations were measured. On the second trial day, a single dose of either 50 mg, 100 mg, 200 mg, or 400 mg of voriconazole was administered, followed by the microdosed probe drugs. A wide range of clearances of midazolam (790–2790 ml/min at baseline; 248–1316 ml/min during VRZ), omeprazole (66.4–2710 ml/min at baseline; 30.1–1420 ml/min during VRZ) was observed and voriconazole exhibited non-linear pharmacokinetics. Clearances of midazolam (geometric mean ration (GMR) 0.586 at VRZ 50 mg decreasing to GMR 0.196 at VRZ 400 mg) and omeprazole (GMR 0.590 at VRZ 50 mg decreasing to GMR 0.166 at 400 mg) were reduced with increasing voriconazole doses. Nonlinear regression showed a correlation between the clearance of midazolam and voriconazole (slope 0.404; adjusted R² 0.521) and between the clearance of omeprazole and voriconazole (slope 1.13; adjusted R² 0.756) during VRZ. Multiple linear regression resulted in an adjusted R² of 0.9968 for the relationship $CL_{VRZ} \sim \log CL_{OMZ} + \log CL_{MDZ}$ using data gathered during VRZ and an adjusted R² of 0.9974 for the relationship $CL_{VRZ} \sim \log CL_{OMZ} + \log CL_{MDZ} + VRZ$ dose using the data for CL_{MDZ} and CL_{OMZ} at baseline. Microdosed probe drugs of CYP3A (midazolam) and CYP2C19 (omeprazole) accurately described and predicted the total clearance of voriconazole.

Keywords: Voriconazole, CYP3A, CYP2C19, midazolam, omeprazole, individualised medicine, microdosing.

Figure 1. Multiple regression estimates.

Figure 2. Best-fit multiple regression models.

Schulz J, et al. Novel insights into the complex pharmacokinetics of voriconazole: a review of its metabolism. Drug Metab Rev. 2019.

Mikus G. Probes and Cocktails for Drug-Drug Interaction Evaluation: The Future Is Microdosing? Clin Pharmacol Ther. 2019.

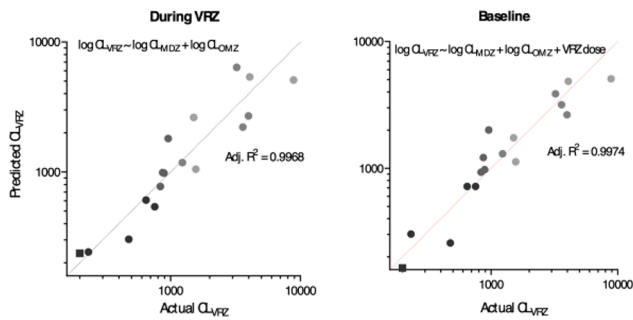
Elbe A, et al. Evaluation of CYP2C19 activity using microdosed oral omeprazole in humans. Eur J Clin Pharmacol. 2022.

Hohmann N, Haefeli WE, Mikus G. CYP3A activity: towards dose adaptation to the individual. Expert Opin Drug Metab Toxicol. 2016.

Fig. 1

Equation	Dose	CL _{MDZ}		CL _{OMZ}	
		Estimate	p-value	Estimate	p-value
log CL _{VRZ} ~ VRZ dose	VRZ	0.009548	0.0004		
log CL _{VRZ} ~ log CL _{MDZ}	VRZ			1.124	<0.0001
	BL			0.961	<0.0001
log CL _{VRZ} ~ log CL _{OMZ}	VRZ			1.282	<0.0001
	BL			1.074	<0.0001
log CL _{VRZ} ~ log CL _{OMZ} + log CL _{MDZ}	VRZ			0.5481	<0.0001
	BL			0.2134	0.1696
log CL _{VRZ} ~ log CL _{OMZ} + log CL _{MDZ} + VRZ dose	VRZ	0.0002546	0.5209	0.4696	0.0099
	BL	-0.001726	<0.0001	0.5609	0.0001
				0.569	<0.0001

Fig. 2



Short talks: Toxins II

26

Inhibition of *Clostridioides difficile* Toxins TcdA and TcdB by Repurposing of the Antiarrhythmic Drug Amiodarone

J. Schumacher¹, A. Nienhaus¹, E. Chaves-Olarte², C. Rodriguez², H. Barth¹, P. Papatheodorou¹

¹Ulm University Medical Center, Institute of Experimental and Clinical Pharmacology, Toxicology and Pharmacology of Natural Products, Ulm, Germany

²Universidad de Costa Rica, Centro de Investigación en Enfermedades Tropicales and Facultad de Microbiología, San José, Costa Rica

The intestinal pathogen *Clostridioides difficile* is a major cause of antibiotic-associated diarrhea and pseudomembranous colitis in humans. Its two toxins TcdA and TcdB, which are responsible for the symptomatology of *C. difficile*-associated diseases (CDADs), enter target cells via receptor-mediated endocytosis and inactivate host Rho and Ras GTPases by glucosylation. Cholesterol plays a crucial role during the intoxication process of TcdA and TcdB, most likely during pore formation of both toxins in endosomal membranes, which represents a key step for the translocation of the glucosyltransferase domain of both toxins from endocytic vesicles into the cytosol of host cells. Recent studies revealed that the licensed antiarrhythmic drug amiodarone, which is a multichannel blocker commonly used in the treatment of atrial and ventricular tachyarrhythmias, inhibited cholesterol biosynthesis in cultured human cells (Allen et al., 2020; Simonen et al., 2020). Prompted by these findings, we investigated whether preincubation of cultured mammalian and human cells and human intestinal organoids with amiodarone protects from TcdA and/or TcdB intoxication. Astonishingly, amiodarone exhibited a protective effect against both toxins and also against toxin variants from the clinically relevant, epidemic *C. difficile* strain NAP1/027. Surprisingly, our data indicates that amiodarone most likely interferes with the membrane pore of the toxins during the translocation process. Due to the fact that amiodarone represents an already approved licensed drug, our study points towards the possibility of repurposing this drug as a novel pan-variant antitoxin therapeutic in the context of CDADs.

References:

Allen, L. B., Genaro-Mattos, T. C., Anderson, A., Porter, N. A., Mimics, K., and Korade, Z. (2020). Amiodarone Alters Cholesterol Biosynthesis through Tissue-Dependent Inhibition of Emopamil Binding Protein and Dehydrocholesterol Reductase 24. *ACS Chem. Neurosci.* doi:10.1021/acscchemneuro.0c00042.

Simonen, P., Li, S., Chua, N. K., Lampi, A. M., Piironen, V., Lommi, J., et al. (2020). Amiodarone disrupts cholesterol biosynthesis pathway and causes accumulation of circulating desmosterol by inhibiting 24-dehydrocholesterol reductase. *J. Intern. Med.* doi:10.1111/joim.13095.

27

European programme for the establishment of validated procedures for the detection and identification of biological toxins (EuroBioTox)

S. Worbs¹, B. Kampa¹, M. Skiba¹, K. Busschots², R. Zeleny², J. Masquelier³, A. Puustinen⁴, P. Vanninen⁴, C. Rasetti-Escargueil⁵, M. Popoff⁶, E. Lemichez⁵, A. S. Mierzaia⁶, H. Volland⁶, F. Becher⁶, S. Simon⁶, B. Boran⁷, Y. Nia⁷, J. A. Hennekinne⁷, J. Weisemann⁸, A. Rummel⁸, D. Jansson⁹, M. A. Avondet¹⁰, M. Wittwer¹⁰, W. Luginbühl¹¹, R. Josuran¹², C. Zaborosch¹², L. Burns¹³, K. Campbell¹³, B. Dörner¹

¹Robert Koch Institute, Biological Toxins, Berlin, Germany

²European Commission, Joint Research Centre, Geel, Belgium

³Sciensano, Tervuren, Belgium

⁴University of Helsinki, Finnish Institute for Verification of the Chemical Weapons Convention, UH/VERIFIN, Helsinki, Finland

⁵Institut Pasteur, Département de Microbiologie, Bactéries Anaérobies et Toxines, Paris, France

⁶CEA-SACLAY, Laboratoire d'Etudes et de Recherche en Immunoanalyse, Gif-sur-Yvette, France

⁷ANSES, Food Safety Laboratory, SBCL Unit, Maisons-Alfort, France

⁸toxogen GmbH, Hannover, Germany

⁹Swedish Defence Research Agency FOI, Umeå, Sweden

¹⁰SPIEZ LABORATORY, Spiez, Switzerland

¹¹ChemStat, Bern, Switzerland

¹²Zürich University of Applied Sciences ZHAW, Institute of Chemistry and Biotechnology, Wädenswil, Switzerland

¹³Queen's University Belfast, Institute for Global Food Security, Belfast, United Kingdom

Biological toxins are known as causative agents of food poisoning, but some of them also have a history as warfare agents and could be used in a bioterrorism context. Previous studies showed that there is a lack of robustness in European preparedness for biotoxin incidents. There is a need for standard analytical tools and procedures, reference materials, state-of-the-art training and establishment of a European proficiency testing scheme.

EuroBioTox is a Horizon 2020 project integrating 13 consortium partners and 50 network partners from 23 countries from the health, food, military and verification sectors. The project aims at establishing a Pan-European network of competence for the analysis of biological toxins of potential bioterrorism threat (1). The toxins in the scope of EuroBioTox comprise selected large protein toxins (ricin, abrin, botulinum neurotoxins [BoNT], staphylococcal enterotoxin B [SEB]) as well as small molecule biotoxins (saxitoxin [STX]).

Using current best practice, the EuroBioTox core members develop and validate improved analytical tools, reagents and standard operating procedures based on realistic incident scenarios. Alternative and more accurate *in vitro* tests for the ethically questionable animal test for BoNT are under evaluation.

Progress beyond state of the art has been achieved by production of five candidate reference materials for different biological toxins to be certified after the current comprehensive molecular characterisation. The first certified reference material has been released this year. Training courses at basic and advanced levels have been conducted within the network tailored to the different methods and toxins, followed by a series of proficiency tests (currently five) to disseminate best practice methods across Europe. The creation of a European repository with proprietary toxin-specific tools was initiated to harmonise detection methods. With respect to the specific needs of first responders, new conceptual guidelines on sampling, detection and decontamination were established focusing on biological toxins.

EuroBioTox is implementing a comprehensive mechanism of training, method sharing, improvement of quality assurance measures and proficiency testing. It is expected that the spreading of good analytical practices will improve preparedness and response planning at national and international level.

Reference: (1) <https://eurobiotox.eu>

28

Endotoxin exacerbates the NLRP3-dependent inflammatory potency of Saharan dust

G. Bredeck¹, M. Busch¹, A. Rossi¹, B. Stahlmecke², K. W. Fomba³, H. Hermann³, R. Schims¹

¹IUF - Leibniz Research Institute for Environmental Medicine, Düsseldorf, Germany

²Institute for Energy and Environmental Technology e.V. (IUTA), Duisburg, Germany

³Leibniz-Institute for Tropospheric Research (TROPOS), Leipzig, Germany

Epidemiological studies have shown that desert dust exposure affects respiratory health. About half of global desert dust is attributable to Saharan dust (SD). SD is a heterogeneous mixture of inorganic and organic components including compounds of microbial origin. We aimed to investigate the NLRP3 inflammasome-caspase-1 pathway-dependent inflammatory properties of SD in a macrophage model and an air-liquid interface (ALI) co-culture model of the alveolar epithelium.

Under submerged conditions wild-type (WT) and *NLRP3*^{-/-} THP-1 cells were exposed to SD at 50 µg/cm². Using a Vitrocell® Cloud 12α, A549/THP-1 WT ALI co-cultures were exposed to SD or DQ12 quartz at non-cytotoxic concentrations of 10, 20, and 30 µg/cm². Additionally, ALI co-cultures containing *NLRP3*^{-/-} or *CASPASE-1*^{-/-} THP-1 cells were exposed to SD.

SD was found to contain endotoxin, detected by LAL assay, and caused manifold higher interleukin (IL)-1β secretion in WT than in *NLRP3*^{-/-} THP-1 cells. Baked SD (220°C, overnight), which was endotoxin-free, induced IL-1β secretion to an approximate 4-fold lower extent. Co-exposure to baked SD and endotoxin synergistically restored the IL-1β secretion. In ALI co-cultures SD but not DQ12 upregulated the expression and secretion of IL-1β, IL-6, IL-8, and tumor necrosis factor α. The secretion of these four cytokines was strongly decreased in co-cultures with *CASPASE-1*^{-/-} or *NLRP3*^{-/-} THP-1 cells. The screening of multiple SD samples on WT THP-1 cells revealed that their inflammatory potencies strongly depended on the sampling day and location.

The surprisingly strong SD-mediated activation of the NLRP3 inflammasome emphasizes its hazardousness and the need for risk mitigation strategies. Therefore, the connection between the toxicity of SD and its composition, especially its microbial components, needs to be further unraveled.

Supported by the Leibniz Collaborative Excellence Programme project DUSTRISK.

29

Identification of the transport subunit C2IIa of the binary *Clostridium botulinum* C2 toxin as a cytosolic protein delivery system for protein cargo into mammalian cells
 S. Heber¹, J. Borho¹, M. Fellemann¹, N. Stadler¹, F. Wondany², J. Michaelis², H. Barth¹
¹Ulm University Medical Center, Institute of Experimental and Clinical Pharmacology, Toxicology and Pharmacology of Natural Products, Ulm, Germany
²Ulm University, Institute of Biophysics, Ulm, Germany

The *Clostridium botulinum* C2 toxin consists of the two individual proteins C2I (enzyme subunit) and C2II (binding/translocation subunit) [1]. Proteolytically activated C2II (C2IIa) forms ring-shaped homoheptamers that bind carbohydrate receptors which are expressed on all mammalian cells investigated so far and interact with C2I. Following binding, C2I/C2IIa-complexes are internalized by receptor-mediated endocytosis. Once taken up into early endosomes, C2IIa heptamers form membrane-spanning pores through which C2I translocates into the cytosol, where it modifies cellular target molecules. Up to this point, no transport of proteins other than the natural cargo C2I or fusion-proteins derived from its N-terminus has been described. Here we showed, that C2IIa is also able to efficiently transport other, foreign cargo proteins into the cytosol of mammalian cells.

As proof of concept enzymatic subunits of other bacterial toxins were chosen as reporter enzymes, each having specific functions within cells. C2IIa as well as the membrane impermeable cargo proteins on their own showed no cellular effects, while the respective combinations led to typical changes in cell morphology and viability, which indicate efficient transport of the cargo into the cytosol. Morphological effects were examined by phase contrast and fluorescent microscopy, cytotoxic effects by MTS assay. Binding of cargo proteins with and without specific modifications to C2IIa was shown *in vitro* by Dot Blot technique. Increased endosomal uptake of cargo proteins in the presence of C2IIa was detected by STED super resolution microscopy whereas the transport of enzymatically active cargo toxins into the cytosol of cells was investigated by Western Blot and Flow cytometry.

All together, we showed that C2IIa delivers not only its original cargo C2I but also a range of different other proteins into the cytosol of cells. Therefore, C2IIa might serve as a cargo delivery platform for enhanced transport of therapeutic proteins into mammalian cells and also might have additional yet undescribed roles in pathophysiology. Furthermore, we could demonstrate that specific modifications of the cargo proteins drastically alter the transport efficiency by C2IIa.

[1] Barth H., Blocker D., Behlke J., Bergsma-Schutter W., Brisson A., Benz R., Aktories K. (2000). Cellular Uptake of Clostridium Botulinum C2 Toxin Requires Oligomerization and Acidification. *J. Biol. Chem.* 275, 18704–18711.

Short talks: Genotoxicity

30

Adduct-specific differences in DNA damage recognition by nucleotide excision repair
 L. Sarmeni¹, M. Meabed¹, A. Khobta¹
¹Friedrich Schiller University Jena, Institute of Nutritional Sciences, Jena, Germany

Introduction and aim: Global genome (GG) and transcription coupled (TC) nucleotide excision repair (NER) remove a broad range of DNA modifications induced in the genome by active metabolites of nutritional and environmental carcinogens. Although GG- and TC-NER share the same set of core components, their adduct recognition spectra may differ. As an extreme example, we previously reported that repair of an exocyclic *N*²-guanosine adduct of N-acetoxy-N-2-acetylaminofluorene (dG(*N*²)-AAF) strictly requires TC-NER in human cells regardless of their GG-NER proficiency [1]. The inability of GG-NER to recognize the damage would be extremely dangerous to the genome integrity. We therefore questioned whether resistance to GG-NER could be more common between adducts of different nature.

Experimental approach: We used cell lines with specific genetic defects of GG-NER or TC-NER to measure host cell reactivation (HCR) as a readout of repair capacities towards structurally defined synthetic DNA adducts incorporated specifically into the transcribed DNA strand of an EGFP reporter gene.

Results and conclusions: Besides dG(*N*²)-AAF, cells derived from TC-NER-compromised Cockayne syndrome (CS) patients showed inability to repair *N*²-ethylguanine and 1-*N*²-ethenoguanine, whereas GG-NER-deficient xeroderma pigmentosum group C (XP-C) cells showed full repair capacities towards these adducts. Independently from the substituent size, all *N*²-guanosine adducts are characterized by minimal structural distortion within DNA and do not destabilize base pairing, which may prevent efficient recognition by GG-NER. Likewise, HCR of (S)-stereoisomers of 8,5'-cyclo-2'-deoxypurine lesions, which also do not induce a significant distortion of the helical structure of DNA, was strongly suppressed in CS but not in XP-C cells. In contrast, repair capacity towards helix-distorting lesions, such as cyclobutane thymine-thymine dimer and N-(deoxyguanosin-8-yl)-2-acetylaminofluorene, could be accomplished by either TC- or GG-NER. These results were independently confirmed in an isogenic cell model. Thus, CSA gene knockout in HeLa cells exactly recapitulated the CS phenotype, whereas knockout of its GG-NER-specific analog *DDB2/XPE* retained normal repair. In summary, our results expose remarkable inefficiency of GG-NER towards physiologically relevant substrates, including adducts arising from the reactive electrophilic and oxidative species.

Reference: [1] Kitsera N, et al. (2014) *PLoS One* 9: e94405

31

The role of NAD⁺ in genotoxic stress response towards sulfur and nitrogen mustards.
 J. Ruzsiewicz¹, F. Eble¹, Y. Papatheodorou¹, N. Jäck¹, S. Rothmiller², A. Bürkle¹, A. Mangerich^{1,3}
¹University of Konstanz, Biology, Konstanz, Germany
²Bundeswehr Institute of Pharmacology and Toxicology, Munich, Germany
³University of Potsdam, Institute Nutritional Science, Potsdam, Germany

Introduction: Nicotinamide adenine dinucleotide (NAD⁺) is essential for energy metabolism, redox regulation, and cell survival pathways. Moreover, NAD⁺ is involved in genome maintenance, as a substrate for DNA repair factors, such as ARTDs (aka PARPs) and SIRT6. Decreased NAD⁺ levels have been observed in the pathomechanism of DNA alkylating agents such as sulfur mustard (SM), suggesting that NAD⁺ supplements might be helpful in mitigating mustard-induced toxicity.

Objectives: The role of NAD⁺ depletion and elevation in the genotoxic stress response towards the sulfur mustard derivatives has been investigated with the use of NAD⁺ synthesis inhibitor FK866 and NAD⁺ booster nicotinamide riboside (NR).

Materials and methods: Cells were exposed to NR in order to boost NAD⁺ levels before and/or after a 30-min exposure to monofunctional agent 2-chloroethyl-ethyl sulfide (CEES) or the crosslinking agent mechlorethamine (HN2). To deplete cellular NAD⁺ levels in the immortalized human keratinocytes (HaCaT), FK866 was applied 24 h prior to and after genotoxic treatment. Subsequently, the cellular NAD⁺ levels were measured via the enzymatic cycling assay, and the clonogenic survival assay was performed. In human immortalized monocyte-like cell line THP-1, the effects of NR supplementation of cellular NAD⁺ levels and cell viability (Alamar Blue) were assessed upon exposure to CEES or HN2.

Results: Depletion of cellular NAD⁺ via FK866 sensitized HaCaT cells to genotoxic stress, particularly to CEES exposure. NR supplementation, by increasing cellular NAD⁺ levels, rescued the effect of FK866. In THP-1 cells, the elevation of basal NAD⁺ levels via NR had a positive effect on cell viability after genotoxic exposure.

Conclusion: Our present results suggest that NAD⁺ is an important molecule in the pathomechanism of SM derivatives with compound-specific outcomes. Protective effects of NR observed in THP-1 cells suggest system specificity of the application of this NAD⁺ booster.

Supported by the German Ministry of Defense (grant number E/U2AD/ID015/IF561).

32

Arsenite-induced epigenetic dysregulation of post-translational histone modifications in DNA repair genes in lung epithelial cells
 T. Lumpp¹, K. Gleiss¹, S. Stöber¹, P. Schumacher¹, A. Hartwig¹
¹Karlsruhe Institute of Technology (KIT), Karlsruhe, Germany

Arsenite contamination of drinking water is a human health concern affecting millions of people worldwide. Adverse outcomes, particularly human carcinogenicity, may result due to a chronic exposure towards elevated levels of inorganic arsenite. Nevertheless, the precise molecular mechanisms of carcinogenicity remain unknown. Several modes of action have been established, with impairment of DNA repair being one of the prominent ones. A number of studies indicate that arsenite negatively affects protein folding, for example by interactions with zinc-binding structures, and expression of DNA repair factors. In this work, the latter was identified gene-specifically by applying a high-throughput RT-qPCR method, which might be caused by an alteration of the epigenome such as modified histone modification patterns.

Within this study, we addressed potential arsenite-induced changes in gene expression and linked them to post-translational histone modification patterns in promoter regions of selected DNA repair genes and genes involved in epigenetic regulation. For this purpose, a ChIP-qPCR method was established to detect specific DNA-histone interactions. DNA repair genes involved in base-excision repair (*MPG*, *XRCC1*), nucleotide-excision repair (*XPA*, *XPC*) and mismatch repair (*MLH1*, *MSH2*) were analyzed concerning the gene activating histone marks H3K18ac and H3K4me3 as well as the gene repressing mark H3K27me3. Further, we examined the impact of arsenite on *EP300*, coding for a histone acetyltransferase.

Initial data revealed that 24-hour non-cytotoxic sodium arsenite treatment of A549 cells induced gene-specific alterations of the active histone modifications H3K18ac and H3K4me3, but not the repressive mark H3K27me3, in close proximity to the promoter regions of the genes investigated. Particularly, *MLH1* and *MPG* showed a decrease in the abundance of both, H3K18ac and H3K4me3. A single modification declines in the case of *EP300*, *XRCC1* (H3K4me3) and *XPA* (H3K18ac). In contrast, no significant changes, either of H3K18ac or of H3K4me3, were detected in the promoter regions of *MSH2* and *XPC*.

The results correspond to the observed downregulation of genes coding for DNA repair and epigenetic factors, which could lead to the inactivation of respective pathways. Altogether, our findings suggest that arsenite is capable of inducing gene-specific epigenetic dysregulation through modifying histone modification in A549 cells.

33

Toxicity and DNA-repair in in vitro and ex vivo skin models after single and combined exposure to benzo[a]pyrene and UV irradiation.C. Kersch¹, V. Masutin¹, R. Alsaieh¹, S. Schmitz-Spanke¹¹Friedrich-Alexander-Universität Erlangen-Nürnberg, Institut und Poliklinik für Arbeits-, Sozial- und Umweltmedizin, Erlangen, Germany

Introduction: Humans are exposed to PAHs and UV radiation in the workplace and in the environment. Both toxicants exert genotoxic effects, so a potential synergistic effect is still under discussion. For this purpose, the study aimed to analyse the dose-response relationship of different toxicological endpoints after single as well as combined exposure to benzo[a]pyrene (B[a]P) and UV irradiation. Skin-related cells and ex vivo skin were used to compare the results in the two models.

Method: KeratinoSens™ and U937 cells were exposed to 0.0004 - 40 µM B[a]P for 24h in absence/presence of UV irradiation (3.5 J 95% UVA, 5% UVB [KeratinoSens™]; 1.7 J UVA [U937]). Freshly prepared ex vivo skin was exposed for 24 h to 0.318, 31.8 and 318 ng/cm² B[a]P or 7 J UV (95% UVA and 5% UVB) and in combination of both. Endpoints for vitality, oxidative stress, enzymatic activity and DNA damage/repair were determined. For the cell models a benchmark approach was utilized to rank the endpoints according to their sensitivity.

Results and conclusions: In our cell models exposure to B[a]P alone did not affect the cells in a meaningful way. The addition of UV irradiation led to synergistic effects on cellular homeostasis and DNA repair with BMD values for non-genotoxic endpoints between 0.005 µM B[a]P (LDH) and 0.2 µM B[a]P (glutathione) for KeratinoSens™. Deviating from that, DNA repair (yH2AX) was the most sensitive endpoint with BMD values of 0.0006 µM B[a]P (KeratinoSens™) 0.001 µM B[a]P (U937).

In ex vivo skin, single and combined exposure to B[a]P and UV had minimal impact on vitality and lipid peroxidation. While the cytochrome activity was slightly elevated under single exposure conditions, combined exposure significantly increased it. Single UV irradiation elevated the level of glutathione, while combined exposure had nearly no effect. DNA repair showed no synergistic effect, in contrast to the in vitro models. On the contrary, single UV irradiation alone reduced the levels of yH2AX while single B[a]P exposure significantly increased it. The combined exposure reached the level under control conditions (-B[a]P/-UV irradiation) only at higher B[a]P concentrations.

In comparison to the cell lines the ex vivo skin was more robust. While the cell lines showed a synergistic effect to the combination of B[a]P and UV, this effect was not observed in ex vivo skin.

This work was supported by the *Deutsche Gesetzliche Unfallversicherung* [grant number FB 275 B].

Short talks: Young Investigator Lectures

34

Human metabolism and urinary excretion of neonicotinoids and neonicotinoid-like compounds in controlled oral dose studiesS. A. Wrobel¹, D. Bury¹, S. Koslitz¹, H. M. Koch¹, H. Hayen², T. Brünig¹, H. U. Käfferlein¹¹Institute for Prevention and Occupational Medicine of the German Social Accident Insurance, Ruhr University Bochum (IPA), Center of Toxicology - Section Biomonitoring, Bochum, Germany²University of Münster, Department of Analytical Chemistry, Münster, Germany

Introduction: Neonicotinoids and neonicotinoid-like compounds (NNIs) are an important group of insecticides frequently applied worldwide. Nevertheless, their use is of growing concern because of toxicity to non-target organisms such as bees. Even though NNIs are well studied in rodents and mice, fundamental human toxicokinetic data is lacking.

Objective: The aim of this study was therefore to investigate human metabolism and urinary excretion of seven selected NNIs – the neonicotinoids acetamiprid (ACE), clothianidin (CLO), imidacloprid (IMI), thiacloprid (THIAC), and thiamethoxam (THIAM), as well as two neonicotinoid-like compounds flupyradifurone (FLUP) and sulfoxaflor (SULF).

Materials and methods: Each NNI was administered separately to male volunteers in controlled oral doses. The respective dose of the NNI was at its current acceptable daily intake (ADI). Complete and consecutive urine samples were collected over 48-hrs post dose. All samples were analyzed by mass spectrometry following chromatographic separation.

Results: In addition to the parent compounds, a total of 24 metabolites were identified, resulting predominately from mono-oxidation and oxidative N-dealkylation. Thus, metabolites known from previous biomonitoring studies such as IMI-olefin, hydroxy-IMI, or N-desmethyl-ACE could be confirmed, but also a variety of new metabolites such as hydroxy-FLUP or N-desdiufluoroethyl-FLUP were newly identified. Urinary excretion fractions (F_{ues}) of these specific metabolites were between 0.3% and 84% with elimination half times between 2.7 and 41 h. To our surprise, 6-chloronicotinic acid (6-CNA) and 2-chlorothiazole-5-carboxylic acid (2-CTA), previously established as biomarkers of NNI exposure, were of low metabolic relevance in humans with F_{ues} <1%. In the case of SULF, no phase I metabolites could be detected.

Conclusion: This study provides a first specific insight into metabolic conversion of NNIs in humans and generates quantitative data on urinary excretion of potential exposure

biomarker. These can be used in future exposure and risk assessment of these compounds based on human biomonitoring data.

35

Biomonitoring of heat-induced food contaminants: Biomarker based approach to exposure assessment of furan in foodC. Kalisch¹, M. Krieger¹, M. Reiter¹, L. Wüst¹, B. Sängner¹, O. Scherf-Clavel², R. Dekant¹, A. Mally¹¹University of Würzburg, Pharmacology and Toxicology, Würzburg, Germany²University of Würzburg, Pharmacy and Food Chemistry, Würzburg, Germany

As a process contaminant, furan occurs in a variety of heat-treated food items, particularly in ground roasted coffee, canned foods and processed baby foods. Due to the high volatility of furan and evaporation losses during home cooking, human exposure assessment based on occurrence and consumption data may not provide reliable estimates. Considering the low margin between estimated human exposure and doses that cause high incidences of neoplastic and non-neoplastic effects in rodents, which indicate a health concern, more accurate exposure assessment of furan is needed. Furan biotransformation via CYP2E1 to the highly reactive dialdehyde *cis*-2-butene-1,4-dial (BDA) and subsequent reaction with glutathione (GSH) or amino acids gives rise to several metabolites which may serve as potential urinary biomarkers of furan exposure. Previous analyses in rats demonstrated a close correlation between urinary biomarker excretion and furan dose, but also revealed substantial background levels of some metabolites, indicating either background exposure or endogenous formation. To better discriminate between external dose and endogenous formation/background exposure, rats were administered isotopically labelled [¹³C₄]-furan, and urinary excretion of metabolites, including mono GSH-BDA, NAcLys-BDA, NAcCys-BDA-NAcLys and NAcCys-BDA-NAcLys sulfoxide was monitored over time using stable isotope dilution ESI-LC-MS/MS. Following a single oral dose of [¹³C₄]-furan (1 mg/kg bw), mono GSH-[¹³C₄]-BDA was rapidly excreted within the first 24h, accounting for 2.2 % of the administered dose. NAcLys-[¹³C₄]-BDA, NAcCys-[¹³C₄]-BDA-NAcLys and NAcCys-[¹³C₄]-BDA-NAcLys sulfoxide were excreted in a delayed and gradual manner, with 24h excretion rates of 0.59, 1.33 and 0.64 % of the administered dose, respectively. In contrast to mono GSH-BDA, which showed no background occurrence, unlabelled NAcLys-BDA, NAcCys-BDA-NAcLys and NAcCys-BDA-NAcLys sulfoxide were also detected in rat urine. Based on the 24h excretion rates, the background levels of NAcCys-BDA-NAcLys and NAcCys-BDA-NAcLys sulfoxide were estimated to correspond to a furan dose of about 60 µg/kg bw per day. However, HS-GC-MS analysis of furan in feed excluded animal feed as a significant source for background exposure, supporting the hypothesis that furan or its reactive metabolite BDA may be formed endogenously. Overall, data obtained so far suggest that mono GSH-BDA may present a specific biomarker of furan exposure via food.

36

Inactivation of HDAC2 attenuates remodeling of Ca²⁺ dynamics and reduces atrial thrombus formation in female CREM-IbΔC-X transgenic mice correlating with the delay in onset of atrial fibrillationL. B. Tardio¹, J. P. Reinhardt¹, M. D. Seidl¹, U. Kirchhefer¹, F. U. Müller¹, J. S. Schulte¹¹Institute of Pharmacology and Toxicology, UKM, University of Münster, Münster, Germany

Objectives: We previously reported that inactivation of histone deacetylase (HDAC) isoform 2 (KO) reduced atrial dilatation and the occurrence of macroscopic spontaneous Ca²⁺ events in atrial cardiomyocytes (ACMs) in CREM-IbΔC-X transgenic mice (TG), a well-characterized model with extensive atrial remodeling and spontaneous onset of atrial fibrillation (AF). However, onset of AF was only delayed in female TGxKO mice. Therefore, we investigated the sex-specific consequences of HDAC2 inactivation for atrial remodeling and intracellular Ca²⁺ dynamics in TG mice.

Material and methods: Mice with cardiomyocyte-specific inactivation of HDAC2 (KO) were generated by crossbreeding HDAC2^{loxP/loxP} and αMHC^{Cre/+} mice and were then mated with TG (CREM-IbΔC-X^{Cre/+}) mice. CTR (FVB/N^{Cre/+}), KO, TG and TGxKO mice were analyzed. Ca²⁺ sparks with Fluo-4/AM were recorded in ACMs. RNA isolated from atrial tissue was analyzed by qPCR. Thrombus frequency was determined in mouse hearts and the amount of atrial fibrosis by Masson-Goldner trichrome staining.

Results: The proportion of thrombus-positive atria increased in TG with age (2% at 6-8 weeks to 64%[#] at 30 weeks, n=25-42). Simultaneous HDAC2 inactivation reduced thrombus formation exclusively in female mice (TG mice: 50%, TGxKO: 9%[#]; 30 weeks, n=11-14). In contrast, increased atrial fibrosis in TG was reduced in TGxKO in both sexes to a similar extent. An increase in Ca²⁺ spark frequency was detected in ACMs from TG mice (µm²/s±SD: CTR: 9.7±10, TG: 15.8±13^{*}; n=6, 58-68 cells), likewise in ACMs from male TGxKO mice (µm²/s±SD: CTR: 10.4±12, TGxKO: 15±14^{*}; n=3-4, 24-36 cells) but not in ACMs from female TGxKO mice vs CTR. mRNA levels of genes involved in Ca²⁺ cycling (*Slc8a1*, *Atp2a2*, *Ryr2*, *Casq2*) were down-regulated in TG by 42-71% compared to CTR (n=10 per genotype). While in male TGxKO mRNA expression was unchanged vs TG, *Slc8a1*, *Ryr2* and *Casq2* down-regulation was limited in female TGxKO vs TG (n=5 *p<0.05 vs CTR, #p<0.05 vs TG).

Conclusion: Cardiomyocyte-specific inactivation of HDAC2 reduced atrial thrombus formation and normalized both Ca²⁺ spark frequency in ACMs and mRNA levels of genes involved in Ca²⁺ cycling in female CREM-IbΔC-X transgenic mice, correlating with the delay in onset of AF. This underscores the importance of these substrates in the development of AF and suggests that inhibition of HDAC2 may represent a therapeutic option against atrial remodeling that may have a greater impact on females.

37

Evaluation of an ERK1/2 autophosphorylation as a pro-inflammatory triggerJ. N. Herbel¹, N. Amézaga Solé², M. Bernhardt³, A. Zemecke-Madsen², K. Lorenz^{1,4}¹Universität Würzburg, Pharmakologie und Toxikologie, Würzburg, Germany²Uniklinikum Würzburg, Experimentelle Biomedizin, Würzburg, Germany³Universität Würzburg, Rudolf-Virchow-Zentrum, Würzburg, Germany⁴Leibniz-Institut für Analytische Wissenschaften, ISAS e.V., Dortmund, Germany

Introduction: The extracellular signal-regulated kinases 1 and 2 (ERK1/2) act at crossroads of protective and maladaptive signaling. They are part of a central signaling cascade in which various extracellular signals converge, thereby playing a crucial role in cardiac hypertrophy and inflammation. An autophosphorylation at threonine 188 in ERK2 (pERK(T188)) has been shown to trigger nuclear ERK signaling and has thus far only been associated with pathological conditions, i.e. cardiac hypertrophy. Interference with ERK dimerization, a prerequisite for pERK(T188), with a peptide termed ERK-dimerization inhibitory peptide "EDI" impedes nuclear ERK signaling and protects from pressure-overload induced heart failure.

Objectives: Since cardiac hypertrophy can comprise inflammatory processes and since ERK1/2 are involved in inflammatory signaling, the ERK(T188) phosphorylation could be of great relevance in inflammation and immune cells. Therefore, this study evaluates the potential role of pERK(T188) in immune cell responses.

Materials and methods: To assess the occurrence and potential function of pERK(T188) in inflammatory cells, we used murine bone marrow-derived macrophages (BMDM), (anti)inflammatory stimuli (LPS, TNF α or IL4) and isolated T cells from spleens of wild-type mice activated by anti-CD3 and anti-CD28 antibodies. Mouse lines with ubiquitous expression of phosphorylation deficient (ERK2(T188A)) or pERK(T188)-simulating (ERK2(T188D)) ERK2 mutants and EDI were used to analyze a potential causative relation of pERK(T188) with inflammation. Inflammatory responses were measured by RT-qPCR, flow cytometry and proteomics.

Results: Exposure of BMDM to inflammatory mediators, but not anti-inflammatory entailed an increase in pERK(T188). The ERK dimerization inhibitor EDI indeed reduced the induction of pERK(T188) by TNF α and LPS. Also, isolated CD8+ T cells activated using anti-CD3 and anti-CD28 antibodies showed an increase of pERK(T188) suggesting an involvement of pERK(T188) in inflammatory signaling. This hypothesis was further supported by proteomics data of BMDM from ERK2(T188D) transgenic mice.

Conclusion: Taken together, pERK(T188) appears to be involved in immune cell signaling and responses. Future analyses will help to clarify the (patho-)physiological impact of pERK(T188) in the development of heart diseases and inflammatory diseases.

38

The RNA-binding Protein KSRP affects the outcome of allergic asthmaK. A. Palzer¹, V. Bolduan², J. Lakus³, M. Bros², A. Pautz¹¹University Medical Center Mainz, Department of Pharmacology, Mainz, Germany²University Medical Center Mainz, Hautklinik & Poliklinik, Mainz, Germany³University Medical Center Mainz, Molecular Medicine, Mainz, Germany

Introduction: Asthma is a chronic inflammatory disease, which is characterized by allergic airway inflammation, IgE- and Th2 cytokine production as well as increased eosinophil and T cell infiltration in the respiratory tract. This results in airway hyperresponsiveness (AHR) and constriction of the airways. The RNA-binding protein KH-type splicing regulatory protein (KSRP) controls the mRNA stability of immune relevant genes by initiation of mRNA decay and inhibition of translation, and by enhancing the maturation of microRNAs.

Objectives: Chronic inflammatory diseases, such as asthma, are characterized by dysregulated immune responses and increased expression of pro-inflammatory genes. Therefore, the characterization of pathways that resolve inflammation is necessary to identify new drug targets. As KSRP plays a pivotal role in innate and adaptive immune cell function, we were interested whether knockdown of the protein KSRP/- affects the outcome of allergic asthma.

Materials and methods: To investigate the role of KSRP in allergic asthma we studied the immunomodulatory effect of KSRP in an *in vivo* ovalbumin (OVA) asthma mouse model. OVA-induced allergic asthma is a well-established model of acute respiratory AHR that is characterized by a Th2-biased immune response. We compared asthma induction in wild type (WT) and KSRP/- mice. Lungs were taken for histological sections and cytokine levels in lung cells and bronchial lavage supernatant (BAL) were determined by qPCR analysis and cytometric bead array analyses (CBA).

Results: We found that KSRP/- mice sensitized with OVA appear to have a higher AHR and increased eosinophil infiltration compared to the OVA WT controls. In accordance, cytokine amounts of several pro-inflammatory factors, like IL-4, IL-5, IL-10, IL-13, IL-17 and eotaxin, was enhanced in lung cells and BAL supernatants of OVA treated KSRP/- compared to OVA WT samples. These results fits to the increased number of immune cells around the bronchi and alveoli as well as the higher number of mucus producing goblet cells and the increased production of OVA-specific IgE and IgG1 in serum of OVA treated KSRP/- mice compared to OVA WT controls.

Conclusion: To sum up, we have strong evidence that allergic asthma is aggravated in KSRP/- mice. These findings indicate that KSRP may play a regulatory role in OVA-induced asthma and may be therapeutically useful for the management of asthma.

39

Transmembrane Transporters in Myocytes: Relevance for Statin-induced MyopathyA. Hafkemeyer¹, V. Rönnpagel¹, F. Morof¹, J. Lange², L. Haralambiev², H. Brinkmeier², M. V. Tzvetkov¹, G. Jedlitschky¹¹University Medicine Greifswald, Department of General Pharmacology, Greifswald, Germany²University Medicine Greifswald, Center for Orthopaedics, Trauma Surgery and Rehabilitation Medicine, Greifswald, Germany³University Medicine Greifswald, Department of Pathophysiology, Greifswald, Germany

Introduction: Statins prevent cardiovascular events by lowering cholesterol levels. Many patients treated with statins experience myalgia or myopathies. Variations in transporter-mediated uptake of statins into hepatocytes are known to affect the frequency of these side effects by influencing the plasma levels of the drugs. However, little is known about the uptake and efflux of statins in skeletal muscle cells.

Objectives: This study aims to characterize the accumulation of various statins in myocytes and identify the transporters that might be involved.

Materials and methods: Transporter expression in the human rhabdomyosarcoma cell line TE671 and in human skeletal muscle tissue was detected by Western blotting and qPCR. Immunofluorescence microscopy was performed to confirm transporter localization. Further, we characterized the cellular uptake of atorvastatin, simvastatin acid, fluvastatin, pravastatin, and rosuvastatin into the TE671 cells in a time- and concentration-dependent manner. Statin transport was also studied in the presence of potentially interfering compounds such as 4,5-dibromofluorescein, prostaglandin E₂ and lactate, that are known substrates of OATP2B1, OATP2A1 and MCT4, respectively. The cellular drug accumulation was determined by HPLC-MS/MS. Cell viability in the presence of statins was measured in resazurin assays.

Results: We could detect OATP2B1, OATP2A1, MCT4, MRP1 and MRP3-5 on transcript and protein level in TE671 cells and in muscle tissue. Immunofluorescence microscopy revealed localization in the cell membrane and in t-tubules. Saturable uptake of statins was detected with K_m values ranging from 142 μ M (simvastatin acid) to 202 μ M (atorvastatin). Remarkably, pravastatin was only transported to a minor extent into the cells. Furthermore, studies with the transporter inhibitors suggested that OATP2B1, OATP2A1 and MCT4 may be involved in the statin uptake to varying degrees. The statin accumulation was partially counteracted by an MRP-mediated efflux. In addition, lipophilic statins reduced the cell viability in a concentration-dependent manner, while only weak effects were observed for hydrophilic statins.

Conclusion: Our findings imply that several transporters are involved to a variable extent in the transmembrane transport of statins in myocytes, including OATP2B1, as well as probably OATP2A1 and MCT4. Furthermore, the efficiency of drug accumulation correlates with the ability of the statins to reduce myocyte viability.

Short talks: G-protein coupled receptors

40

Two lysines in the N-terminus of arrestin control binding and release of the arrestin C-terminus upon binding to GPCRsC. Krasel¹, N. Mösslein¹, D. Zindel¹, M. Bünemann¹¹Philipps-Universität Marburg, FB Pharmazie, Institut für Pharmakologie und Klinische Pharmazie, Marburg, Germany

Introduction: One of the many different ways of classifying G protein-coupled receptors (GPCRs) is their behaviour towards arrestins. Upon agonist stimulation, class A GPCRs interact with arrestins only transiently and internalize in endosomes while the arrestins remain at the plasma membrane. In contrast, class B GPCRs show a more stable interaction with arrestins and co-internalize with arrestins into endosomes. We have previously shown that increasing the affinity of a GPCR to arrestin by the introduction of additional phosphorylation sites in the receptor can convert a class A to a class B receptor. Likewise, reducing the affinity of a GPCR to arrestin by removal of some phosphorylation sites in the receptor converted a class B to a class A receptor.

Objective: It has been described that mutation of Lys11 and Lys12 in the N-terminus of arrestin3 to arginine alters the behaviour of arrestin3 towards some but not all GPCRs. We therefore wanted to investigate whether this mutation alters arrestin3 affinity to GPCRs.

Materials and methods: Arrestin trafficking upon GPCR stimulation was assessed by confocal microscopy. The affinity of arrestin to GPCRs was measured by dual-color fluorescence recovery after photobleaching (FRAP) after immobilization of the GPCR with antibodies. Arrestin3 ubiquitination was investigated by immunoprecipitation of Flag-tagged arrestin followed by Western blotting with a ubiquitin antibody.

Results: The arrestin3 K11,12R mutant did not co-internalize with several class B receptors, including the PTH and neurotensin receptor. Co-internalization with the angiotensin AT1 receptor was compromised but not completely abolished, similar to what was previously described. Affinity of arrestin3 K11,12R to several class B receptors was reduced compared to wild-type arrestin3. Ubiquitination of the arrestin3 K11,12R mutation was also reduced in comparison to wild-type. Arrestin affinity, trafficking and ubiquitination could be rescued by mutating two acidic residues in the C-terminus to alanine.

Conclusion: Mutation of lysine to arginine is generally thought to be very conservative. However, mutation of Lys11 and 12 to Arg completely alters the behaviour of arrestin3,

probably by reducing the ability of the arrestin3 C-terminus to be released from the arrestin core upon contact with activated GPCRs.

41

Oligomerization of β AR and AT1R increases AT1R signalling leading to enhanced aldosterone synthesis and cardiomyocyte hypertrophy

J. Fender¹, V. Boivin-Jahns¹, K. Lorenz^{1,2}

¹Universität Würzburg, Institut für Pharmakologie und Toxikologie, Würzburg, Germany
²Leibniz-Institut für Analytische Wissenschaften—ISAS e.V., Dortmund, Germany

Background: G-protein-coupled receptors (GPCR) are key modulators for cardiac performance and homeostasis. Angiotensin II type 1 receptors (AT1R) and β -adrenergic receptors (β AR) are activated in several diseases under neurohumoral stress conditions and they are common drug targets in e.g. hypertension, acute and chronic heart failure or asthma therapy.

Objective: Since a functional interconnection between these two receptor types has been proposed, we aimed to investigate the potential crosstalk between AT1R with β AR (β 1AR and β 2AR) and its potential (patho) physiological consequences.

Methods and results: A bioluminescence resonance energy transfer (BRET)-based donor saturation assay suggests an oligomerization between AT1R and β 2AR as well as between AT1R and β 1AR under baseline conditions. Stimulation of AT1R reduced BRET signal suggesting a reorganization of the receptors. A BRET-based arrestin recruitment assay revealed significantly potentiated recruitment of β arr1 and 2 to the AT1R after co-activation of AT1R and β AR compared to AT1R stimulation alone. Of interest, co-activation of β 1AR was not sufficient to induce this effect.

To investigate the physiological consequences of this crosstalk we used human adrenocortical cells and evaluated the mRNA levels of genes involved in the angiotensin II-dependent aldosterone synthesis. Indeed, mRNA-expression levels of steroidogenic acute regulatory (STAR) protein and aldosterone synthase (CYP11B2) were potentiated by co-stimulation of β AR and AT1R. This stimulatory conditions also induced an overadditive hypertrophic response in cardiomyocytes.

Conclusion: Our results strongly suggest a crosstalk between AT1R and β AR as a result of oligomerization. Mechanistically the co-activation of AT1R and β AR led to an increased AT1R arrestin recruitment and AT1R signalling. In line with this cardiomyocyte hypertrophy and aldosterone synthesis were potentiated. This could be particularly interesting in chronic heart failure patients where catecholamines and Angiotensin II are highly upregulated and this mechanism could contribute significantly to the disease progression.

42

Insights into the molecular mechanism of glucagon receptor signaling and its modulation by RAMP2

D. Hilger¹, K. Krishna Kumar², E. O'Brien², H. Hu², C. Habrian², N. Latorraca³, H. Wang², I. Tuneew⁴, L. Giehm⁴, C. Jennings⁵, M. Fabricius Pedersen⁶, G. Eskici², E. Montabana², E. Isakoff⁶, M. Lerch⁵, A. Inoue⁶, S. Maqusee³, G. Skiniotis², J. Mosolf Mathiesen⁴, B. Kobilka²

¹Philipps-Universität Marburg, Pharmazeutische Chemie, Marburg, Germany
²Stanford University, Stanford, United States
³UC Berkeley, Berkeley, United States
⁴Zealand Pharma, Søborg, Denmark
⁵Medical College of Wisconsin, Milwaukee, United States
⁶Tohoku University, Sendai, Japan

The endocrine hormone glucagon plays a key role in blood sugar homeostasis. Binding of glucagon activates the class B G protein-coupled glucagon receptor (GCGR) in the liver to predominantly signal via the G protein Gs, leading to the glucose release from hepatocytes. GCGR pharmacology is further modulated through interaction of the receptor with the Receptor Activity Modifying Protein 2 (RAMP2). Co-localization of GCGR with this accessory protein has been shown to result in changes of glucagon potency, receptor targeting, and transducer coupling. However, the mechanistic basis of GCGR activation and G protein signaling and their modulation by RAMP2 remains incompletely understood. Using a series of biochemical, biophysical, and cell-based assays, we show that glucagon binding to GCGR does not induce outward movement of TM6, resulting in a decreased G protein activation rate compared to the prototypical class A b2-adrenergic receptor. Using cryo-electron microscopy (cryoEM), we determined the structure of the GCGR-Gs complex. The structure shows that G protein binding induces the formation of a distinct kink in TM6 of GCGR that requires overcoming a higher energy barrier for receptor activation compared to the gradual outward bending of TM6 in class A receptors. Cellular signaling data and Hydrogen-deuterium exchange mass spectrometry (HDX-MS) show that RAMP2 interacts with the receptor and decreases GCGR-induced downstream signaling by enhancing the conformational heterogeneity in and near the receptor extracellular domain (ECD) as well as at the kink region of TM6. Single-molecule fluorescence resonance energy transfer (smFRET) measurements show that the RAMP2-induced dynamics prevent the formation of active and intermediate states of the intracellular face of the receptor. In addition we determined the cryo-EM structure of the RAMP2-GCGR-Gs complex. Even though RAMP2 does not interact with GCGR in an ordered manner, transient interactions between the two proteins lead to a largely disordered ECD of GCGR. This disorder is accompanied by rearrangements of several key areas of the receptor, resulting in the formation of a likely unproductive G protein complex. Together, our studies provide mechanistic insights into GCGR activation and signaling and suggest that RAMP2 acts as a negative allosteric modulator of the receptor by enhancing conformational sampling of the ECD of GCGR.

43

Modulation of adrenergic-mediated signaling by cell swelling - a fluorescence spectroscopy investigation

A. Sirbu¹, M. J. Lohse², P. Annibale^{1,3}

¹Max Delbrück Center for Molecular Medicine, Receptor Signaling Lab, Berlin, Germany
²ISAR Bioscience, Planegg-Munich, Germany
³University of St Andrews, School of Physics and Astronomy, St Andrews, United Kingdom

Introduction: Osmotic swelling is a physiological process, which takes place in several pathological conditions like the ischemia/reperfusion scenario or cellular acidosis. It is known to cause substantial alteration to intracellular architecture, ranging from membrane curvature to actin polymerization, altering the environment of the transmembrane proteins.

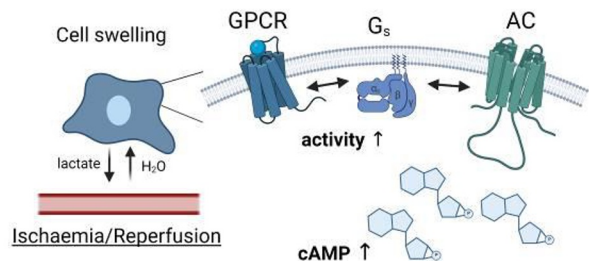
Objectives: Our aim is to study if and how the signaling of G protein-coupled receptors, a key family of transmembrane signaling proteins, is altered in the context of cell swelling and to determine how their signaling efficiency can be affected at the molecular level by alterations to the subplasmalemmal biophysical environment.

Materials and methods: Here, we employ a comprehensive set of fluorescence-based methods, ranging from FRET-based biosensors to nanobody recruitment assays, to dissect the individual steps of the signaling cascade, from upstream stimulation of β -adrenergic receptors (β -AR) down to cAMP production.

Results: Notably, we observe that swollen cells yield increased cAMP production in response to stimulation of Gs-coupled receptors. Upon direct adenylyl cyclase stimulation with forskolin, cell swelling increases cAMP production, but fails to elicit comparable effects when using a Gs-knockout cell line. Further studying the β 2-AR, we don't observe any changes to ligand binding affinity by osmotic swelling. At the same time, nanobody recruitment experiments show an increased extent of receptor activation along with elevated levels of active Gs. Based on these results, we hypothesize that signal transduction by the Gs-coupled receptors and the Gs-protein is enhanced by the intracellular reorganization arising upon cell swelling.

Conclusion: Our findings uncover a novel effect of cell swelling on cellular signaling, but also open interesting perspectives on whether what we observe here is a general mechanism common to other GPCRs, with biophysical changes of the local environment of a receptor acting as an allosteric modulator of its function.

Fig. 1



44

LPA receptor 1 (LPAR1) interacts with Myocardin-related transcription factor A (MRTF-A) to promote SRF target gene expression and HCC proliferation

A. Konopa¹, M. Sergeev¹, M. A. Meier¹, S. Muehlich¹

¹Friedrich-Alexander University Erlangen-Nürnberg, Department of Chemistry and Pharmacy, Erlangen, Germany

Myocardin-related transcription factors A and B (MRTFs) are coactivators of Serum Response Factor (SRF), which controls fundamental biological processes such as cell growth, migration and differentiation. MRTF and SRF transcriptional activity plays an important role in hepatocellular carcinoma (HCC) growth. In search for druggable therapeutic targets in HCC inhibiting MRTF/SRF target gene expression, we identified the G protein-coupled lysophosphatidic acid receptor 1 (LPAR1) as a novel interaction partner of MRTF-A using fluorescence resonance energy transfer- (FRET) and proximity ligation assays (PLA) in HCC cells and in organoids. Pharmacological blockade of LPAR1 prevents complex formation with MRTF-A, resulting in reduced MRTF/SRF target gene expression and HCC cell proliferation by oncogene-induced senescence. Thus, dissociation of the novel LPAR1-MRTF-A interaction represents a promising strategy for HCC therapy.

45

Unexpected activity of the histamine H1-receptor inverse agonist mepyramine in human colon carcinoma-derived HT29 cellsM. Kirsten¹, B. Schirmer¹, R. Seifert¹, D. Neumann¹¹Hannover Medical School, Institute of Pharmacology, Hannover, Germany

The biogenic amine histamine mediates its pleiotropic effects via four G protein-coupled receptors, referred to as histamine H₁-receptor (H₁R), H₂R, H₃R, and H₄R. In addition to its role in immune modulation, histamine is involved in several other physiological processes. Pathophysiological effects have also been demonstrated, e.g. in chronic inflammatory bowel diseases (IBDs) and colon carcinoma. The involvement of histamine in carcinogenesis and tumor progression is currently being discussed. The human colon cancer-derived cell line HT29 serves as a versatile model system for the analysis of colon epithelial functions. In these cells, histamine induces a significant increase in calcium mobilization. The application of antagonists/inverse agonists at H₂R, H₃R, and H₄R did not interfere with this histamine-induced effect. Unexpectedly, mepyramine, an inverse H₁R agonist that is approved for its use in anti-allergic therapies, massively enhanced the histamine-induced calcium mobilization. This effect of mepyramine was neither recapitulated by cetirizine, a chemically different H₁R inverse agonist, nor by the CRISPR/Cas9-mediated knockout of H₁R in HT29 cells. Interestingly, in H₁R-KO HT29 cells, mepyramine in combination with histamine still led to a massive calcium mobilization.

We conclude that the combination of mepyramine and histamine may bind to a so far not identified structure present in HT29 cells.

Short talks: Pharmacoepidemiology and drug safety

46

Analysis of sex-specific differences in spontaneously submitted and systematically collected reports of serious adverse drug reactionsD. Dubrall^{1,2}, P. Christ³, K. Just⁴, M. Below⁵, M. Schmid¹, J. Stingl⁴, B. Sachs^{2,6}¹University Hospital of Bonn, Bonn, Germany²Bundesinstitut für Arzneimittel und Medizinprodukte, Forschung, Bonn, Germany³Federal Institute for Drugs and Medical Devices, Bonn, Germany⁴University Hospital RWTH Aachen, Aachen, Germany⁵Central Research Institute of Ambulatory Health Care in Germany, Berlin, Germany⁶University Hospital (RWTH) Aachen, Clinic for Dermatology and Allergology, Aachen, Germany

Introduction: Sex is known to be a risk factor for certain adverse drug reactions (ADRs). Among others, sex-specific differences in pharmacokinetics or genetics may influence the occurrence of ADRs. So far, results of published studies are inconsistent possibly due to varying study designs.

Objectives: The first aim of our study was to identify all drugs, ADRs and drug-ADR combinations more frequently reported for either females or males in i) ADR reports submitted spontaneously to EudraVigilance and, ii) ADR cases collected systematically from the ADRED study. The second aim was to compare the results from both data sources.

Materials and methods: ADRED was a multi-center prospective observational study analysing ADR cases of adults presenting to 4 German emergency departments between 09/2015 and 12/2018. The identified cases have been submitted to EudraVigilance and were identified by their case report numbers. Complementary to the study design of ADRED, we identified all spontaneously submitted ADR reports in EudraVigilance. In both data sets, the drugs, ADRs, and drug-ADR combinations more frequently reported for females or males were identified by calculation of odds ratios with 95% confidence intervals. The identified drug-ADR combinations in the spontaneously submitted ADR reports were set in context to the number of drug prescriptions.

Results: In both data sets, we identified drugs, ADRs, and drug-ADR combinations more frequently reported for either females or males. Similar findings could be observed in both data sets, however, the drugs, ADRs or drug-ADR combinations reported were mostly not identical. As an example for the ADRs, gastrointestinal ADRs were more frequently reported for females and respiratory and cardiovascular ADRs for males, in both data sets. After considering the number of drug prescriptions, the number of identified drug-ADR combinations being more frequently reported for either females or males decreased. As an example, the drug-ADR combination hydrochlorothiazide - sodium imbalance and antithrombotics - cerebral injuries remained more frequently reported for females and males, respectively.

Conclusion: Investigating sex-differences in ADR reports collected via two complementary methodological approaches may help to strengthen findings. Our analysis highlights the importance to consider the number of drug prescriptions for sex-specific ADRs. The findings suggesting sex-specific differences in our study should further be investigated.

47

Comparison of provided information and quality of documentation in spontaneous reports of adverse drug reactions from consumers, physicians and pharmacistsP. Christ¹, D. Dubrall¹, M. Schmid², B. Sachs¹¹Federal Institute for Drugs and Medical Devices, Research, Bonn, Germany²University Hospital of Bonn, IMBIE, Bonn, Germany

Introduction: The analyses of spontaneous reports of suspected adverse drug reactions (ADRs) play a major role in the post-approval surveillance of drugs. In the European Union, alongside healthcare professionals (e.g. physicians, pharmacists) patients are also encouraged to report suspected ADRs. In fact, over the past few years the number of ADR reports originating from patients as a so called primary reporter has increased. Differences in quality of documentation dependent on the primary reporter have been shown for different countries. To the best of our knowledge, no such analysis has been performed for reports from Germany.

Objectives: The aim of this study was to compare all spontaneous ADR reports originating from Germany exclusively reported by either physicians, pharmacists, or patients regarding the information provided and the quality of documentation.

Materials and methods: All spontaneously submitted ADR reports originating from Germany received between 2018 and 2021 were extracted from the EudraVigilance database (EV) where a physician, pharmacist, or patient has been coded as the primary source qualification. A descriptive analysis of demographical parameters was performed in each group. In addition, we assessed for each report if information was provided or not for several categories (e.g. indication of the drug, medical history). As a higher-level estimate, an automated calculation of the vigiGrade score was performed for all reports.

Results: In total 233,516 reports were extracted from EV. About half of them were reported by patients (52%). In all three groups, more reports referred to females, with a higher proportion in the reports from patients and pharmacists (~65% each) compared to physicians (~55%). Differences in the quality of documentation according to vigiGrade were found. Reports by physicians, on average, scored the highest vigiGrade score.

Conclusion: Our analysis found differences regarding the documentation quality and presence of information in spontaneously submitted ADR reports from patients, physicians and pharmacists. As a limitation, these differences could be influenced by obligations and contributions of the stakeholders involved in the reporting and processing of the report. However, our results may be of help for studies aiming to analyse the underlying reasons for these differences and, subsequently to foster improvement initiatives.

48

Documentation of drug-related problems with ICD-11 – development and application of a decision algorithm for clinicians and clinical codersL. Jung-Poppe¹, W. Andrikyan¹, H. F. Nicolaus¹, A. Altenbuchner¹, B. Pfistermeister², H. Dormann³, M. F. Fromm¹, R. Maas¹¹Friedrich-Alexander-Universität Erlangen-Nürnberg, Institute of Experimental and Clinical Pharmacology and Toxicology, Erlangen, Germany²Fürth Hospital, Hospital Pharmacy, Fürth, Germany³Fürth Hospital, Central Emergency Department, Fürth, Germany

Introduction: Drug-related problems (DRPs), i.e., adverse drug reactions (ADRs) and medication errors (MEs), can affect patients' treatment outcomes negatively. Their accurate documentation enables strategies for improvement in the prescribing and treatment processes through quality assurance and research. The 11th revision of the "International Statistical Classification of Diseases and Related Health Problems" (ICD) provides a new code-set for documentation of DRPs. However, the coding process of DRPs in ICD-11 is complex and requires sufficient training.

Objectives: The aim of this work was to develop and apply a usable decision algorithm for the coding of DRPs with ICD-11 for clinicians and clinical coders.

Materials and methods: We used the "Quality and Safety Algorithm" from the ICD-11 Reference Guide and refined it for DRP reporting. Matching codes for four prespecified categories (harm, cause, drugs, and mode) according to the WHO's proposed framework for describing healthcare-related events ("3-part Quality and Safety model") were identified. The final algorithm was then applied to 100 different DRPs (50 ADRs and 50 MEs) from clinical routine data of a German hospital.

Results: We identified ICD-11 chapters containing codes for the four prespecified categories and portrayed these results as a decision algorithm. Applying this algorithm, we coded all 50 ADRs from clinical routine data with 38 (100%) ICD-11 codes describing harm. Of these, 27 (71.1%) codes cannot be fully coded according to the 3-part model due to sanctioning rules that prevent the combination of specific codes. Additionally, we identified 17 (44.7%) codes that do not have sufficient granularity for describing the clinical event. The 3-part model is not specifically designed for reporting MEs. However, we were able to code all 50 MEs with 13 (100%) different codes. None of these codes allow the combination with the causing drug and 4 (30.8%) of the codes were not specific enough for describing the MEs.

Conclusion: Due to the sophisticated ICD-11 system, sufficient training and teaching for adequate documentation of DRPs are necessary. With our decision algorithm we provide a vivid guide on how to code DRPs. Nevertheless, a majority of the identified ICD-11 codes do not allow the combination with other codes to further specify the DRP. This system could be substantially improved by modifications of sanctioning rules and by addition of new codes for the detailed documentation of DRPs.

49**Drug consumption in German cities and municipalities during the COVID-19 lockdown: a wastewater analysis**

R. Oertel¹, S. Schubert¹, B. Helm², R. Mayer², R. Dumke³, A. El-Armouche⁴, B. Renner¹
¹TU Dresden, Institute of Clinical Pharmacology, Dresden, Germany
²TU Dresden, Institute of Urban and Industrial Water Management, Dresden, Germany
³TU Dresden, Institute of Medical Microbiology and Virology, Dresden, Germany
⁴TU Dresden, Institute of Pharmacology and Toxicology, Dresden, Germany

Introduction: Analysis of illicit drugs, medicines and pathogens in wastewater is a powerful tool for epidemiological studies to monitor public health trends.

Objectives: The aims of this study were to (i) assess spatial and temporal trends of population-normalized mass loads of illicit drugs and nicotine in raw wastewater in the time of regulations against SARS-CoV-2 infections (2020–21); (ii) find suitable markers to characterize the occurrence of selected drugs in wastewater.

Materials and methods: Analysis of raw sewage 24-hour composite samples of 15 German wastewater treatment plants in urban, small-town and rural areas collected during different lockdown phases from April 2020 to December 2021.

Results: Parent substances (amphetamine, methamphetamine, 3,4-Methylenedioxy-N-methylamphetamin (MDMA), carbamazepine, gabapentin and metoprolol) and the metabolites of cocaine (benzoylecgonine) and nicotine (cotinine) were measured in wastewater using liquid chromatography–tandem mass spectrometry. The daily discharge of WWTP influents were used to calculate the daily load (mg/day) normalized by population equivalents (PE) in drained catchment areas (in mg/1,000 persons/day) and, further, converted to the number of combined doses ingested per day. Otherwise, normalization was carried out using marker substances. The beta blocker metoprolol and the nicotine metabolite cotinine were found to be suitable as marker substances for the characterization of wastewater. An influence of the regulations to reduce SARS-CoV-2 infections such as contact bans and border closures on drug consumption has been proven in some cases and refuted in several.

Conclusions: A change in drug use was visible at the beginning of the Corona crisis. Starting from mid-2020, no obvious effect was detected with regard to the regulations against SARS-CoV-2 infections on concentration of drugs in wastewater. Wastewater-based monitoring might be a useful tool to identify variability in illicit drug consumption, medication and pathogens occurrence and spreading in different wastewater systems.

50**Prescribing practices of antipsychotics for the treatment of schizophrenia in older age**

O. Zolk¹, T. Greiner¹, M. Schneider², M. Heinze², V. Dahling², T. Ramin¹, R. Grohmann³, S. Bleich⁴, S. Toto⁴, J. Seifert⁴
¹Brandenburg Medical School, Institute of Clinical Pharmacology, Rüdersdorf, Germany
²Brandenburg Medical School, University Clinic for Psychiatry and Psychotherapy, Rüdersdorf, Germany
³LMU University Hospital Munich, Department of Psychiatry and Psychotherapy, Munich, Germany
⁴Hannover Medical School, Department of Psychiatry, Social Psychiatry and Psychotherapy, Hannover, Germany

Objectives: To investigate the relationship between patient age and the selection and dosage of antipsychotic drugs (APDs) for treatment of schizophrenia. We describe age effects for multiple individual APDs, thus allowing comparisons between drugs.

Methods: Prescription data of 32,062 inpatients with schizophrenia from 2000 to 2017 were obtained from the Drug Safety Program in Psychiatry (AMSP) database. APD selection and dosage were related to patient age with sex as an influencing variable. Dose equivalents were used to combine dose data from oral and long-acting injectable formulations of a drug or to estimate the patient's total APD exposition. Moreover, a systematic search of current guideline recommendations on APD treatment in patients with schizophrenia aged ≥65 years was performed.

Results: Eighty percent of elderly patients (≥65 years) received a second-generation APD, most commonly risperidone. We observed changes in the spectrum of APDs used depending on the age of the patients. Clozapine, olanzapine and quetiapine prescription rates decreased in older adults, while use of risperidone increased. We found an inverted U-shaped relationship of dosage and age. The dosage of APDs increased with age until about age 40 years, then decreased slowly at first and more steeply beyond age 55 years. For example, the dose of haloperidol and clozapine prescribed to patients older than 75 years was only 41% (95% confidence interval 34–48) and 42% (95% CI 36–50), respectively, of the dose prescribed to patients younger than 65 years (p<0.001 each). The influence of age as well as sex on dosage partly differed between the individual drugs. For example, the dose of amisulpride was not significantly changed in older patients compared with younger patients. Only one of eight schizophrenia guidelines systematically addressed specific aspects of pharmacotherapy in older adults.

Conclusions: In clinical routine, age has a significant impact on selection and dosing of APDs. The natural history of schizophrenia, physiological aging and comorbidities may contribute to dose adjustments in older age. Information on optimizing pharmacotherapy in older adults with schizophrenia from clinical trials is needed. Guidelines should be improved regarding APD therapy specifically for older adults.

51**Pre-operative medication assessment and optimization to improve clinical outcomes of women with ovarian cancer: subproject of the prospective KORE-INNOVATION trial.**

F. Meiner¹, E. Algharably¹, R. Kreutz¹, T. I.², M. Lee², M. E. Liebi³, P. Harter⁴, S. Schneider⁴, E. Schnura⁴, J. Klews⁵, R. Lohrmann⁵, L. Zwanzleitner⁶, J. Sehouli²
¹Charité – Universitätsmedizin Berlin, Institut of Clinical Pharmacology and Toxicology, Berlin, Germany
²Charité – Universitätsmedizin Berlin, Department of Gynecology including center of oncological surgery (CVK), Berlin, Germany
³Charité – Universitätsmedizin Berlin, Department for Physical Medicine, Berlin, Germany
⁴KEM I Evang. Kliniken Essen-Mitte GmbH, Department for Gynecology and Gynecologic Oncology, Essen, Germany
⁵Charité – Universitätsmedizin Berlin, Department of Nursing Science, Berlin, Germany
⁶Techniker Krankenkasse, ..., Germany

Methods: Overall, 414 patient records will be reviewed at the following time points: pre-operative, at discharge from hospital, and at 30 days post-operative follow-up. Reviewed data include medical history, comorbidities, prescribed and over the counter medication as well as dietary supplements, and complementary medication. The data will be matched with clinical parameters and guideline recommendations for the identification of drug-related problems (DRPs) including potential over- and under-treatment, inappropriate dosing, adverse effects, and drug-drug interactions (DDIs). Based on this review, recommendations for each assessment point will be provided.

Results: Preliminary data for 55 patients were available for assessment of all time-points. We identified DRPs in 15(27.3%) patients preoperatively, in 13(23.6%) at discharge and 8(14.5%) at follow-up. DRPs included over- and under-treatment and over- and under-dosing. Polypharmacy was detected in 7(12.7%) patients preoperatively, in 28(50.9%) at discharge and in 13(23.6%) at follow-up. Relevant DDIs were detected in 6(10.9%) patients preoperatively, in 12(21.8%) at discharge and in 5(9.1%) at follow-up. Recommendations for medication change were made in 8(14.5%) patients preoperatively, in 7(12.7%) at discharge and in 5(9.1%) at follow-up. Inadequate medication in older patients were detected in 3(5.5%) both preoperatively and at discharge.

Conclusion: Preliminary data show a trend for reduced DRPs in the course of the trial, which correlates with the number of drug therapy recommendations made. Therefore, patients may benefit from a medication review in the perioperative setting. Pharmacological assessment and optimization should be routinely integrated in the ERAS perioperative pathways.

References: Parrish RH et al. J Clin Med. 2022 24;11(19):5628

Short talks: Toxicological Methods I**52****Establishment of an *in vitro* foreign body reaction model for medical device testing**

J. Sündermann¹, C. Ziemann¹, S. M. Reamon-Buettner¹, M. Engelke¹, H. Brockmeyer¹, R. Kellner¹, A. Bitsch¹, T. Doll¹

¹Fraunhofer ITEM, Hannover, Germany

Introduction: The foreign body reaction (FBR) is defined as the response of the host tissue towards implanted material. FBR can lead to serious impairment of medical devices and is one major cause for their failure. After implantation, proteins are adsorbed to the material's surface, followed by recruitment of immune cells such as macrophages participating in the acute inflammation. The macrophages then undergo "frustrated fusion" to form foreign body giant cells (FBGC). Finally, since the immune cells are not able to remove the material, a fibrotic encapsulation is established.

Objectives: FBR is currently not part of biocompatibility testing, according to ISO 10993 for accreditation of medical devices. Therefore, it is of interest to establish a protocol in assessing FBR induction to better ensure patient's safety.

Materials and methods: Since macrophages are orchestrating FBR signalling, primary rat alveolar macrophages were chosen as the model system. To assess their acute activation status when exposed to different implantable polyethylene materials, production of the chemokine CINC-1 served as the major endpoint. After 4, 12, and 72 h of seeding 2x10⁵ macrophages into a 24-well plate onto implant materials, supernatants were collected to measure membrane damage and CINC-1 release. The formation FBGC was also analyzed after 72 h of incubation by confocal microscopy using DAPI staining and alpha-tubulin immunofluorescence to assess a later stage of FBR.

Results: In line with its use as an implant material, high density polyethylene did not induce cytotoxicity (0 ± 0.2 % cytotoxicity) or CINC-1 release (33 ± 3.7 pg/mL) after 24 h of incubation, as compared to untreated cells (33 ± 13.5 pg/mL, 0 ± 2.5 % cytotoxicity). In contrast, ultra-high molecular weight polyethylene (UHMWPE) led to significant, time-dependent CINC-1 release (782 ± 154.1 pg/mL), however, without inducing membrane damage (1 ± 2.0 % cytotoxicity). Formation of FBGC upon UHMWPE exposure was clearly shown by confocal microscopy.

Conclusion: The results indicate that UHMWPE exhibited a pro-inflammatory potential with induction of FBR in the absence of cytotoxicity. Based on cytotoxicity testing only, UHMWPE might, therefore, pass ISO 10993-5 testing, irrespective of causing FBR, as a considerable adverse reaction. The present approach for FBR detection, thus, might represent an important add-on for ISO 10993 biocompatibility testing to better ensure patient's safety.

53

Assessing Hepatotoxic and Non-hepatotoxic Compounds by Means of New Approach Methods

K. Jochum¹, A. Miccoli^{1,2,3}, H. Hammer⁴, O. Poetz^{4,5}, A. Braeuning³, T. Tralau¹, P. Marx-Stoelting¹

¹German Federal Institute for Risk Assessment, Dept. Pesticides Safety, Berlin, Germany

²University of Tuscia, Department for Innovation in Biological, Agro-food and Forest Systems, Viterbo, Italy

³German Federal Institute for Risk Assessment, Dept. Food Safety, Berlin, Germany

⁴SIGNATOPE GmbH, Reutlingen, Germany

⁵University of Tübingen, NMI Natural and Medical Sciences Institute, Reutlingen, Germany

Introduction: The implementation of new approach methods (NAMs) to reduce, replace or refine animal testing is a major challenge in risk assessment. One aspect that has to be considered is their applicability in different regulatory domains. In addition, the robustness and the accuracy of testing has to be thoroughly evaluated before a consensus can be reached in scientific and regulatory communities.

Objectives: This study aimed at investigating the effects of xenobiotics belonging to different regulatory domains, for which toxicity is mostly known *in vivo*, using NAMs.

Materials and methods: A total of 11 xenobiotics with known *in vivo* toxicity but partially unknown toxicological modes of action were selected. This included 6 pesticide active substances and 5 food contaminants. Differentiated HepaRG cells were used as a model of the human liver. Non-cytotoxic concentrations were determined based on the WST-1 and the neutral red assays. Changes in the expression of proteins indicative of select endpoints were assessed using a multiplex assay, and an LC-MS-based proteomics approach was applied for major cytochrome P450 enzymes and transporters. Subsequently, transcriptomics of the most promising test conditions based on the previous results were determined by PCR profiler arrays.

Results: A successful protocol for mRNA and protein extraction with subsequent multiplex, LC-MS and PCR measurements could be established. Exposure of the cell model to selected xenobiotics led to the triggering of various pathways. These comprise well established effects as well as pathways associated with hitherto undescribed endpoints.

Conclusion: The conducted assessment indicates the suitability of the HepaRG model as well as a combination of omics techniques for the toxicological evaluation of novel substances in an animal-free manner. Future efforts will be dedicated to obtaining dose-response curves with the multiplex assay and focusing on the impacts of mixtures.

Keywords: New Approach Methods, Omics data, *in vitro* techniques, Pesticides, Contaminants, HepaRG

54

Thyroid hormones system disruption after exposure to mixtures of triazole fungicides *in vivo* and *in vitro*

A. E. Reetz¹, A. Kadic¹, B. C. Fischer¹, T. Heise¹, V. Ritz¹, P. Marx-Stoelting¹, P. Oles¹, K. Renko¹, M. D. L. Marzo Solano¹

¹BfR, Berlin, Germany

Introduction: Changes in thyroid hormone (TH) and TSH levels are often found following exposure to chemical substances and the effects of their have also been discussed in the context of endocrine disruption. Thyroid effects may be caused by a variety of mechanisms, of which increased hepatic metabolism of T3 and T4 and a compensatory up-regulation of TSH is the most prominent one following exposure to environmental chemicals (ECs) in animal experiments.

Methods: 28-day feeding study in rats examining the effects of treatment with the hepatotoxic fungicides cyproconazole, epoxiconazole and prochloraz as well as combinations thereof was performed as already described. Serum hormone concentrations were analysed by MagPix multiplex assays *post hoc*. Thyroid histopathology was conducted and the severity of the effects are being analyzed by thyroid follicular cells morphometry. Induction of hepatic metabolism was measured by qRT PCR and hepatic T3/T4 clearance and UGT were measured by a microsomal enzyme activity assay. With cyproconazole, additional *in vitro* assays were conducted including thyroidal I-uptake (NIS), thyroperoxidase (TPO) and iodothyronine deiodinases (D1-D3) inhibition.

Results: Decrease in serum T4 levels and an increase in TSH levels were observed in rats treated with 1000 ppm cyproconazole and with theazole mixtures that contained a corresponding amount of cyproconazole. At the same doses, hepatocyte hypertrophy, thyroid follicular hypertrophy and hyperplasia, UGT activity and gene expression inductions, and T3 and T4 metabolism were increased. Thus the effect on thyroid hormones and tissue may be secondary to hepatic enzyme induction. Preliminary results of *in vitro* assays dedicated to HPT axis-specific interference by cyproconazole are supporting the proposed MoA as none of the other targets were affected.

Conclusion: This study shows the application of a method battery for *in vivo* and *in vitro* characterization of potential endocrine disruptors also in a mixture inducing changes in TH serum levels and tissue by HPT primary and secondary mechanisms. Cyproconazole and its mixtures provoked hepatic UGT activities followed by T4 decline (and TSH induction), with consequent thyroid follicular hyperplasia and hypertrophy.

Keywords: thyroid adverse outcome pathway, liver enzyme induction, endocrine disruption, cyproconazole.

55

Disruption of the 6-formylindolo[3,2-b]carbazole (FICZ) metabolism sensitizes keratinocytes for drug-induced phototoxicity

F. Hartung¹, T. Haarmann-Stemann¹

¹IUF – Leibniz Research Institute for Environmental Medicine, Düsseldorf, Germany

Introduction: Drug-induced cutaneous adverse reactions are a common side effect of a wide variety of systemically and topically applied drugs. Recently, it was shown that an accumulation of the endogenous photosensitizer 6-formylindolo[3,2-b]carbazole (FICZ) and associated sensitization to ultraviolet A (UVA)-induced oxidative stress and apoptosis may determine the phototoxicity of the BRAF inhibitor vemurafenib. The underlying molecular mechanism appears to be an inhibition of the FICZ metabolism via disruption of the aryl hydrocarbon receptor (AHR)-cytochrome P450 monooxygenase 1A1 (CYP1A1) axis.

Objectives: Various drugs which are metabolized by CYP1 isoforms and are known to be phototoxic were investigated with regard to their interference with FICZ metabolism and stimulation of the FICZ/UVA-mediated phototoxicity. The data may be useful to obtain a better *in vitro* prediction of phototoxic drugs and suggest that a disruption of the metabolism of endogenous photosensitizers like FICZ should be considered in regulatory guidelines.

Materials and methods: *in vitro* studies, cell culture, UVA radiation, apoptosis and ROS measurement.

Results: Drugs from different substance classes stimulated the FICZ/UVA-mediated phototoxicity in HaCaT keratinocytes. The findings suggest that drug-induced phototoxicity may underlie a disturbance in FICZ metabolism. In addition, this study provides a basis for the development of appropriate *in vitro* assay strategies to evaluate phototoxicity in regulatory toxicology.

Conclusion: Disruption of the FICZ metabolism by interference with the AHR-CYP1A1 axis may be an underlying mechanism of the phototoxicity of the EGFR inhibitor erlotinib and the immunosuppressive disease-modifying antirheumatic drug leflunomide. Therefore, interference with FICZ metabolism should be considered when developing new *in vitro* strategies for regulatory assessment of the phototoxic potential of drugs.

Short talks: Cancer pharmacology and treatment

56

Mechanisms of drug resistance in chronic myeloid leukemia – The role of cell adhesion signaling and fibronectin 1

M. Kähler¹, L. Tiedemann¹, C. Pott², L. S. Schmidt¹, M. Litterst¹, H. Bruckmüller^{1,3}, I. Nagel^{1,4}, I. Cascorbi¹

¹Institute of Pharmacology, UKSH Campus Kiel, Kiel, Germany

²Department of Internal Medicine II, UKSH Campus Kiel, Kiel, Germany

³The Arctic University of Tromsø, Department of Pharmacy, Tromsø, Norway

⁴Institute of Human Genetics, UKSH Campus Kiel, Kiel, Germany

Introduction: The hematopoietic malignancy chronic myeloid leukemia (CML) predominantly caused by the formation of the BCR-ABL1 fusion protein can be successfully treated with tyrosine kinase inhibitors (TKIs), e.g. imatinib. Nevertheless, therapy failure still is a clinical problem in 25 % of CML patients.

Objectives: To study mechanisms of TKI resistance, we established an *in vitro*-TKI-resistance cell line model analyzing genome-wide gene expression of imatinib and nilotinib resistant cell lines. Further, the role of cell adhesion signaling and the putative candidate gene fibronectin 1 (FN1) in TKI resistance was investigated.

Methods: The *in vitro*-TKI-resistance K-562 cell model was established against 2 µM imatinib, 0.1 µM nilotinib and 0.01 µM dasatinib. Genome-wide gene expression was measured using HuGene 2.0 ST arrays. mRNA and protein levels were validated using qPCR and immunoblotting in cell lines and a cohort of ten CML patients. Transfection experiments were performed with an FN1-specific siRNA or -encoding plasmid challenging the cells with BCR-ABL1 TKIs followed by analyses of cell fitness on the level of total cell number, cell viability, proliferation and cell cycle distribution. Cell adhesion was measured using Matrigel-coated plates and Vybrant cell adhesion assay.

Results: Genome-wide expression analyses revealed a downregulation of FN1 expression (-9.8-fold, padj=9.5x10⁻¹⁵) accompanied by deregulation in focal adhesion and PI3K-Akt-pathways in imatinib and nilotinib-resistance compared to native cells. FN1 expression was confirmed to be downregulated also in dasatinib-resistant sublines on mRNA and protein level. In native cells, siRNA-mediated FN1-downregulation led to the development of imatinib resistance, as TKI susceptibility against all BCR-ABL1 TKIs was reduced, while cell adhesion was increased (p=0.02), e.g. after 48 h imatinib treatment (cell number: +1.5-fold, p=0.04; proliferation: +1.45-fold, p=0.005). Restoration of FN1-expression in TKI-resistant sublines restored TKI sensitivity as seen for imatinib, nilotinib and dasatinib-resistance. FN1 expression was also decreased in CML patients lacking molecular response to TKI treatment.

Conclusion: Our data suggest that FN1 expression influences the response to all BCR-ABL1 TKIs. Restoration of FN1 is able to overcome resistance potentially by altered cell adhesion signaling. These findings indicate that FN1 could be a promising target to overcome TKI resistant CML.

58

A mutation in the Btk SH2 domain, known to mediate ibrutinib resistance in chronic lymphocytic leukemia, causes a significant increase in kinase function by enhancing its binding affinity to regulatory proteins or peptides

M. Wist¹, S. Endres¹, P. Gierschik¹

¹University of Ulm Medical Center, Institute of Experimental and Clinical Pharmacology, Toxicology and Pharmacology of Natural Products, Ulm, Germany

Introduction: The approval of Brutons tyrosine kinase (BTK) inhibitor ibrutinib has changed the field of chronic lymphocytic leukemia (CLL). By blocking the kinase function and thus abrogating the B-cell receptor signaling pathway being crucial for both proliferation and survival of malignant B cells, ibrutinib has proven to be very effective and has become a first-line therapy for CLL. However, over the years some patients developed resistance to the drug by acquiring mutations mainly affecting Btk. While most of the mutations in Btk affect the kinase domain and interfere with drug binding, there are few resistance-mediating-mutations like T316A in the Btk SH2 domain where the mechanism of resistance has not been understood

Objectives: As little is known about the functional consequences of the T316A mutation, we intended to investigate its effect on both Btk kinase function and driving the BCR signaling pathway to unveil the mechanism by which this mutation provides drug resistance

Materials and methods: We have established a reconstituted system in COS-7 cells to investigate the functional interaction of WT and mutant Btk with their effector protein PLC γ 2. Moreover, we reconstituted Btk-deficient DT40 cells with either WT or mutant Btk for comparison in a B cell background. As the mutation affects BTKs SH2 domain, we generated recombinant Btk-SH2 protein either WT or mutant and compared their binding affinity to specific peptides using Fluorescence Polarization binding assay

Results: We could show that the T316A mutation strikingly enhances the ability of Btk to activate PLC γ 2 and, thus the BCR signaling pathway. Moreover, in DT40 cells, we observed that in contrast to WT the mutant cells display ibrutinib resistance although the kinase per se seems to be sensitive towards the inhibitor. Interestingly we observed that the mutation massively augments the binding affinity of BTKs SH2 domain to peptides obtained from the kinase interaction partner B cell linker protein (BLNK)

Conclusion: Together this data confirm that the T316A mutation mediates drug resistance most likely by significantly increasing the catalytic functions of the kinase to a level that even few percent of ibrutinib-free Btk might be sufficient to compensate for the entire Btk. It seems most likely that the gain of catalytic function is triggered by the increased binding affinity of Btk to regulatory proteins including BLNK, which may help to stabilize the active conformation of the kinase

59

Molecular prediction of clinical response to anti-PD-1/anti-PD-L1 immune checkpoint inhibitors: new perspectives for precision medicine and mass spectrometry-based investigations.

R. Longuespée¹, W. E. Haefeli¹, M. Fresnais¹

¹University Hospital Heidelberg, Department of Clinical Pharmacology and Pharmacoepidemiology, Heidelberg, Germany

Immune checkpoint inhibitors (ICIs), such as monoclonal antibodies targeting the program cell death 1 protein (PD-1) or its ligand (PD-L1), are among the most frequently used immunotherapies in oncology ¹. However, precision medicine approaches to adapt the treatment to each patient are still poorly exploited. A large proportion of patients do not respond to ICIs and often develop severe adverse reactions, while existing predictive biomarkers still do not reliably predict outcome for many patients. Identifying new biomarkers to predict ICI efficacy or resistance as early as possible, and finding relevant clinical pharmacological parameters to better estimate ICI exposure would thus open new paths for precision medicine. This necessitates a broader view on intended and unintended events of ICI disposition. ICIs are administered intravenously and further diffuse from the blood compartment into interstitial compartments to reach the cellular site of action (SOA) where it binds non-covalently to its molecular SOA (i.e., PD-1 or PD-L1) to display the therapeutic action ². However, interfering events influence ICI efficacy, such as (i) off-site binding between the ICI and its molecular target circulating in the blood (e.g., soluble or exosomal), and (ii) *in vivo* chemical modifications, degradation, and aggregation of the ICI and its molecular target. These represent relevant hints of investigation to predict therapy efficacy or resistance.

Today, the extended panel of mass spectrometric approaches, accompanied by newly developed sample preparation methods offer multiple options for molecular quantification in biological matrices. These virtually allow for investigations of interfering events of ICI disposition and for the possible stratification of responders and non-responders on a molecular basis ³, and early detection of resistance. Especially, three target groups of proteins appear interesting to investigate: the ICI, the immune checkpoint molecules, and the other endogenous proteins. In this presentation, we will review the current knowledge of ICI disposition and interfering events, and present recent results of quantification of the anti-PD-1 ICI pembrolizumab and its circulating molecular target in plasma from patients with non-small cell lung cancer.

1. Baumeister et al. *Annu Rev Immunol* 2016, 34, 539-73.
2. Longuespée et al. *Br J Clin Pharmacol* 2021, 87 (3), 858-874.
3. Srivastava et al. *Proteomics* 2019, 19 (10), e1700448.

Short talks: CNS / endocrine pharmacology and treatment

60

The influence of the AT1-receptor blocker Telmisartan on endothelial function in AAV-PCSK9^{DY} atherosclerosis mice is dependent on the ACE2/Ang(1-7)/Mas axis

T. Klersy¹, L. Achner¹, Z. Aherrahrou², B. Fels³, O. Müller⁴, F. Rezende⁵, R. Brandes⁵, M. Bader⁶, K. Kusche-Vihrog³, W. Raasch¹

¹University of Lübeck, Institute of Experimental and Clinical Pharmacology and Toxicology, Lübeck, Germany

²University of Lübeck, Institute for Cardiogenetics, Lübeck, Germany

³University of Lübeck, Institute for Physiology, Lübeck, Germany

⁴University Hospital Schleswig-Holstein, Campus Kiel, Clinic for Internal Medicine III, Kiel, Germany

⁵Goethe-Universität, Institut für Kardiovaskuläre Physiologie, Frankfurt, Germany

⁶MDC, Berlin, Germany

Recently, we demonstrated that the mechanical stiffness of in situ endothelial cells of aortas from AAV-PCSK9^{DY}-induced mice is increased as a functional correlate of atherosclerosis.

Because AT₁ receptor blockers (ARBs) have anti-atherosclerotic effects, the aim of the present study was to investigate whether ARB treatment reduces the endothelial stiffness in the AAV-PCSK9^{DY} model and whether this is mediated via an ACE2/Ang(1-7)/Mas-dependent mechanism.

Male C57BL/6N, Mas-ko and ACE2-ko mice were employed. We induced atherosclerosis by an AAV-PCSK9^{DY} (2x10¹¹ VG) injection plus cholesterol-rich Western diet (WD). Controls received chow and no PCSK9^{DY}. Additional groups of all mouse strains were treated with telmisartan (TEL, 8 mg/kg/d) upon AAV-PCSK9^{DY} injection+WD. After 3 months, endothelial stiffness was quantified by Atomic Force Microscopy (AFM) and the extent of atherosclerotic lesions was determined by Oil Red-O staining. Cholesterol (TC) and nitrite was measured in plasma of all mice.

Regardless of the mouse strain, plaque burden was significantly increased in all mice as a result of AAV-PCSK9^{DY}+WD, but decreased again by TEL. Although TC was also increased upon AAV-PCSK9^{DY}+WD, TEL reduced TC only in C57BL/6N but not in ACE2- or Mas-ko mice. Endothelial stiffness was higher per se in Mas-ko and ACE2-ko compared with C57BL/6N mice and was increased in all strains by AAV-PCSK9^{DY}+WD. However, a reduction was observed under TEL only in the C57BL/6N, while it remained still high in the two ko strains. Correlation analyses confirmed the association between atherosclerotic lesions and functional vascular damage, due to a positive correlation between endothelial stiffness on one side and TC, plaque content and fat content on the other side, and a negative correlation between cortical stiffness and plasma nitrite in C57BL/6N controls. Interestingly, these positive and negative correlations were abolished or even convert to the opposite in the Mas-ko and ACE2-ko mice, respectively.

In agreement with the literature, we here confirmed that PCSK9^{DY}/WD-treated mice developed profound atherosclerosis resulting in a vascular dysfunction as demonstrated by the AFM analyses. Since TEL-induced improvement of endothelial stiffness was only seen in the C57BL/6N but not the Mas-ko and ACE2-ko mice, we suggest that the protective TEL effect is at least partly due to an Ang(1-7)/ACE2/Mas axis mediated mechanism.

61

Cognitive function and cerebral blood flow are impaired in AAV-PCSK9^{DY} atherosclerotic mice

L. D. Hernandez Torres¹, Z. Aherrahrou², K. Kusche-Vihrog³, J. B. Hoeverner⁴, F. Rezende⁵, R. Brandes⁵, O. Müller⁶, W. Raasch¹

¹University of Lübeck, Institute of Experimental and Clinical Pharmacology and Toxicology, Lübeck, Germany

²University of Lübeck, Institute for Cardiogenetics, Lübeck, Germany

³University of Lübeck, Institute for Physiology, Lübeck, Germany

⁴UKSH, Kiel University, MOIN CC, Department of Radiology and Neuroradiology, Kiel, Germany

⁵Goethe-Universität, Institut für Kardiovaskuläre Physiologie, Frankfurt, Germany

⁶University Hospital Schleswig-Holstein, Campus Kiel, Clinic for Internal Medicine III, Kiel, Germany

We recently showed that mice exhibit increased anxiety behavior as a result of diet-induced obesity while cognitive function remained normal. We speculated that cognitive dysfunction may require additional vascular damage.

We aimed to investigate whether atherosclerotic mice have impaired learning and memory and whether this is associated with a decrease in cerebral blood flow.

We induced atherosclerosis by an AAV-PCSK9^{DY} (2x10¹¹ VG) injection plus cholesterol-rich Western diet in male C57BL/6N mice (called in the following as verum mice). After 3 months, we examined these mice and chow-fed controls for cognition using Barnes maze procedure for spatial learning (within a 5d-lasting training period) and memory at d6

(short-term memory) and at d17 (long-term memory). Cerebral blood flow was determined by using ASL-MRI. Using CD31/Col IV immunofluorescence, we determined vascular morphology in specific cerebral areas.

Compared with controls, verum mice developed obesity, massive aortic plaque burden, and marked elevation of plasma cholesterol and triglycerides, demonstrating atherosclerosis in these mice. RNAseq analyses followed by KEGG pathway evaluation confirmed marked inflammatory processes in the aortas of verum mice. Verum mice had a delay to learn the Barnes maze task as well as an impaired long-term memory, as they shown increased number of primary errors and higher latency to have the first contact with the exit hole at d17. Verum mice used less efficient search strategies to locate the escape hole. Short-term memory was not affected. Compared to controls, the blood flow was reduced in verum mice in, among other areas, the cingulate cortex, caudate putamen and the hippocampus. Immunostaining indicated more string vessels in the cingulate cortex and the hippocampus in verum mice.

We conclude that as consequences of atherosclerotic vascular lesions and obesity, the spatial learning and long-term memory of the animals were decreased due to the formation of string vessels which further causes decreased blood flow in certain brain areas. Particularly noteworthy is the reduced blood flow in the caudate putamen and the cingulate cortex, which are related to the learning and decision-making processes, respectively as well as the hippocampus, which correlates with the reduced capacity of generating long-term memory. These findings make the AAV-PCSK9^{DY} mouse model valuable for research in obesity-associated dementia.

62

The role of VDAC1 inhibitor Akos-22 in ferroptotic cell death

S. Tang^{1,2}, C. Culmsee^{1,2}

¹Institute of Pharmacology and Clinical Pharmacy, Marburg, Germany

²Center of Mind, Brain and Behavior, Marburg, Germany

During regulated cell death, mitochondrial apoptosis is executed by the permeabilization of the mitochondrial outer membrane. During this process, pro-apoptotic proteins of the Bcl-2 family interact with voltage-dependent anion channels (VDACs) to form pores in the mitochondrial membrane, leading to devastating mitochondrial damage and ultimately to cell death [1].

Recent findings underline an essential role of mitochondrial integrity during ferroptotic cell death [2], which is defined as an iron-dependent cell death mechanism, characterized by massive lipid peroxidation. Inhibition of mitochondrial respiration contributes positively to cellular integrity by suppressing the generation of mitochondrial reactive oxygen species [2].

In this study, we investigated the impact of Akos-22, a selective VDAC1-inhibitor, during erastin and RSL3-mediated ferroptotic cell death. Fluorescence-activated cell sorting (FACS) measurements were conducted after respective cell labelling to detect cell death (Annexin V/Propidium iodide), mitochondrial membrane potential (TMRE) and mitochondrial superoxide formation (MitoSox). Mitochondrial morphology and mitochondrial iron uptake was assessed by fluorescence microscopy after staining the cells with MitoTracker Deep Red or Mito-FerroGreen respectively. Further, the Seahorse XF Analyzer was used for detecting mitochondrial respiration and glycolytic activity.

Flow cytometric analyses revealed alleviated lipid peroxidation, as well as reduced ferroptotic cell death in Akos-22 treated mouse hippocampal HT22 cells. Ferroptosis-mediated excessive mitochondrial iron uptake, mitochondrial ROS formation and the loss of mitochondrial membrane potential were attenuated by the inhibition of VDAC1. Strikingly, incubation with Akos-22 alone leads to mitochondrial fragmentation and suppressed mitochondrial respiration while preserving glycolytic activity.

These findings suggest a role of Akos-22 in regulating mitochondrial dynamics, function and integrity during the execution of ferroptotic cell death. During ferroptosis, excessive ROS formation and the loss of mitochondrial integrity leads to cellular demise, that were impeded by the inhibition of VDAC1 by Akos-22.

References:

[1]: Dadsena et al.: Cell Mol Life Sci, 2021, 78(8), 3777–3790.

[2]: Clemente et al.: Cells, 2020, 9(10), 2259.

Short talks: Ion channels, drug development

64

Improving chemosensitivity in cancer - A novel role for Two Pore Channel 2

F. Geisslinger¹, M. Müller², Y. K. Chao³, C. Grimm³, A. Vollmar^{2,4}, K. Bartel²

¹Ludwig-Maximilians-University Munich, Pharmacy, Munich, Germany

²Ludwig-Maximilians-University Munich, Pharmacy, Pharmaceutical Biology, Munich, Germany

³Ludwig-Maximilians-University Munich, Walter-Straub-Institute for Pharmacology and Toxicology, Munich, Germany

⁴Ludwig-Maximilians-University Munich, München, Germany

Introduction: Even though a variety of targeted cancer therapies exist, chemotherapy regimens still include classic cytostatics e.g., vincristine and doxorubicin. A major problem

that often leads to decreased therapy efficacy is the development of resistance against cytostatics. Interestingly, the lysosome has recently been implicated in chemoresistance. Drugs can accumulate within the organelle by which they are prevented from reaching their intracellular targets and the release of lysosomal proteases into the cytosol upon lysosomal membrane damage can initiate lysosomal cell death.

Objectives: In this study, we investigated the role of Two-Pore Channel 2 (TPC2), a lysosomal cation channel important for lysosomal and cellular function. We posed the hypothesis that targeting TPC2 can manipulate lysosomal function in a way that restores chemosensitivity in leukemia cells.

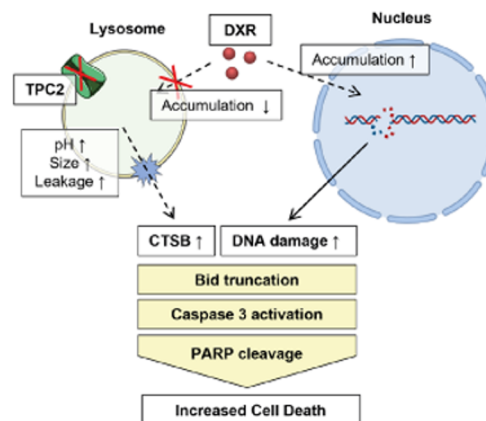
Materials and methods: TPC2 knock-out (KO) cells were generated using CRISPR/Cas9. Cell survival and signalling pathways were analyzed by cell biological methods, including qPCR, immunoblotting, flow cytometry, confocal microscopy and CellTiter-Blue.

Results: We provide novel data that loss of TPC2 function sensitizes multidrug-resistant acute lymphoblastic leukemia (ALL) cells to various cytostatics such as vincristine, doxorubicin and topotecan in a cell culture model. Importantly, also pharmacological channel inhibition by naringenin or tetrandrine proved beneficial in several leukemic cell lines or patient-derived xenograft ALL cells when combined with vincristine. Underlying this chemo-sensitization is a dual mode of action. Upon TPC2 loss of function, lysosomal drug sequestration is impaired and concurrently susceptibility to lysosomal damage is increased. This results in increased drug abundance at the respective target site and induction of lysosomal cell death by cathepsin B release from damaged lysosomes into the cytosol.

Conclusion Our work presents, for the first time, TPC2 as a promising target for overcoming chemoresistance in ALL. These beneficial effects of impairing TPC2 function on chemosensitivity are mediated by manipulation of lysosomal function.

Geisslinger F et al., Cell Death Dis. 2022 Aug 1;13(8):668.

Fig. 1



65

TRPC5 controls the adrenaline-mediated counter regulation of hypoglycemia

J. Bröker-Lai^{1,2}, J. Rego Terol³, C. Richter¹, I. Mathar^{1,2}, A. Wirth^{1,2}, S. Kopf^{4,5}, A. Moreno-Pérez⁶, E. Heidenreich⁶, L. Liqi Tan¹, Y. Schwarz³, G. Poschet⁶, J. Hermann¹, V. Tsvilovsky^{1,2}, U. Haberkorn⁷, P. Wartenberg⁸, M. Berlin^{1,2}, R. Ottenheim^{1,2}, N. Agarwal¹, B. Kleb⁹, K. Dinke⁹, F. Zufal³, P. Nussbaumer⁹, L. Birnbaumer⁹, U. Boehm¹⁰, R. Hell⁶, P. Nawroth^{4,5}, T. Leinders-Zufal³, R. Kuner¹, M. Zorn⁴, D. Bruns³, M. Freichel^{1,2}

¹Heidelberg University, Institute of Pharmacology, Heidelberg, Germany

²DZHK, Partner site Heidelberg/Mannheim, Heidelberg, Germany

³Saarland University, Center for Integrative Physiology and Molecular Medicine, Homburg, Germany

⁴Klinik für Endokrinologie, Diabetologie, Stoffwechsel und Klinische Chemie, Heidelberg, Germany

⁵Deutsches Zentrum für Diabetesforschung, München-Nueherburg, Germany

⁶Centre for Organismal Studies Heidelberg, Metabolomics Core Technology Platform, Heidelberg, Germany

⁷Heidelberg University Hospital, Nuclear Medicine, Heidelberg, Germany

⁸Pontifical Catholic University of Argentina, Institute of Biomedical Research, Buenos Aires, Argentina

⁹Lead Discovery Center GmbH, Dortmund, Germany

¹⁰Saarland University, Experimental and Clinical Pharmacology and Toxicology, Center for Molecular Signaling, Homburg, Germany

Diabetes mellitus is a global pandemic leading to numerous micro- and macrovascular long-term complications as well as neuropathies. The latter include hypoglycemia-associated autonomic failure (HAAF), which represents a defect in the modulation of glucose homeostasis by the autonomous nervous system. HAAF patients experience life-threatening hypoglycemic episodes, but neither specific treatment options nor diagnostic tools, that allow to predict susceptibility for HAAF episodes, are currently available. Therefore, patient management is restricted to the avoidance of hypoglycemic events.

Using a combination of TRPC-deficient mouse models and pharmacological approaches, we demonstrate for the first time that TRPC5 activity selectively in catecholaminergic cells

is instrumental for the counter regulation following insulin-evoked hypoglycemia and the subsequent plasma adrenaline rise, thereby allowing the reestablishment of euglycemia. Specifically, our experiments pinpoint a failure in the in the autonomous nervous system of TRPC5-deficient animals, which show strongly impaired catecholamine release from chromaffin cells in response to stimulation with the neurotransmitter PACAP, that is co-released with acetylcholine from sympathetic neurons innervating the adrenal medulla. Furthermore, the comparative metabolome analysis in TRPC5-deficient mice and HAAF patients identified striking commonalities in the metabolic signature. Collectively, our new results assign TRPC channels a crucial role in the stress response to hypoglycemia and pinpoint them as potential targets for diagnostic and pharmacological interventions in diabetes patients with HAAF complications.

66

Enhanced inactivation increases the sensitivity of pathogenic Cav1.3 L-type Ca²⁺-channel variants to dihydropyridine Ca²⁺ channel blockers

F. TORÖK¹, N. J. ORTNER¹, J. STRIESSNIG¹

¹University of Innsbruck, Department of Pharmacology and Toxicology, Institute of Pharmacy and Center for Molecular Biosciences Innsbruck, Innsbruck, Austria

Introduction: Pathogenic de novo missense mutations in the pore-forming $\alpha 1$ -subunit of Cav1.3 voltage-gated L-type Ca²⁺-channels (*CACNA1D*) confer high risk for neurodevelopmental disorders. Most mutations cause pronounced shifts of the steady-state inactivation (SSI) and conductance curve towards negative potentials enabling a channel gain-of-function. Such mutants (A749T, S652L, F747S) exhibit increased sensitivity for clinically approved brain-permeable dihydropyridines (e.g. isradipine), which therefore appear suitable for symptomatic off-label treatment.

Objectives: We tested if isradipine preferentially binds to the inactivated state of Cav1.3 channels predicted by the modulated receptor hypothesis (MRH) (Bean BP, PNAS 1984;81:6388), and if a more negative inactivation voltage of mutant channel A749T can account for its higher drug sensitivity.

Methods: Human wild-type (WT) Cav1.3 $\alpha 1$ -subunits and the pathogenic A749T variant were heterologously expressed in HEK-293T cells with $\beta 2a$ and $\alpha 2\delta 1$ subunits. Isradipine sensitivity was measured by 50 ms pulses (0.1 Hz) from various holding potentials (HP, -89 - -27 mV).

Results: The half-maximal voltage for SSI was 18.8 mV more negative for A749T channels (-35.3 mV) as compared to WT. At -89 mV HP A749T was 1.4-fold more sensitive to isradipine (IC₅₀=97.7 nM) than WT (IC₅₀=135.8 nM, p=0.0007). Isradipine potency increased at more positive holding potentials. This voltage-dependence was more pronounced for A749T leading to a 2.4-fold higher potency at -54 mV HP (A749T: IC₅₀=17.3 nM; WT: IC₅₀=41.6 nM, p<0.0001). At HPs providing 10% or 20% SSI in both WT and A749T channels, IC₅₀s further decreased but were no longer distinguishable (10%: A749T: IC₅₀=6.22 nM; WT: IC₅₀ = 6.55 nM, p=0.2254; 20%: A749T: IC₅₀=2.12 nM; WT: IC₅₀=3.94 nM, p=0.0681). Assuming zero SSI of WT channels at -89 mV, an isradipine K_d of 135.8 nM for the resting channel and a K_d of 0.7nM for inactivated channels (from radioligand binding studies), the measured IC₅₀ values closely followed the IC₅₀s predicted by the MRH.

Conclusion: Voltage-dependent isradipine inhibition of WT Cav1.3 and its A749T variant can be explained by preferential inhibition of inactivated channel states. Higher isradipine sensitivity of A749T in comparison to WT at a given HP can therefore be explained by its more negative SSI.

Funding: Marie Skłodowska-Curie COFUND (ARDRE, 847681); FWF (P35722, P35087, DOC 30/CavX); Univ. of Innsbruck (Erika-Cremer fellowship).

67

Regulation of Raf kinase inhibitor protein levels under ischemic condition

C. Schanbacher^{1,2}, S. Herrmann³, P. Nordbeck^{4,5}, F. Weidemann⁶, K. Lorenz^{1,2}

¹Institute of Pharmacology and Toxicology, University of Würzburg, Würzburg, Germany

²Leibniz-Institut für Analytische Wissenschaften - ISAS - e.V., Dortmund, Germany

³Caritas-Krankenhaus Bad Mergentheim, Medical Clinic I, Bad Mergentheim, Germany

⁴University Hospital of Würzburg, Medical Clinic and Policlinic I - Cardiology, Würzburg, Germany

⁵Comprehensive Heart Failure Center, Würzburg, Germany

⁶Clinic Vest, Medical Clinic I - Cardiology, Recklinghausen, Germany

Introduction: The Raf kinase inhibitor protein (RKIP) was found to protect from pressure overload-induced heart failure. Since RKIP is upregulated under these conditions, this was considered as protective endogenous feedback mechanism. However, we could also show that RKIP is differentially regulated in two patient entities of aortic valve stenosis (AS): while RKIP expression was increased in patients with high transvalvular pressure gradients, there was a decline of RKIP levels in patients with low pressure gradients.

Objective: As low gradient AS is often accompanied by coronary artery disease we asked if ischemic conditions may counteract the protective upregulation of RKIP in these patients and therefore analyzed RKIP levels under ischemic conditions.

Methods: To simulate ischemia, we induced myocardial infarction (MI) by ligation of the left anterior descending coronary artery in mice with cardiac specific overexpression of RKIP (RKIP-Ig) and wild-type controls. RKIP protein and mRNA levels were analyzed by western blot and rt-PCR. Cardiac function was assessed by echocardiography and MI

induced mortality was monitored. To further assess RKIP expression, cardiomyocytes were treated with ischemic buffer and different inhibitors of protein degradation mechanisms, e.g. 3-methyladenine for autophagy or clasto-lactacystin β -lactone for the ubiquitin proteasome system (UPS).

Results: Similar as seen in low gradient AS patients, RKIP levels were significantly reduced 4 weeks after induction of MI. Downregulation of RKIP in response to ischemia was further reproduced *in vitro* suggesting a general repressive mechanism of ischemia on RKIP expression. Unaltered RKIP mRNA levels suggest that this mechanism is rather based on protein degradation than on gene regulation. As observed in pressure overload induced heart failure, cardiac RKIP overexpression also improved cardiac function and survival after MI compared to control mice. *In vitro* experiments using cardiomyocytes and inhibitors of different protein degradation pathways revealed autophagy and the UPS as central mechanisms for the downregulation of RKIP under ischemic conditions.

Conclusion: Our study further underscores the protective role of RKIP in the heart. However, we could also show that different disease stimuli have differential impact on endogenous RKIP levels. The herein gained insights in regulatory mechanisms of RKIP may help to define new therapeutic targeting strategies in heart failure.

Short talks: Biotransformation and Toxicokinetics

68

Studies investigating the side-chain hydroxylation of 2,5-dimethylfuran

D. Bohlen¹, L. Eichel¹, S. Stegmüller¹, E. Richling¹

¹University of Kaiserslautern-Landau, Kaiserslautern, Germany

Introduction: 2,5-Dimethylfuran (DMF) is a volatile organic compound which occurs as heat induced contaminant in food. It is mainly formed in food during roasting, grilling, frying, and baking via the Maillard reaction. Data to evaluate an average exposure scenario is rather scarce. Orally administered DMF is known to be metabolized in an analogous way as furan: CYP450 mediated epoxidation of the aromatic ring is followed by ring opening and formation of 3(Z)-hexene-2,5-dione (HD). Furthermore, studies showed that the highly reactive HD is able to bind to amino acid residues and proteins.¹ Previous research results by our group have shown that in general alkylpyrazines can be metabolized to carboxylic acids in humans. 2,5-Dimethylpyrazine was mainly transformed to the 5-carboxylic acid form in humans after coffee intake.² In this work a potential analog side-chain hydroxylation of DMF was investigated.

Objectives: The objective of this study was to investigate the phase 1 metabolism of DMF in pooled human liver microsomes with focus on potential side-chain hydroxylation and carboxylic acid formation.

Materials and methods: To investigate the possible formation of side-chain hydroxylated and oxidized metabolites a GC-MS method was developed to detect 5-methylfurfuryl alcohol (MFM), 5-methylfurfural (MFA), and 5-methylfuran-2-carboxylic acid (MFC). Commercially available human liver microsomes from 50 pooled liver donors were used.

Results: After incubation of microsomes with DMF the time- as well as a dose-dependent formation of MFM, MFA, and MFC was investigated. Formation of MFM was observed during the first minutes of the incubation with a maximum velocity at 8.1 min, whereas formation of MFA and MFC occurred delayed.

Conclusion: The human metabolism of DMF is not limited to oxidative ring opening to the highly reactive HD. Formation of a side-chain hydroxylated metabolite, such as MFM, was also observed resulting in a broader spectrum of metabolites with regard to alternative modes of action or detoxification mechanisms. Furthermore, other alkylfurans, such as 2-ethylfuran will be investigated analogously.

The studies were carried out within the framework of the DFG project RI 1176/12-1.

References:

- ¹ EFSA (2017) *EFSA Journal* 15 (10). DOI: 10.2903/j.efsa.2017.5005.
- ² Kremer *et al.* (2019) *Molecular nutrition & food research* 63 (14), 1801341. DOI: 10.1002/mnfr.201801341.

69

Toxicokinetic study of *cis*- and *trans*-homosalate in humans after oral dose.

K. E. Ebert¹, P. Griem², T. Weiss¹, T. Bruening¹, H. Hayden³, H. M. Koch¹, D. Bury¹

¹Institute for Prevention and Occupational Medicine of the German Social Accident Insurance, Institute of the Ruhr University Bochum (IPA), Bochum, Germany

²Symrise AG, Holzminden, Germany

³Institute of Inorganic and Analytical Chemistry, University of Münster, Münster, Germany

Homosalate (HMS) is a salicylate UV filter used worldwide in sunscreens and other personal care products at maximum concentrations of 10-15%. However, additional animal experiments have been requested by the ECHA due to concerns about possible reproductive toxicity. In 2021, the Scientific Committee on Consumer Products has suggested a reduced safe maximum concentration of 0.5%. Commercial products generally contain mixtures of *cis*- and *trans*-HMS. However, previous studies have not

addressed these isomers separately. We therefore investigated human toxicokinetics of HMS separately for *cis*- and *trans*-HMS.

Toxicokinetics in plasma and urine was investigated after a single oral dose of 10 mg HMS to four volunteers (two male, two female). Full urine voids were collected for 48 hours and 8 plasma samples were taken within the first 24 hours. Both a *cis*-rich and a *trans*-rich HMS isomer mixture were studied. The two parent isomers and four previously identified HMS-specific hydroxy (OH) and carboxylic acid (CA) metabolites, tHMS-CA, cHMS-CA, 3OH-tHMS and 3OH-cHMS, were investigated using LC-MS/MS and isotope dilution analysis, and further isomers were investigated semi-quantitatively.

Maximum plasma concentrations were reached 1–2 h post-dose for the parent isomers and 1–6 h post-dose for the metabolites. Mean plasma half-lives (in the first of two phases in the case of parent HMS and hydroxy metabolites, which all showed biphasic elimination) ranged between 1–6 h. In urine, peak concentrations were reached 1.5–6.3 h post-dose. Within 24 h $\geq 70\%$ of these metabolites were excreted. The mean (n=4) urinary excretion fraction (F_{ue}) was 0.045% for the sum of all oxidized metabolites derived from *cis*-HMS (range 0.036–0.049%) and 6.4% for those derived from *trans*-HMS (range 4.5–9.2%). According to our plasma and urine data, the availability of *trans*-HMS in plasma after oral administration is about 10-fold higher and the formation of its oxidized metabolites even two orders of magnitude higher than that of *cis*-HMS. Differences between oral and dermal HMS application are currently being investigated.

The data from the present study proves diastereoselectivity in toxicokinetics of *cis/trans*-HMS, emphasizing the necessity to address isomer ratios in future studies. The reported biomarkers and toxicokinetic data will be used in future exposure (and eventually risk) assessments within the scope of human biomonitoring population studies.

70

Metabolic activation of 2-methylfuran and reactivity towards biomolecules

V. Kirsch¹, S. Stegmüller¹, E. Richling¹

¹RPTU Kaiserslautern-Landau, Food Chemistry and Toxicology, Kaiserslautern, Germany

Introduction: 2-Methylfuran (MF) is a contaminant found primarily in heat-treated foods such as coffee or canned food. However, EFSA reported that the data for risk assessment is incomplete in terms of exposure and also terms of toxicity. *In vivo* studies indicate that the liver is the target organ for histopathological changes. The metabolic activation of MF to the reactive intermediate acetylacrolein (AcA) was hypothesized, but not validated yet.

Objective: The molecular and chemical mechanisms of MF metabolism to AcA was investigated to draw conclusions about the reactivity of AcA and toxicological effects of MF.

Materials and methods: AcA was synthesized and its reactivity towards N-acetyl-L-cysteine (AcCys), N-acetyl-L-lysine (AcLys), 2'-deoxyadenosine (dA), 2'-deoxyguanosine (dG), 2'-deoxycytosine (dC), and 2'-deoxythymidine (dT) was investigated. Adducts were characterized and quantified by (U)HPLC-MS/MS. Additionally, the metabolic activation of MF to AcA was verified using human (HLM) as well as rat liver microsomes (RLM). With supersomesTM (CYP 1A2, 2A6, 2C9, 2D6, 2E1, and 3A4) the key cytochrome P450 isoenzyme was identified. Primary rat hepatocytes (pRH) were incubated with MF or AcA and afterwards the DNA adducts, AcCys and AcLys adducts of AcA were determined in the cell supernatants by UPLC-MS/MS.

Results: Investigating the reactivity, for all nucleosides, except for dT, AcA adducts were formed as well as adducts with AcCys and AcLys. For the conversion of MF to AcA CYP 2E1 was found to be a key enzyme within the tested supersomesTM. When pRH were incubated with MF and AcA, AcLys-AcA was detected in the cell supernatants in a time- and dose-dependent manner. In addition, the results showed that AcA was indeed formed at the cellular level. Neither AcCys-AcA nor the DNA adducts dA-AcA, dG-AcA or dC-AcA were detectable *in vitro*. This indicated efficient detoxification, or reactivity towards biomolecules in cells.

Conclusion: AcA was determined as a reactive metabolite of MF *in vitro*, and its adduct formation with nucleophilic cellular components was evaluated. The metabolites were characterized and identified as potential biomarker for the first time *in vitro*.

71

Species-differences in the *in vitro* biotransformation of 1,1,2-trifluoroethene (HFO-1123)

R. Dekant¹, J. Serban¹, S. Sharma¹, R. Bertermann², M. Shinohara³, Y. Morosawa³, H. Okamoto³, W. J. Brock⁴, W. Dekant¹, A. Mally¹

¹University of Wuerzburg, Pharmacology and Toxicology, Wuerzburg, Germany

²University of Wuerzburg, Inorganic Chemistry, Wuerzburg, Germany

³AGC Inc., Tokyo, Japan

⁴Brock Scientific Consulting LLC, Hilton Head, United States

1,1,2-Trifluoroethene (HFO-1123) is anticipated for use as a refrigerant with low global warming potential. Inhalation studies on HFO-1123 in rats suggested a low potential for toxicity (NOAEL $\geq 20,000$ ppm), whereas single inhalation exposure of minipigs (≥ 500 ppm) and rabbits (≥ 1250 ppm) resulted in mortality. It has been suggested that the marked species-differences in HFO-1123 toxicity may be due to species-differences in biotransformation of HFO-1123 via the mercapturic acid pathway.

Thus, overall objective of this study was to analyse species-differences in glutathione (GSH) dependent *in vitro* biotransformation of HFO-1123 in susceptible vs. less susceptible species and humans as a basis for human risk assessment. Specifically, *in vitro* biotransformation of HFO-1123 to S-(1,1,2-trifluoroethyl)-L-glutathione (1123-GSH) and subsequent β -lyase mediated cleavage of the corresponding cysteine conjugate (1123-CYS) were investigated in subcellular fractions of mice, rats, minipigs, rabbits and humans. LC-MS/MS was used to quantify formation of 1123-GSH. Enzyme kinetics of β -lyase mediated cleavage of 1123-CYS were determined by spectrometric assay, and fluorine containing metabolites were monitored by ¹⁹F-NMR.

While 1123-GSH formation occurred at higher rates in rat liver S₉ as compared to rabbit, minipig and human S₉, increased β -lyase mediated cleavage of 1123-CYS was observed in renal cytosol of minipigs as compared to subcellular fractions of other species. Increased β -lyase activity in minipig was associated with time-dependent formation of monofluoroacetic acid (MFA), a highly toxic metabolite that interferes with cellular energy production through inhibition of aconitase. The intensity of the MFA signal in human kidney cytosol was only a fraction of the signal obtained in minipig cytosol, consistent with a lower β -lyase activity towards 1123-CYS in human cytosolic fractions. While these data may suggest that humans may be less susceptible to HFO-1123 toxicity as compared to minipig, the inconsistencies between GST and β -lyase mediated biotransformation observed *in vitro* do not allow to draw firm conclusions on the overall contribution of the mercapturic acid pathway to HFO-1123 biotransformation and toxicity *in vivo*.

Short talks: Toxicological Methods II

72

Impact of exposure to different ultrafine particles (UFP) aerosols on the metabolome of a lung model

R. Alsaleh¹, C. Kersch¹, J. Pantzke², A. Das², M. N. Delaval², M. Sklorz², S. Di

Bucchianico², R. Zimmermann², S. Schmitz-Spanke¹

¹Institute and Outpatient Clinic of Occupational, Social and Environmental Medicine, University of Erlangen-Nuremberg, Erlangen, Germany

²Comprehensive Molecular Analytics, Helmholtz Zentrum München, Munich, Germany

Introduction: The assessment of potential adverse health-related effects of ultrafine particles (UFP, diameter of $<0.1 \mu\text{m}$) is still ongoing. Since the exposure occurs mainly via inhalation, a triple cell culture model of lung cells was exposed to UFP containing aerosols with different chemical composition and similar physical characteristics at the air-liquid interface (ALI).

Objectives: This study aims to investigate the effect of *in vitro* exposure on the metabolome of lung cells model system.

Materials and methods: A triple cell culture model was established by seeding alveolar epithelial cells (A549) and macrophages (THP-1) on top of insert membranes, and fibroblasts (MRC-5) on beneath the insert. After this model adapted to the ALI condition, cells were exposed to different aerosols, which were generated by a combustion aerosol standard (CAST) soot generator. Exposures implicated UFP with either high or low content of semi-volatile organic compounds (SVOC) and were applied in a concentration of $10 \mu\text{g}/\text{m}^3$. Clean air (CA) served as negative control. For the current study, metabolites were extracted from cell lysates of the apical side. Metabolomics data acquisition was performed by GC-MS and processed with R software. Finally, MetaboAnalyst platform was used to analyse the data for various statistical tests in addition to KEGG based pathway analysis.

Results: Several metabolites have been significantly up or downregulated (fold change: 1.5, p threshold: 0.05). Multivariate tests showed that 2 amino acids, namely tryptophan (Trp) and lysine, accounted for the top metabolites differentiating high SVOC from CA. On the other hand, 5-methylthioadenosine and 5-methoxyindoleacetate were characteristic for low SVOC. Focusing on tryptophan metabolism, which modulates cells immunity and inflammation, Trp and its metabolite 5-hydroxy-Trp were significantly upregulated in high SVOC exposed model compared to upregulated 5-methoxyindoleacetate in low SVOC. Purine metabolism was among the top significant pathways in both high and low SVOC groups. Additionally, Trp metabolism pathway was enriched with similar significance levels in both groups.

Conclusion: In conclusion, this study could elucidate how chemical identity of UFP modulates the metabolism of lung cells and give more insights on the underlying mechanisms.

This work was funded by Bayerische Staatsministeriums für Umwelt und Verbraucherschutz (BayUFP).

73

Development of a human ex-vivo model for characterizing the dermal absorption of toxic substances - as demonstrated by hydrofluoric acid

S. Kilo¹, S. Mini Vijayan¹, F. Kiesewetter², T. Göen¹, H. Drexler¹

¹Friedrich-Alexander-Universität Erlangen-Nürnberg (FAU), Institut für Arbeits-, Sozial- und Umweltmedizin, Erlangen, Germany

²Sozialstiftung Bamberg, Pathologie, Bamberg, Germany

Introduction: Dermal exposure to toxic or carcinogenic substances can pose a major health risk in many industrial and other applications. Therefore, characterization of dermal

uptake and decontamination measures can be important cornerstones of risk assessment. Despite being an extremely hazardous liquid, hydrofluoric acid (HF) is indispensable in many industries. Following dermal contact, damage to deep tissue layers may occur, although at low HF concentrations a warning pain and externally visible skin damage may not occur for several hours. In addition, severe systemic poisoning and even death can result from fluoride absorption. Both factors make decontamination of exposed skin sites a crucial first aid measure to reduce adverse health effects.

Objectives: Since it is ethically unacceptable to perform such studies *in-vivo*, an *ex-vivo* human skin model was developed to study HF-induced local damage, fluoride uptake and its influencing factors.

Materials and methods: Static diffusion cells were used to study penetration of fluoride for up to 72 hours following application of HF (c: 5-50%, 1-10 min.) through excised human abdominal skin (0.64cm² exposure area, thickness 0.9 or 2.5 mm). Fluoride was measured by liquid chromatography (LC-ICP-MS) or fluoride-sensitive electrode. Intradermal pH was determined using a microminiature pH electrode, and skin integrity was assessed histologically.

Results: Dermal absorption of fluoride increased exponentially with increasing HF concentration. Furthermore, penetration increased significantly when the exposure time was extended from 1 to 3 min. In contrast, when the HF application time was extended from 5 to 10 min, there was hardly any further increase in fluoride absorption. Intradermal accumulation of fluoride also increased in a concentration-dependent manner, but to a lesser extent. Intradermal pH decreased with increasing HF concentration and exposure time. In addition, the lag time between HF application and the onset of pH changes decreased with increasing HF concentration and application time. Histological changes in the skin were detectable depending on the HF concentration and application time.

Conclusion: Considering our results, the human *ex vivo* skin model is suitable for the study of transdermal penetration and skin damage after HF exposure. Because of the very quick dermal absorption and the formation of a large skin depot, immediate intervention is advised, at best within the first minute after exposure to HF.

74

Senescence contributes to the wound healing disorder after sulfur mustard exposure

S. Rothmiller¹, G. Horn¹, C. Schäfers¹, N. Jäger¹, A. Neu¹, A. Bürkle², F. Worek¹, D. Steinritz¹, A. Schmidt³

¹Bundeswehr Institute of Pharmacology and Toxicology, München, Germany

²University of Konstanz, Department of Biology, Konstanz, Germany

³University of the Bundeswehr Munich, München, Germany

Introduction: Wound healing is a complex, well-orchestrated process. Disturbance of that process results in chronic wounds that are challenging to treat. Long lasting wounds are common after the exposure to alkylating sulfur mustard (SM). Treatments are still insufficient and mostly supportive. The underlying cellular pathomechanisms are not yet fully understood. Senescence of key player cells in wound healing might affect wound healing due to the longevity and the proinflammatory microenvironment of the cells.

Objectives: Identification of senescence as a new pathomechanism after SM exposure in wound healing associated cell lines.

Materials and methods: Human mesenchymal stem cells (MSC) and human dermal fibroblasts (HDF) were exposed to SM. Senescence was determined by senescence-associated β -galactosidase (SA- β -gal) staining. Various additional senescence-associated markers were identified by quantitative real time PCR and western blot. Senescence associated secretory phenotype (SASP) was determined by Bio-Plex assay. Migration was analyzed by IncuCyte. Senolytics were applied and cell viability was measured by XTT assay.

Results: SM induces senescence in MSC and HDF in a time- and concentration-dependent manner. Both cell lines exhibit various senescence markers, such as SA- β -gal, expression changes in cell cycle regulators as well as DNA damage and repair pathway, and SASP. Senescent MSC showed migration deficiencies. The senolytic compound ABT-263 had some beneficial effects by affecting the viability of senescent cells significantly more than of non-senescent cells.

Conclusion: Senescence after single dose SM exposure in wound healing associated MSC and HDF was identified as novel pathomechanism. Both cell lines showed various senescence markers, suggesting a common cellular answer to this stressor. These could serve as potential new drug targets to counteract chronic wounds after SM in a broader context.

75

Mixture effects of co-formulants and two plant protection products in a liver cell line

K. Feiertag¹, P. Marx-Stoelting¹, D. Bloch¹, B. Fischer¹, C. Kneuer¹, T. Opialla¹, T. Heise¹, T. Tralau¹, M. Karaca¹

¹The German Federal Institute for Risk Assessment, Pesticides, Berlin, Germany

Background: Plant protection products (PPPs) are extensively used in agriculture to protect desirable plants against diseases, pests and other unwanted plants. PPPs consist

of one or more active substances and a number of co-formulants. Active substances provide the functionality of the plant protection product and are also assumed to contribute to the entirety of its toxicity. Consequently, active substances are evaluated according to standard test methods set by legal data requirements before they are approved. In contrast, the relevance of co-formulants' toxicity is not always clear. However, mixture effects have been reported between active substances and co-formulants within plant protection products in both *in vivo* and *in vitro* studies.

Aim: This study aims to investigate the differential effects of two plant protection products, their active substances in combination and some of their co-formulants on the HepaRG liver cell line.

Method: The cytotoxicity of the two plant protection products, their active substances in combination, and their co-formulants on HepaRG cells, were investigated using Neutral Red uptake assays and WST-1 assay. Cyproconazole and azoxystrobin (Product A) were investigated in combination and epoxiconazole and fluxapyroxad (Product B) were investigated in combination, while a few known co-formulants were investigated individually. Transcriptomic and proteomic analyses were done. In addition, LC-MS/MS was used to determine the intracellular concentration of the active substances in the cells treated.

Results: Cell viability results show a dose-response relationship for cytotoxicity in HepaRG cells with increasing concentrations of the substances used. Products are more cytotoxic than their active substances alone. Gene expression profiles of products are similar to those of their active substances with minor differences. Proteomics results show that the transporters ABCB1 and ABCG2 are induced by a co-formulant. LC-MS/MS analyses reveal higher intracellular concentration of active substances in the cells treated with PPPs compared to those treated with the respective active substances mix.

Conclusion: PPPs show increased toxicity as compared to their active substances alone and results indicate the potential of co-formulants to contribute to this increase. Related kinetic interaction could be attributed to CYP enzyme and active transporter induction.

Short talks: Signal transduction, second messengers, nuclear receptors and other targets

76

Pharmacological Targeting of Platelet ACKR3/CXCR7 Modulates the Platelet Lipidome To Regulate Thrombotic and Thrombo-inflammatory Functions

K. Dittrich¹, X. Fu¹, M. Cebo¹, M. Manke², J. Sudman², S. Beer-Hammer³, B. Nürnberg³, T. Geisler², M. Gawaz², T. Bakchoul⁴, M. Lämmerhofer¹, M. Chatterjee³

¹University of Tübingen, Institute of Pharmaceutical Sciences, Tübingen, Germany

²University Hospital Tübingen, Department of Cardiology and Angiology, Tübingen, Germany

³University Hospital Tübingen, Dept. of Pharmacology, Experimental Therapy and Toxicology, Tübingen, Germany

⁴University Hospital Tübingen, Institute for Clinical and Experimental Transfusion Medicine, Tübingen, Germany

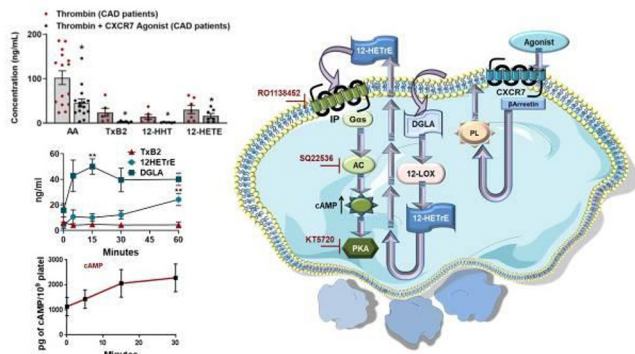
Introduction: Surface availability of platelet atypical chemokine receptor 3 or CXCR7 is significantly enhanced in acute coronary syndrome (ACS) patients post-myocardial infarction (MI), is associated with improved myocardial functional recovery and prognosis. Physiological ligand macrophage migration inhibitory factor (MIF) regulates thrombotic response through CXCR7 while CXCL12/SDF1- α acting through CXCR4 synergistically prompts prothrombotic response. Current investigation explored the therapeutic potential of platelet CXCR7 in modulating thrombotic and thrombo-inflammatory responses post-MI, in arterial thrombosis and in Heparin induced thrombocytopenia (HIT).

Methods: Lipidomics analysis by UHPLC-QTOF-MS/MS; flow cytometry; impedance and lumiaggregometry; T-TAS; calibrated automated thrombinolysis (CAT); murine MI and arterial thrombosis models.

Results: Pharmacological CXCR7-agonist (VUF11207) regulated platelet degranulation (CD62P surface expression, release of thrombo-inflammatory mediators, ATP), α IIb β 3-integrin activation and thrombotic propensity in blood from ACS patients *ex vivo* and post-MI in murine models *in vivo*. VUF11207 retarded arterial thrombosis *in vivo*, regulated thrombo-inflammatory functions triggered by HIT antibodies *ex vivo*. CXCR7-ligation preferentially limited the metabolism and release of COX-1 and 12-LOX derived pro-thrombotic oxylipins, and phospholipase-derived atherogenic lipids, while favouring the generation of antiplatelet lipid, dihomoy-linolenic acid (DGLA)-derived 12-hydroxyeicosatrienoic acid (12-HETE). Through 12-HETE, noncanonical CXCR7 coordinated with the Gas-coupled IP receptor to elevate platelet inhibitory cAMP levels and inhibit platelet response through the AC-cAMP-PKA pathway. VUF11207 counteracted activated platelet-driven procoagulant response, e.g. thrombin generation by reducing the externalization of thrombogenic phospholipid phosphatidylserine and generation of Factor-Xa inhibiting long-chain-acylcarnitines (16:0, 18:1, 18:2). It affected ADP-induced blood clot formation in thromboelastographic assays, but not basal hemostatic response (tail bleeding time) or plasma coagulation profile (APTT, PT) or availability of receptors that mediate platelet response (GPIIb α , GPV, GPIIb, GPIX, α v- β III-integrins) following administration in mice.

Conclusion: Therefore, therapeutic targeting of CXCR7 may modulate thrombotic and thrombo-inflammatory platelet functions, sparing basal hemostasis.

Fig. 1



77

Increase of RSL-3-induced HT22 cell death by NIST DEP involves ferroptosis and Epac1 but not caspases and Epac2

H. Yan¹, M. Veen¹, F. Lezoualc'h¹, A. Dolga¹, M. Schmidt¹

¹Faculty of Science and Engineering, Department of Molecular Pharmacology, Groningen, Netherlands

Introduction: Air pollution exposure is one of the important threats to human health. Diesel combustion produces diesel exhaust particles (DEP) which seem to contribute to the onset of different neurological diseases due to the induction of oxidative stress, inflammation and neuronal degeneration [1]. Underlying molecular mechanisms are ill defined. RSL-3-induced neurotoxicity has been linked to the newly identified iron-dependent form of cell death ferroptosis [2]. Cyclic adenosine monophosphate (cAMP) seems to be linked to ferroptosis type of cell death in processes involving Epac (exchange protein directly activated by cAMP) [3].

Methods: HT22 cells were treated with increasing concentrations of NIST DEP (24h) or RSL-3 (17h) alone and with different concentrations of NIST DEP and RSL-3 (17h) in combination. Cell viability was measured by MTT assay and Hoechst 33342/PI double staining assay. To further determine the basis of NIST DEP and RSL-3-mediated cell death, pan-caspase inhibitor QVD (10 μ M) and ferroptosis inhibitor ferrostatin-1 (5 μ M) were used. To elucidate the role of cAMP/Epac1 signaling in regulating the response to the combined effect, the expression of Epac1 was analyzed by western blotting, and Epac1 inhibitor CE3F4 (30 μ M) and Epac2 inhibitor ESI-05 (30 μ M) were used.

Results: NIST DEP alone does not significantly change HT22 cell viability. Importantly, co-treatment with NIST DEP further increased RSL-3-induced cell death by MTT assay and increased the number of PI-positive cells. Ferrostatin-1 but not QVD restored cell viability after treatment of RSL-3 and NIST DEP. Epac1 expression is detectable in HT22 cells. CE3F4 but not ESI-05 prevented cell death after NIST DEP and RSL-3 cotreatment.

Conclusions: Our current work demonstrates that co-treatment of HT22 cells with RSL-3 and NIST DEP caused a significant increase in cell death compared with RSL-3 treatment alone. Accelerated cell death of HT22 cells by RSL-3 and NIST DEP seems to involve ferroptosis, in a process independent of caspase but dependent on Epac1.

References:

1. Sermin, G., et al., *The Adverse Effects of Air Pollution on the Nervous System*. 2012. **2012**: p. 782462.
2. Wan et al., S.Y. and B.R.J.T.i.c.b. Stockwell, *Ferroptosis: Death by Lipid Peroxidation*. 2015. **26**(3): p. 165-176.
3. Musheshe, N., et al., *Pharmacological Inhibition of Epac1 Averts Ferroptosis Cell Death by Preserving Mitochondrial Integrity*. 2022. **11**(2): p. 314.

78

Two NO-GC isoforms, two different pathways to regulate airway tone.

M. Verheyen¹, D. Koesling¹, M. Peters², E. Merzgia¹

¹Institute for Pharmacology and Toxicology, Ruhr-University Bochum, Bochum, Germany

²Ruhr-University, Department of Molecular Immunology, Bochum, Germany

The NO-sensitive guanylyl cyclase (NO-GC; also referred to as sGC) catalyses the formation of cGMP in response to NO binding to the enzyme's prosthetic haem group. NO-GC-mediated signalling participate in many functions, with relaxation of vascular smooth muscle being the most well-known. In this regard, drugs that activate NO-GC in the lung are known to reduce pulmonary vascular resistance. However, whether NO-GC's activation also affects airway tone it is unclear. Moreover, it is not established that NO-GC signalling is accomplished by two isoforms, NO-GC1 ($\alpha_1\beta_1$) and NO-GC2 ($\alpha_2\beta_1$). The isoforms possess very similar regulatory and enzymatic properties with a PDZ domain in NO-GC2 representing the major distinguishing feature between the isoforms that probably targets the enzyme to signalling complexes. Studies of KO mice lacking either one isoform revealed a synergistic action of both enzymes in mediating vascular smooth muscle relaxation.

Herein, we investigated the functional roles of the NO-GC isoforms in respiration by measuring lung function parameters of isoform-specific KO mice using noninvasive and invasive techniques.

Our data revealed that NO-GC1 or NO-GC2 deficiency resulted in altered functional properties of the lungs suggesting participation of both isoforms in respiration. NO-GC1 KO mice showed enhanced respiratory resistance, which increased more pronouncedly with the bronchoconstrictor methacholine (Mch), but normalized with a bronchodilator. Contrariwise, NO-GC2 KO mice displayed reduced airway reactivity to Mch, which was also observed in an ovalbumin model of asthma that enhanced airway responsiveness in WT and NO-GC1 KO mice. A general impairment of NO-GC2 airways could be excluded because serotonin provocation resulted in a WT-like response. Furthermore, conscious NO-GC2 KO mice displayed altered breathing patterns at rest and after challenge of the mice with a bronchoconstrictor that point to altered vagal reflexes in these mice. Thus, we assume that a reduced cholinergic input into the airways of NO-GC2 KO mice may account for the lower response to Mch. Indeed, application of a ganglion blocker elicited a greater effect on Mch response in WT than in NO-GC2 KOs.

In conclusion, our data support the concept that both NO-GC isoforms are involved in the adjustment of airway muscle tone, but participate in distinct pathways with opposite effects on airway reactivity.

79

Impact of G-protein-coupled-receptor kinase 4 on GPCR signaling activity.

M. Burkhalter¹, M. Heßlinger¹, S. A. Sailer¹, M. Philipp¹

¹University Hospital Tübingen, Department of Experimental and Clinical Pharmacology and Pharmacogenomics, Section of Pharmacogenomics, Tübingen, Germany

Introduction: The signaling activity of GPCRs upon ligand binding is mainly regulated by G-protein-coupled-receptor kinases (GRKs) and β -arrestins. How GRKs carry out their part in this process has been studied in great detail for six of the seven members of this protein family. GRK4, however, remains only poorly analyzed. One reason for this lack of data could be an underestimation of the spatial expression of GRK4.

Objectives: Here, we aim to provide insight into how GRK4 affects signaling of activated GPCRs.

Materials and methods: This study was carried out in HEK 293T cells, which represents a widely used model system to analyze GPCR signaling. To assess molecular processes, we mainly applied Western blotting. Additionally, we used CRISPR/CAS9 and siRNA technology, respectively, to remove or reduce gene expression, which was controlled via qPCR.

Results: To study the influence of GRK4 on the signaling capacity of activated GPCRs, we generated a new HEK knock out (KO) line that lacks functional GRK4 using a CRISPR/CAS9 approach. Loss of *GRK4* mRNA in these KO cells verified the KO. We stimulated cells of this GRK4 KO line as well as of the parental line with ligands for different endogenously expressed GPCRs. We assessed phosphorylation of ERK1/2 as a read-out for signaling activity. Interestingly, stimulation of β -adrenoceptors, somatostatin receptors, muscarinic receptors as well as angiotensin receptors in every case caused pronounced exacerbation of ERK1/2 phosphorylation in GRK4 KO cells as compared to wild-type cells. Yet, we did not detect alterations of the kinetics of activation *per se*. To test, if other GRKs are involved in ERK1/2 overactivation in GRK4 KO cells, we overexpressed a dominant negative version of GRK2. However, reduction of GRK2 activity did not ameliorate ERK1/2 overactivation. Currently, we study recruitment of β -arrestin 1 and 2 in GRK4 KO cells after activation of the GPCRs named above.

Conclusion: Our newly generated GRK4 KO cell line revealed a so far underappreciated role of GRK4 regarding control of GPCRs. GRK4 appears to be instrumental in keeping signaling at bay and preventing an overactivation of intracellular signal transduction.

80

Real-Time Monitoring of GRK2-Induced Effects on Beta-Adrenoceptor-Stimulated cAMP Signaling by an EPAC-Based cAMP FRET Biosensor

C. Weinmann¹, A. Perhal¹, A. Langer¹, U. Quittner¹

¹ETH Zurich, Molecular Pharmacology, Zurich, Switzerland

Up-regulation of the G-protein-coupled receptor kinase 2 (GRK2) exerts fundamental pathological effects in heart failure. Major detrimental effects of GRK2 are attributed to exaggerated desensitization of beta-adrenoceptor-stimulated cAMP signaling and impairment of the inotropic reserve of failing hearts. In agreement with this concept, GRK2 inhibition shows beneficial effects in experimental models of heart failure, in part by restoration of the reduced inotropic response. To better understand effects of GRK2 inhibition on beta-adrenoceptor cAMP signaling, we established cellular models and measured the kinetics of receptor-stimulated cAMP signaling in real-time with an EPAC-based cAMP FRET (Foerster resonance energy transfer) biosensor. Three different HEK (human embryonic kidney) cell lines were established with comparable levels of the EPAC-based cAMP FRET biosensor: (I) HEK cells with endogenous GRK2 levels, (II) HEK cells with 8.9-fold increased GRK2 protein levels, and (III) HEK cells with 19.9-fold increased protein levels of the dominant-negative, kinase-deficient GRK2-K220R mutant. Endogenous beta-adrenoceptors were stimulated with 3 μ M of the agonist isoproterenol. Experimental data show that 8.9-fold increased GRK2 levels significantly decreased the isoproterenol-stimulated cAMP peak, which was 26 ± 4 % lower than that of cells with endogenous GRK2 levels and 20 ± 4 % lower than that of GRK2-K220R-expressing cells. In addition, the total isoproterenol-stimulated cAMP signal was strongly

decreased by GRK2, and the area of the cAMP transient in cells with 8.9-fold increased GRK2 levels was 54 ± 5 % smaller than that of cells with endogenous GRK2 levels and 52 ± 6 % smaller than that of GRK2-K220R-expressing cells (mean \pm s.d., $n=5$). To investigate the effect of a GRK2/3-specific inhibitor, we applied CMPD101. Cell pre-treatment with 30 μ M of the small-molecule GRK2 inhibitor, CMPD101, prevented the GRK2-induced cAMP signal desensitization and significantly increased the cAMP peak and the area of the cAMP transient in cells with 8.9-fold increased GRK2 levels and in cells with endogenous GRK2 levels. In contrast, CMPD101 had no effect in cells with expression of the dominant-negative GRK2-K220R mutant. Taken together, we established cellular models, which monitor GRK2-induced desensitization of beta-adrenoceptor-stimulated cAMP signaling in real-time, and visualize effects of a small-molecule GRK2 inhibitor.

81

Androgen receptor signaling guides vertebrate heart development
D. M. Duong Phu¹, S. Matysik², K. Aßfalg², M. Burczyk², M. Burkhalter¹, M. Philipp¹
¹University Hospital Tübingen, Pharmacogenomics, Tübingen, Germany
²Ulm University, Ulm, Germany

Introduction: Anomalies in cellular signaling during heart development may give rise to congenital heart defects (CHD). In fact, nearly 1 in 100 newborns is diagnosed with an abnormality in heart structure. In severe cases, surgical interventions are required early during life. Such patients with corrected heart defects are more prone to cardiovascular disease later in life.

Objectives: In spite of intensive research on the molecular and cellular causes underlying CHDs, the exact mechanistic pathways underlying regular heart development are not yet completely understood.

Material and methods: We conducted a small chemical compound screen in zebrafish embryos and identified lead compounds causing abnormal heart development. Phenotypes were verified by additional compounds targeting the same protein as the lead compound. In addition, knockdown experiments were performed. Changes in gene expression were investigated by qPCR and whole-mount *in situ* hybridization analysis.

Results: We identified the androgen receptor as a potential candidate in guiding vertebrate heart development. Pharmacological blockade of the androgen receptor caused morphological and functional defects. We observed bradycardia and edema of the inflow tract. Importantly, knockdown experiments confirmed these observations. Mechanistically we uncovered upregulation of adrenomedullin, which controls heart development and elevated expression of the close homolog of *lyve1*, a gene known to be regulated by adrenomedullin. Interestingly, the zebrafish homolog of *lyve1* was detected in the region of the inflow tract, which may be the cause for the observed congestion and/or the reduced heart rate.

Conclusion: Taken together, our data suggest an essential role for androgen receptor signaling during vertebrate heart development.

Short talks – Disease models, drug development

82

Topical application of inhaled macrophage-specific carbohydrate-coupled anti-miR-21 attenuates pulmonary inflammation and fibrosis – two hallmarks of COVID-19.
C. Beck^{1,2}, D. P. Ramanujam^{1,2}, P. Vaccarello¹, F. Widenmeyer¹, M. Feuerherd³, C. C. Cheng³, A. Bomhard¹, J. Schädler⁴, J. P. Sperhake⁴, S. Safi⁵, H. Hoffmann⁵, C. Staab-Weijnitz⁶, R. Rad⁷, U. Protzer⁸, T. Frischmuth⁹, S. Engelhardt^{1,2}

¹Institut für Pharmakologie und Toxikologie, Technische Universität München,

Medizinische Fakultät, München, Germany

²DZHK (German Centre for Cardiovascular Research), partner site Munich Heart Alliance, München, Germany

³Technische Universität München, Medizinische Fakultät, Institut für Virologie, München, Germany

⁴UKE Hamburg, Institut für Rechtsmedizin, Hamburg, Germany

⁵Technische Universität München, Klinikum rechts der Isar, Thoraxchirurgie, München, Germany

⁶Comprehensive Pneumology Center, Institute of Lung Biology and Disease, Helmholtz-Zentrum, München, Germany

⁷Institute of Molecular Oncology and Functional Genomics, Translational Cancer Center, Technische Universität München, München, Germany

⁸Baseclick GmbH, Neuried, Germany

One predominant characteristic of COVID-19 is pulmonary hyperinflammation associated with a strong leukocyte recruitment. Macrophages are key drivers in acute lung damage and pulmonary fibrosis, making them suitable targets for intervention. Here, we report on the development of RCS-21, a macrophage-specific carbohydrate-coupled inhibitor of microRNA-21 (miR-21), which acts as an anti-inflammatory and anti-fibrotic agent in the treatment of lung injury and lung fibrosis - major problems in acute and long COVID.

Small RNA-Seq identified miR-21 as the top expressed microRNA in pulmonary macrophages and one of the strongest upregulated microRNAs in a mouse model of pulmonary inflammation and fibrosis. Inhalation of a locked-nucleic acid-based 15-mer oligonucleotide inhibitor of miR-21 linked to trimeric mannose (RCS-21) achieved specific uptake via MRC1 in macrophages and prevented pulmonary dysfunction and fibrosis in these mice.

Furthermore, *in situ* hybridization showed the same degree of miR-21 upregulation in COVID-19 human lung tissue compared to control tissue. Applying RCS-21 to human precision-cut lung slices infected with severe acute respiratory syndrome coronavirus 2 (SARS-CoV-2) effectively prevented the exaggerated inflammatory immune response and improved tissue viability.

In summary, our data reports on a first-in-class ligand-coupled anti-miR-modality and its therapeutic efficacy against COVID-19. Based on the mechanism of action, our treatment is independent of current and future variants of SARS-CoV-2.

83

In vivo microRNA activity sensing of the mammalian heart at single-cell resolution reveals selective uptake of antisense oligonucleotides by injured cardiomyocytes
P. Avramopoulos¹, R. Babaei Khorzoughi¹, S. Werfel¹, Y. Sassi¹, D. Esfandyari¹, J. Ludwig¹, D. Ramanujam¹, S. Engelhardt¹

¹Technical University of Munich, Institute of Pharmacology and Toxicology, Munich, Germany

MicroRNAs are small noncoding RNAs that post-transcriptionally regulate gene expression, and many are involved in the development of diseases, including those affecting the cardiovascular system. Concerning the heart, several oligonucleotide therapeutics are currently under preclinical and early clinical development. The most significant hurdle to their widespread application is the delivery of microRNA therapeutics to the target cells and organs *in vivo*. However, methodology to quantitatively determine the efficacy of oligonucleotide therapeutics in the mammalian heart has been lacking and hampers the development of cardiac nucleic acid-based therapeutics.

Here, we report on the development of a microRNA activity sensing methodology in the mammalian heart *in vivo*, spatially resolved and at single-cell resolution, and its application to assess oligonucleotide delivery in disease.

We developed an optimized microRNA activity sensor based on fluorescence to evaluate anti-miR efficacy at the single-cell level. *In vitro* evaluation of the sensor revealed a high specificity and sensitivity in the subnanomolar range. Adeno-associated virus serotype 9 (AAV9) was then employed to deliver this optimized sensor to the cardiomyocytes of mice. The efficacy of systemically administered anti-miR was then assessed in a mouse model of acute myocardial infarction (MI) induced by ligation of the left anterior descending coronary artery (LAD) and was compared to SHAM-operated animals. Analyzing the fluorescent signal of the sensor, we did not observe any anti-miR uptake by the cardiomyocytes in SHAM mice. In contrast, we detected a significant de-repression of the sensor -as a result of anti-miR efficacy- in cardiomyocytes of mice that had previously undergone MI. Spatial analysis of the sensor's signature at the single cell level revealed a preferential uptake at the border zone compared to the remote area.

The sensor we developed is superior to the currently used methodology and would be a valuable tool to assess the efficacy of newly developed microRNA therapeutics at the single-cell level. The results of this study indicate that microRNA therapeutics are preferentially taken up by injured cardiomyocytes, a fact that calls for a reinterpretation of the targeting strategies of nucleic acid-based therapeutics in the diseased myocardium.

84

From bioinformatic profiling to the development of siRNA-loaded nanoparticle-based therapy against lung fibrosis

M. Otto^{1,2}, M. Fuchs^{1,2}, S. Rosencrantz^{2,3}, T. Weigel^{2,4}, B. Christ^{2,4}, V. Benke^{1,2}, J. Steinke¹, A. Pfanne⁵, A. Just⁵, S. Dembski^{2,4,6}, K. Sewald^{1,2,7}, G. Pohlmann^{1,2}, A. Braun^{1,2,7}, T. Thum^{1,2,5,8}, J. Fiedler^{1,2,5}

¹Fraunhofer Institute for Toxicology and Experimental Medicine (ITEM), Hannover, Germany

²Fraunhofer Cluster of Excellence for Immune Mediated Diseases, Hannover, Germany

³Fraunhofer Institute for Applied Polymer Research (IAP), Potsdam, Germany

⁴Fraunhofer Institute for Silicate Research (ISC), Würzburg, Germany

⁵Institute of Molecular and Translational Therapeutic Strategies (IMTTS), Hanover Medical School, Hannover, Germany

⁶Department Tissue Engineering and Regenerative Medicine, Würzburg, Germany

⁷Member of German Center for Lung Research (DZL), Hannover, Germany; Biomedical Research in Endstage and Obstructive Lung Disease Hannover (BREATH), Member of

Fraunhofer International Consortium for Anti-Infective Research (ICAIR), Hannover, Germany

⁸REBIRTH Center for Translational Regenerative Medicine, Hannover Medical School, Hannover, Germany

Introduction: The cure of life threatening diseases like pulmonary fibrosis is still not possible. The combination of *in silico* analyses, *in vitro* and *ex vivo* models offer strong opportunities to obtain relevant, mechanistic data and knowledge with high predictive power to further develop clinical therapeutic interventions. For some years now, RNA-based therapeutics have been the future for the modulation of molecular disease patterns.

Objectives: We hypothesized that siRNA, specifically repressing hallmarks of fibrosis like inflammation and proliferation, promote effective treatments to target fibrosis onset. In line, we aimed to promote effective packaging strategies of RNA molecules to enable precise and targeted delivery.

Materials and methods: An *in silico*-based interaction study revealed 15 repressed key factors in human lung fibroblast (MRC-5) treated with an anti-fibrotic drug and this set of

genes served as potential downstream effectors. Five selected mediators with unknown function in fibrotic signaling were specifically repressed *in vitro* using appropriate gene-specific siRNA. Functional assays testing, among others, viability, migration, and inflammatory response were performed *in vitro* under control and siRNA conditions to validate fibrotic key characteristics in MRC-5 cells. siRNA packaging optimization was performed applying six different nanoparticles to deliver fluorophore-coupled mock-siRNA and functional-siRNA into *ex vivo*-cultured 3D human precision cut lung slices (PCLS) and MRC-5 cells. Additionally, nanoparticles were nebulized using M-neb® mobile mesh nebulizer MN-300/9 (NEBUTEK).

Results: qPCR analysis revealed significant downregulation of *cafib3* and *cafib9* expression ($P < 0.01$, $P < 0.001$) after siRNA transfection highlighting efficient siRNA-mediated repression. The following analyses demonstrated that both siRNAs, interfere with fibrotic processes in MRC-5 ($P < 0.01$) without affecting viability. In both *in vitro* systems, MRC-5 and PCLS, the nanoparticles tested were highly effective and importantly, non-toxic to deliver siRNA into cells ($P < 0.001$, $P < 0.001$). The combination of anti-inflammatory siRNA and target cell-specific modified polymers provide potential new treatment strategies to target fibrosis in a tissue- or cell type-specific manner. Collectively, nebulization of siRNA-loaded nanoparticles bridges the gap to RNA-based airway-therapeutics in clinical translation.

85

Cardioprotective MicroRNAs (ProtectomiRs) as potential novel cardioprotective therapeutics for acute myocardial infarction

*P. L. Wiederanders*¹, *R. N. Nagy*², *A. Makkos*², *T. Baranyai*², *Z. Giricz*², *B. Kiss*², *L. G. Puskás*³, *N. Farago*³, *R. Schulz*⁴, *M. Gyöngyösi*⁵, *Z. V. Varga*², *A. Görbe*², *P. Ferdinandy*²

¹University of Medicine, Pharmacy, Science and Technology "George Emil Palade" of Tirgu Mures, Pharmacology, Tirgu Mures, Romania

²Cardiovascular and Metabolic Research Group, Department of Pharmacology and Pharmacotherapy, Semmelweis University, Pharmacology and Pharmacotherapy, Budapest, Hungary

³Institute of Genetics, Biological Research Center of the Hungarian Academy of Sciences, Szeged, Hungary

⁴Institute of Physiology, Justus-Liebig University of Giessen, Giessen, Germany

⁵Department of Cardiology, Medical University of Vienna, Wien, Austria

Introduction: Ischemic heart disease and its complications, like acute myocardial infarction (AMI) are still causing millions of deaths worldwide. The currently best treatment option for various types of AMI in the acute phase is an early reperfusion of the severely narrowed or blocked coronary artery. Although reperfusion seems to be a good treatment option of AMI, it also contributes to ischemia-reperfusion (I/R) injury, leading to irreversible myocardial damage which underlines the need of cardioprotective treatment options. The alterations in expression pattern of microRNAs (miRNAs) was shown to be involved in I/R injury and that modulating cardioprotective miRNAs, named protectomiRs, could be used in the development of novel therapeutics.

Objectives: We aimed to validate in an *in vitro* experiment the cardioprotective effect of previously identified potential protectomiRs which were altered after ischemic conditioning stimuli in a closed-chest porcine model of AMI.

Material and methods: We selected protectomiR candidates based on their expression pattern in ischemic conditioning in a translational porcine model and identified their rat homologues. Primary cardiomyocytes of neonatal rats were transfected *in vitro* with the selected protectomiRs at 3 different concentrations (25, 50, 100nM) or non-targeting negative control miRNAs. ProtectomiRs were either miRNA mimics to increase, or inhibitors (antagomiRs) to decrease the expression of certain miRNAs. After transfection, simulated ischemia for 6 hours, followed by reperfusion for 2 hours was performed. To quantify the cardioprotective effect, cell survival was determined by a fluorescence-based viability assay.

Results: We assessed 12 protectomiR candidates in our *in vitro* experiment, out of which 4 were miRNA mimics and 8 antagomiRs. We showed that 2 of the investigated miRNA mimics (25nM) have a significant cardioprotective effect after simulated I/R as compared to the negative control. Due to ongoing patenting, we do not disclose these protectomiRs. The other protectomiR candidates showed no improvement on cell viability compared to the control.

Conclusion: This *in vitro* validation is an important step in the development of novel therapeutics against I/R injury, contributing to a better clinical outcome for patients suffering from an acute myocardial infarction and a better understanding of cellular mechanisms involved in cardioprotection.

86

A chronic lung infection model with *P. aeruginosa* for evaluation of novel anti-infectives

K. Rox^{1,2}, *M. C. Greweling-Pils*³, *S. Häussler*⁴, *E. Medina*^{1,5}

¹German Center for Infection Research (DZIF), DZIF Partner site Hannover-Braunschweig, Braunschweig, Germany

²Helmholtz Centre for Infection Research (HZI), Department of Chemical Biology, Braunschweig, Germany

³Helmholtz Centre for Infection Research (HZI), Mouse pathology, Braunschweig, Germany

⁴Helmholtz Centre for Infection Research (HZI), Department of Molecular Bacteriology, Braunschweig, Germany

⁵Helmholtz Centre for Infection Research (HZI), Infection Immunology Research Group, Braunschweig, Germany

Introduction: *P. aeruginosa* is a critical priority I pathogen (WHO, 2017) and a serious threat for human health. Vulnerable populations (i.e. immunocompromised as well as cystic fibrosis or chronic obstructive pulmonary disease (COPD) patients), are at high risk for chronic infections *inter alia* leading to recurrent pneumonia. According to the ECDC, around 20 % of pneumonia acquired in the ICU is associated with *P. aeruginosa*. Consequently, it is of utmost importance to find novel anti-infectives that enable to control or cure chronic lung infections caused by *P. aeruginosa*.

Objectives: In this study, an animal model mimicking the clinical situation of chronic *P. aeruginosa* lung infections was developed to enable assessment of "classical" antibiotics as well as of novel approaches, i.e. targeting virulence mechanisms, to facilitate translation.

Materials and methods: *P. aeruginosa* isolates were obtained from COPD or cystic fibrosis patients and evaluated *in vitro* based on their morphology and their potential to survive in agarbeads based on the procedure described by Facchini and colleagues (J Vis Exp, 2014). Next, C57Bl/6J mice were infected intratracheally with different clinical isolates. Bacterial burden was determined on day 3 and day 7 post infection (phase I), day 3, 7, 14 and 28 (phase II + III). Inflammatory markers were assessed in phase II and III. In phase III, the positive control with inhalative tobramycin was validated. Finally, histopathological evaluation of lung tissue was performed in phase III.

Results: In phase I, 18 clinical isolates were tested. Only 6 out of 18 isolates showed a sustained bacterial burden until day 7. Next, evaluation of the 6 isolates showed that only 4 out of 6 isolates achieved a sustained bacterial burden until day 28 post infection. Moreover, only one clinical isolate showed a persistent low-level inflammatory response for markers associated with lung tissue remodeling. Finally, in phase III, tobramycin administered via inhalation showed a significant reduction of bacterial burden compared to vehicle control and was successfully validated as positive control.

Conclusion: We present a chronic *P. aeruginosa* lung infection model using a clinical isolate with inhalative tobramycin as validated positive control. The model enables three different readouts: bacterial burden, inflammatory response and histopathology. This is valuable for "classical" novel antibiotics, but also for compounds targeting virulence.

87

High-Throughput Morphological and Behavioral Screening of Zebrafish Embryos for Pharmacological and Toxicological Applications

*R. Peravali*¹, *Y. Wang*², *A. Rajendra Kumar*¹, *G. Hayot*¹, *E. Gursky*¹, *J. Stegmaier*³, *C. A. Cramer von Clausbruch*¹, *R. Geisler*¹, *T. Dickmeis*¹, *C. Weiss*¹, *U. Strähle*⁴, *C. Pylatiuk*², *M. Reischl*², *R. Mikut*²

¹Karlsruhe Institute of Technology, Institute of Biological and Chemical Systems - Biological Information Processing, Eggenstein-Leopoldshafen, Germany

²Karlsruhe Institute of Technology, Institute for Automation and Applied Informatics, Eggenstein-Leopoldshafen, Germany

³RWTH Aachen University, Institute of Imaging and Computer Vision, Aachen, Germany

⁴Karlsruhe Institute of Technology and Heidelberg University, Eggenstein-Leopoldshafen and Heidelberg, Germany

Introduction: In recent years there has been an increasing need for *in vivo* screening and testing of chemical compounds to identify novel drug candidates and in evaluating their toxic effects. Zebrafish embryos have emerged as a robust model organism for such investigations owing to their genomic similarity to humans, high fecundity, transparency of the embryos, ease of genetic manipulation and the availability of a wealth of genetic tools. Besides in-depth mechanistic studies, the zebrafish embryo model permits systematic screening of large numbers of compounds in parallel in a fast and unsupervised manner.

Objectives: Several (semi-)automated systems have been developed for chemical screening in zebrafish. However, they are often inflexible and expensive. Here we describe the development of high-throughput screening platforms that are low-cost and modular. These platforms integrate information from embryo morphology and early behavioral phenotypes to comprehensively test teratogenic and neuroactive compounds.

Materials and methods: The screening devices were custom-designed and built using commercially available imaging and robotic components. Zebrafish embryos of the AB wildtype strain were used. Matlab and C# scientific programming constructs were used for imaging, control and image analysis.

Results: The screening suite consists of four assays: **1. Morphological phenotyping** - using novel methods for feature extraction, zebrafish embryos in different multi-well plate formats can be screened automatically and in high-throughput to identify early mortality and malformations in conformance with the OECD Fish Embryo Toxicity test requirements. **2. Photomotor response** - this assay characterizes the earliest behavioral response of embryos (~1000 embryos in a 96-well plate) to a series of short light pulses. The response reveals compound effects on neurotransmitter systems. **3. Touch response** - tactile stimuli applied via a needle to a 3 day old embryo elicits an escape response. **4. Vibration startle response** - at 4 days post fertilization, embryos respond to a vibrational stimulus by executing a characteristic "C-bend" followed by an escape movement. We demonstrate the functioning of our robotic systems and show example data from selected compounds and genetic mutations.

Conclusions: We present integrated morphological and behavioral screening platforms for rapid assessment of compounds on development and neuromuscular activity using zebrafish embryos.

Clinical pharmacology – Disease models, drug development

79P001

Experimental characterization of human hepatic spheroids for enzyme induction studies in drug development

A. K. Lenich¹, J. Tuckermann², S. Ruez¹

¹Boehringer Ingelheim, DMPK, Biberach, Germany

²Ulm University, Ulm, Germany

Introduction: The current gold standard to investigate *in vitro* cytochrome P450 (CYP) enzyme induction are sandwich cultured primary human hepatocytes. However, spheroid culture has a longer stability and exhibits a more stable cellular phenotype, which is closer to the physiological situation.

Objective: Characterization of human liver spheroids, commercially available at InSphero AG, including general behavior in culture and the performance in CYP enzyme induction studies during drug development.

Materials and methods: Spheroids were purchased at InSphero AG in 96-well format. Three single donors and one multi donor (5 males, 5 females) were examined. Long-term survival of spheroids was investigated by cultivation until cell death (max. 12 weeks), measurement of spheroid size, visual assessment of morphology and analysis of albumin and LDH secretion. CYP enzyme induction was assessed by applying prototypical inducers for 48 hours and subsequent analysis of CYP1A2, CYP2B6 and CYP3A4 mRNA (via qRT-PCR) and enzyme activity (via LC-MS/MS). In comparison, sandwich cultured hepatocytes were incubated. Furthermore, monocultured spheroids (hepatocytes) and cocultured spheroids (hepatocytes, endothelial cells and Kupffer cells) of all four investigated donors were compared.

Results: Overall, spheroids were morphologically and functionally stable for at least 5 weeks in culture. CYP1A2, CYP2B6 and CYP3A4 mRNA expression was induced with a fold-change of 4-18, 2-8 and 3-35, respectively. Enzyme activity of CYP1A2, CYP2B6 and CYP3A4 was induced with a fold-change of 2-14, 5-31 and 3-23, respectively. The multi donor exhibited lower induction than the single donors. Fold induction of monocultured and cocultured spheroids was similar. In 80 % of investigations, induction in spheroids was significantly lower compared to sandwich culture.

Conclusion: CYP enzyme induction with prototypical inducers could be measured in spheroids on mRNA and enzyme activity levels. Surprisingly, no significant difference was observed in monocultured and cocultured spheroids. Lower induction of all CYP enzymes in spheroids compared to sandwich culture could potentially point to a more physiological system that is closer to the clinical situation. The possibility to have a stable, inducible long-term culture of human primary hepatocytes during drug development is of high potential.

P002

Targeted degradation of the protein kinase DYRK1A using PROTACs

G. Wilms¹, K. Schofield², C. Hulme^{2,3}, W. Becker¹

¹Uniklinik RWTH Aachen, Institute of Pharmacology and Toxicology, Aachen, Germany

²The University of Arizona, Department of Chemistry and Biochemistry, Tucson, United States

³The University of Arizona, Department of Pharmacology and Toxicology, Tucson, United States

Introduction: Increased activity of the protein kinase DYRK1A has been implicated in the pathogenesis of several human diseases. Therefore, pharmacological inhibition of DYRK1A is discussed as a therapeutic principle. Recently developed DYRK1A inhibitors are mostly ATP-competitive type-I inhibitors. However, such inhibitors usually require high intracellular drug concentrations to achieve sufficient target occupancy, which in turn increases the risk of adverse off-target effects. Besides inhibiting the catalytic activity, protein kinase functions can also be suppressed by induced degradation through hetero bifunctional molecules known as proteolysis-targeting chimeras (PROTACs).

Objectives: Our aim was to develop and characterize the first compound that can effectively and potently induce targeted degradation of DYRK1A in cultivated cells.

Materials and methods: A series of candidate PROTACs was synthesized by linking a DYRK1A inhibitor moiety to an E3 ligase-binding molecule. For screening of potential PROTACs, the amount of soluble DYRK1A was measured in HEK293 cells stably overexpressing a DYRK1A luciferase fusion protein (split luciferase assay) after treatment with the test compounds. The best hit compound was further analyzed for degradation of endogenous DYRK1A as well as cellular DYRK1A-dependent downstream functions by western immunoblot.

Results: Candidate compound DYR684 degraded >90% of endogenous DYRK1A protein levels at a final concentration of 100 nM in various cell lines (HEK293 and SH-SY5Y neuroblastoma cells). Degradation of DYRK1A was prevented by treatment with the proteasome inhibitor bortezomib. Further mechanistic studies showed that the effect of DYR684 was also blocked by pevonedistat, which inhibits the activation of cullin-RING ubiquitin ligases, or by inhibition of p97 unfoldase (CB-5083). Finally, nanomolar concentrations of DYR684 eliminated the phosphorylation of splicing factor 3B1 (SF3B1), a known downstream target of DYRK1A.

Conclusion: We have developed the first hetero-bifunctional small-molecule degrader for the protein kinase DYRK1A. DYR684 induces the targeted degradation DYRK1A and thereby interferes with DYRK1A downstream effects in cell culture.

P003

Drug Repurposing Strategy for Treatment of Idiopathic Pulmonary Fibrosis

M. Jordan^{1,2}, K. Schmidt^{1,2,3}, M. Fuchs^{1,3}, T. Thum^{1,2,3}, J. Fiedler^{1,2,3}

¹Fraunhofer Institute for Toxicology and Experimental Medicine ITEM, Hannover, Germany

²Institute of Molecular and Translational Therapeutic Strategies (IMTTS), Hannover Medical School, Hannover, Germany

³Fraunhofer Cluster of Excellence for Immune Mediated Diseases, Hannover, Germany

Introduction: Idiopathic pulmonary fibrosis (IPF) is a highly mortal chronic fibrotic interstitial lung disease and affects up to 3.5 million people globally. Pulmonary fibrosis causes scarring of the lung tissue and leads to a reduced total lung capacity and forced vital capacity. The treatment options of IPF are currently very limited with nintedanib and pirfenidone which only slows down the progression but does not lead to recovery. Via repurposing of existing compounds, an alternative to the two drugs could be found. Drug repurposing is cost-effective and shortens drug development timeline.

Objective: The aim of this study was to identify an alternative antifibrotic drug for IPF patients through *in silico*-based drug screening and to characterize therapeutic outcome in human lung fibroblasts (MRC-5) *in vitro*.

Material and methods: *In silico* drug screening aimed to investigate approved drugs which interact with the aforementioned discovered, deregulated quaking (QKI) interactome in IPF patients. The human embryonic lung fibroblasts MRC-5 cells were treated in a dose-dependent manner with the compound ITEM-Fib001 to validate the antifibrotic potential by performing various *in vitro* analyses to examine wound healing capacity, cell proliferation and viability. In addition, we executed a quantification of secreted fibrotic factors after treatment with ITEM-Fib001.

Results: The *in silico* approach revealed ITEM-Fib001 as an inhibitor of the upregulated vascular cell adhesion molecule1 in the QKI signaling axis as the most promising candidate for IPF treatment. The treatment with ITEM-Fib001 triggered reduced metabolic activity, inhibited cell proliferation, and led to decreased migratory activity in lung fibroblasts *in vitro* underlying anti-fibrotic mechanism. Moreover, the ITEM-Fib001 treatment led to repression of profibrotic galectin-3.

Conclusion: We applied high content bioinformatical transcriptome analysis combined with screening of approved drugs and discovered the drug ITEM-Fib001 as a promising agent for the treatment of IPF. Furthermore, the first *in vitro* studies confirmed the antifibrotic effect of ITEM-Fib001 on migratory activity, proliferation, and metabolism in lung fibroblasts. Therefore, further *in vitro* functional investigations and *ex vivo* experiments are planned to further validate the potential of ITEM-Fib001 in the clinical setting of lung fibrosis.

P004

Parthenolide accelerates functional nerve regeneration by VASH1/VASH2 inhibition

P. Gobrecht^{1,2}, J. Gebe^{1,2}, A. Hilla^{1,2}, G. Gisselmann³, D. Fischer^{1,2}

¹Universität Köln, Institut für Pharmakologie, Köln, Germany

²Universität Köln, Institut für Pharmakologie, Köln, Germany

³Ruhr Universität Bochum, Fakultät für Biologie und Biotechnologie, Bochum, Germany

Treatments accelerating axon regeneration in the nervous system are still unavailable in the clinic. However, in culture, parthenolide markedly promotes adult sensory neurons' axon growth by inhibiting microtubule deetyrosination. Here, we show that overexpression of vasohibins increases microtubule deetyrosination in growth cones and compromises growth in culture and *in vivo*. Moreover, overexpression of these proteins increases the required parthenolide concentrations to promote axon regeneration, while the knockdown of vasohibins or their enhancer SVBP abolishes parthenolide's effects, verifying them as pharmacological targets for promoting axon growth. *In vivo*, repeated intravenous application of parthenolide or its prodrug di-methyl-amino-parthenolide (DMAPT) markedly facilitates regeneration of sensory, motor, and sympathetic axons in injured murine and rat nerves and accelerates functional recovery. Moreover, orally applied DMAPT was similarly effective in promoting nerve regeneration. Thus, pharmacological inhibition of vasohibins facilitates axon regeneration in different species and nerves, making parthenolide and DMAPT promising drugs for curing nerve injury.

P005

Novel selenocompounds for pharmacological inhibition of ferroptosis in HT22 cells

M. Merkel¹, A. Peter-Ventura², M. Schlitzer², C. Culumsee¹

¹Philipps-Universität Marburg, Clinical Pharmacy and Pharmacology, Marburg, Germany

²Philipps-Universität, Marburg, Germany

Ferroptosis is a form of caspase-independent regulated cell death mediated by iron-dependent accumulation of reactive oxygen species (ROS), predominantly through lipid peroxidation and mitochondrial ROS formation. Mechanistically, decreased glutathione peroxidase (GPx4) activity and enhanced activation of lipoxygenases are regarded as key trigger mechanisms in ferroptosis. In particular, GPx4 was identified as the key regulator of ferroptosis, due to its unique function to reduce complex hydroperoxides thereby disrupting the chain reaction of lipid peroxidation. Since Ebselen exhibits antioxidant activity mimicking the active site of GPx4, novel Ebselen-derivatives were synthesized and characterized in this study.

Mouse hippocampal HT22 neurons were treated with erastin, hemin or RSL-3, to induce oxidative cell death. Effects of Ebselen and three selenocompounds were analyzed using

FACS for detecting lipid peroxidation and cell death. Furthermore, cell viability was determined through MTT- and ATP assays and xCELLigence measurements. Cytosolic and mitochondrial iron measurements were performed using the fluorescent probes Phen Green SK diacetate and Mito-FerroGreen, respectively.

Ebselen and the derivatives prevented oxidative cell death induced by the various substances in a concentration-dependent manner. While 10 µM of Ebselen were required to protect the HT22 cells, the novel selenocompounds were more potent and only concentrations up to 1 µM were needed to reduce lipid peroxidation and to achieve protection from oxidative cell death. Post-treatment experiments demonstrated that cell viability could be preserved, also when the selenocompounds were applied 4 hours after the induction of ferroptosis. Furthermore, the selenocompounds reduced cytosolic iron levels in the cells comparable and even stronger than Deferoxamine, and they prevented erastin-induced accumulation of mitochondrial iron.

These results showed that Ebselen exerted protective effects against ferroptosis. In comparison, the selenocompounds exhibit potent protective effects on metabolic activity, cell death, lipid peroxidation, cytosolic and mitochondrial iron accumulation at low concentrations. The pronounced protective effects of the selenocompounds occurred at 10-fold lower concentrations and with stronger protective effects compared to Ebselen. Therefore, it can be concluded, that the selenocompounds are promising for therapeutic purposes to attenuate ferroptosis.

P006

A sufficient Cav-1 level is required for the maintenance of proper vascular function via VEGFR2 in the retina

Y. Wang¹, M. Halawa¹, R. Eshwaran¹, A. Chatterjee¹, T. Wieland¹, Y. Feng¹

¹Medical Faculty Mannheim, Experimental Pharmacology Mannheim, Mannheim, Germany

Introduction: Caveolin-1 (Cav-1) is one of the essential structural proteins required for caveolae formation at the plasma membrane. Studies with Cav-1 knockout mice showed that Cav-1 is critical for angiogenesis and vascular function, especially in the retina. However, it is unclear whether a reduction in Cav-1 content already hampers the vascular function in the retina. Thus, the vascular function in the heterozygote Cav-1 deficient (Cav-1^{+/−}) mouse retinas was analyzed.

Objectives: Here, we investigated how the reduction of Cav-1 in the mouse retinas influences vascular function and identified the underlying mechanisms of action both in vivo and in vitro.

Materials and methods: Retinal morphometry was performed in 8- and 1-month old mice to assess the coverage of pericytes and endothelial cells in the retina. Immunofluorescence staining with lectin was used to study vessel formation at postnatal day (p) 5 and p10. Immunoblotting and a cell fractionation were employed to detect the expression of VEGFR2 in the retina and human umbilical vein endothelial cells (HUVECs) upon knockdown of Cav-1 with Cav-1 siRNA, respectively.

Results: Cav-1^{+/−} retinas showed significant lower pericyte coverage and higher numbers of acellular capillaries in the retina compared to controls at 8 month, but not at 1 month of age. Analysis of vascular development in the retina demonstrated a transient significant delay in retinal angiogenesis in Cav-1^{+/−} retinas at p5, which was however no longer detectable at p10. The VEGFR2 content was significantly reduced by about 25% in 8-month Cav-1^{+/−} retinas compared with WT retinas. In vitro knockdown experiments in HUVECs revealed that the loss of Cav-1 in ECs resulted in a decrease in plasma membrane VEGFR2 and a concomitant increase in VEGFR2 content in the soluble fraction.

Conclusion: Our results indicate that a certain Cav-1 level is required for the maintenance VEGFR2 localization at the plasma membrane, which is required for a proper vascular function in the retina.

P007

Bactericidal potential of drugs targeting the mevalonate pathway

L. Weber¹, A. Hagemann¹, H. Jebens¹, M. Besse², J. Schlobach², P. Rockenfeller³, A. Ehrhardt⁴, E. Stürmer^{2,5}, H. S. Bachmann¹

¹Witten/Herdecke University, Institute of Pharmacology and Toxicology, Centre for Biomedical Education and Research (ZBAF), School of Medicine, Faculty of Health, Witten, Germany

²Witten/Herdecke University, Translational Wound Research, Centre for Biomedical Education and Research (ZBAF), School of Medicine, Faculty of Health, Witten, Germany

³Witten/Herdecke University, Institute of Biochemistry and Molecular Medicine, Centre for Biomedical Education and Research (ZBAF), School of Medicine, Faculty of Health, Witten, Germany

⁴Witten/Herdecke University, Institute of Virology and Microbiology, Centre for Biomedical Education and Research (ZBAF), School of Medicine, Faculty of Health, Witten, Germany

⁵University Medical Center Hamburg-Eppendorf, Department of Vascular Medicine, University Heart Center, Translational Wound Research, Hamburg, Germany

Question: The mevalonate pathway provides targets for several drugs effective in diseases like cancer, progeria or hepatitis delta. Various infectious diseases, like African sleeping sickness, hepatitis or leishmaniasis are targeted by Farnesyltransferase inhibitors (FTIs) and in a recent study, we demonstrated the bactericidal effects of the FTIs Lonafamib and Tipifamib on different pathogenic bacteria. In order to identify possible targets, we conducted transcriptome analyses of FTI-treated *S. aureus* cells.

Furthermore, we analyzed the effect of other substances affecting the human mevalonate pathway, pointing at the identification of antibacterial points of attack as well as possible homologue target structures.

Materials and methods: Transcriptome analyses were conducted using the Illumina Sequencing platform. *S. aureus* cells were treated with Lonafamib and Tipifamib (500 µM) or control for 6 h, generating 30 Mio reads à 150 bp, paired-end. Bactericidal activity was analyzed using a time kill assay. Here, bacterial suspensions were prepared in CSB and adjusted to a 0.5 McFarland standard. Added inhibitors in different concentrations (Lonafamib, Tipifamib, Atorvastatin) were incubated for 0 h, 6 h, 12 h, and 24 h and suspensions were serially diluted and plated on CSA.

Results: The treatment of *S. aureus* by Tipifamib led to significant transcriptional changes. A downregulation was observed for transcripts encoding delta-hemolysin (*hld*), a transglycosylase (*SceD*), staphylococcal secretory antigen (*SsaA*), a choline dehydrogenase (*betA*), and several transport proteins. Significant upregulated transcripts encoded for a hemin transport system permease protein (*hrtB*), the betaine aldehyde dehydrogenase (SAOUHSC_02933) and ABC-transporters. Lonafamib did not induce significant changes in the transcriptome of *S. aureus* after 6 h. Atorvastatin, another drug targeting the human mevalonate pathway, also showed bactericidal efficacy like the FTIs, however, higher concentrations are needed.

Conclusion: Farnesyltransferase inhibitors are capable of inhibiting bacterial growth of different pathogenic strains. Transcriptome analyses of FTI-treated *S. aureus* revealed several interesting candidates for further studies. Furthermore, we could show that Atorvastatin is able to inhibit bacterial growth as well. Next, we aim to clarify whether the bactericidal effects induced by different drugs addressing the human mevalonate pathway can be attributed to yet unknown analogous bacterial structures or completely different targets

P008

PANHPVAX: Study design for dose titration of two first-in-human molecules (human papillomavirus L2 antigen with cyclic di-AMP) in a single vaccine trial

K. S. Gümüs¹, M. Kratzmann², W. E. Haefeli¹, M. Müller³, A. Blank¹

¹Heidelberg University Hospital, Department of Clinical Pharmacology and Pharmacoepidemiology, Heidelberg, Germany

²National Center for Tumor Diseases, Heidelberg, Germany

³German Cancer Research Center, Heidelberg, Germany

Introduction: PANHPVAX, a new vaccine targeting human papillomavirus L2 antigen, will be tested in a recently approved first-in-human trial (EudraCT No. 2021-002584-22). The vaccine consists of two substances entering clinical development, the thermostable vaccine antigen PANHPVAX and the novel adjuvant cyclic di-AMP (cDA). The trial design should allow independent dose titration of both molecules.

Objectives: The primary objective of the trial is to assess safety of ascending doses of PANHPVAX formulated with and without cDA as adjuvant. Further objectives are definition of the recommended phase 2 dose and determination of immunogenicity. The design must ensure a guideline adherent, safe and timely way to define the ideal composition of the two compounds with the lowest required amount of adjuvant and the lowest possible number of volunteers.

Patients and methods: A first-in-human, open-label, prime/boost trial with ascending doses of vaccine antigen and adjuvant will be conducted in healthy volunteers. Because both antigen and adjuvant are novel immunologic compounds, the trial design involves a dose escalation strategy exploring effects of different doses of both compounds.

Results: To our knowledge, this is the first trial to simultaneously examine two novel compounds used for the first time in humans. Its design allows titration of vaccine antigen and adjuvant independently to find the ideal dose composition and the lowest adjuvant dose required for vaccine success. Different antigen doses will be tested in cohorts of 15 healthy volunteers each, which will be exposed in a staggered manner. Each of these antigen dose cohorts will be divided into groups receiving either no adjuvant (N = 3) or different doses of cDA (N = 6) (Fig. 1). Study participants will receive 3 dose-identical vaccinations (at month 1, 2, and 7). The trial protocol sets safety rules for dose escalation of groups and cohorts separately. Escalation of the antigen dose requires recommendation of a Data Safety Monitoring Board (DSMB) whereas the adjuvant dose may be increased by the investigator (Fig. 2).

Conclusion: Simultaneous testing of two novel substances requires a complex titration scheme to safely and timely determine the ideal dose composition, in this case especially the lowest adjuvant dose required for vaccine success.

Fig. 1: Safety rules for prime and boost vaccination within a cohort (shown for cohort 1 as example)

Fig. 2: Trial overview (D, day; SC, steering committee)

Fig. 1

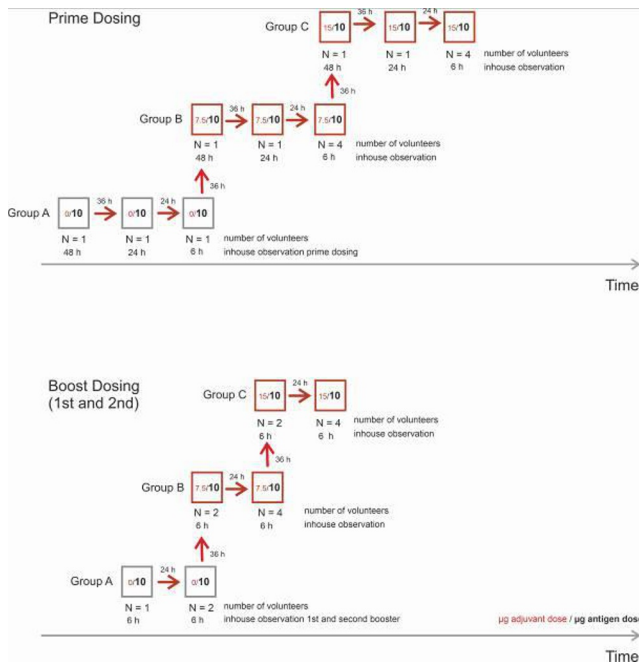
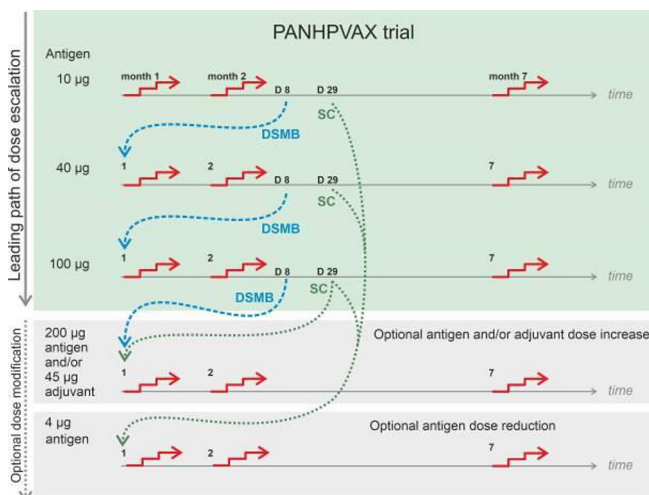


Fig. 2



P009

A novel organoid model of acute kidney injury allows for identification and characterization of drug effects on renal repair

M. Torres-Pereiro¹, L. Zhou¹, T. Worzfeld¹, H. J. Gröne^{1,2}

¹Philipps-Universität Marburg, Institute of Pharmacology - BPC, Marburg, Germany

²German Cancer Research Center (DKFZ), Cellular and Molecular Pathology, Heidelberg, Germany

Acute kidney injury (AKI) is a frequent and challenging clinical problem associated with high risk of morbidity and mortality. Dialysis is currently the only therapeutic intervention to treat AKI patients. Therefore, the development of alternative AKI treatments represents an urgent unmet medical need. In contrast to other epithelial organs such as the intestine or the skin, the kidney lacks a functionally relevant stem cell compartment driving its regeneration. Rather, renal tubular repair after damage relies on surviving renal tubular epithelial cells, which dedifferentiate into a progenitor-like state, proliferate and, eventually, re-differentiate to restore renal architecture and function. These dynamic changes in cellular differentiation are known as epithelial plasticity. The identification of drugs promoting or interfering with renal repair has so far been hampered by the lack of suitable *in vitro* models, which faithfully recapitulate the complex pathophysiological processes in AKI. Here, we established a novel three-dimensional organoid model of AKI derived from mouse and human primary kidney cortex tissue. We demonstrate that upon toxin-induced damage, these so-called tubuloids undergo characteristic morphological and molecular changes highly similar to renal proximal tubules after AKI *in vivo*. Moreover, we employ this organoid model to identify and characterize previously unknown adverse drug effects on renal repair. In summary, this novel organoid model of AKI holds promise as a tool to identify the molecular mechanisms of renal plasticity and to uncover and characterize effects of pharmacological drugs on renal repair.

P010

Caenorhabditis elegans: A simple model to screen neuroprotective effects of olive (Olea europaea L.) leaf extracts

C. Büchter¹, J. Matzner¹, C. Saier¹, W. Wätjen¹

¹Martin-Luther-University Halle-Wittenberg, Inst. of Agricultural and Nutritional Sciences, Halle (Saale), Germany

Introduction: Alzheimer's disease, Chorea Huntington and Parkinson's disease are neurodegenerative diseases in humans. Molecular mechanisms of these diseases are complex and not completely understood.

Objectives: We used the nematode *C. elegans* as a model organism to investigate the ability of different olive leaf extracts to modulate pathological mechanisms involved in the neurodegenerative diseases.

Materials and methods: *C. elegans* strains, e.g. expressing human amyloid-β in muscle cells (M. Alzheimer), GFP in dopaminergic neurons (M. Parkinson) or human huntingtin 513 (C. Huntington). Neurodegeneration was induced e.g. by 6-hydroxydopamine or overproducing of dopamine. Olive leaf extracts were generated via cascade valorization of olive leaf biomass (OLEAF4VALUE) and analyzed in comparison to isolated compounds (e.g. oleuropein, oleoanolic acid, hydroxytyrosol).

Results: The various olive leaf extracts generated during the OLEAF4VALUE project showed selective protective effects in the *C. elegans* models used: An extract containing 70% pentacyclic triterpenes (1 µg/ml) was efficient in the C. Huntington model, while its effect in the M. Alzheimer model was only poor and in the M. Parkinson model not significant. A similar protection in the C. Huntington model was achieved using hydroxytyrosol or hydroxytyrosol (100 µM), but not oleoanolic acid or oleuropein. We performed further experiments (DAF16 activation, antioxidative capacity...) to elucidate the molecular mechanisms responsible for the beneficial effects.

Conclusion: *C. elegans* can be used as a tool to identify bioactive olive leaf extracts which may have the potential to modulate neurodegenerative diseases. Due to the huge amounts of phytochemicals, olive leaves represent a valuable biomass.

Funding: This research has received funding from the Bio-Based Industries Joint Undertaking under the European Union's Horizon 2020 research and innovation programme under grant agreement n° 101023256. www.oleaf4value.eu

P011

Klf4 is a key determinant factor for AVM pathogenesis in HHT-JP mouse model

K. Banerjee¹, Y. Lin¹, J. Gahn¹, P. Gupta¹, I. Mohamed¹, M. Graupera², G. Dobrev^{3,4}, M. A. Schwartz⁵, R. Olat¹

¹Heidelberg University, Experimental Pharmacology Mannheim (EPM), European Center for Angioscience (ECAS), Medical Faculty Mannheim, Mannheim, Germany

²Josep Carreras Leukaemia Research Institute (IJC), Badalona, Spain

³Heidelberg University, Department of Cardiovascular Genomics and Epigenomics, European Center for Angioscience (ECAS), Medical Faculty Mannheim, Mannheim, Germany

⁴German Centre for Cardiovascular Research (DZHK), ..., Germany

⁵Yale School of Medicine, Yale Cardiovascular Research Center, New Haven, United States

Introduction: Vascular networks form, remodel and mature under the influence of both fluid shear stress (FSS) and soluble factors. For example, FSS at physiological levels promotes vascular stability via a synergy with Bone Morphogenic Protein 9 (BMP9) and BMP10 mediated activation of Smad1/5 pathway. Conversely, mutation of the BMP receptors *ALK1*, *Endoglin* or the downstream effector *Smad4* leads to Hereditary Hemorrhagic Telangiectasia (HHT), characterized by fragile and leaky arterial-venous malformations (AVMs). But how endothelial cells (EC) integrate FSS and BMP signals in normal vascular development and homeostasis, and how mutations give rise to vascular malformations is not well understood.

Materials and methods: We used *in vitro* loss and gain approaches: siRNA and overexpression vectors in HUVECs, ex vivo: cultures of isolated mouse lung ECs, RNA sequencing from isolated ECs from retinas, immunofluorescence, RT-PCR and *in vivo* approaches: tamoxifen inducible loss of function mice and blocking antibodies treatment.

Results: Using both *in vitro* analysis of ECs under flow and *in vivo* analysis of *Smad4* ECKO mice, we found that loss of *Smad4* in murine ECs increases cells' sensitivity to flow by lowering the FSS set point. The proliferating AVMs thus exhibit features of excessive flow-mediated morphological responses. Mechanistically, loss of *Smad4* disinhibits flow-mediated KLF4-P13K/Akt signaling to activate cyclin dependent Kinase (CDK), leading to excessive EC proliferation and loss of arterial identity. AVMs caused by *Smad4* deletion are thus characterized by chronic high flow remodeling with loss of arterial identity.

Discussion and conclusions: Our results show that loss of flow-mediated cell cycle arrest leading to loss of arterial identity due to flow-induced Klf4-P13K/Akt hyperactivation and *Cdk4/6/2* upregulation drive AVM formation upon *Smad4* loss of function in the ECs.

Clinical pharmacology – Drug transport/delivery and metabolism

P012

Characterization of the suitability of a primary cell airway model from the porcine trachea for up-take and permeations studies and as a potential model for mucociliary clearance

J. Martin¹, R. Rittersberger¹, K. Schindowski¹

¹Institute of Applied Biotechnology/ University of Applied Sciences, Biberach an der Riss, Germany

Introduction: At the end of 2019, the coronavirus SARS-CoV-2 started to spread worldwide. This virus can lead to slight cold and severe diseases like Middle East Respiratory Syndrome and Severe Acute Respiratory Syndrome. This fact increased the interest in inhalative drug administration for local treatment of respiratory diseases. Besides viruses like SARS-CoV-2, and influenza, pathogenic bacteria are the primary pathogens that cause severe respiratory diseases like pneumonia. Thus, inhalation is a potential drug delivery route to target directly the regions of interest in the respiratory system. Although, targeting the respiratory system comes up with challenges like mucociliary clearance, proteases in the mucus, and the barrier function of epithelial cells.

Objectives: The aim of this work was to establish and characterize an *in vitro* model using primary porcine tracheal epithelial cells (TEC). This model shall be used to study uptake, permeation and mucociliary clearance of for example small molecules.

Material and methods: An isolation and cultivating procedure was developed for TEC based on earlier research. RPMI2650 cells were used for comparison. Both types of cells were cultivated at the air-liquid interface (ALI) and then compared regarding different properties like transepithelial electrical resistance and fluorescein-labeled isothiocyanate-dextran permeation. Further, gene expression of different markers was characterized for TEC. In the end, first approaches were performed to enhance cilia formation in the established TEC model.

Results: Clear differences in barrier integrity and function, permeation, and morphology were observed between RPMI2650 cells and TEC. Gene expression analysis enabled further characterization of the new *in vitro* model. Different media compositions and cultivation conditions have been tested, but increasing the number of ciliated cells with beating cilia was challenging and the result was not sufficient.

Conclusion: The established *in vitro* TEC model is suitable for a variety of applications focused on respiratory drug delivery. Nevertheless, increasing the number of beating cilia would further improve this model.

P013

CYP dependent drug interactions in polypharmacy: a personalized medicine approach

J. Wozniak¹, J. C. Radermacher¹, K. Just¹, J. Stingl¹

¹Pharmacology at the University Hospital Aachen, Clinical Pharmacology, Aachen, Germany

Background: Drug-drug-interactions (DDI) in metabolic elimination pathways are common as most drugs share similar metabolic enzymes, leading to adverse drug reactions. The most important enzymes involved in metabolism of drugs are the cytochrome P450 enzymes CYP2D6, CYP3A, CYP2C19, CYP2C9, CYP2C8 and CYP1A2 [1]. DDIs and the influence of pharmacogenetics on a particular drug depend on how much a pathway is involved in drug elimination. Being a CYP substrate does not tell about quantitative influences an interacting drug will have on the substrate plasma level. To estimate DDIs in polypharmaceutical situations where several substrates of one enzyme may be administered simultaneously, the participation of a single enzymatic pathway in the overall metabolism of the drug must be known.

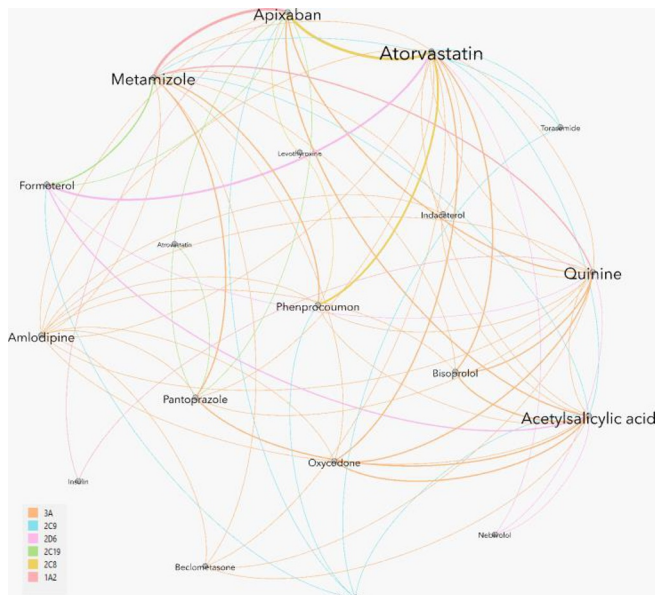
Methods: In this analysis, we used the clinical drug interaction database MediQ to derive clinically important potential drug interactions in patient polytherapy profiles (n=50) stratified for CYPs.

Results: The most frequently affected metabolic pathway was CYP3A, followed by CYP2C19, CYP2D6 and CYP2C9. The number of interactions between the shared pathways in each patient correlated only weakly with the number of drugs. It can be assumed that interaction with another substrate of a particular enzyme is clinically relevant if it is a major or minor pathway of the drug. In MediQ the levels of clinical relevance have been discriminated, reflecting the involvement of a single enzyme in the overall drug metabolism. Susceptibility of patients to side effects depends on the number of interactions but can also be stratified according to the individual metabolic pathways and its importance. We modelled the interaction as a function of the metabolic pathway's involvement in drug metabolism to create the patient dependent individual interaction score. Further analysis included the correlation of the interaction score with side effects, depending on their severity and number, showing that an individual medication interaction check depending on CYP pathways should be a crucial step in every poly-medicated patient.

1. Leone, R., et al., *Identifying adverse drug reactions associated with drug-drug interactions: data mining of a spontaneous reporting database in Italy*. Drug Saf, 2010. 33(8): p. 667-75.

Figure 1 Individual DDI analysis. The amount of influence on the drug itself due to is represented by its label size, the amount of change in the associated pathway by line thickness.

Fig. 1



P014

Comparison transporter expression in mouse hepatocytes and non-parenchymal mouse liver cells

V. Rönnpagel¹, D. Runge², A. Ullrich², M. Grube¹

¹Institute of Pharmacology, General Pharmacology, Greifswald, Germany

²PRIMACYT Cell Culture Technology GmbH, Schwerin, Germany

Primary hepatocytes are widely used as a standard *in vitro* model in preclinical drug development. Therefore, hepatocytes are well characterized in terms of expression of drug transporters and transporters of endogenous substrates. However, the predictive value of hepatocytes is limited because they alone do not fully represent the whole liver. Also, rapid changes in their gene expression under culturing conditions are problematic. Moreover, non-parenchymal liver cells (NPCs) like sinusoidal endothelial and Kupffer cells represent 40% of the liver cell population. The aim of this study was the characterization of transporter expression in NPCs in addition to hepatocytes to improve the liver *in vitro* models. We characterized Kupffer and sinusoidal endothelial cells in comparison to hepatocytes and analyzed effects of coculture on gene expression of drug transporters. To this end, hepatocytes and NPCs were isolated from mouse liver by collagenase perfusion followed by differential centrifugation. Cells were separated using magnetic activated cell sorting and specific antibodies against Kupffer (F4/80) and sinusoidal endothelial cells (CD146). For characterization of specific cell markers, the mRNA expression of reference genes and drug transporters was analyzed using a TaqMan[®] low density array. For cell culture effects, hepatocytes were seeded in a single culture at 1-3 × 10⁵ cells/well and in a coculture at 1 × 10⁵ hepatocytes/well and 3 × 10⁵ NPCs/well in 24-well plates for 2, 4 and 7 days and the expression of single genes was analyzed over time. We observed expression of drug transporters Mrp1, Mrp5, PepT2 and Oatp3A1 in NPCs that differed in part from expression in hepatocytes. NPCs showed a 55-fold higher Mrp1 and a 50-fold higher Mrp5 expression compared to hepatocytes. The NPCs hardly differed in expression of transporters, but in Kupffer cells Mrp3 expression was 6-fold higher than in sinusoidal endothelial cells. Culturing for 2 days led to a rapid downregulation of transporter expression in single culture and coculture. However, after 4 days, a slight trend towards increased expression of Bsep and Ntcp in coculture was observed. In conclusion, efflux transporters Mrp1 and Mrp5 are highly expressed in NPCs. Therefore, also NPCs could be of relevance for drug metabolism and should be included in *in vitro* preclinical testing. Coculture slightly improved transporter expression after 4 days, but could not prevent a general downregulation of expression.

P015

Development of a fast multiplexed UHPLC-MS/MS method for the determination of substrates and metabolites of the Aachen Phenotyping Cocktail to assess individual cytochrome P450 metabolism

J. P. Müller¹, P. Ziegler², K. S. Just¹, J. C. Stingl¹

¹University Hospital RWTH Aachen, Institute for Clinical Pharmacology, Aachen, Germany

²University Hospital RWTH Aachen, Institute for Occupational, Social and Environmental Medicine, Aachen, Germany

Introduction: The activity of cytochrome P450 (CYP) enzymes is crucial for the metabolism of a wide variety of drugs and toxins, thereby influencing efficacy, side-effects and toxicity. Activity of CYP enzymes is highly variable due to genetic and environmental factors. The quantification of drug metabolism capacity (phenotyping) by genotyping, usually cannot reflect individual variability caused by factors such as drug-drug interactions and health-state.

Objectives: Our aim was to establish a rapid multiplexed quantification method of a drug metabolism phenotyping cocktail to assess enzyme activity of CYP1A2 (50 mg caffeine), CYP2B6 (20 mg bupropion), CYP2D6 (12.5 mg metoprolol), CYP2C19 (10 mg omeprazole), CYP3A4 (1 mg midazolam) as well as CYP2C9 (2.5 mg torsemide) in humans.

Methods: The used probe drugs were previously validated in human cocktail studies (Basel Cocktail, Geneva Cocktail, TWIN Study Göttingen). The phenotype will be determined by measuring the kinetics and metabolic ratios of metabolite and parent drug in plasma from healthy volunteers with blood sampling over 24 hours. The study has been registered in the German Clinical Trials Register under the number DRKS00028922. Quantification will be performed by UHPLC-MS/MS. An analytical method for simultaneous measurement of all probe drugs and metabolites in plasma was developed, consisting of quick sample preparation with a simple protein precipitation step followed by centrifugation and dilution. Plasma samples are analyzed for cocktail drugs and metabolites in a single fast multi-method with a run-time of 7.5 minutes by using multiple reaction monitoring (MRM) with scheduled MRM algorithm. A specific deuterated internal standard is used for each substrate and metabolite.

Results and conclusion: The developed method showed good sensitivity, linearity, accuracy and precision over the desired concentration range. The sample preparation is fast, easy and allows a high throughput. The method is suited to assess CYP metabolism in healthy individuals or patients after oral intake of the probe drugs.

P016

Cytochrome P450-based Metabolism of Pipamperone

T. Pfaff¹, U. Walther¹

¹Rostock University Medical Center, Institute of Pharmacology and Toxicology, Rostock, Germany

Introduction: The evaluation of pharmacokinetic interactions is based on the knowledge of enzymatic metabolism e. g. by cytochrome P450 (CYP) enzymes or cellular transport processes. Research on these topics regarding pipamperone has not yet shown conclusive results in animal models or in human materials. In the current in vitro study, six different human CYP enzymes were investigated with respect to their possible involvement in the metabolism of pipamperone.

Material and methods: The human CYP enzymes used, i. e. CYP1A2, CYP2B6, CYP2C9, CYP2C19, CYP2D6 and CYP3A4 were recombinantly produced in *Pichia* cells and were commercially available. FDA-recommended clinical index substrates were used to develop optimal incubation conditions for each enzyme. The generated metabolites of index substrates and of pipamperone as well as of pipamperone itself were analyzed by GC-MS. In addition, a qualitative comparison of the metabolites from these in vitro experiments was performed with the metabolites found in urine samples from pipamperone-treated patients and A549 cell culture supernatants.

Results: Of the pipamperone concentration used in vitro, only 3 to 10 % could be detected in the form of metabolites after enzymatic reaction, while the decrease in pipamperone concentration compared with frozen control samples was 10 to 25 %. A small pipamperone decrease of 5 to 10% was also found in incubated samples without CYP. Of the enzymes tested, CYP3A4 proved to be the isoform that most strongly metabolized pipamperone, with the other isoenzymes tested producing a similar pattern of metabolites. Remarkably, the metabolite found in the CYP experiments was not detected in the patients' urine samples or in the cell culture experiments.

Conclusions: Our results obtained so far indicate that other metabolizing systems should be involved in the phase I metabolism of pipamperone in addition to mostly tested CYP enzymes. The quantitative divergence between pipamperone decrease and metabolite increase as well as between the different metabolite spectrum in the enzymatic assays and in the biological matrices indicates the need for further research on the metabolism of pipamperone.

Clinical pharmacology – Ion channels and membrane transporters

P017

Establishing an overexpression system for studying genetic variability in green tea catechins inhibition of organic anion transporting polypeptide 1A2 (OATP1A2) in vitro

P. Koczera¹, J. Müller¹, D. Gründemann², J. Stingl¹

¹University Hospital RWTH Aachen, Institute of Clinical Pharmacology, Aachen, Germany

²Faculty of Medicine and University Hospital Cologne, Department of Pharmacology, Cologne, Germany

Introduction: While green tea and dietary supplements containing its components are said to have positive effects on health with a favourable risk-benefit ratio, alteration of drug absorption, distribution and metabolism is possible by impairing activity of the transporter OATP1A2, which is considered to be responsible for the uptake of a variety of drugs [1]. OATP1A2 is expressed in various organs and tissues including the intestine. Higher catechin levels are present locally in the intestine increasing the possibility of interactions with OATP1A2 and thus interfering drug uptake. The results of a clinical study on colon cancer protective properties of green tea extract by reduction of adenoma reoccurrence in healthy participants reduced reoccurrence with an effect most significant

in men compared to women [2]. Since hormones are another endogenous substrate of OATP1A2 possible interactions and differences between the sexes are also possible.

Objectives: Establish a OATP1A2 overexpression system in cell culture with a high signal to noise ratio in order to investigate OATP1A2 activity in different genetic variants. Investigate transporter activity changes with different test substrates in the presence of green tea catechins and naringenin to evaluate possible interactions.

Methods: HEK 293 cells were transfected with a plasmid containing OATP1A2 and different drugs were utilized as test substrates to investigate uptake into the cells. Green tea catechins and naringenin were investigated and changes in intracellular drug uptake were measured via LC-MS/MS.

Results: HEK 293 cells were successfully transfected with high signal to noise ratios up to 40. Catechins and naringenin showed inhibition (100 µM EGCG 94,1%; 100 µM EGC 71,4%; 100 µM Naringenin 86,5%) and yielded lower intracellular concentrations of the substrates.

Conclusion: The uptake of different drugs by OATP1A2 is impaired by a variety of compounds found in green tea. This impairment could decrease the drug amount absorbed into the body and therefore alter its therapeutic activity. Caution for people using drugs and dietary green tea supplements is advised.

[1] Roth, M. et al., 2011. Interactions of Green Tea Catechins with Organic Anion-

Transporting Polypeptides. *Drug Metab. Dispos.*, 39, pp. 920 – 926.

[2] Seufferlein, T. et al., 2022. Green tea extracts to prevent colorectal adenomas, results of a randomized, placebo-controlled clinical trial. *Am. J. Gastroenterol.*, 117, pp. 884 – 894.

P018

TRPM7 kinase modulates insulin production and compensatory islet response to obesogenic diet

N. Khajavi¹, A. Beck², S. Zierler³, T. Müller⁴, T. Gudermann^{1,5,6}

¹Walther-Straub-Institut für Pharmakologie und Toxikologie, München, Germany

²Institut für Experimentelle und Klinische Pharmakologie und Toxikologie, Universität des Saarlandes, Homburg, Germany

³Walther-Straub-institute, München, Germany

⁴German Center for Diabetes Research (DZD), Neuherberg, Germany

⁵German Center for Lung Research, München, Germany

⁶Munich Heart Alliance, German Center for Cardiovascular Research, München, Germany

The melastatin transient-receptor-potential-7 protein (TRPM7), harboring a cation channel and a serine/threonine kinase, has been implicated in numerous cellular processes including cell cycle regulation, growth, and proliferation. Here, we show that selective deletion of *Trpm7* in β -cells disrupts insulin secretion and leads to progressive glucose intolerance. Our results indicate that the impairment of glucose metabolism in β -cell-specific *Trpm7* knockout mice (β *Trpm7* KO) is caused by an impaired kinase function in this mouse model. Strikingly, mice with a genetic loss of TRPM7 kinase activity (*Trpm7R/R*) exhibit the same metabolic phenotype as β *Trpm7* KO mice. The diminished insulinotropic response in *Trpm7R/R* mice can be attributed to decreased insulin synthesis due to downregulation of gene programs implicated in insulin production including pancreatic duodenal homeobox 1 (*Pdx1*) and insulin-2 precursor (*Ins2*). Accordingly, *Trpm7R/R* mice fed a high-fat diet develop profoundly impaired glucose tolerance accompanied by hyperglycemia and decreased plasma insulin. These detrimental glucoregulatory effects are engendered by reduced compensatory β -cell hypertrophy and proliferation due to a mitigated AKT/ERK signaling pathway linked to the dysfunctional TRPM7 kinase moiety. Taken together, our data identify TRPM7 kinase as a novel key regulator of insulin synthesis, β -cell dynamics, and glucose homeostasis under conditions of diet-induced obesity.

P019

The importance of stereoselectivity in drug membrane transporter inhibition

L. Gebauer¹, J. Brockmüller¹, M. Rafehi¹

¹Institute of Clinical Pharmacology, University Medical Center Göttingen, Göttingen, Germany

Introduction: Stereoselectivity is a most prominent feature in receptor binding and drug metabolism. However, in drug membrane transport, it has not been studied in detail yet. Solute carriers, including the organic cation transporters (OCTs), are important for the absorption, distribution and elimination of many drugs and other substances. Inhibition of such drug membrane transporters may thus be an important mode of drug-drug interactions that could lead to therapeutic failure or cause severe adverse effects. Stereospecific differences in the inhibition of membrane transporters could be a reason to prefer enantiopure drugs over their racemic mixtures. In addition, studying stereospecificity could contribute to a better molecular understanding of the transporter-substrate interactions.

Objectives: In this study, we aimed to characterize the extent of stereoselectivity in the inhibition of OCT1, 2, and 3. We tested 31 pairs of enantiomers for differences in OCT inhibition. The 31 chiral inhibitors investigated here covered a broad range of different drug classes.

Results: Using several model substrates in screening OCT inhibition, the majority of the analyzed enantiomers showed little to no differences in their OCT inhibition. Particularly,

OCT1 inhibition was characterized by almost no stereoselectivity, whereas OCT2 was stereoselectively inhibited by amisulpride, citalopram, pramipexole, and verapamil with an up to 4-fold difference between enantiomers. OCT3, on the other hand, showed remarkably high stereospecific inhibition by the muscarinic acetylcholine receptor antagonist tolterodine. Here, (*R*)-tolterodine showed a 10-fold stronger inhibition than the respective (*S*)-enantiomer. Other drugs, such as palonosetron, atomoxetine, and verapamil, showed stereoselective inhibition of OCT3 as well.

Conclusions: Stereoselectivity in OCT inhibition was highly substance- and transporter-specific and appears to be rather the exception than the rule. Considering that for chiral drugs one enantiomer is usually more active than the other, this data further substantiates that the less active enantiomer has also the potential to significantly interfere with unintended biological targets.

P020

Differential modulation of ventricular Ca^{2+} currents by absence of $G_{\alpha 2}$ or $G_{\alpha 3}$ in a murine $\beta 1$ -transgenic heart failure model

N. Katnabji¹, J. Matthes¹

¹University of Cologne, Pharmacology, Cologne, Germany

Introduction: Lack of $G_{\alpha 2}$ ($G_{\alpha 2}^{-/-}$) aggravates murine cardiomyopathy caused by cardiac $\beta 1$ -adrenoceptor overexpression ($\beta 1$ -tg), while lack of $G_{\alpha 3}$ ($G_{\alpha 3}^{-/-}$) is preventive. L-type Ca^{2+} channel (LTCC) activity is altered in heart failure, modulated by β -adrenergic signaling and differentially affected by lack of either the $G_{\alpha 2}$ or the $G_{\alpha 3}$ isoform of Gi-proteins. Thus, altered Ca^{2+} currents may be involved in isoform-specific Gi effects on cardiomyopathy in $\beta 1$ -tg.

Objective: To study ventricular L-type Ca^{2+} -current density (I_{CaL}) in wildtype, $\beta 1$ -tg, and $\beta 1$ -tg/ $G_{\alpha 3}^{-/-}$ and $\beta 1$ -tg/ $G_{\alpha 2}^{-/-}$ mice.

Materials and methods: We isolated ventricular myocytes from male mice at 4-5 months of age, for the study of the effects of $G_{\alpha 2}^{-/-}$ and 10-11 months of $G_{\alpha 3}^{-/-}$. Whole-cell I_{CaL} was recorded under basal conditions and after preincubation with 1 μ M isoproterenol (iso) at RT. Data are given as mean \pm SD.

Results: Peak I_{CaL} density was significantly reduced in myocytes from $\beta 1$ -tg compared to wildtype mice (-5.5 \pm 1.6 vs. -8.1 \pm 1.6 pA/pF). In $\beta 1$ -tg mice lacking $G_{\alpha 3}$, I_{CaL} was raised towards wildtype level (-7.3 \pm 1.5 pA/pF). I_{CaL} activation was significantly shifted towards more depolarized potentials in $\beta 1$ -tg mice compared to wildtypes ($V_{0.5}$: -7.7 \pm 2.8 vs. -11.3 \pm 2.5 mV), while it was pretty normal in $\beta 1$ -tg/ $G_{\alpha 3}^{-/-}$ mice (-10.3 \pm 5.0 mV). As expected, iso significantly increased I_{CaL} density and caused a left-shift of activation in wildtype myocytes (to -14.3 \pm 5.6 pA/pF and -17.0 \pm 4.0 mV, respectively). These effects were significantly attenuated in both $\beta 1$ -tg (-7.4 \pm 1.9 pA/pF and -9.7 \pm 4.6 mV) and $\beta 1$ -tg/ $G_{\alpha 3}^{-/-}$ mice (-8.5 \pm 2.7 pA/pF and -12.7 \pm 5.2 mV). Effects observed in mice lacking $G_{\alpha 2}$ were opposite. I_{CaL} also appeared to be reduced in $\beta 1$ -tg at younger ages, but the absence of $G_{\alpha 2}$ had no effect on this. Furthermore, both $\beta 1$ -tg and $\beta 1$ -tg/ $G_{\alpha 2}^{-/-}$ showed a significantly more positive I_{CaL} activation potential. In $\beta 1$ -tg mice lacking $G_{\alpha 2}$, I_{CaL} response to iso was not impaired but similar to wildtypes (e.g. peak I_{CaL} increase from -5.8 \pm 2.1 to -10.2 \pm 2.6 pA/pF).

Conclusion: It is tempting to speculate that in $\beta 1$ -adrenoceptor overexpressing mice $G_{\alpha 3}$ -deficiency is cardioprotective, restoring basal LTCC function and attenuating β -adrenergic effects, whereas $G_{\alpha 2}$ -deficiency is detrimental, neither restoring basal I_{CaL} nor protecting the cell from β -adrenergic stimulation.

P021

Optimization of the conditions for visualization of a homodimeric assembly state of voltage-gated ion channels by BN-PAGE and high-resolution clear native PAGE

L. Li¹, G. Schmalzing¹

¹Institute of Clinical Pharmacology, Medical Faculty of the RWTH Aachen University, Aachen, Germany

Voltage-gated Na^{+} channels are integral membrane proteins consisting of a principal pore-forming α subunit (Nav1.1-Nav1.9) in complex with one or two smaller auxiliary β subunits (Nav β 1-Nav β 4). The Nav1.5 channel encoded by the SCN5A gene plays a crucial role in generating and propagating the cardiac action potentials. As such, Nav1.5 is an important target for class I antiarrhythmic drugs, but also for off-target drug side effects in general. There is growing evidence including our own work (A. Rühlmann et al, Brit. J. Pharmacol. 177, 4481-4496, 2020) that Nav α subunits can exist as obligate homodimers and exhibit coupled gating. Here we screened for optimal conditions to detect the oligomeric state of the human hNav1.5 protein expressed in *Xenopus laevis* oocytes by blue native and high-resolution clear native polyacrylamide electrophoresis (BN- and hCN-PAGE). Among various non-ionic detergents tested, none was better than digitonin in terms of extraction efficiency and preserving the homodimeric state of hNav1.5. Various N- and C-terminally fused fluorescent proteins including different versions of enhanced GFP (conventional, monomeric, superfolder, ultrasuperfolder), mGreenLantern and ZsGreen were equally well suited for in-gel detection of hNav1.5 homodimers. Co-expressed auxiliary hNav β 1-4 subunits enhanced the expression of the hNav1.5 α subunits. However, the interaction of the co-expressed hNav β 1-4 subunits with the hNav1.5 subunit was too weak to allow the visualization of hNav α - β complexes in the native PAGE gels. Further experiments were performed to investigate the gel running conditions required to sufficiently negatively charge the Nav1.5 proteins to allow them to migrate in the electric field. We anticipate that our results will enable us to study the oligomeric state of splice isoforms and pathogenic loss-of-function and gain-of-function mutations of hNav1.5 and their impact on coupled gating.

Financial supported by the Interdisciplinary Centre for Clinical Research of the Medical Faculty of RWTH Aachen University (IZKF TN1-8/IA 532008) and the German Research Foundation (Sino-German project SCHM 536/12-1).

P022

BK contributes to resistance against diet-induced obesity through functions in hypothalamic neurons and brown adipocytes

J. Brueckner¹, D. Spaehn¹, S. Fromknecht¹, P. Krefl¹, L. Wolf¹, L. Matt¹, R. Lukowski¹

¹University of Tuebingen, Institute of Pharmacy, Department of Pharmacology, Toxicology and Clinical Pharmacy, Tuebingen, Germany

Introduction: Obesity and its associated secondary health issues present a growing global health burden. A genome-wide association study linked expression of voltage- and Ca^{2+} -activated K^{+} channels of big conductance (BK) to morbid obesity [1]. Global BK knock-out (KO) mice are protected from diet-induced obesity (DIO). This protection is partly replicated by total brain and white adipocyte-specific conditional KO (cKO) of BK [2].

Objectives: To study BK's role in a subset of orexigenic hypothalamic nuclei and in brown adipocytes for the development of DIO and associated cardio-metabolic impairments.

Materials and methods: BK was conditionally deleted from orexigenic AgRP-positive hypothalamic neurons (AgRP-KO) and brown adipocytes (Ucp1-KO) by mating mice carrying floxed BK alleles to the respective Cre driver mouse models. cKO mice and respective controls (CTR) were subjected to control and high-fat diet (HFD) for 18 weeks. Body weight development was analysed over time and body composition at the end of the feeding. Blood plasma and tissue samples as well as glucose tolerance tests were used to assess the metabolic status of these animals. Further, we used an AgRP-positive (AgRP⁺) neuronal cell line as well as primary brown adipocyte cultures to examine BK function *in vitro*.

Results: Female AgRP-KO showed an 18% reduced body weight increase under HFD compared to CTR while males were not protected against DIO. Blood lipid and body fat depot composition were not different between AgRP-KO and CTR. However, HFD-fed AgRP-KO females displayed higher blood sugar levels after i.p. glucose administration. In AgRP⁺ neurons of CTR mice and in a AgRP⁺ hypothalamic cell line, the presence of BK was demonstrated by western blot and immunofluorescence, respectively. Compared to controls, Ucp1-KO males, but not females accumulated significantly reduced amounts of body fat during HFD. In *in vitro* cultures of primary brown adipocytes, blocking BK with paxilline or ibertoxin provoked a cytosolic Ca^{2+} signal that was abolished when maintaining the cells in Ca^{2+} -free medium. Furthermore, pre-treatment with paxilline significantly augmented Ca^{2+} -influx upon adrenergic stimulation.

Conclusion: BK in AgRP⁺ hypothalamic neurons and brown adipocytes clearly contributes to DIO resistance by differing mechanisms in both sexes. Next, we aim to further investigate altered phenotypes *in vivo* and BK's function(s) on a cellular level.

[1] Jiao *et al.*, 2011; [2] Ilison *et al.*, 2016

P023

Anti-hormonal therapy provokes BK_{Ca} channel-dependent K^{+} dynamics in human and murine breast cancer cells

S. Maier^{1,2}, H. Bischof¹, D. Grob¹, D. Stojkov³, S. Madden⁴, P. Ruth¹, M. Schwab^{2,5}, H. Brauch², W. Schroth², R. Lukowski¹

¹Department of Experimental Pharmacology and Pharmacology, Toxicology and Clinical Pharmacy, Tuebingen, Germany

²Dr. Margarete Fischer-Bosch-Institute of Clinical Pharmacology, Stuttgart, Germany

³Institute of Pharmacology, Bern, Switzerland

⁴RCSI Division of Population Health Sciences, Dublin, Ireland

⁵Departments of Clinical Pharmacology, and of Biochemistry and Pharmacy, Tuebingen, Germany

Background: Calcium (Ca^{2+})-activated potassium (K^{+}) channels of big conductance (BK_{Ca}) are strongly expressed in breast cancer (BC) [1]. In murine BC models, the pore-forming α -subunit of the BK_{Ca} channel promotes breast carcinogenesis. Interestingly, instead of inhibiting, treatment by low-dose anti-estrogens induced BC cell proliferation in BK_{Ca}-expressing cells *in vitro*. Considering recurrence-free survival (RFS) of estrogen receptor (ER)-positive BC patients treated with tamoxifen (TAM), higher expression of BK_{Ca} together with ER status contributed in worse clinical outcomes [2].

Objective: To investigate the underlying molecular mechanisms by which anti-estrogens affect BK_{Ca} channel activity and thus K^{+} - and Ca^{2+} homeostasis, thereby driving proliferation in human and murine BC cell models.

Methods: Intracellular K^{+} ($[K^{+}]$) and Ca^{2+} concentrations ($[Ca^{2+}]$) were monitored by genetically encoded potassium ion indicators using Förster Resonance Energy Transfer (FRET)-based [3] or Fura-2AM single cell live imaging, respectively. Kaplan-Meier survival analysis of BC patients (BreastMark database) was performed to evaluate the correlation of BK_{Ca} subunit expression levels and clinical outcome.

Results: Our results imply that BK_{Ca} channel activity is targeted by active TAM metabolites independent of BC cells' ER status. Highly BK_{Ca}-expressing human BC cell lines (BK_{Ca}^{high}) responded immediately to TAM metabolites by depletion of $[K^{+}]$, while BK_{Ca} low expressing cells (BK_{Ca}^{low}) exhibit minor responses. Additionally, the BK_{Ca}-specific

inhibitor paxilline reduced TAM-specific effects. Because BK_{Ca} activation and [Ca²⁺]_i dynamics are directly linked, [Ca²⁺]_i in BC cells was monitored resulting in TAM-induced elevation of [Ca²⁺]_i. In addition, Kaplan-Meier analysis revealed a clinical relevance of the BK subunit β₁. *In vitro*, overexpression of β₁-subunit was associated with a decreased loss of [K⁺]_i suggesting that in addition to the α-subunit, other auxiliary subunits may contribute to influence [K⁺]_i homeostasis as well as tumorigenesis and proliferation in BC cells.

Conclusion: Anti-estrogens have a BK_{Ca}-mediated effect on [K⁺]_i homeostasis *in vitro*. Thus, we suggest that established BC treatment regimens could be improved by subunit expression analysis and targeted pharmacological inhibition of the BK_{Ca} channel.

References:

1. Huang *et al.* Jan, 2014
2. Mohr *et al.* 2020
3. Bischof *et al.* 2017

P024

K_{Na} Slick channel in myo-fibroblast function and post-infarction induced cardiac remodeling

J. Yang¹, A. Roslan¹, M. Cruz Santos¹, S. Schanz¹, L. Birkenfeld¹, H. Bischof¹, R. Lukowski¹

¹Institute of Pharmacy, University of Tübingen, Tübingen, Germany

Background: Acute myocardial infarction (MI) leads to ventricular dysfunction and is associated with poor prognosis. Scar formation in the infarcted area in post-MI hearts is promoted by the conversion of resident cardiac fibroblast (RCF) to cardiac myofibroblast (CMF), which is implicated in excess deposition of extracellular matrix (ECM) proteins, such as collagen. The Na⁺-activated K⁺ channel (K_{Na}) Slick (Slc12.1) was previously detected in cardiomyocyte (CMs) mitochondria, and its activity was shown to confer the protection afforded by anesthetic pre-conditioning (APC) in murine CMs *ex vivo*. Interestingly, Slick transcripts are highly abundant in RCF, but their role in post-MI hearts is completely unclear.

Objective: Our study examines whether and how Slick affects the function of RCF and thereby the cardiac post-injury RCF-to-CMF conversion, excessive ECM deposition, and/or chamber remodeling.

Method: *In vitro*: RCFs were purified from global Slick deficient (KO) and proficient (WT) murine hearts. Subsequently, Förster resonance energy transfer (FRET)-based live-cell imaging based on genetically encoded K⁺ indicators (GEPH) was applied to visualize Slick-dependent K⁺ dynamics in real-time.

In vivo: An open- (acute) and closed-chest (chronic) cardiac ischemia/reperfusion (I/R) *in situ* model was applied to address whether infarct size formation and/or the amount of myocardial fibrosis after 4 weeks of reperfusion are dependent on Slick, respectively.

Results: *In vitro*: Strong Slick mRNA expression was detected in freshly isolated murine RCFs. Immunoblotting and immunofluorescence staining further confirmed the presence of Slick channels in this cardiac cell type. Opening of Slick channels resulted in a massive cytosolic K⁺ loss that correlated with an increased expression of alpha-smooth muscle actin (α-SMA) in WT *versus* Slick KO RCF.

In vivo: Lack of Slick did not affect infarct size formation nor the acute CM death in I/R-exposed hearts *in vivo*. However, our preliminary findings suggest that Slick deficiency limits the fibrotic scarring in post-MI hearts.

Conclusion: Our study validates the presence of Slick channels in RCF. Slick-dependent changes in K⁺ may contribute to the injury-induced RCF-to-CMF conversion. Interestingly, Slick activity, possibly by a CM-independent function of the channel, seems to promote myocardial fibrosis in post-MI hearts.

Clinical pharmacology – Pharmacoepidemiology and drug safety

P025

PK/PD Modeling for Deriving Health Based Exposure Limits

E. Zeller¹, C. Sehner¹

¹Boehringer Ingelheim Pharma GmbH & Co. KG, Nonclinical Drug Safety, Biberach, Germany

In the pharmaceutical industry, Health Based Exposure Limits (HBELs) are set for active pharmaceutical ingredients (APIs) for controlling potential exposure on a safe level. This includes for example Occupational Exposure Limits (OELs) to control worker exposure and Permitted Daily Exposure (PDE) to control cross-contamination during manufacturing in shared facilities. HBELs are set using all available pharmacological and toxicological data from nonclinical as well as clinical studies. They are calculated using a Point of Departure (POD), e.g., the NOAEL for a critical effect, and applying different adjustment factors. HBELs are also set for biological products such as antibodies. However, for those it is often difficult to set these limits, as they generally have very flat dose-response

curves, have long half-lives, are not administered daily, and may be administered by unusual routes such as intravitreal or intrathecal. In addition, in early phases of development only limited nonclinical and no clinical data are available. Here, an approach is presented, how PK/PD modeling is used to determine the minimum anticipated biological effect level (MABEL), used for setting safe limits.

P026

Patient satisfaction in randomized controlled trials (RCTs) and pharmacy based (PB) studies investigating aspirin, ibuprofen, and the combination aspirin, paracetamol and caffeine (APC) for the treatment of acute migraine.

T. Weiser¹, H. Gräter¹, M. Plomer¹

¹Sanofi Deutschland, CHC Medical Affairs, Frankfurt am Main, Germany

Introduction and objective: OTC analgesics are first-line therapy for treating acute migraine [1]. For differentiation, patients' perspective on treatment may be useful. We compared patient ratings of treatment satisfaction between RCTs and PB studies investigating the same active ingredients.

Methods: Studies were included when they contained data on patient-reported satisfaction measured on four- or five-point verbal rating scales. For RCTs, percentages of the top two categories ("excellent/good" or "very good/good") were calculated for verum and placebo (PLA). Treatment benefit (delta) was verum minus PLA.

Results: Data were found for effervescent aspirin (3 RCTs, 1 PB study; [2-5]), ibuprofen (1 RCT, 1 PB study [2,6]), and APC (4 RCTs, 1 PB study [7-9]). In RCTs, 40.3% of patients were satisfied with aspirin (PLA: 22.4%, delta: 17.9%), 38.2% with ibuprofen (PLA: 16.7%; delta: 21.5%), and 59.3% with APC (PLA: 22.9%; delta: 36.4%). Patient satisfaction was higher in the PB studies: aspirin: 76.8%; ibuprofen: 75.6%; APC: 93%. See figure for details.

Discussion: As expected, satisfaction was lower in RCTs than in PB studies (e.g. due to selection bias based on treatment experience and the unblinded design of the latter). Aspirin and ibuprofen scored less favorable than APC in RCTs, as well as in PB studies. Since patients use their favorite product in the PB studies, equally high satisfaction rates would be expected. However, satisfaction was different, i.e. lowest with ibuprofen and highest with APC. A PB study with the combination of ibuprofen plus caffeine showed satisfaction in 85% of migraine patients giving reason to speculate that also in RCTs this combination will be superior to the above-mentioned treatments [10].

Sponsored by Sanofi

Fig. 1

Figure

	RCT			PBPS
	Verum	Placebo	Delta (Verum-Placebo)	Verum
Aspirin	204/526[2,3,4] 40.3%	123/548[2,3,4] 22.4%	17.9%	227/296[5] 76.8%
Ibuprofen	81/211[3] 38.2%	37/222[3] 16.7%	21.5%	139/184[6] 75.6%
Aspirin/paracetamol /caffeine	594/1001[7,8] 59.3%	167/729[7,8] 22.9%	36.4%	190/204[9] 93.0%
Ibuprofen/caffeine	---	---	---	136/160[10] 85.0%

Patient satisfaction in RCTs and PBPSs. Patient in the two top satisfaction categories are divided by the total number of patients in the respective trial arms to give the percentages.

References: [1] Haag *et al.* (2011) *J Headache Pain* 12:201ff; [2] Diener *et al.* (2004) *Cephalalgia* 24:947ff; [3] Diener *et al.* (2004) *Eur Neurol* 52:50ff; [4] Lange *et al.* (2000) *Cephalalgia* 20:663ff; [5] Göbel *et al.* (2007) *Schmerz* 21:49ff; [6] Krall *et al.* (2007) *Pharm Zg* 152:86ff; [7] Lipton *et al.* (1998) *Arch Neurol* 55:210ff; [8] Diener *et al.* (2005) (only migraine patients) *Cephalalgia* 25:776ff; [9] Gaul *et al.* (2013) *SpringerPlus* 5:721ff; [10] Gaul *et al.* (2022) *Frontiers Neurology*, 13: 902020

P027

Onset of action of a conventional spasmolytic in patients with menstrual pain and their treatment satisfaction - Real world evidence data from a pharmacy-based patient survey

P. Nonnenmacher¹, H. Weigmann¹, S. Landes¹, T. Weiser¹

¹Sanofi Deutschland, CHC Medical Affairs, Frankfurt am Main, Germany

Introduction and objective: Dysmenorrhea is one of the most common gynecological dysfunctions in women of childbearing age and is characterized by abdominal pain during menstruation. For the treatment, spasmolytic medications can be used. However, as there are only limited data available on women's perceived effectiveness, tolerability, and satisfaction of such interventions in real life, data of a pharmacy-based patient survey were analyzed.

Patients and methods: Pharmacy customers purchasing a fixed-dose combination product (HBB+) of 10 mg hyoscine butylbromide and 500 mg paracetamol were offered to participate in a survey. The survey captured amongst others the time to perceived onset of pain relief quantitatively (categories: 0–5, 6–15, 16–30, 31–45, 46–60, >60 min) as well as the perceived onset of action qualitatively (categories: very fast, fast, moderate, slow). In addition, participants were asked about treatment satisfaction, treatment tolerability, as well as their willingness and reason for recommendation to others.

Results: Of 641 participants completing the survey, 329 females (mean age 32.8 ± 10.1 years) used HBB+ to treat their menstrual pain and thus were subject for further analysis.

The majority (93.6%) of these women reported an onset of pain relief within 1 hour after HBB+ intake, with 50.5% resp. 82.7% experiencing an onset within 30 min resp. within 45 min. Besides, 70.2% of the women using HBB+ for their menstrual pain rated the onset of action as very *fast/fast*. Interestingly, of those rating the onset of action as very *fast* 52.8% perceived relief within 15 min and 36.1% within 16 – 30 min. Of those, rating the onset of action as *fast* 10.3% perceived relief within 15 min, 48.7% within 16 – 30 min and 31.8% within 31 – 45 min.

Overall, most women (96.6%) were very *satisfied/satisfied* with the effectiveness of HBB+ in menstrual pain, with 97.3% rating tolerability as very *good/good*. 97.3% of the women would recommend HBB+ to others. The top-3 reasons (multiple answers possible) for recommendation were the very *good pain relief* (87.5%), very *good tolerability* (75.0%) and very *fast effect* (55.9%).

Conclusion: HBB+ provides fast pain relief in patients with menstrual pain, with over 80% perceiving onset of action within 45 minutes. This, together with very good tolerability, leads to high patient satisfaction. Therefore, HBB+ constitutes a valuable option in the treatment of dysmenorrhea.

The study was sponsored by Sanofi.

Clinical pharmacology – Biotransformation and toxicokinetics

P028

Prediction of dutasteride disposition in zebrafish embryos using a toxicokinetic modeling approach

B. Him-Derksen¹, C. Ryu², H. Cho², Y. J. Kim², G. Hempel¹

¹University of Muenster, Institute for Pharmaceutical and Medicinal Chemistry, Münster, Germany

²Korea Institute of Science and Technology (KIST) Europe, Saarbrücken, Germany

Introduction: In the last 20 years, the zebrafish and its embryos gained a lot of interest as animal models especially in toxicokinetics. Reasons are i.e. the genetic conformity with the human genome and the easy and cost-effective handling of the embryos [1]. However, to extrapolate a certain effect of a xenobiotic to the embryos the (toxico-)kinetic behaviour must be known. For this reason, we built a pharmacokinetic model to predict the concentration after medium exposure in zebrafish embryos and choose dutasteride as example substance.

Objectives: This work aims to predict the disposition and time course of dutasteride in zebrafish embryos for pharmaco- or toxicokinetic analysis.

Material and methods: Based on a published model for zebrafish embryos we built a two-compartment model including the yolk sac and the embryo itself using GNU MCSim[3,4]. First estimations of different model parameters were done using Quantity Structure-Activity Relationship- (QSAR) and Virtual in vitro distribution (VIVD) model approaches [5,6]. Furthermore, we created an estimation method for absorption rate constant estimating the absorption rate only with a less amount of data. We also integrated a plastic adsorption model to account for the adsorption to wells [7]. Parameter calibration was done using the Marcov Chain Monte Carlo (MCMC) algorithm. The performance of the calibrated model was checked against datasets of either 30 or 60 embryos per exposure vessel treated with different concentrations of dutasteride. In addition to the actual fitting process, other optimization approaches were tested in order to improve the model quality.

Results: The model is able to describe the toxicokinetic profile in zebrafish embryos for dutasteride at different exposure concentrations. Mean absolute prediction error (MAPE) of the final model were 15.2 % for the 1000 nM experiment 9.09 % for the 500 nM experiment, 14.45 % for the 100 nM experiment, 19.92 % for the 50 nM experiment and 38.69 % for 5 nM experiment.

Conclusion: It was possible to build a simple and dynamic model for zebrafish embryos which also accounts for decrease of medium concentration due to plastic adsorption. Also, we could show that initial predictions, in case of dutasteride, serve as a good starting point. This finding must be proved by extending the model to other xenobiotics.

References:

- [1] Cassar S et al. Chem Res Toxicol. 2019;33(1):95-118.
- [2] Siméon S et al. Reprod Toxicol. 2020;93:219-229.
- [3] Bois F. Bioinformatics. 2009;25(11):1453-1454.
- [4] Fischer F et al. Environ Sci Technol. 2018;52(22):13511-13522.
- [5] Fisher C et al. Toxicol in Vitro. 2019;58:42-50.
- [6] Spacie A et al. Envir Toxicol and Chem. 1982;1(4):309-320.

Toxicology – Food toxicology

P029

How safe are hemp-based food products in Germany? Suggesting new exposure limits for cannabinoids.

F. Steinmetz¹, C. Conerney², J. Wakefield³

¹Delphic HSE, Schiphol, Netherlands

²Delphic HSE, Farnborough, United Kingdom

³Delphic HSE, Shatin, Hong Kong

Hemp-based food products and supplements have gained popularity within recent years in Europe. Apart from the non-psychoactive cannabinoid, cannabidiol (CBD), these products may also contain Δ^9 -tetrahydrocannabinol (THC), which can be of concern due to its impairing properties. The currently accepted limit for THC in hemp in the European Union is 0.3%. As many hemp-based products have been withdrawn from the German market within recent years, this study aims to investigate the current safety limit and potential concerns based on available analytical data. Furthermore, safety of natural CBD exposure is assessed based on clinical data and history of safe use. Exposure limits for food products have been suggested as 0.8 mg/kg bw/day for CBD and 0.012 mg/kg bw/day for THC. For CBD supplements with appropriate labeling, a CBD exposure up to 1.67 mg/kg bw/day could be justifiable. Regarding THC, only few products exceeded the limit moderately. Overall, risks for adverse/impairing reactions are considered low for hemp-based food products on the German market. Regarding a recreational cannabis market, as planned by the current government, higher limits and sufficient risk mitigation strategies must be applied.

P030

Loss of monoterpenes by polystyrene-sorption influences the toxic potential towards *Salmonella typhimurium*

T. Jochum¹, S. Stegmüller¹, E. Richling¹

¹University of Kaiserslautern-Landau, Food Chemistry and Toxicology, Kaiserslautern, Germany

Introduction: Sorption of test compounds by cell culture equipment made of polystyrene (PS) can deplete substance concentrations especially for molecules with log K_{ow} >3 in serum free assays. Losses due to sorption can lead to an underestimated toxicity^{1,2}.

Monoterpenes such as (R)-(+)-limonene (Rlim; log K_{ow} =4.57) and β -myrcene (β Myr; log K_{ow} =4.33) are known to be sorbed by various polymers whereas the sorption of monoterpenoids such as (\pm)-linalool (Lin; log K_{ow} =2.97) was expected to be much lower^{3,4}. In the past, none of these substances showed indications for mutagenicity or genotoxicity in various *in vitro* assay⁵⁻⁷.

Objectives: The influence of PS-sorption on the toxic potential of Rlim, β Myr and Lin was investigated in the Ames fluctuation test (AFT). Cytotoxicity and mutagenicity were determined after incubation of *S. typhimurium* TA98 in a PS-free setup in comparison to the conventional setup (ISO 11350:2012). Furthermore, final concentrations in the cell culture media were checked analytically and related to nominal substance concentrations.

Materials and methods: AFT was performed following ISO 11350:2012 and cytotoxicity was assessed via resazurin reduction assay. Separately, test substance concentrations in the media were analyzed via headspace-GC-MS before and after 100 min incubation in the conventional and PS-free setup in the absence of cells to quantitate sorptive losses.

Results: For Rlim and β Myr EC₅₀ values were 64±5 μ M and 114±37 μ M in the PS-free incubation setup respectively, whereas no significant decrease in relative vitality could be observed for nominal concentrations up to 600 μ M (Rlim) and 400 μ M (β Myr) in the conventional (PS) setup. Differences in the EC₅₀ values for Lin were less distinct with 4030±220 μ M for conventional and 2556±199 μ M for PS-free incubation setup. None of the substances tested showed an increase in mutant colonies in AFT for each respective incubation setup.

Conclusion: EC₅₀ values after PS-free incubations indicated significant substance losses in the conventional incubation setup for the AFT. In the future, the use of PS cell culture equipment to evaluate toxicity of lipophilic compounds has to be questioned.

[1] Riedl und Altenburger, *Chemosphere* 2006, 67 [2] Fischer et al., *Environ Sci Technol* 2018, 52, 22 [3] Charara et al., *J Food Sci* 1992, 57, 4 [5] IARC, *IARC Monog Eval Carc* 1999, 73 [6] IARC, *IARC Monog Eval Carc* 2019, 119 [7] Letizia et al., *Food Chem Toxicol* 2003, 41, 7

P031

Conceptual considerations on dealing with intermediary effects as reference points for the derivation of health-based guidance values

M. Balke¹, R. FitzGerald², U. Gundert-Remy³

¹Hochschule Emden/Leer, Naturwissenschaftliche Technik, 26723, Germany

²Université de Bâle, SCAHT - Swiss Centre for Applied Human Toxicology, Basel, Switzerland

³Charité - Universitätsmedizin Berlin and Berlin Institute of Health, Institute of Clinical Pharmacology and Toxicology, Berlin, Germany

Question: Health-based guidance values (HBGV) are usually based on apical effects in animal studies from which a reference point (RP) is derived. In order to extrapolate the RP to the human population, inter-species differences and intra-human variability in toxicokinetics (TK) and toxicodynamics (TD) are taken into consideration. The question is whether this procedure or another approach should be applied when an intermediate effect (i.e. an effect biomarker for organ toxicity or disease) is used to derive an HBGV.

Methods: A selective non-systematic literature search was performed to find relevant data and publications.

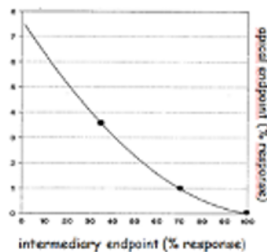
Results and discussion: In terms of the adverse output pathway (AOP) framework, an "intermediate effect" is defined as a key event (KE) upstream to the apical adverse outcome (AO); KEs are defined as measurable and necessary, but not necessarily sufficient, to induce an adverse outcome (OECD 2017). Even late intermediary effects may be related to the apical adverse effect in a non-linear fashion (Fig. 1). To estimate the probability that occurrence of an upstream KE will trigger an AO, quantitative AOPs (qAOPs) are in development (e.g. Spinu et al 2022), but many uncertainties remain, e.g. whether a qAOP calibrated with data from a particular type of cell can be used to predict quantitatively the toxicity with a KE in another cell type, and whether qAOPs have to include all the possible mechanisms of action relevant to activation of the AO to be chemical-independent (Tebby et al 2022). Current default or substance specific TK and TD factors are based on apical adverse effects (Bhat et al 2017). TK factors are independent of the effect, thus can be applied to both KE and AO. A TD factor should however, either by default or based on specific information, reflect the mechanism of action and may be modified by an additional factor based on probability of triggering AO.

Conclusion: The quantitative relationship between intermediary and apical endpoint must be derived using endpoint-specific data obtained from appropriate studies which is the present challenge.

Fig. 1 Non-linear relationship between intermediary endpoint and apical endpoint (Garbe et al., 1993, redrawn)

Garbe et al. Eur J Clin Pharmacol. 1993;45(1):1-7
OECD 2017; ISSN: 20777876
Spinu et al. Comput Toxicol 2022;21:100206
Tebby et al. Toxicol In Vitro. 2022;81:105345

Fig. 1



P032

Time trend of internal exposure to perfluoroalkyl substances (PFAS) in vegans and omnivores within 4 years

J. Menzel¹, C. Weikert¹, W. Völkel², B. Monien¹, K. Abraham¹

¹German Federal Institute for Risk Assessment, Department of Food Safety, Berlin, Germany

²Bavarian Health and Food Safety Authority, Department of Chemical Safety and Toxicology, Munich, Germany

Introduction: Consumption of food and drinking water is the main route of background exposure to per- and polyfluoroalkyl substances (PFAS) in humans. The daily low-level exposure leads to an accumulation especially of four compounds: perfluorooctane sulfonic acid (PFOS), perfluorooctanoic acid (PFOA), perfluorohexane sulfonic acid (PFHxS) and perfluorononanoic acid (PFNA). Animal-based foods are thought to be the main contributors.

Objectives: To compare the internal exposure to PFAS in vegans and omnivores, and to investigate its time trend within 4 years.

Participants and methods: 24 vegans and 26 omnivores were investigated, participating in the cross-sectional study "Risks and Benefits of a Vegan Diet" (RBVD) at two time points (RBVD1: year 2017, and RBVD2: year 2021). PFOS, PFOA, PFHxS, and PFNA were quantified in plasma using a triple-stage quadrupole mass spectrometer.

Results: In 2017, lower median plasma for PFOS and PFNA were observed in vegans compared to omnivores (Menzel et al. 2021, Int J Hyg Environ Health 237, 113808). The investigations in 2021 confirmed these differences for PFOS (median 0.98 vs. 1.86 µg/L, resp., p = 0.001) and PFNA (<0.25 vs. 0.30 µg/L, resp., p < 0.0001), whereas no significant differences were observed for PFOA (1.42 vs. 1.10 µg/L, resp., p = 0.07) and PFHxS (1.85 vs. 1.44 µg/L, resp., p = 0.38). For the whole group of 50 participants, the median PFAS levels measured in 2017 and 2021 are compiled in Table 1. Within the 4 years, we observed a decreasing time trend of PFAS levels, which was significant for all

four compounds. However, the rates of the decrease were different (PFOS > PFNA > PFOA > PFHxS).

Conclusion: Lower levels of PFOS and PFNA, but not of PFOA and PFHxS were observed in vegans compared to omnivores. The decreasing trend is in line with many other studies, but was found to be surprisingly strong especially for PFOS. Its half-life of about 4 to 5 years (literature data) and the observed decline of -55 % in 4 years leads to the conclusion that the ongoing exposure in Berlin (Germany) obviously is relatively low.

Fig. 1

Table 1. Time trend of different PFAS between RBVD1 and RBVD2

	PFOS	PFOA	PFHxS	PFNA
RBVD1 median level 2017 (µg/L)	2.59	1.58	1.86	0.32
RBVD2 median level 2021 (µg/L)	1.25	1.31	1.67	<0.25
Median of indiv. differences (µg/L)	-1.5	-0.5	-0.2	-0.2
Median difference to 2017 (%)	-55.0	-25.7	-12.2	-39.4

P033

Analyzing the fate of heme and NO-heme after (processed) red meat consumption using the INFOGEST 2.0 digestion model

T. Kostka¹, P. Boden², J. Fahrner¹

¹Technical University of Kaiserslautern, Division of Food Chemistry and Toxicology, Kaiserslautern, Germany

²Technical University of Kaiserslautern, Department of Chemistry and State Research Center OPTIMAS, Kaiserslautern, Germany

The consumption of processed and red meat is associated with a higher risk of developing colorectal cancer (CRC). While heme may be responsible for the red meat-mediated higher CRC incidence, the influence of processed meat on CRC development is less known. The addition of curing salt (sodium nitrite) to meat induces the formation of *N*-nitroso compounds, mainly nitrosylated heme (NO-heme). Previous studies showed a high genotoxic and mutagenic potential for both compounds, i.e. heme as well as NO-heme, while the effects of NO-heme were generally lower than those induced by heme alone. This lower toxicity of NO-heme suggested that endogenous modifications of heme compounds may lead to the formation of other compounds or activate/increase their toxicity in the colon.

The aim of the study was to analyze the fate of heme and NO-heme in the human digestion process. Therefore, highly purified NO-heme was synthesized and chemically characterized. Then, the digestion of heme compounds was simulated in an *in vitro* digestion model to analyze the composition, concentrations and potential chemical modifications of heme and NO-heme in each digestion compartment.

NO-heme was synthesized by heme nitrosylation, followed by purification using dialysis cassettes and concentration by a vacuum concentrator. The purity was verified by photometric nitrite quantification as well as UV/Vis and FTIR spectra of NO-heme. The *in vitro* digestion will be done according to the INFOGEST 2.0 digestion model, while the NO-heme will be quantified using the NO chemiluminescence detection method. Differentiation of heme compounds will be performed by liquid-liquid-extraction, followed by photometric quantification.

The NO-heme synthesis and analytical characterization was successfully established with an average loss of 38% of the substance. Nevertheless, more than 99% of nitrite as nitrosylation byproduct was removed by dialysis, while the high purity was also confirmed by FTIR spectra. Substance stabilization studies reveal the transformation of NO-heme into β-hematin, a heme dimer, which was never associated with the human diet. For the *in vitro* digestion model, enzyme activity assays proved the suitability of the different enzymes origin from human, rabbit and porcine.

The above-mentioned lower toxicity of NO-heme may result from its chemical instability and transformation to β-hematin. Its potential endogenous formation will be investigated in the *in vitro* digestion studies.

P034

Lupine alkaloids as food contaminants: Investigation of mutagenic potential

U. Schreiber¹, M. Esselen¹

¹Institute of Food Chemistry, WWU Münster, Münster, Germany

Alternative sources for protein are becoming more popular. One of these sources are lupine seeds, which can be processed to flour, yogurt, pasta and other products. However, lupines contain a variety of quinolizidine alkaloids (QA). It was shown that some of these alkaloids can be found in lupine food products in concentrations of several mg/kg [1]. Moreover, in a recent feeding study by the German Federal Institute for Risk Assessment lupine alkaloids migrated into milk after cattle was fed with a diet containing lupine seeds [2]. The health risks by the presence of quinolizidine alkaloids in feed and food was evaluated by the European Food Safety Authority (EFSA) in 2019. However, EFSA stated that "very limited information is available on the genotoxicity of QAs" [3].

To begin the evaluation of the genotoxic and mutagenic potential of a test compound EFSA recommends to use a "basic battery of *in vitro* tests" [4]. This includes a Bacterial

Reverse Mutation Assay and a Micronucleus test. In the study at hand five of the most frequently found QA (Angustifoline, 13-OH-Lupanine, Lupanine, Lupinine and Sparteine) were tested for their mutagenic potential in the Ames test with and without metabolic activation as recommended in OECD TG 471. Four *S. typhimurium* strains (TA97a, TA98, TA100 and TA11535) and one *E. coli* strain (*E. coli* WP2) were used. Furthermore, the test compounds were examined for their potential to cause chromosomal damage in the Micronucleus test using human liver carcinoma (HepG2) cells.

In conclusion with this study we close a knowledge gap on potential mutagenic effects by lupine alkaloids using a battery of *in vitro* tests.

References:

- [1] Hwang IM et al. Rapid and Simultaneous Quantification of Five Quinolizidine Alkaloids in *Lupinus angustifolius* L. and Its Processed Foods by UPLC-MS/MS. ACS Omega. 2020 Aug 10;5(33):20825-20830.
 [2] Engel AM et al. Investigations on the Transfer of Quinolizidine Alkaloids from *Lupinus angustifolius* into the Milk of Dairy Cows. J Agric Food Chem. 2022 Sep 21;70(37):11749-11758.
 [3] FSA Panel on Contaminants in the Food Chain (CONTAM). Scientific opinion on the risks for animal and human health related to the presence of quinolizidine alkaloids in feed and food, in particular in lupins and lupin-derived products. EFSA J. 2019 Nov 5;17(11):e05860.
 [4] EFSAScientificCommittee.Scientific opinion on genotoxicity testing strategies applicable to food and feed safety assessment. EFSA J.2011;9(9):2379

Toxicology – Genotoxicity and carcinogenesis

P037

The pyrrolizidine alkaloid lasiocarpine affects cell cycle progression in metabolic competent liver cell lines

M. Beckschulte¹, A. Peters¹, J. Buchmüller¹, J. H. Kupper², B. Sachse¹, B. Schäfer¹, S. Hessel-Pras³

¹German Federal Institute for Risk Assessment, Food Safety, Berlin, Germany

²Brandenburg University of Technology (BTU), Molecular Cell Biology, Cottbus, Germany

³German Federal Institute for Risk Assessment, Food Safety, Berlin, Germany

Introduction: The majority of pyrrolizidine alkaloids are produced as secondary metabolites in plants where they presumably act as a protection mechanism against herbivores. Foods like herbs or tea, or animal feed can be contaminated by pyrrolizidine alkaloid-producing plants. The exposure to high amounts of 1,2-unsaturated pyrrolizidine alkaloids (PAs) can lead to severe acute liver damage while perpetual ingestion of lower amounts has been associated with carcinogenic effects.

Objective: Albeit the general mode of action leading to PA-induced toxicity is widely understood, there is still uncertainty about the mechanism in detail, including the impact on cell cycle. Therefore, we used the open-chain diester lasiocarpine (Lc), a well-described hepatotoxic PA known to be bioactivated by human cytochrome P450 monooxygenase (hCYP) 3A4, to investigate the interaction with cell cycle progression.

Material and methods: Induction of cytotoxicity and micronuclei formation was elucidated in hCYP3A4-overexpressing HepG2 cells (HepG2h3A4) and wild-type cells (HepG2wt) exhibiting low hCYP activity. Subsequently, the effect of Lc on cell cycle progression was evaluated by flow cytometry in synchronized HepG2h3A4 and HepG2wt cells using a subtoxic dose of Lc (10 µM). Furthermore, RT-PCR analysis was used to investigate the expression of specific cell cycle-associated genes such as *PLK1*, *CHEK1*, *BRCA1*, *CDC2*, *CDK2* or *Ki-67*.

Results: In the HepG2 cells, cytotoxicity depends on Lc concentration and on hCYP3A4 activity. Furthermore, micronuclei were induced after metabolism of Lc. FISH experiments using a centromere specific probe suggest that micronuclei formation is the result of an aneuploid effect. In addition, Lc led to an accumulation of HepG2 cells in S- and G2/M phase, solely in the hCYP3A4-competent cell line. Analysis of expression of cell cycle associated genes revealed a decrease of e.g. *PLK1*, *CHEK1* or *Ki-67* transcripts after hCYP3A4 mediated metabolism of Lc.

Conclusion: Following hCYP3A4 mediated metabolism, Lc induced the formation of micronuclei concentration-dependently. Based on our results, these micronuclei seem to be of an aneuploid origin, probably due to cell cycle disturbance in S and G2/M phase. We will have to further clarify whether structurally different PAs also induce the formation of micronuclei of aneuploid origin due to cell cycle disruption, in order to better characterize the structure-dependency of the toxicity.

P038

The concept of the German Human Biomonitoring Commission for the health risk assessment of carcinogenic substances in the human body

C. Röhl¹, P. Apel², Y. Chovolou³, M. Kolossa-Gehring², U. Pabel⁴, T. Schettgen⁵, K. M. Wollin⁵

¹State Agency for social Services Schleswig-Holstein, Environmental Medicine and Toxicology, Neumünster, Germany

²German Environment Agency (UBA), Berlin, Germany

³North Rhine-Westphalia State Agency for Nature, Environment and Consumer Protection, Recklinghausen, Germany

⁴German Federal Institute for Risk Assessment (BfR), Berlin, Germany

⁵RWTH Aachen University, Aachen, Germany

⁶Formerly Governmental Institute of Public Health Lower Saxony, Hannover, Germany

For the risk assessment of environmental chemicals in the human body the German Human Biomonitoring Commission at the German Environment Agency (UBA) derives health based guidance values (HBM-I and HBM-II values). Prerequisite for the derivation of HBM values is an existing dose, that can be assumed to be harmless to health. For non-threshold carcinogenic substances no HBM values are derived. So far, only population-based reference values have allowed a contextualization of body burdens of these substances found in studies of the general population or in environmental medicine. Health-based measures are needed to assess human biomonitoring data especially for those substances of very high concern.

Therefore, we developed a supplementary risk assessment concept for threshold and non-threshold carcinogens. With its risk-based approach, this concept goes decisively beyond the purely descriptive-statistical reference value concept. Instead of HBM values quantitative dose descriptors of the internal body load are derived. These measures allow to calculate for any concentration of a carcinogen, e.g. in urine or blood, an additional lifetime cancer risk, which can be used for the further evaluation of the measured internal exposure.

First of all, the mechanism of carcinogenesis has to be determined. For genotoxic carcinogens in general a non-threshold mechanism is assumed. Based on quantitative dose descriptors of the external exposure (e.g. Unit Risk, Oral Slope Factor), knowledge on the toxicokinetics and specific carcinogen biomarkers for humans the quantitative dose descriptors of the internal body load are derived. By means of these dose-descriptors, finally, additional lifetime cancer risk for measured concentrations and vice versa can be calculated. The concept, its prerequisites and uncertainties will be presented using benzene as example.

Calculated lifetime cancer risks can be used to justify and prioritize risk management measures. The concept intentionally does not include any a priori-suggestions, e.g., for certain guidance values, to clearly separate the scientific method of toxicological risk assessment from the risk evaluation process as part of the risk management procedure.

The applicability of the concept will be further tested and evaluated to decide in the near future if any aspects can be modified and improved.

P039

In depth genotoxic analysis in a time- and dose-dependent manner in different urothelial cells after exposure to benzo[a]pyrene

J. Zaloga¹, C. Kersch¹, R. Alsaleh¹, S. Schmitz-Spanke¹

¹Friedrich-Alexander Universität Erlangen-Nürnberg, Institute and Outpatient Clinic of Occupational, Social and Environmental Medicine, Erlangen, Germany

Introduction: Benzo(a)pyrene (B[a]P) is suspected to be involved in the development of bladder cancer, but the data are not conclusive. Therefore, primary porcine urothelial cells (PUBEC) and cells of a urinary bladder carcinoma cell line (T24) were exposed to a wide dose range of B[a]P in a time-dependent manner. The aim of this study was to perform an in-depth investigation regarding the genotoxicity of B[a]P in different urothelial cell types, including differences in susceptibility.

Method: PUBEC and T24 cells were exposed to 0.001 µM - 10 µM B[a]P for 4, 24, and 48 h, respectively. The following parameters were examined: MTT (metabolic activity), clonogenic assay (cell survival), micronucleus (genomic instability) and neutral comet assay (DNA damage). A benchmark calculation (BMD) was performed using the Comet assay data in PUBEC cells.

Results and conclusions: No significant cytotoxicity was detected. In T24 cells, time- and dose-dependent cytoxicity was observed. In PUBEC cells, there was a slight increase in proliferation after 4 h.

24-h exposure induced the most severe dose-dependent DNA damage with primary cells responding more strongly than T24 cells. Even 4-h exposure induced DNA damage with BMD's of 0.0027 µM B[a]P after 4 h and 0.00023 µM after 24 h exposure in PUBEC cells. The frequency of micronucleus formation increased more markedly in T24 cells, especially after 24 h. In PUBEC cells, 48 h exposure induced the formation of nucleoplasmic bridges and nuclear buds. In conclusion, our results highlighted the potential of B[a]P to induce and promote bladder cancer even at very low concentrations.

P040

Threshold concentrations for BPDE-induced cell death are characterised by altered DNA damage signalling and associated with unrepaired double-strand breaks

A. Schmidt¹, R. Kitzinger¹, A. Pöschmann¹, M. T. Tomičić¹, M. Christmann¹

¹Universitätsmedizin Mainz, Toxicology, Mainz, Germany

The environmental carcinogen benzo(a)pyrene (B[a]P) is not carcinogenic unless metabolically activated to benzo(a)pyrene 9,10-diol-7,8-epoxide (BPDE). In our previous work, we showed that exposure of human VH10tert fibroblasts to non-toxic concentrations of BPDE induces p53-dependent transcriptional activation of the nucleotide excision repair as well as p53/p21-dependent induction of senescence, leading to cellular survival. In contrast, high BPDE concentrations result in p53 mediated cell death via apoptosis,

suggesting the existence of specific thresholds at which the p53-dependent pro-survival signalling turns into p53-dependent pro-death signalling.

The initial activation of the DNA damage response does not differ between toxic and non-toxic BPDE concentrations, whereas at later time points toxic concentrations cause complex changes in the DNA damage response resulting in cell death. In summary, protective ATR-CHK1-p53^{Ser15}-p21 dependent signalling changes upon toxic concentrations into ATM-CHK2-p53^{Ser46}-NOXA dependent signalling, mediating induction of apoptosis. Preliminary data further suggest that this threshold is caused by unrepaired DNA double-strand breaks.

P041

Characterization of the genotoxic potential of the anthraquinone dye Alizarin Red S

H. Rossi¹, B. Bauer¹, H. Hintzsche¹

¹Rheinische Friedrich-Wilhelms Universität Bonn, Institute of Nutritional and Food Sciences, Bonn, Germany

The substance class of anthraquinones contains a plethora of approximately 700 compounds of natural or synthetic origin. Members of this class have been used as antineoplastic or laxative drugs, the use of anthraquinones, e.g. alizarins, as staining dyes even dates back to ancient times. However, besides these beneficial characteristics, health concerns were raised due to the genotoxic/mutagenic properties of certain anthraquinones. The dye Alizarin Red S (ARS) is currently used as a tool in European eel stock monitoring by marking the caught fish with the dye before releasing them back into the wild. As ARS can be found in recaptured eels even years later, knowledge of potential health risks of ARS is crucial for assessing the food safety of eels, marked with this dye, for human consumption. To date, no data for the characterization of the hazard potential of ARS is available. In the present study we aimed at filling this data gap. To this end, we investigate the cytotoxic and genotoxic potential of Alizarin Red S in HepG2 cells, preliminary results from the micronucleus test and the alkaline comet assay will be presented.

P042

Establishment of an *in vivo* micronucleus test using flow cytometry

A. Hellmann¹, S. Weber¹, J. Lott¹

¹Boehringer-Ingelheim Pharma GmbH & Co. KG, NDS (Nonclinical Drug Safety), Ulm, Germany

The micronucleus test is an essential part in the characterization of the genotoxic potential of a test compound. This assay is used for the detection of chromosomal damage by evaluating the formed micronuclei. Micronuclei emerge from chromosome fragments or whole chromosomes, which have failed to be incorporated correctly into one of the daughter nuclei during cell division. As genotoxic substances are known to be potentially mutagenic, the micronucleus test is an inherent part in the safety evaluation of pharmaceuticals. In this study an *in vivo* micronucleus test using flow cytometry on peripheral blood was established. Experiments were performed with the alkylating compounds cyclophosphamide (CP) and ethyl methanesulfonate (EMS). Measurements were restricted to the youngest reticulocytes, displaying the transferrin receptor (CD71). This ensured that only recent DNA lesions were observed. To avoid the splenic elimination of micronucleated reticulocytes (MN-RETs) reported in rats, CD-1 mice were used through the study. 24 hours after treatment on two consecutive days, peripheral blood from the vena facialis was collected. The frequency of micronucleated reticulocytes was determined by measuring 20 000 reticulocytes using flow cytometry. In contrast to previously published data, both EMS concentrations with 200 and 225 mg/kg bodyweight displayed only moderate effects with an overall 1.7-fold increase in MN-RETs. CP at a dosage of 20 mg/kg bodyweight resulted in a 3.8-fold inductions of MN-RETs and may serve as a validated positive control in further studies. It could be demonstrated that flow cytometry is excellent for the evaluation of the micronucleus test, as it is a reliable, time-saving method for the measurement of micronuclei in the peripheral blood of mice.

P043

More Models, More Complexity, More Confusion? Comparisons and Combinations of (Q)SAR Tools for Ames Mutagenicity in Pesticide Regulation

D. Fojl¹, J. König¹, K. Hermann¹, C. Kneuer¹, B. C. Fischer¹

¹Bundesinstitut für Risikobewertung, Sicherheit von Pestiziden; Toxikologie der Wirkstoffe und ihrer Metabolite, Berlin, Germany

Introduction: From the regulatory perspective, the Ames test for bacterial mutagenicity is required for the approval of pesticides. In some cases where experimental evidence is unattainable - particularly for impurities and metabolites - a combination of a structure-alert based Structure Activity Relationship (SAR) model and a statistically-based Quantitative Structure Activity Relationship (QSAR) model may be used to provide insight into potential mutagenicity.

Objectives: Herein we sought to compare the performance of model suites from different developers, and to test different combinations of the models, in order to better understand the factors that influence model performance and to examine the relative performance of said model combinations. The ultimate aim is to give recommendations for appropriate model combinations.

Materials and methods: An in-house test set comprising 15 known Ames negative and 15 known Ames positive substances of relevance to pesticides (active ingredients,

impurities, and metabolites) was used to evaluate the performance of various QSAR model combinations. Nexus (Lhasa Ltd., UK) includes one SAR (Derek) and one QSAR (Sarah) for Ames, while VEGA (Istituto di Ricerche Farmacologiche Mario Negri, IT), includes two SARs (ISS, SarPy), two QSARs (CAESAR, KNN), and a consensus model which incorporates predictions from all of the individual models. Model combinations both within each model suite and combining models from the different developers were evaluated.

Results: The Nexus model suite performed better than the individual VEGA model combinations, especially with regard to false negatives and false positives. VEGA consensus made predictions for more molecules than any of the individual model combinations, but at a cost of more false positives and false negatives. Combining VEGA and Nexus models improved predictive success relative to VEGA models alone.

Conclusion: The size and quality of the rule- or training set seem to be critically important to the model performance. Well-suited model combinations more reliably predict the mutagenicity of pesticide-relevant chemicals, enabling a greater degree of certainty in regulatory decision-making. In this respect, the advantages of having more models available outweigh the disadvantages if they are chosen carefully.

P044

Pharmacological inhibition of the small Rho-GTPase Cdc42 reduces the doxorubicin-induced DNA damage response in NIH-3T3 cells

K. Reiffert¹, C. Henninger¹, G. Fritz¹

¹Medical Faculty of the Heinrich-Heine University Düsseldorf, Institute of Toxicology, Düsseldorf, Germany

Introduction: Small GTPase homologous (Rho)-GTPases act as molecular switches that transduce extracellular stimuli to signaling networks of the inner cell. The Rho-GTPases Rac1 and Cdc42 regulate actin dynamics and affect plasma membrane protrusion as well as vesicle traffic. Beyond that, inhibition of small Rho-GTPase like Rac1 was shown to reduce the amount of doxorubicin (DOX)-induced DNA double-strand breaks (DSB) and cell death in rat cardiomyocytes, human umbilical vein cells and in mouse embryonic fibroblasts.

Objectives: Here, we investigated whether the guanine nucleotide exchange factor (GEF) Tiam1 that is a regulator of the small GTPases Rac1 and Cdc42 has an impact on the doxorubicin-induced DNA damage response (DDR). Moreover, we tested whether or not Cdc42 - a close relative to the Rac1 subfamily - plays a role in the DOX-induced DDR.

Materials and methods: To this end, we used the mouse fibroblasts cell line NIH-3T3 as *in vitro* test system and targeted Rac1 and/or Cdc42 with specific small-molecular pharmacological inhibitors or made use of siRNA directed against those Rho-GTPases as well as the Rho-GEF Tiam1. Subsequently, we treated the cells with DOX and measured DSB-formation (γH2AX / 53BP1 co-localization), cell viability (resazurin reduction assay), cell cycle distribution and apoptosis (propidium iodide-based flow cytometry). The activation of a subset of DDR-related proteins was detected by Western blot analyses.

Results: Pharmacological inhibition of Rac1 and/or Cdc42 resulted in a diminished DOX-induced DDR to a similar extent. The use of siRNA against the Rho-GTPases was not as potent as the pharmacological inhibitors but tended to cause a reduction of the DOX-induced DDR, too. The Tiam1 siRNA did not cause a sufficient knockdown efficiency to evaluate a possible impact of this GEF on the DOX-induced DDR.

Conclusion: Besides Rac1, Cdc42 is an additional Rho-GTPase that is involved in the regulation of the DOX-induced DDR and the data point to a possible crosstalk with Rac1. Since the pharmacological inhibition of those small GTPases showed more potent effects on the DOX-induced DDR than the siRNA approach, it is feasible that cells are able to partially compensate for a slow loss of the GTPases but cannot counteract a sudden deficiency of Rac1 or Cdc42 to activate a full-blown DDR following DOX treatment.

P045

Assessment of the Mutagenic Potential of a Protoporphyrinogen-Oxidase Inhibitor Herbicide

N. Honarvar¹, A. Zander¹, E. Dony², B. Williamson Riffle³, M. Frericks¹, T. Seiser¹, M.

Shigano⁴, D. Funk Weyer¹, R. Landsiedel¹

¹BASF SE, Ludwigshafen, Germany

²CCR-Roßdorf GmbH, Roßdorf, Germany

³BASF Corp., Research Triangle Park, United States

⁴L SIM Safety Institute Corporation, Ibaraki, Japan

Protoporphyrinogen-oxidase inhibitors (PPOi) is a class of herbicides, which acts on chlorophyll synthesis. Likewise, it affects heme synthesis resulting in anaemia in mammals to varying degrees. A series of experimental PPOi candidates showed, despite their clear negative *in vitro* mutagenic profile, enhanced micronucleus formation in rodent bone marrow *in vivo*. Since increased erythropoiesis may result in increased micronucleus formation, a series of investigations were performed to determine whether the micronucleus findings were attributed to a mutagenic effect or linked to the observed anaemia.

One of these PPOi candidates was tested *in vivo* by oral gavage in rats; micronucleus assays in the liver and bone marrow were performed on day 14. The data showed an increase in the micronucleus counts in the bone marrow whereas the hepatocyte micronucleus frequency was not affected. In another study, 24 hours after a single gavage

administration in mice a portion of the bone marrow was assessed for micronucleus formation while the rest was subjected to a subpopulation separation process isolating erythroid (selected via their Ter119 surface expression) and non-erythroid (selected by their CD45 surface expression) cells, which were then assessed in a comet assay. Results showed a dose dependent increase in micronucleus frequencies. However, increases in % DNA tail intensities in the comet assay were confined only to the erythroid Ter119+ subpopulation.

In conclusion, it can be stated that the observed induced micronucleus frequencies using the PPOi candidate is most probably a product of enhanced erythropoiesis and not linked to a direct DNA damaging effect.

P046

Life cycle toxicities of DNA alkylating agents using *C. elegans* as a 3R-compliant organismic model system.

J. Ruzkiewicz¹, L. Endig¹, E. Guver¹, A. Bürkle¹, A. Mangerich^{2,1}
¹University of Konstanz, Molecular Toxicology, Konstanz, Germany
²Universität Potsdam, Nutritional Toxicology, Nuthetal, Germany

C. elegans is a popular model in aging research is emerging as an attractive organismic model in toxicity testing in compliance with the 3Rs concept to avoid the use of vertebrate animal testing. We investigated the toxicities of DNA alkylating agents at different life cycle stages of the nematode. To this end, sulfur mustard analogues, i.e., the monofunctional agent 2-chloroethyl-ethyl sulfide (CEES) and the bifunctional, crosslinking agent mechlorethamine (HN2) were investigated for biological effects and population-based read-outs such as worms' survival, fertility, and germline apoptosis. Additionally, the levels of NAD⁺, a versatile factor in energy metabolism, redox regulation, and genome maintenance have been examined.

Synchronized worms at different life cycle stages (from L1 to adult day 10) were exposed to CEES or HN2 for 30 min. For survival assay, viability of wild-type (N2) worms was scored 24 h later. For reproduction assay, N2 worms were exposed to CEES or HN2 during the L4 stage. 24 h later adult hermaphrodites were allowed to lay eggs for 24 h. Then adults were removed, and plates were kept for an additional 24 h to allow egg hatching. For each hermaphrodite, the number of offspring and the percentage of unhatched eggs were determined. For germline apoptosis assay, CED-1:GFP worms were exposed to CEES or HN2 during the L4 stage. Adult hermaphrodites were picked 24 h later and the number of CED-1:GFP-positive cells was scored. For the NAD⁺ assay, NAD⁺ was extracted from N2 worms and NAD⁺ levels were determined using an enzymatic cycling assay.

General susceptibility of *C. elegans* to alkylating agents exhibited similarities with human cell culture models, such as higher toxicity of HN2 than CEES, with LC50 values in the high µM to low mM range, respectively. Of note, the effects were dependent on worms' developmental stage and age. Thus, L1 exhibited the highest susceptibility, whereas L4 the lowest. For adult worms, susceptibility decreased with advanced age, especially for HN2. At low-toxicity concentrations in adult worms, both agents potentiated germline apoptosis, as well as impaired reproduction measured with offspring number and eggs hatching rate. Again HN2 showed stronger effects than CEES. Analogously, NAD⁺ levels were also greater affected by HN2 treatment. Together, the data indicate high toxicity of DNA alkylating agents to germline cells, as well as increased toxicity in early larval development as well with advanced age.

P047

(Oxy-)Matrine in liquorice – a genotoxic threat?

Y. Musenji¹, K. Hermann¹, S. Hessel-Pras², C. Kneuer¹, J. König¹, B. Sachse², B. C. Fischer¹
¹BfR, Pesticide Safety, Berlin, Germany
²BfR, Food Safety, Berlin, Germany

Introduction and objective: Liquorice is a confectionery flavoured with extracts of the liquorice plant (*Glycyrrhiza glabra*). Recently, liquorice products were found to be contaminated with matrine and oxymatrine, being quinolizidine alkaloids from *Sophora* roots. These roots are used in traditional Chinese medicine and extracts thereof as biopesticides in some countries. Further, the roots may be confused with liquorice roots. There are some indications for genotoxic activity from studies with *Sophora* root extracts. However, no reliable data on genotoxicity of the pure compounds is available as previous studies mainly investigated plant extracts of unknown composition. Furthermore, experimental protocols did not meet current test guidelines and reporting was limited. Therefore, the potential of pure matrine and oxymatrine to cause gene mutations and/or chromosomal damage was investigated in this study using *in vitro* genotoxicity tests.

Materials and methods: We conducted the bacterial reverse mutation test (Ames test/OECD TG 471) with the strains TA98, TA100, TA1535, TA1537 and *E.coli* WP2 uvrA using the plate-incorporation and the pre-incubation method with and without metabolic activation. Additionally, we performed the *in vitro* micronucleus test with V79 cells (OECD TG 487) with and without metabolic activation. All experiments were carried out using matrine and oxymatrine with ≥ 98% certified purity.

Results: The Ames-test demonstrated that neither matrine nor oxymatrine are cytotoxic or mutagenic in the bacterial test system up to the maximum dose of 5000 µg/plate independent of metabolic activation. Assay performance was confirmed by strain specific positive controls. However, in the *in vitro* micronucleus assays, there was a dose-related response for matrine in the number of counted micronuclei per 1000 events. Relative survival decreased to < 55% at the maximum test concentration of 1500 µg/ml after 24 h

incubation. Our results suggested, that matrine may be clastogenic and/or aneugenic *in vitro* at concentrations ≥ 1250 µg/ml.

Conclusion: Matrine and oxymatrine were found to be non-mutagenic in the Ames-test. However, matrine was clastogenic and/or aneugenic in the *in vitro* micronucleus assay. Our findings indicate a concern for genotoxicity *in vitro*. The relevance for the *in vivo* situation needs to be elucidated in appropriate follow up studies.

P048

Towards *in vivo* genotoxicity assessment in *C. elegans* via the automated fluorometric analysis of DNA unwinding (FADU) assay.

J. Ruzkiewicz¹, E. Nurray¹, A. Bürkle¹, A. Mangerich^{1,2}
¹University of Konstanz, Biology, Konstanz, Germany
²University of Potsdam, Institute Nutritional Science, Potsdam, Germany

Introduction: The automated fluorometric analysis of DNA unwinding (FADU) assay is a DNA damage assay that had been developed as a very sensitive screening tool to monitor various types of DNA damage, such as strand breaks, crosslinks, alkylating adducts, or oxidative damage *in vitro* in human cell culture models and primary lymphocytes. *C. elegans* is a popular model in pharmaceutical and toxicological studies, and its implementation in genotoxicity testing and DNA damage research is continuously growing. The nematode has been utilized in studies of environmental genotoxins or DNA-damaging anticancer drugs. Besides, multiple homologs and orthologs of key genes and gene products within human DNA damage response and DNA repair pathways have been discovered in the nematode, granting its suitability in studying the molecular mechanisms of genetic integrity.

Objectives: In this project, the application of *C. elegans* in the detection of DNA strand breaks via the FADU assay has been investigated.

Materials and methods: The method principle is based on DNA alkaline unwinding under highly controlled conditions of pH, temperature, and time, managed by an automated liquid handling device (LHD). After genotoxic treatment samples are sonicated and transferred into the LHD which performs further steps, such as the addition of lysis, alkaline, and/or neutralisation reagents. Lastly, fluorescence dye for double-stranded DNA (SYBRGreen) is added, followed by a fluorescent readout.

Results: Our preliminary results indicate the feasibility of the detection of DNA strand breaks in the nematode via the FADU assay. Cells isolated from *C. elegans* embryos, as well as worms at larval stage L1 and L4 exposed to genotoxic agents such as hydrogen peroxide, tert-butyl hydroperoxide, or bleomycin, showed a dose-dependent induction of DNA strand breaks.

Conclusion: After successful optimization, this novel assay with its time- and cost-effective, high-throughput screening application will be a significant addition to currently used techniques in studies investigating genetic toxicity *in vivo* with a wide range of potential applications.

This research was supported by the Zukunftskolleg, University of Konstanz with funding from the Excellence Strategy of the German Federal and State Governments (grant number 1414 547 66 82 to JR).

P049

The human endometrial adenocarcinoma Ishikawa cell line as promising test system for SULT-mediated activation of genotoxins

E. Veh¹, F. Schulze¹, D. Leonhardt¹, C. Kleider¹, L. Lehmann¹
¹University of Würzburg, Chair of Food Chemistry, Würzburg, Germany

The experimental evaluation of genotoxicity *in vitro* requires testing in the absence and presence of metabolic activation. In most cases, metabolic activation is referred to as CYP-mediated hydroxylation (or oxidation), which can be achieved by incorporating rat liver S9 mix into the test system, resulting eventually in the formation of electrophilic metabolites able to cause genotoxicity. However, some hydroxylation products, e.g. benzylic alcohols like 1-hydroxymethylpyrene (1-HMP), the main human metabolite of the environmental contaminant methylpyrene, become genotoxic only after SULT-mediated sulfonation because in a benzylic position, the resulting sulfate group is a good leaving group.

Unfortunately, this SULT-mediated metabolic activation is not represented in the current standard genotoxicity test battery and recently it has been observed that also the metabolically competent cultured human hepatocellular carcinoma cell line HepG2 failed to activate 1-HMP. Thus, testing SULT-mediated metabolic activation *in vitro* is currently possible only by genetically modified mammalian cells or *Salmonella* strains.

We hypothesized that the SULT-expressing human endometrial adenocarcinoma Ishikawa cell line is able to metabolically activate 1-HMP resulting in the formation of micronuclei. Thus, Ishikawa cells were seeded on glass slides and treated with 1-HMP (up to 50 µM) for 18 h in the absence and presence of STX-64 (used as SULT inhibitor). After the substance free post-incubation period of 2 doubling times cells were fixed with paraformaldehyde, immunostained (alpha-tubulin, centromere proteins) and evaluated fluorescence-microscopically for micronuclei containing whole chromosomes (centromere positive) or chromosome fragments (centromere negative). DMSO and ethyl methanesulfonate were used as negative and positive control, respectively. Inhibition of SULT activity by STX-64 was verified in parallel incubations using estradiol as SULT substrate and monitoring formation of estrogen sulfates in incubation medium by UHPLC-MS/MS.

1-HMP increased dose-dependently the frequency of micronuclei containing chromosome fragments, whereas in the presence of STX-64 no increase in micronucleated cells was observed.

Thus, the Ishikawa cell line seems a suitable candidate to test SULT-mediated metabolic activation of genotoxins.

P050

Improving human relevance of Ames tests for regulatory use via *in silico* predicted metabolites

A. Drees¹, V. O. Jejenywa², A. Schütte², S. E. Escher³, M. Batke², J. vom Brocke¹

¹ECHA, Helsinki, Finland

²Hochschule Emden-Leer, Emden, Germany

³Fraunhofer ITEM, Hannover, Germany

Introduction: The information requirements for substances of low annual production volumes (1-10 t/y) under REACH are so limited that they can hardly support regulatory risk management for ca. 3500 substances. Although the bacterial gene mutation (Ames) assay is frequently considered over-predictive, an analysis of the REACH database identified >50 substances out of 10800 with reliable data, which were negative in the Ames assay and positive in other genotoxicity tests.

Objectives: One area for potential improvement is increasing the relevance of metabolites to humans, e.g. in the Ames test system, which commonly uses rat-derived induced-liver S9 homogenates for metabolism of test substances.

Materials and methods: Our analysis starts from a curated pool of a hundred substances that are negative in the Ames assay and predicts metabolites with human relevance using Meteor Nexus v.3.1.0 by Lhasa as well as the OECD QSAR Toolbox in a first step. These are then matched with data base entries from human *in vitro* screening data from high quality inventories such as ToxCast and Tox21, entries of genotoxic or carcinogenic substances in the REACH database, and CPDB from CEFIC LRI B18 project. In case no match is found, the metabolites are subjected to DNA-reactivity profiling using the LMC module of the OECD QSAR toolbox.

Results: We identified three outcome types for the predicted metabolites: identification of additional substances with a concern for mutagenicity, confirmation of low concern for DNA reactivity of all metabolites, or equivocal results. Groups for which additional concerns for mutagenicity were identified are alkenes, nitro-compounds, amines and ethers.

Conclusion: There is potential for improvement of genotoxicity assessment using not only *in-vitro* but also *in-silico* approaches for targeting gaps that are left especially by *in-vitro* metabolism. This will support clarifying the impact of metabolite predictions in our effort to identify and address substances of concern as quickly as possible.

P051

Role of ascorbic acid in the chromate-induced cytotoxicity and gene expression profiles in human lung epithelial cells

F. Fischer¹, E. Veh¹, S. Schorb¹, P. Schumacher¹, A. Hartwig¹

¹Karlsruhe Institute of Technology, Institute of Applied Biosciences, Department of Food Chemistry and Toxicology, Karlsruhe, Germany

Ascorbic acid (AA) is an essential cofactor for many enzymes involved in processes of barrier integrity, transcription, hormone regulation and epigenetics. Furthermore, it plays a pivotal role in the maintenance of genomic stability as an antioxidant. However, cell cultures lack AA due to its rapid degradation in culture medium. Thus, it may be prudent to load the cells with AA in order to reflect the physiological conditions more closely. This is particularly critical for toxicological studies of chromate since ascorbate acts as an intracellular reductant and has been proposed to strongly affect toxicity, genotoxicity as well as epigenetic alterations caused by chromate.

Within the present study, A549 and Beas-2B cells were preincubated with dehydroascorbic acid (DHA) to receive an intracellular AA level in the physiological range (1-5 mM). Preincubated cells (DHA+) and DHA-free cells (DHA-) were tested for chromate-induced cytotoxicity via ATP-Assay and intracellular uptake of chromium using atomic absorption spectrometry. Additionally, transcriptional toxicity profiles were obtained by a high-throughput RT-qPCR.

Treatment with chromate resulted in a concentration-dependent cytotoxicity in both cell lines, which was reduced in DHA+ A549 cells but not in DHA+ Beas-2B cells. Uptake studies were performed to rule out the possibility that the reduced cytotoxicity was caused by extracellular reduction of chromium(VI) to chromium(III), since chromium(III) cannot cross the plasma membrane. In both cell lines a difference in chromium uptake was observed between DHA+ and DHA- cells. The gene expression profile obtained in this study using high-throughput RT-qPCR indicates a complex mode of action of chromate. Many genes coding for proteins involved in epigenetic regulation, DNA damage response, inflammation, oxidative stress response, cell cycle progression and apoptosis were affected by chromate. In addition, the gene expression profile of some investigated genes differ between DHA+ cells and DHA- cells in a quantitative manner. In conclusion, preincubation with DHA leads to a higher acute cytotoxicity of chromate in Beas-2B cells but not in A549 cells. This effect as well as the differences in gene expression profiles highlight the importance of further research in this area.

P052

Optimization of the *in vitro* alkaline comet assay with HepG2 cells for genotoxicity testing of N-nitrosamines

M. Divari¹, L. Elenschneider¹, M. Engelke¹, C. Ziemann¹

¹Fraunhofer Institute for Toxicology and Experimental Medicine, Hannover, Germany

N-Nitrosamines (NAs) are currently of high concern for pharmaceuticals, due to detection of potentially carcinogenic NA impurities in certain products. The European Medicine Agency-funded Mutamind project aims at investigating, amongst others, the predictivity of the *in vitro* alkaline Comet assay (CA) for a carcinogenic outcome of NA exposure. As *in vitro* test systems, different liver cell models were chosen, as the liver represents a target organ for NAs, and NAs need cytochrome P450-dependent metabolic activation for DNA adduct formation. The objective of the present experiments was to optimize the standard CA protocol for genotoxicity testing of NAs. Hepatocellular carcinoma HepG2 cells, supposed to exhibit some metabolic competence, were initially used as an easy-to-handle liver cell model. The known carcinogen N-nitrosodimethylamine (NDMA, 0.1 – 20 mM) served as NA and ethyl methanesulfonate (EMS, -S9-mix) and cyclophosphamide (CP, +S9-mix) as established clastogenic positive controls. HepG2 cells precultured for either 24 or 48 h were exposed to NDMA (4 – 24 h) with cytotoxicity determined by cell counting. After characterization of the used HepG2 batch regarding morphology, population doubling time and sensitivity towards relevant solvents and CP and EMS as CA positive controls, it turned out that S9-mix, as exogenous metabolic system should be added to the CA treatment protocol, as HepG2 cells were not able to metabolically activate CP. However, initial experiments with 4 and 6 h of incubation with NDMA (1, 5, 10, and 20 mM) without S9-mix demonstrated that HepG2 cells were, nevertheless, able to directly activate NDMA. Observed concentration-dependent increase in mean tail intensity was comparable for both incubation times, amounting to 16.9% (4 h) and 18% (6 h) at 20 mM NDMA versus 5.5% for negative control. Subsequent experiments further demonstrated that the effect was independent of the preculture time, and both 24 h of incubation and addition of S9-mix did not markedly alter the genotoxic response to NDMA. Regarding cytotoxicity, slight NDMA-mediated decrease in cell count was noted in higher concentrations. In conclusion, the CA was able to clearly detect genotoxicity of NDMA using HepG2 cells even without S9-mix. However, since HepG2 cells were not able to metabolically activate CP, their overall metabolic competence seems limited. Thus, NAs with unknown genotoxicity/carcinogenicity should be tested ± S9-mix to avoid false-negative results.

Toxicology – Nanomaterials

P054

Refinement of the acute inhalation limit dose test for inert particles: An *in silico* model to set reasonable upper aerosol concentrations

L. Ma-Hock¹, H. Stratemann², R. Corley³

¹BASF SE, Ludwigshafen / Rhein, Germany

²Sun Chemical, Basel, Switzerland

³Greek Creek Toxicokinetics Consulting, LLC, Idaho 83714, United States

Introduction: According to the REACH regulation acute inhalation toxicity is an information requirement for nanoparticles. The OECD guidance document No. 39 recommends a top dose concentration of 2 mg/L to avoid unnecessarily high exposure concentrations. Yet, the classification criterion for GHS category 4 is a LC50 below 5 mg/L. This poses a regulatory dilemma: Test guideline and classification criteria do not match. Hoffmann et al. (2016) showed that rats die of suffocation due to particles clogging the airways. This is an artifact of too high aerosol concentrations in rats. Yet, testing these high concentrations would be necessary to avoid classification as "harmful".

Objectives: We examined whether *in silico* models can predict obstruction of the airway of the rat by clogging particles and whether this effect would be relevant to humans.

Materials and method: Acute inhalation of copper phthalocyanine pigment was tested in Wistar rats according to OECD guideline 403 (nose-only). The mass of deposited particles in the airways was modeled by Multiple Path Particle Dosimetry (MPPD) model for rats and human. The total mass of aerosol particles that were retained in each tracheobronchial and pulmonary airway at the end of the four-hour exposure were assumed to form a single spherical particle agglomerate. The diameters of these agglomerates were then compared with airway diameters of rats and humans.

Results: In the acute inhalation toxicity testing all rats died at 5 mg/L. Histopathological examinations revealed that many airways were obstructed with agglomerated particles. Ratios of the diameters of the agglomerates and the corresponding airway diameters of the tracheobronchial and pulmonary regions in the rat were >0.5 and in some cases >1.0, indicating that some airways were blocked. When cumulative deposited mass is normalized to respective airway surface areas, the rat received a 5-10-fold higher dose per airway surface in the tracheobronchial regions than the human.

Conclusion: *In silico* models support the hypothesis, that high aerosol concentrations (>2 mg/L) of inert particles may lead to blocking of rat airways leading to death by suffocation. Indeed, suffocation seems not to be likely in human. This would support the upper concentration of 2 mg/L suggested by the OECD guidance no. 39, rather than the GHS classification limit of 5 mg/L. The *in silico* model could be used to provide a rationale for limiting the upper aerosol concentration for inert particles.

P055**Comparison of a 3D co-culture and a mini organ culture by testing barium sulphate and titanium dioxide nanoparticle aerosols.**D. Eckstein¹, B. Schumann¹, F. Glahn¹, O. Krings¹, A. Schober², H. Foth¹¹MLU Halle-Wittenberg, Environmental Toxicology, Halle (Saale), Germany²TU Ilmenau, Nanobiosystemtechnik, Ilmenau, Germany

Nowadays, the demand for in vivo alternatives is increasing. We established 2 in vitro methods for lung tox. testing with aerosols of nanoparticles (NP), a 3D co-culture (PLC/EA.hy926) on a 3D membrane & a mini organ culture (MOC). NP can be found in many products of the daily use. They can be emitted at different stages of the product's life. Our models were exposed to barium sulphate (BaSO₄) and titanium dioxide (TiO₂) NP aerosols.

Viability of 3D co-cultures and MOC was determined by Resazurin assay. The size distribution of the particles in the aerosols was determined by SMPS and OPS.

For acute tox. testing, we exposed our cultures to NP aerosols for 1 h (23 h & 71 h post-incub.). For chronic tox. testing we exposed the 3D co-culture to NP aerosols (washing & additive exposure) 2 times and the MOC to NP aerosols 4 times. In the Resazurin assay acute exposure of co-cultures to 0.9 g/l BaSO₄ aerosol (conc. of stock suspen. resulting in averagely 5x10⁴ particles/cm³ in the aerosol) shows a distinct viability decreasing effect after 24 h. The exposure of co-cultures to 0.9 g/l TiO₂ aerosol (conc. of stock suspen. resulting in averagely 1x10⁵ particles/cm³ in the aerosol) shows a noticeable decreasing effect after 24 h, too. MOC show no decrease of viability after short term exposure for 1 h and postincub. for 23 h & 71 h with BaSO₄ NP and TiO₂ NP aerosols at the highest conc. of 0.9 g/l (conc. of stock suspen., resulting in averagely 4.5x10⁴ particles/cm³ for BaSO₄ NP aerosol and 8x10⁴ particles/cm³ for TiO₂ NP aerosol). In the chronic exposure of co-cultures to 0.9 g/l BaSO₄ aerosols the viability decreases to 40 - 60 % (depending on the patient) when 3D co-cultures were washed before exposure. Exposure of co-cultures to 0.9 g/l TiO₂ aerosols under such conditions shows a clear decrease to 0 - 30 % (depending on the patient). Contrary to these findings, there was no decrease of viability after chronic exposure of MOC to BaSO₄ NP and TiO₂ NP aerosols at the highest conc. of 0.9 g/l (exposure 4 times in 2 weeks). Based on the number size distribution more than 50 % of particles had a size below 100 nm.

The applied NP aerosols of BaSO₄ & TiO₂ cause more toxic effects in the 3D co-cultures than in MOC. This might be due to the fact that the remaining natural 3D structure of the cells in the MOC may be beneficial for the protection of the whole cell complex. Furthermore, in case of the MOC the exposed surface is much smaller than in the 3D co-cultures.

Toxicology – Organ toxicology**P056****Human liver spheroids: optimized cold storage and investigation of oxime-induced hepatotoxicity**G. Hom¹, T. Kranawetvogl¹, H. John¹, C. Weigel¹, U. Rauen², F. Worek¹, T. Wille¹¹Institut für Pharmakologie und Toxikologie der Bundeswehr, München, Germany²Institut für Physiologische Chemie, Essen, Germany

Introduction: To enable storage of liver spheroids, hypothermic storage in preservation solutions was optimized (ion composition and iron chelators). Oximes are antidotes in the therapy of organophosphorus compound (OP) poisoning. Pathologic liver parameters were observed in some case reports of OP poisoning and associated with oxime treatment. In this study, oxime-induced hepatotoxic effects were investigated with human liver spheroids.

Methods: Viability of liver spheroids was assessed after 24 h to 72 h cold storage at 4 °C in culture medium and two tissue preservation solutions with different content of deferoxamine (0.1 mM versus 0.5 mM) and subsequent rewarming at 37 °C. Additionally, liver spheroids were exposed to the oximes pralidoxime, obidoxime, HI-6, MMB-4 and to the OP malathion and malaoxon alone or in combination with obidoxime. Effective concentrations (EC50) were determined with an ATP assay at several time points. Aspartate aminotransferase (AST), alanine aminotransferase (ALT) and albumin were measured in supernatants. Diclofenac was used as positive hepatotoxic control.

Results: Cold storage for 72 h in standard culture medium with subsequent rewarming in culture medium solution resulted in a complete loss of viability (<1 %). Both tissue preservation solutions preserved viability without significant difference (86 ± 4 %, 0.1 mM deferoxamine vs. 95 ± 3 %, 0.5 mM deferoxamine).

The individually tested oximes and OP showed a low cytotoxicity with EC50 mostly > 2 mM. Exposure to malathion in the presence of 1 mM obidoxime up to 96 h resulted in EC50 values > 2 mM and no significant changes in albumin, AST or ALT release. In contrast, the exposure to malaoxon in the presence of 1 mM obidoxime resulted in a marked decrease of viability (EC50 = 532 ± 33 µM) and an increased AST release after 72 h (77.7 ± 4 ng/mL for 2 mM malaoxon with 1 mM obidoxime vs. 31.8 ± 1 ng/mL with control). Data are given as mean ± SEM.

Conclusion: The preservation of liver spheroids during cold storage at 4 °C with subsequent rewarming can be optimized with specifically designed tissue preservation solutions. The cytotoxicity of the individual oximes and malathion in liver spheroids is low. The decrease of viability and the increased release of AST after exposure to malaoxon in the presence of 1 mM obidoxime supports the assumption that impaired liver function after OP poisoning may be provoked only if oximes are used in supratherapeutic concentrations.

P057**Reactivation of organophosphorus compound-inhibited acetylcholinesterase in rat precision cut lung slices**F. Göllitz¹, F. Worek¹, T. Wille¹¹Bundeswehr Institute of Pharmacology and Toxicology/ LMU, Munich, Germany

Question: The recent use of organophosphorus nerve agents (OPNA) underlines the need of an optimized medical treatment. OPNA inhibit acetylcholinesterase (AChE) activity with subsequent acetylcholine overflow resulting in bronchoconstriction and bronchorrhea. Thus, precision cut lung slices (PCLS) are a meaningful model to investigate (experimental) therapeutic approaches. In the current study the AChE activities were investigated in OPNA-exposed and reactivator-treated PCLS and correlated with the respective airway areas.

Methods: AChE activity in rat PCLS was determined with a colorimetric reaction (modified Ellman assay). PCLS were exposed to cyclosarin (GF), sarin (GB) or VX. Then, as the oximes obidoxime (OBI) and HI-6 or the experimental reactivator NOX-6 was added to OPNA-inhibited AChE and the AChE reactivation was assessed for 30 min. Changes in airway area were observed by video-microscopy in a similar experimental setting for selected conditions.

Results: Colorimetric determination of AChE activities in intact PCLS was successfully assessed here for the first time. Exposure with GB, VX or GF resulted in residual AChE activities ≤ 12±2% and airway areas ≤ 13±4% suggesting good correlation of both parameters. For GB-inhibited AChE reactivation was highest with OBI 83±6% and HI-6 64±1%. For VX-inhibited AChE reactivation data were lower for OBI 71±3%, NOX-6 55±4% followed by HI-6 51±1%. AChE reactivation was lowest for GF-inhibited AChE OBI 13±3% and HI-6 15±3% - those results are comparable to the residual activity after OPNA exposure and therefore nearly no AChE was reactivated. For selected OPNAs and reactivators airway area changes were assessed as well. For GB- or GF-exposed PCLS, both reactivated with OBI, similar data to AChE reactivation were recorded (OBI 74±6% and HI-6 11±3%), suggesting good correlation of AChE activities with airway area data.

Conclusion: PCLS can be used to determine the AChE activity in intact tissue. Reactivation data of rat PCLS are in line with data of rat red blood cell AChE which were published previously. Bronchoconstriction and bronchorrhea in OPNA poisoning are typically addressed by administration of atropine. However, current data show, that AChE reactivators contribute to counteract bronchoconstriction by reactivation of AChE targeting the pathomechanism more upstream than atropine does.

P058**Preclinical safety assessment of selected extracts of pyrrolizidine alkaloid producing plants**A. Müller¹, C. Turek¹, N. Mörbt¹, P. Vögele¹, F. C. Stintzing¹¹WALA Heilmittel GmbH, Bad Boll/Eckwälden, Germany

Pyrrolizidine alkaloids (PAs) are among the most important plant toxins. They are produced as defense compounds against herbivores by more than 6,000 plant species, mainly belonging to the *Asteraceae*, *Boraginaceae* and the *Fabaceae*. PAs themselves are chemically non-reactive, only their metabolic activation of the 1,2-unsaturated necine backbone results in carcinogenic, genotoxic, and hepatotoxic properties. Due to hepatic metabolism, hepatotoxicity, ultimately leading to liver damage, is a potentially serious result following ingestion of PAs. Humans, livestock and wildlife are at risk by accidental uptake of PA containing contaminated food and feed. However, extracts from PA producing plant species also possess various pharmacological properties and therefore are part of traditional medicinal products. Considering that PAs are natural constituents in a number of plants used for medicinal purposes and that PAs might be part of the food chain, the Committee on Herbal Medicinal Products (HMPC) of the European Medicines Agency (EMA) issued a *Public statement on the use of herbal medicinal products containing toxic, unsaturated pyrrolizidine alkaloids (PAs) including recommendations regarding contamination of herbal medicinal products with PAs* [EMA, 2021]. Consequently, the aim of the present study was to close the gap between the high safety requirements for medicinal products produced from typical PA plants and the lack of extract specific data. To achieve this, aqueous and ethanolic extracts from *Borago officinalis*, *Petasites hybridus* and *Symphytum officinale* were analysed for their PA content and their mutagenic as well as hepatotoxic potential *in vitro*. Primary human hepatocytes were exposed to different concentration levels of the test items and cytotoxicity was determined by MTT kits. Concomitantly, extracts were subjected to bacterial reverse mutation assays following OECD standards, with and without exogenous metabolic activation. None of the extracts analysed showed any cytotoxic effect on primary human hepatocytes and no evidence for genotoxic potential was found in any of the test items. As a key step of preclinical safety assessment, these new data contribute to a thorough risk assessment of the selected plant extracts as well as preparations thereof, ensuring a safe application of medicinal products containing these.

P059**Are murine air liquid interface (ALI) models suitable for toxicity testing of cigarette smoke extract (CSE)?**J. Müller¹, P. Alt¹, T. Gudermann¹, C. Staab-Weijnitz², A. Dietrich¹¹Walther-Straub-Institut für Pharmakologie und Toxikologie, Munich, Germany²Comprehensive Pneumology Center Helmholtz-Zentrum München, Munich, Germany

Introduction: Cigarette smoke exposure is one of the main causes of Chronic Obstructive Pulmonary Disease (COPD), which is characterized by an altered composition of the airway epithelium. Chronic application of Cigarette Smoke Extract (CSE) during the differentiation of human bronchial epithelial cells at the Air Liquid Interface (ALI)

decreases the number of ciliated cells, while the populations of club and goblet cells were increased [1]. However, COPD-promoting pathways induced by CSE are not fully understood. ALI models from available gene-deficient mouse models would be extremely helpful for a detailed molecular and cellular analysis of these pathways. Therefore, we asked if primary murine tracheal epithelial cells (mTec) differentiated in a murine ALI model behave similar to the human model after exposure to CSE.

Methods: mTec including basal cells from wild-type mice were isolated, cultured and differentiated to a pseudostratified epithelium in a murine ALI model. CSE was freshly diluted in medium to a concentration of 5% to allow for chronic basolateral treatment of airlifted cells. H&E stained sections were prepared to monitor the differentiation process. Ciliated, goblet and club cells were quantified by immunofluorescence (IF) with cell type specific antibodies. mRNA expression of smoke exposure regulated genes (SERGs) identified in human ALI models [2] was quantified by RT-qPCR. Cell viability was analyzed by an LDH assay.

Results: We established a reproducible protocol for the generation of CSE that is applicable on differentiating ALI-cultures of murine tracheal basal cells. mRNA expression of SERGs was up-regulated by CSE in murine cells similar to the human ALI model, validating CSE potency. Cell viability assays showed no acute toxicity of 5% CSE and basal cells differentiated into a pseudostratified epithelium. Identification of epithelial cells was performed by IF-staining, and revealed no altered cell differentiation pattern after chronic CSE application for four weeks. However, at the mRNA level, we found a downregulation of cell specific markers.

Discussion:

Our data in the murine ALI model showed no differences in cell types following chronic CSE exposure compared to the human model. Therefore, murine ALI models may not be suitable to dissect molecular steps in CSE-associated human diseases like COPD.

[1] Schamberger et al., Sci. Rep. **2015**, 5, 8163

[2] Mastalerz et al., AJP Lung **2022**, 322, L129

P060

Differences between humans and rats in chloroform-induced effects on the olfactory epithelium

N. Hund¹, B. Brinkmann¹, R. Bartsch¹, G. Schriever-Schwemmer¹, G. Jahnke¹, A. Hartwig¹

¹MAK Kommission, Karlsruher Institut für Technologie (KIT) Institut für Angewandte Biowissenschaften Abteilung Lebensmittelchemie und Toxikologie, Karlsruhe, Germany

Introduction: The Permanent Senate Commission for the Investigation of Health Hazards of Chemical Compounds in the Work Area (MAK Commission) proposes maximum workplace concentrations (MAK values) for chemicals in order to provide comprehensive information for workplace safety professionals and researchers and to give scientific policy advice. Recently, the MAK Commission re-evaluated the hazard of chloroform at the workplace.

Objectives: Chloroform affects the central nervous system, liver and kidneys after oral and inhalation exposure. A new 2-year inhalation study in rats and mice indicated that nasal lesions play a major role in chloroform-induced toxicity. However, differences in anatomy, physiology and air flow dynamics in the nasal cavity between humans and rodents raise the question if rodents are more sensitive for effects in the olfactory epithelium (OE).

Methods: A comprehensive literature search on the toxicity of chloroform was performed. Reviews by other regulatory bodies and original studies on inhalation toxicity and metabolism were evaluated.

Results: In the new 2-year inhalation study, thickening of the bone in the nasal cavity and respiratory metaplasia of the OE were observed. The pathomechanism of thickening of the bone is due to a degeneration of the Bowman's glands, which are located in the OE. Rats and mice have a much higher proportion of olfactory epithelium than humans. Substances that cause effects in the Bowman's glands are therefore particularly effective for rodents. Furthermore, rodents exhibit significantly higher metabolic activity of cytochrome P450 (CYP) 2E1 in the OE than humans. As CYP2E1 is the key enzyme that metabolizes chloroform to the toxic phosgene, it is assumed that rodents are more sensitive than humans.

Detailed data are published in the journal of the MAK Commission: https://doi.org/10.34865/mb6766d7_4ad

Conclusion: Rodents are very likely more vulnerable for effects in the OE induced by chloroform than humans.

Toxicology – Toxic compounds

P061

Early hazard assessment of drug-induced phospholipidosis using *in vitro* and *in silico* approaches – investigation of metabolic capacity of HepG2-based *in vitro* assay and implications on *in silico* screening strategy

L. T. Anger¹, K. C. Wu¹, Y. Melnikov¹, C. Hasselgren¹

¹Genentech, Inc., Safety Assessment, San Francisco, United States

Over 50 approved drugs are on the market that cause drug-induced phospholipidosis (PLD). PLD is a lipid storage disorder, which is characterized by excessive accumulation of drug and polar phospholipids in lysosomes. On the one hand, PLD is considered adaptive and reversible, on the other hand it may negatively impact labeling and market development. Therefore, PLD is one endpoint for which drug candidates are screened early in pharmaceutical industry using *in vitro* and/or *in silico* approaches.

A challenge when predicting PLD is that some drugs like Ketoconazole and Loratadine are reported to induce PLD *in vivo*, where PLD is in fact caused by their respective N-dealkylation metabolites.

The simple but robust *in silico* approach developed by Ploemen et al., based on lipophilicity (logP) and basicity (pKa) descriptors, fails to classify both drugs as PLD-positive due to their low most basic pKa values. Both compounds are however experimentally positive in the HepG2-based PLD assay, suggesting the possible formation of the suspected metabolites *in vitro*, despite the reported low metabolic capacity for HepG2 cells.

We investigated whether N-dealkylation biotransformations, similar to those reported for Ketoconazole and Loratadine, might affect the PLD *in vitro* readout of 4 internal drug candidates. N-dealkylation often results in metabolites with higher basicity that are more likely to accumulate in lysosomes and therefore have a higher propensity to result in PLD.

Metabolite identification (MetID) studies were conducted in-house on compounds incubated in HepG2 cells following the PLD *in vitro* assay protocol. MetID studies confirmed formation of the suspected N-dealkylation metabolites for all 4 parent compounds. Co-incubation with CYP inhibitor 1-Aminobenzotriazole and pre-incubation with S9 additionally showed that the PLD signal can be shifted to higher or to lower concentrations, respectively.

We concluded that the HepG2-based PLD assay showed unexpected metabolic capacity, which may lead to positive PLD assay results that in fact need to be attributed to metabolites being formed *in vitro*. This comes with further practical implications for the *in silico* PLD model: If formation of metabolites with higher basicity (e.g. through N-dealkylation) seems likely, it is prudent to also run metabolite structures through the *in silico* model in parallel to their parent structures. For this more conservative approach, metabolite structures can be either obtained from MetID experiments - or Phase I metabolites can also be predicted *in silico* using commercial software.

P062

Chlorinated paraffins in food contact materials – a risk for consumers?

S. Zellmer¹, T. Tietz¹, T. Schulz², S. Schweizer², W. Vetter², S. Merkel¹, A. Luch¹

¹German Federal Institute for Risk Assessment (BfR), Department of Chemical and Product Safety, Berlin, Germany

²University of Hohenheim, Institute of Food Chemistry (170B), Stuttgart, Germany

Introduction: Chlorinated paraffins (CP) consist of polychlorinated alkanes with a degree of chlorination between 30 and 70%. Based on the carbon chain lengths, a classification into short-chain CP (SCCP, C10–13), medium chain CP (MCCP, C14–17) and long-chain CP (LCCP, C18–30) have been introduced. CP are used as pressure additives in the metal working industry, as plasticizers in the polyvinyl chloride (PVC) production, as additives to rubber, paints and lacquers, adhesive sealants and other polymer material, such as polyurethane, and as lubricants and flame retardants. Guida et al. (2022) showed that 48% PVC products for consumers (n = 87) from the Japanese market contained SCCP and/or MCCP. Also, 27 of 28 consumer products from the Belgian market contained SCCP, but mainly at very low concentrations. MCCP was detected in 5 samples, only (McGrath et al. 2021). The total global production of CP from 1930 to 2020 amounted to about 32.5 million metric tons (Chen et al. 2022). Target organs of repeated dose studies are liver, kidney and thyroid (EFSA 2020). SCCP are classified as Carc.2 (regulation EC 1272/2008) and are listed as persistent organic pollutants (POP) under the Stockholm convention and the European POP regulation (EU) 2019/1021. Hence, placing on the market and use of substances or mixtures containing SCCPs in concentrations above 1% by weight or articles containing SCCPs in concentrations above 0.15 % by weight is forbidden. MCCPs are candidates for listing as POPs, which might include LCCP as well.

Question: Are food contact materials made of PVC or rubber a source of CP, which are a potential exposure source for humans?

Method: A method was developed to isolate CP from PVC and rubber. More than thirty samples were extracted with n-hexane, followed by a cleaning step using silica gel. A subsequent analysis was performed with GC/NCI-MS for screening and quantification of the CP.

Result: First results showed that some market samples contained CP. The resulting potential human exposure through food contact materials is estimated.

Conclusions: Food contact materials made of PVC or rubber can be an additional source of CP, contributing to human exposure.

References:

- Chen C et al. 2022 (10.1021/acs.est.2c00264)
 EFSA 2020 (10.2903/j.efsa.2020.5991)
 Guida Y et al. 2022 (10.1016/j.scitotenv.2022.157762)
 McGrath T et al. 2021 (10.3390/ijerph18031069)

P063

A Method for the Extraction of Per- and Polyfluoroalkyl Substances (PFASs) from Wild Boar Tissues

H. Junk¹, T. Schwerdtle¹, K. Abraham¹, B. Monien¹

¹Bundesinstitut für Risikobewertung, Lebensmittelsicherheit, Berlin, Germany

Introduction: Per- and polyfluoroalkyl substances (PFASs) have many desirable properties, like water- and grease repellency or high thermal and chemical stability, so they are used widely in industry and consumer products. Due to bioaccumulation and persistence, some PFASs have attracted high attention as environmental contaminants. They are detected in serum samples of aquatic and terrestrial organisms, however, it is unclear to what extent individual PFASs accumulate in different tissues.

Objectives: The PFAS extraction from tissue samples is demanding due to the complexity of the matrices. The aim of the current work was to discover and optimize the most efficient among common extraction strategies.

Methods: Test samples were from wild boar tissues (liver, kidney and lung), spiked with isotope-labeled standards of eight perfluorocarboxylic acids and three perfluoroalkylsulfonates. A primary extraction (with or without a previous pepsin digestion) was selected from four different methods using either methanol at acidic, neutral or alkaline conditions, or methyl *tert*-butyl ether (MTBE) after ion-pairing with tributylamine. For the choice of a second purification step, we compared different SPE cartridges and various combinations thereof (Oasis WAX, ENVI-Carb, Hybrid Phospholipid) or dispersive SPE with C18 and ENVI-Carb material. The efficiencies of the extractions were evaluated after UPLC-MS/MS analysis at hand of 1) the recovery of spiked isotope-labeled standards, and 2) the signal intensities and signal-to-noise ratios of unlabeled PFASs.

Results: Preceding pepsin digestions had no effect on the extraction efficiency. The primary PFAS extraction of tissues homogenates with methanol under neutral conditions yielded the best recoveries. The most efficient matrix depletion by SPE was achieved using a sequence of a Hybrid Phospholipid cartridge and an ENVI-Carb column yielding recoveries typically in the range of 30 – 90%.

Conclusions: The comparison of different methods for the extraction and enrichment of PFASs from tissue samples allowed a reasonable selection of the fastest and most efficient of the clean-up methods. The limits of quantification of the ensuing UPLC-MS/MS analysis were in the range of 100 ng/kg tissue. The validated method will be used to determine PFAS levels in serum and different tissues to study the accumulation in wild boars in the region of Brandenburg.

P064

Long-term trends for blue mussels from the German Environmental Specimen Bank show first evidence of munition contaminants uptake

J. S. Strehse¹, T. H. Bünnig¹, J. Koschorreck², A. Künitzer², E. Maser¹

¹Institute of Toxicology and Pharmacology for Natural Scientists, University Medical School Schleswig-Holstein Campus Kiel, Kiel, Germany

²German Environment Agency, Dessau, Germany

Question: Submerged munitions are present in marine waters across the globe. They contain energetic compounds (EC) such as TNT and metabolites thereof. EC may cause threats to the marine flora and fauna as well as human health even decades after the disposal. Several studies have shown that TNT and its metabolites are carcinogenic and exhibit other acute and chronic toxic effects in a wide range of marine organisms. The aim of our study was to investigate the occurrence and trends of EC and TNT metabolites in blue mussels from the annual collections of the German Environmental Specimen Bank (ESB) sampled in the North Sea and Baltic Sea over the last 30 years.

Methods: Blue mussels were sampled at three different locations – one at the coastline of the Baltic Sea and two in the North Sea region. The mussel homogenates were retrieved from the German ESB archive and lyophilized at the Fraunhofer IME. Samples were extracted in the lab and analysed by GC-MS/MS for their concentrations of the EC 1,3-DNB, 2,4-DNT, TNT, and its metabolites 2- and 4-ADNT.

Results: While EC were not detected in blue mussels from any of the sampling regions before the year 1999, first signals indicating trace levels of 1,3-DNB were observed in the years 1999 and 2000 in samples from one of the North Sea regions. EC were also found below the limit of detection (LoD) in mussels from the other sampled regions in subsequent years. From 2012 onwards, signals just above the LoD, but below the limit of quantification (LoQ) were detected in blue mussels from one of the North Sea regions. In the other regions EC remained below the LoD for the subsequent years, with the exception in the years 2013, 2015, 2017, and 2019, where the LoD was just exceeded. The highest concentrations of 2-ADNT and 4-ADNT, just below the LoQ (0.14 ng/g d.w. for 2-ADNT, 0.17 ng/g d.w. for 4-ADNT), were measured in one of the North Sea regions in 2019 and 2020.

Conclusion: This study clearly shows that corroding submerged munitions are gradually releasing more and more toxic EC into the waters; and that toxic EC can be detected in randomly sampled blue mussels. Even though the concentrations measured are still in the non-quantifiable trace range, it has been clearly observed that the concentrations and abundances of these EC are increasing. It can therefore not be ruled out that contamination will worsen in the coming years if the munitions are not removed from the seas.

P065

World War Wrecks as a Point Source of Contamination of the Marine Environment with Energetic Compounds – The INTERREG North Sea Wrecks Project

T. Bünnig¹, E. Maser¹, J. S. Strehse¹, K. J. Andresen², M. Brenner³, S. Van Haelst⁴, M. De Rijcke⁴, U. Wichert⁵, P. Müller⁶

¹Institute of Toxicology and Pharmacology for Natural Scientists, University Medical School Schleswig-Holstein, Kiel, Germany

²Aarhus University, Department of Geosciences, Aarhus, Denmark

³Alfred Wegener Institute Helmholtz Centre for Polar and Marine Research, Bremerhaven, Germany

⁴Flanders Marine Institute, Oostende, Belgium

⁵Consultant BLANO, MEKUN and HELCOM SUBMERGED, Damp, Germany

⁶Freelancer, Bonn, Germany

Question: Hundreds of shipwrecks from both World Wars lie at the bottom of the North Sea, sunk by different acts of war. The spectrum of wrecks ranges from lightly armed guard units to full armored battle and transport ships, fully loaded with ammunition containing thousand tons of explosives. The fact that submerged munitions pose a threat to the marine environment has been demonstrated in various research projects in recent years. Whether this also applies to munitions on shipwrecks is the aim of the North Sea Wrecks Project.

Methods: Together with nine partner institutions participating in this INTERREG North Sea Region program-funded North Sea Wrecks project, we have analyzed whether munition loaded wrecks are a potential threat to the surrounding marine environment. After extensive archival research, fifteen wrecks off the coasts of the five countries were selected for sampling. Water and sediment samples were collected using CTD water samplers, Van Veen grabs, and by divers directly on the wreck. Biomonitoring using blue mussels and passive samplers were conducted on the vessels, as well as biota and scratch sampling. In addition, common dab (*Limanda limanda*) and pouting (*Trisopterus luscus*), sedentary species, were caught for histological and toxicological examination. Samples were analyzed by GC-MS/MS and LC-MS/MS for the explosives 1,3-DNB, 2,4-DNT, RDX, HMX, TNT and its metabolites 4-ADNT and 2-ADNT.

Results and conclusion: The investigations revealed different releases of energetic compounds from the wrecks. While on some wrecks the amounts were barely above the detection limit, on other wrecks, such as the WW I minelayer submarine UC30, the small WW I cruiser SMS Ariadne, and the WW II outpost boat V1302, significantly elevated concentrations of TNT and its metabolites 2- and 4-ADNT were detected in all sample types examined. In some sediment and water samples from the wreck of the UC30, TNT concentrations could be measured up to the µg/kg and µg/L range, respectively. On all three wrecks, TNT or its metabolites 2- and 4-ADNT were also detected in bile and muscle tissue of fish. In addition, there is evidence of a correlation between TNT concentration in tissues and an accumulation of liver diseases including liver tumors in adult fish, compared to a reference area considered uncontaminated. The results will be used for risk assessments, on the basis of which recommendations are to be made for administration and politics.

P066

Influence of physicochemical parameters on the dermal absorption of 1,4-dioxane and hydrofluoric acid: An ex-vivo diffusion cell study in human skin

S. Mini Vijayan¹, T. Göen¹, H. Drexler¹, S. Kilo¹

¹Friedrich Alexander Universität, Erlangen-Nürnberg, Erlangen, Germany

Introduction: The physical and chemical parameters of the skin are not constant. Intradermally, pH and temperature may be affected by inflammation and environmental conditions, respectively. This can influence the dermal absorption of substances. The aim of the study was to investigate the effect of these two parameters on the transdermal penetration of two substances, fluoride (hydrofluoric acid, HF) and the hydrophilic 1,4-dioxane.

Methods: Using an ex-vivo static diffusion cell model, dermal absorption was studied at two intradermal pH values, 7.2 (physiological) and 6.5, and at two skin temperature ranges, 32°C (high) and 24-25°C (low). 1,4-Dioxane (100%, 128 µl, 8 h) and HF (30%, 100 µl, 3 min) were applied to freshly excised human skin (0.9 mm thick, 0.64 cm² exposure area). Samples of the receptor solution were taken at regular intervals over a period of 8 h and tested for their fluoride (fluoride-sensitive electrode) and 1,4-dioxane (headspace GC-MS) content.

Results: At low pH, transdermal fluoride penetration increased by a factor of 1.7 compared to physiological pH, while absorption of 1,4-dioxane remained unaffected with maximum fluxes (absorption/time/area) of 30 and 13.8 µg/h/cm² and 41 and 39.5 µg/h/cm² for fluoride and 1,4-dioxane, respectively. In parallel, the lag time of fluoride absorption at both intradermal pH values was 20 min and 44 min, respectively, or remained at ~2 h for 1,4-dioxane. At low skin temperature, fluoride absorption decreased 1.3-fold compared with 32°C, whereas it increased 1.8-fold for 1,4-dioxane. Accordingly, higher flux values were observed for fluoride at 32°C (1.75-fold) and for 1,4-dioxane at 24°C (1.2-fold) and the lag time for fluoride absorption doubled to ~16 min and decreased from ~2 h to ~1.5 h for 1,4-dioxane, respectively.

Conclusion: Both substances showed temperature- and/or pH-dependent impact on their penetration behavior. Thus, changes in the intradermal properties of the skin, such as a pH decrease due to an inflammatory response (e.g., sunburn), can significantly affect the amount and kinetics of absorption of (toxic) substances. To understand the modulation mechanism of dermal absorption by variations in the physicochemical state, additional substances with different chemical properties (e.g. lipophilicity or polarity) shall be analyzed.

P067

Beeswax cloths – a safe alternative to plastic foils?

T. Tietz¹, I. Ebner², S. Zellmer¹, F. Kühne¹, S. Merkel¹, A. Luch¹

¹German Federal Institute for Risk Assessment (BfR), Chemicals and product safety, Berlin, Germany

²Berliner Hochschule für Technik, Fachbereich V – Life Sciences and Technology, Berlin, Germany

Introduction: Beeswax clothes are pieces of tissues, drenched in or coated with beeswax. They are marketed as an ecological and safe alternative to plastic or aluminium foils to wrap up food for storage or transportation and are used by an increasing number of consumers. The beeswax can contain additives like resins (e.g. rosin) and oils (e.g. jojoba, coconut oil) to improve the properties of the wax.

Objectives: Are beeswax clothes safe when repeatedly used in direct contact with food? What should be considered when using beeswax cloths with respect to use conditions and wax additives? In particular, is the use of Jojoba oil as wax additive likely to pose a health risk?

Method: In absence of experimental data, the possible migration of Jojoba oil from beeswax tissues was estimated using data from literature (1, 2) and reasonable assumptions on wrapped food item and contact area. In addition, toxicological studies and information on Jojoba oil and other ingredients were retrieved from the literature. Combining both, a provisional risk assessment was performed.

Result: The Jojoba oil exposure was estimated to be significantly higher than 50 µg/person/ day, both with worst case and reasonable best case assumptions.

From the data available and based on the structure of its components, Jojoba oil is most likely not genotoxic. A subacute oral study (28 days) showed damage of liver and intestine at high doses (4.5 and 9% in the food) as well as increased immune activity and inflammation. Data gaps were identified with respect to accumulation in man and long term toxicity.

Conclusions: Until data gaps on migration and toxicity are closed, Jojoba oil should not be used as substance with oral exposure, like an additive for beeswax cloths. This is in accordance with literature (3, 4, 5). Additional information on safe use of beeswax cloths in food contact were published by the BfR (6).

References:

- 1: <https://de.beeskin.com/blogs/interesting-reads/criticism-of-beeswax-wraps>
- 2: Grob et al. 1991. Zeits. f. Lebensm.-Unt. u. Forschung, 193: 213-219.
- 3: Verschuren et al. 1989: Food and Chemical Toxicology 27(1), 35-44.
- 4: Gruenwald et al. 2007: Physicians' Desk Reference for Herbal Medicines.
- 5: Natural Medicines (2022): Food, Herbs & Supplements. Jojoba
- 6: https://www.bfr.bund.de/en/beeswax_cloths__what_should_you_look_out_for_-271075.html

P068

Lithium Ion Battery Electrolyte Additives – Better Performance but Increased Health Risk?

E. Muschio¹, M. Kubot², M. Esselen¹

¹Westfälische Wilhelms-Universität Münster, Institute of Food Chemistry, Münster, Germany

²Westfälische Wilhelms-Universität Münster, MEET Battery Research Center, Münster, Germany

Lithium-ion batteries (LIB) can be found in consumer electronics as well as in (plug-in hybrid) electric vehicles (EVs). Especially as the EU wants to ban the production of cars with combustion engines from 2035 on, the number of LIBs and their average size will increase, thus enhancing the probability of accidents involving LIBs and the release of their compounds. With this perspective, toxicological investigations of LIB compounds are highly relevant.

The state-of-the-art electrolytes contain additives known to show acute toxicity and to damage organs at repeated exposure. For their degradation products, little toxicological data is available. Does the cycling/aging of the electrolytes increase or reduce their toxicity? Which influence do traces of water have? Starting point for the investigations were organo(fluoro)phosphates (OFPs), which are known as degradation products and show structural similarities to pesticides and chemical warfare agents.

Electrolytes have been studied before use, thermally (80°C, different durations) and electrochemically aged. The inhibition of acetylcholinesterase (AChE) is measured by a modified Ellman Assay. Cell viability was tested on HepG2 cells using the resazurin

assay. Also, DNA-damaging properties of the electrolytes are assessed and still under investigation.

Lithium difluorophosphate (LiDFP), a beneficial additive from the application perspective, yields the highest amount of AChE inhibition. Fluoroethylene carbonate (FEC) leads to a worse battery performance, but also to a lower OFP content. In the course of the thermal aging, e.g. FEC showed an increasing, LiDFP a decreasing cell viability. Water addition seems to accelerate the reaction speed, thus AChE inhibition and cell viability increase/decrease faster.

To conclude, the extent of OFP formation clearly differs depending on the additives used. Often additives with good performance are also more toxic, and the ones which show less toxicity cannot compete in efficiency. A solution could be the use of additive combinations, some of which were investigated as well.

Pharmacology – Cancer pharmacology

P069

Treatment of Cancer by targeting Histone deacetylase 8

S. Khatoon¹, S. Gayen¹

¹Jadavpur University, Department of Pharmaceutical Technology, Kolkata, India

Histone deacetylase 8 (HDAC8) selectivity over other HDACs is a major concern of interest since HDAC8 has been implicated as a potential drug target for many diseases including hematological malignancy. A quantitative activity-activity relationship (QAAR) study is a good strategy to explore the possible features to design HDAC8 selective inhibitors. Here, a mathematical framework was constructed to understand the important molecular fragments responsible for HDAC8 selectivity over HDAC1, 2, and 3. This study also deals with binary QAAR-based HDAC8 selectivity screening of some *in-house* molecules and understanding the reactivity and stability of the *in-house* molecules using DFT-based reactivity descriptors. Further, this study explores the possible binding mechanism of *in-house* compounds with HDAC8 through DFT and molecular dynamic simulation. Taken together, this study validates our previously proposed structural features for better HDAC8 inhibition. The comparative learning among the mathematical models, DFT-based calculation, and molecular dynamic simulation methods will surely enrich the scientific community to design selective HDAC8 inhibitors in the future.

P070

The role of steroid hormone levels on the E2-mediated CYP2B6 regulation in breast cancer cells in vitro

M. Hoffmann¹, J. Müller¹, S. Yamoune^{1,2}, J. C. Stingl¹

¹University Hospital RWTH Aachen, Institute of Clinical Pharmacology, Aachen, Germany

²Federal Institute for Drugs and Medical Devices (BfArM), Bonn, Germany

Introduction: Levels of steroid hormones like estradiol (E2) are relevant for the development and progression of breast cancer (BC). Systemic E2 levels are variable and strongly decrease with menopause or under endocrine BC therapy, which is often used in the treatment of estrogen receptor α (ER α) positive BC. Besides the proliferative effect of E2, its metabolites can also influence progression and prognosis. E2 is metabolized by the cytochrome P450 enzymes CYP1B1 to the cancerogenic 4-hydroxyestradiol and by CYP2B6 to 2-hydroxyestradiol, which is associated to better BC prognosis [1, 2]. The expression of CYP2B6 in BC tissue is linked to ER α expression [3] and the lower activity variant CYP2B6*6 is associated with increased BC risk [4].

Objectives: Our aim was to study the impact of systemic changes of steroid hormone levels on the expression and the E2-mediated regulation of CYP2B6 and the estrogen receptors.

Methods: To assess the E2-dependent regulation of CYP2B6, ER α -positive T47D cells were cultivated with either charcoal-stripped FBS or normal FBS before they were treated with 10 nM of E2. The transcriptional regulation was assessed by using qPCR.

Results: Pretreatment of T47D cells with different medium conditions led to a completely differential regulation of CYP2B6 by E2. Prior cultivation of T47D cells with FBS led to a downregulation of CYP2B6 mRNA expression by E2 treatment of approx. 0.5-fold, while cultivation in charcoal-stripped (steroid-hormone deprived) FBS led to a roughly 2-fold upregulation of CYP2B6 mRNA after incubation with E2.

Conclusion: Our results indicate that transcriptional regulation of CYP2B6 by E2 strongly depends on systemic steroid hormone levels. Hence, women who are exposed to strong hormonal fluctuations e.g., due to menopause or endocrine therapy receive or termination, may show highly different levels of CYP2B6 in BC tissue, potentially affecting BC progression and therapy efficacy.

[1] Fernandez et al. Estradiol and its metabolites 4-hydroxyestradiol and 2-hydroxyestradiol induce mutations in human breast epithelial cells. *Int. J. Cancer*. 2006

[2] Schneider et al. Antiestrogen action of 2-hydroxyestrone on MCF-7 human breast cancer cells. *J. Biol. Chem.* 1984

[3] Lo et al. Estrogen receptor-dependent regulation of CYP2B6 in human breast cancer cells. *Biochim Biophys Acta*. 2010

[4] Justenhoven et al. CYP2B6*6 is associated with increased breast cancer risk. *Int. J. Cancer*. 2014

P071**Potential influence of cancer-patient derived mutations in the MAP kinase negative regulator DUSP2 (dual-specificity phosphatase 2) on phosphatase activity**S. Malek¹, O. M. Setemes², I. Cascorbi¹, H. Bruckmüller^{1,2}¹UKSH Kiel, Institute for Experimental and Clinical Pharmacology, Kiel, Germany²The Arctic University of Tromsø, Department of Pharmacy, Tromsø, Norway

Introduction: The diffuse large B cell lymphoma (DLBCL) is a common malignancy which is characterized by high genetic and clinical heterogeneity leading to considerable differences in therapeutic response of patients. The MAP kinase (MAPK) signalling pathway is dysregulated in 85% of human cancers and found to be hyperactivated in DLBCL patients. However, the underlying molecular mechanisms are only poorly understood.

Objective: The dual-specificity phosphatase 2 (DUSP2), one of the major negative regulators of MAPKs, was shown to be frequently mutated in DLBCL patients. We aimed to investigate whether DUSP2 gene mutations could affect the phosphatase function and might thereby contribute to MAPK hyperactivation.

Methods: A cell-free expression system based on wheat germ extract was established to express the human DUSP2 protein as wild-type, phosphatase dead variant C1S as well as different patient-specific genetic variants. After expression and purification of DUSP2 proteins, their phosphatase activity was analyzed using DifMUP (6,8-difluoro-4-methylumbelliferyl phosphate) as fluorescent phosphatase substrate. The phosphatase activity of the DUSP2 wild type and variant proteins was compared in the presence and absence of various human MAP kinases (ERK1, ERK2, p38 α , p38 β , JNK1, JNK2).

Results: We were able to produce and purify wild-type and variant DUSP2 proteins. The phosphatase activity of DUSP2 wild-type protein was significantly increased by addition of all human MAPKs ($p < 0.001$) except by JNK2. ERK2 lead to the highest induction of phosphatase activity by 2,75-fold, followed by p38 β , p38 α , ERK1 and JNK1. For the DUSP2 proteins C1S and a frame shift variant phosphatase activity was lacking in absence and presence of MAPKs.

Conclusion: We established an expression system for human DUSP2 protein as well as a sensitive DifMUP based phosphatase assay to analyze DUSP2 activity in presence and absence of MAPK. First results indicate that DUSP2 mutations even outside the catalytic center compromise substantially the phosphatase activity as shown for the frame shift mutation, detected in a DLBCL patient. Additional patient-specific DUSP2 mutations ($n > 4$) will be investigated thereby aiming to determine if knowledge on DUSP2 mutations state might support individual treatment stratification.

P072**Role of fibronectin 1 in tyrosine kinase inhibitor resistance in chronic myeloid leukemia**L. Tiedemann¹, C. Pott², L. S. Schmidt¹, M. Litterst¹, I. Cascorbi¹, M. Kähler¹¹Institute of Pharmacology, UKSH Campus Kiel, Kiel, Germany²Department of Internal Medicine II, UKSH Campus Kiel, Kiel, Germany

Introduction: Chronic myeloid leukemia (CML) is a malignant hematopoietic neoplasm concomitant with the BCR-ABL1 kinase. It can successfully be treated with targeted therapy using tyrosine kinase inhibitors (TKIs), i.e. imatinib. However, therapeutic success is limited by resistances.

Objectives: Analyses of an in vitro-CML cell line model revealed altered cell adhesion signaling in TKI resistance. In particular, the expression level of the extracellular matrix protein fibronectin 1 (FN1) was decreased, however, its role in drug resistant CML remains unclear. Here, we investigate the impact of FN1 in therapy resistance against TKIs in CML.

Methods: An in vitro-TKI resistance K-562 cell line model of 2 μ M imatinib or 10 nM dasatinib was used for studies. FN1 downregulation was performed by siRNA transfection, FN1 overexpression by plasmid transfection with subsequent treatment of imatinib, as well as nilotinib, dasatinib, bosutinib, ponatinib or asciminib. Cellular fitness was analyzed by total cell number, cell viability, proliferation and cell cycle analyses. Cell adhesion was investigated using Matrigel-coated plates and Vybrant cell adhesion assay. FN1 expression in cell and in a cohort of ten CML-patients under TKI therapy was analyzed on mRNA and protein level by RT-qPCR and immunoblotting. FN1 location was investigated using immunofluorescence.

Results: siRNA-mediated FN1-knockdown in K-562 led to a significant reduction of TKI susceptibility to all BCR-ABL1 TKIs visible e.g. for bosutinib in an increased cell number (+31%, $p < 0.001$), cell viability (+47%, $p = 0.006$) and proliferation (+93%, $p < 0.001$). Restoration of FN1 in TKI resistant cells reinstated TKI susceptibility, as e.g. in dasatinib resistance cellular fitness was significantly decreased (cell number $p < 0.001$, cell viability $p = 0.004$, proliferation $p < 0.001$), cell adhesion was increased ($p = 0.01$). Regarding FN1 expression in CML-patients, FN1 downregulation was observed in patients lacking molecular response to their TKI therapy, whereas molecular remission was associated with 1.5-fold higher FN1 expression ($p = 0.04$).

Conclusion: Our data showed that FN1 expression in TKI resistant cells results in a restoration of TKI susceptibility, whereas its downregulation leads to resistance to all BCR-ABL1 TKIs. These effects are likewise observed in CML-patients suggesting that FN1 plays a role in TKI resistance in CML. These findings might offer a potential use of FN1 in TKI resistant CML treatment.

P073**Profiling changes in the cancer HLA-I peptide repertoire upon pharmacological intervention with kinase inhibitors and epigenetic modifiers**M. Bernhardt¹, A. Rech², B. Schilling², J. N. Herber³, F. Erhard⁴, A. Schlosser¹¹Julius-Maximilians-University, Rudolf Virchow Center, Würzburg, Germany²University Hospital Würzburg, Department of Dermatology, Venereology, and Allergology, Würzburg, Germany³Julius-Maximilians-University, Institut für Pharmakologie und Toxikologie, Würzburg, Germany⁴Julius-Maximilians-University, Institute for Virology and Immunobiology, Würzburg, Germany

Introduction: Success of cancer therapy often relies on effective pharmacological interventions. A broad repertoire of drugs with different therapeutic strategies enables the treatment of multiple cancers. The administered drug can induce alterations in the tumor (epi)genome or phenotype, leading to apoptosis or tumor growth inhibition.

Objectives: Drug-induced modulation of the HLA-I peptide repertoire (immunopeptidome) can bare promising targets, that can optimize anticancer effects by combining pharmacological treatment and immunotherapy. We therefore addressed the questions how anti-cancer drugs shape the HLA-I immunopeptidome and if we can identify drug-induced antigens that are suitable candidates for add-on immunotherapy.

Methods: First, to reliably profile ongoing immunopeptidomic changes, we established an in-vitro quantitative mass spectrometry-based approach, which we validated by monitoring the immunopeptidomic changes upon IFN γ treatment in melanoma cells. Next, we screened a panel of therapeutically relevant drugs for their ability to substantially modulate the HLA-I peptide repertoire upon drug-exposure. Our studies included kinase inhibitors for therapy of malignant melanoma, targeting BRAF (Vemurafenib) and MEK (Cobimetinib) or MNK (Tomivosertib), as well as epigenetically acting DNMT-1 inhibitors Decitabine and 5-Azacytidine, which are a therapeutic option for AML.

Results: Whereas inhibition of BRAF/MEK-signaling and inhibition of MNK induced only moderate but reproducible global ligandome alterations, the DNMT-1 inhibitors dynamically altered the immunopeptidome. Furthermore, we identified some tumor-associated antigens being cell specifically upregulated upon treatment with promising immunogenicity. However, we also observed downregulation of melanoma differentiation antigens, that could potentially decrease the tumor immunogenicity upon treatment with DNMT-1-inhibitors. Interestingly, we detected recurrent downregulation of some peptides, that occurred upon all conducted anti-cancer drug treatments and inhibition of oncogenic activity, thus, making them attractive tumor-related candidates for cancer vaccine development.

Conclusion: In summary, we could show that pharmacological treatment can modulate the HLA-I peptidome and can thereby determine cancer immunogenicity. We envision to further complement our findings with T-cell based immunogenicity assays and to include more cancer-therapeutic agents to our test panel.

P074**Medication review and therapy optimization in ovarian cancer patients as part of the KORE-OVAR-INNOVATION trial.**F. Meinerz¹, E. Algharably¹, R. Kreutz¹¹Charité – Universitätsmedizin Berlin, Institute of Clinical Pharmacology and Toxicology, Berlin, Germany

Introduction: The influence of pharmacotherapy during the perioperative management of surgical patients is important for outcome (1). KORE-OVAR-INNOVATION is an ongoing clinical trial to assess an innovative perioperative care pathway to reduce complications for patients undergoing surgery for ovarian cancer. The trial is supported by Innovationsfonds of the Gemeinsame Bundesausschuss (01NVF18021). We present first data regarding the structured medication review implemented in this trial to improve outcome.

Objective: To improve the pharmacological treatment of patients in the perioperative setting during their participation in the KORE-OVAR-INNOVATION trial by implementing a structured medication review.

Patients and methods: Overall, 414 electronic patient records will be reviewed in the preoperative, postoperative at from hospital discharge setting and at 30-day post discharge follow-up. Reviewed data include medical history, comorbidities, prescribed and over the counter medication as well as dietary supplements and complementary medication. The data will be matched with clinical parameters and current guideline recommendations for the identification of drug-related problems (DRPs) including potential over- and under-treatment, inappropriate dosing, adverse effects and drug-drug interactions (DDIs). Based on this review, recommendations for each assessment point will be provided.

Results: Preliminary data for 55 patients were available for assessment of all time-points. We identified DRPs in 15 (27.3%) patients preoperatively, in 13(23.6%) at discharge and 8(14.5%) at follow-up. These DRPs included over- and under-treatment and over- and under-dosing. Polypharmacy was detected in 7(12.7%) patients preoperatively, in 28 (50.9%) at discharge and in 13 (23.6%) at follow-up. Relevant DDIs were detected in 6 (10.9%) patients preoperatively, in 12(21.8%) at discharge and in 5(9.1%) at follow-up. Recommendations for medication change where made in 8(14.5%) patients preoperatively, in 7 (12.7%) at discharge and in 5 (9.1%) at follow-up. Inadequate medication in older patients were detected in 3 patients (5.5%) both preoperatively and at discharge.

Conclusion: Preliminary data show a trend for reduced DRPs in the course of the trial, which also correlates with the number of drug therapy recommendations made. Therefore, surgical patients may benefit from a medication review in the perioperative setting.

References: Parrish RH et al. J Clin Med. 2022 24;11(19):5628.

P076

Ascites reprograms peritoneal mesothelial cells to promote ovarian cancer cell migration

V. Shinkevich^{1,2}, L. Sommerfeld³, W. Szymanski⁴, J. Graumann^{2,4}, S. Reinartz^{2,3}, T. Worzfeld^{1,2}

¹Institute of Pharmacology, Biochemical-Pharmacological Center, Philipps University, Marburg, Germany

²DFG Research Training Group "The inflammatory tumor secretome" GRK2573, Marburg, Germany

³Department of Translational Oncology, Center for Tumor Biology and Immunology (ZTI), Philipps University, Marburg, Germany

⁴Institute of Translational Proteomics, Biochemical-Pharmacological Center, Philipps University, Marburg, Germany

Advanced stages of high-grade serous ovarian carcinoma (HGSOC) are characterized by the presence of malignant ascites and peritoneal dissemination of ovarian cancer cells (OCC). Peritoneal metastasis represents the key prognostic factor in HGSOC patients. In order to metastasize, OCC need to attach to and invade through a layer of mesothelial cells (HPMC), which line the peritoneal cavity. The functional role and the molecular mechanisms of the interaction between HPMC and OCC remain largely unclear. Here, we show that, unexpectedly, primary HPMC from HGSOC patients promote, rather than inhibit, migration of primary OCC. Our data indicate that this pro-migratory effect is mediated by an indirect communication mechanism, i.e. via the secretion of soluble factors. Moreover, we find that this secretion from HPMC is induced by malignant ascites. To identify the pro-migratory factors released from HPMC in response to ascites, we performed transcriptomic and proteomic analyses. Based on these systematic unbiased analyses, we tested candidate genes and proteins in functional assays. Altogether our data strongly suggest that HPMC have an important function in ovarian cancer cell metastasis into peritoneal organs, and that molecules in the tumor microenvironment result in the reprogramming of HPMC, which in turn contribute to tumor motility by secretion of soluble factors.

Pharmacology – Cardiac pharmacology

P077

Impairment of the antiplatelet effect of acetylsalicylic acid in patients early after cardiac surgery: Comparative impact of metamizole versus paracetamol

D. Trenk¹, B. Hainke², C. Lehane², E. Niebergall-Joos², S. Leggewie¹, S. Twarock³, T. Hohlfeld³, K. Schrör³, M. Siepe⁴, C. Keyl²

¹Universitätsklinikum Freiburg, Klinik für Kardiologie und Angiologie Bad Krozingen - Klinische Pharmakologie, Bad Krozingen, Germany

²Universitätsklinikum Freiburg, Klinik für Anästhesiologie und Intensivmedizin, Bad Krozingen, Germany

³Heinrich-Heine-Universität, Institut für Pharmakologie und Klinische Pharmakologie, Düsseldorf, Germany

⁴Universitätsklinikum Freiburg, Klinik für Herz- und Gefäßchirurgie, Bad Krozingen, Germany

Background: Low-dose acetylsalicylic acid (ASA) is recommended in current guidelines for a period of 3 months after surgical replacement of the aortic valve by a bioprosthesis as well as after surgical reconstruction of the mitral valve. Metamizole (dipyrone) and paracetamol (acetaminophen) are frequently used non-opioid analgesics after surgery. The active metabolite of metamizole (4-methylaminoantipyrine) is a reversible inhibitor of cyclooxygenase-1 and an interaction with the antiplatelet effect of ASA in more than 50 % of patients has been reported. Prospective randomized studies investigating the potential drug-drug interaction between ASA and high-dose metamizole in cardiac surgical patients are lacking so far.

Material and methods: We enrolled 162 patients in this prospective clinical study. Patients after surgical implantation of a bioprosthetic valve in aortic position or after mitral valve repair were eligible for enrollment. Patients were randomized at day 1 after surgery to either 4 x 1 g metamizole iv/day or 4 x 1 g paracetamol iv/day. All patients were on ASA 100 mg od. The primary endpoint was the proportion of patients with adequate antiplatelet response to ASA assessed via determination of thromboxane B2 in platelet rich plasma after stimulation with arachidonic acid (AA) at day 4/5 after surgery (cutpoint ≤ 209.8 ng/ml thromboxane B2). Key secondary endpoints comprised platelet reactivity assessed by light transmission aggregometry [LTA] and by multiple electrode impedance aggregometry [MEIA].

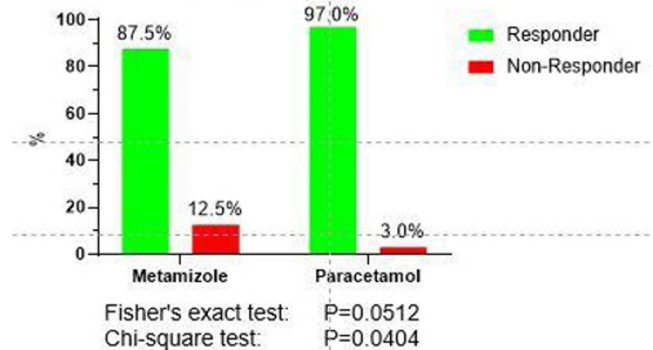
Results: 15 patients dropped out of the study. Thus, data from 71 patients randomized to metamizole and 76 patients randomized to paracetamol were available for data analysis. The primary endpoint analyzed at day 4/5 after surgery is shown in the Figure. The proportion of non-responders in patients treated with metamizole was lower than expected (12.5%) which is 4-fold higher compared with patients on paracetamol. The difference between the treatment groups was, however, of borderline statistical significance only. Platelet reactivity at day 4/5 after surgery assessed by LTA or MEIA was not statistically different between both treatment regimens.

Summary and conclusion: The proportion of non-responders to ASA is higher in patients treated with metamizole compared to paracetamol. The proportion of non-

responders in the metamizole-treated group in our study is substantially lower than reported in previous studies.

Fig. 1

Proportion of Responders/Non-Responders to ASA at Day 4/5



P078

Molecular fingerprints of SGLT2 inhibitors in non-myocyte cardiovascular cell models

K. Schmidt^{1,2}, A. Schmidt^{1,2}, M. Fuchs², S. Groß¹, A. Just¹, A. Pfanne¹, A. Pich¹, T. Thum^{1,2}, J. Fiedler^{1,2}

¹MH Hannover, IMTTS, Hannover, Germany

²Fraunhofer, ITEM, Hannover, Germany

Background: Sodium glucose co-transporter 2 inhibitors (SGLT2i) are approved anti-diabetic drugs with a wide clinical use. Beneficial effects of SGLT2i Dapagliflozin (DAPA) and Empagliflozin (EMPA) on cardiovascular (CV) adverse events have been reported in multiple clinical trials highlighting a novel class of CV therapeutics. However, considering the absence of SGLT2 in the CV system and beneficial effects in non-diabetic patients, various studies suggest SGLT2 independent *modi operandi* in the CV environment, which remain largely undisclosed and need to be defined.

Methods and results: Initially, proteomics datasets from human umbilical vein endothelial cells (HUVECs) treated with DAPA or EMPA were generated, and gene set enrichment analyses were performed to screen for deregulated nodes. Next to altered levels of interleukin-6 and intercellular adhesion molecule 1, reflecting impacted inflammatory signaling, we discovered regulation of clusters involved in reactive oxygen homeostasis, mitochondrial respiration, and actin cytoskeleton. Subsequently, we validated the suggested modes of action using various *in vitro* functional assays as well as transcriptome evaluations. We detected NFKB-repressive activity of SGLT2i using an NFKB-dependent reporter assay. Decreased respiratory capacity and ATP production of mitochondria combined with a reduced lactate production suggested an interference of DAPA with glycolytic metabolism. Moreover, DAPA reduced oxidative stress in HUVECs and decelerated primary human cardiac fibroblast (HCF) proliferation. In line with the described impact on actin cytoskeleton, DAPA slightly disturbed the angiogenic capacity of HUVECs modelled in tube formation assays and inhibited HUVEC and HCF migration in wound healing assays. This however, in both cell types, was not mediated by proposed interactions of SGLT2i with the sodium proton exchanger 1 (NHE1) confirmed by siRNA-knockdown experiments.

Conclusion: We screened for the impact of SGLT2i on non-myocyte CV cells applying bioinformatics-based processing of proteomics data coupled with various *in vitro* assays. Our findings underline an alteration of inflammatory signaling, oxidative stress regulation, glycolytic metabolism and migratory capacity in endothelial cells elicited by SGLT2i and, additionally suggest anti-fibrotic potential of these drugs. In conclusion, the presented data grant further insights into CV-protective mechanisms of SGLT2i to support clinical decision making.

P079

Upregulation of protease-activated receptors contributes to the molecular atrial substrate associated with post-operative atrial fibrillation (POAF)

C. Mittendorff¹, I. Abu-Taha¹, M. Kamler², D. Dobrev¹, A. Fender¹

¹Medical Faculty, University Duisburg-Essen, Institute of Pharmacology, Essen, Germany

²Medical Faculty, University Duisburg-Essen, Department of Thoracic and Cardiovascular Surgery, Essen, Germany

Introduction: New-onset POAF occurs in 30% of patients undergoing cardiovascular surgery and increases risk of stroke and mortality. Why some patients but not others develop POAF despite experiencing the same perioperative triggers is poorly understood, and clinical management remains challenging. Pre-existing Ca²⁺-handling abnormalities and NLRP3-inflammasome/CaMKII signaling sensitize atrial cardiomyocytes to pro-arrhythmic triggers, but the upstream regulators have not been identified. Surgery-associated coagulopathy substantially activates thrombin, which elicits coagulation-independent inflammation via protease-activated receptors (PAR). The role of PAR in the context of POAF is unknown.

Objectives: To identify PAR as candidate regulators of the POAF-prone molecular substrate.

Patients and methods: Right atrial appendages (RAA) of patients undergoing cardiac surgery were snap-frozen or enzymatically digested for cardiomyocyte isolation. Atria were collected from wildtype (WT) and PAR4^{-/-} mice and from mice subjected to sham hepatectomy (HPx) as a model of vascular surgery. HL-1 atrial cardiomyocytes were stimulated with thrombin or specific PAR-activating peptides (AP). Tissue and cell lysates were assayed by Western blot for markers of NLRP3 inflammasome and kinase activation and modification of Ca²⁺-handling proteins.

Results: RAA from POAF-prone patients exhibited higher abundance of thrombin receptors PAR1 and PAR4 in whole tissue lysates and at the cardiomyocyte level, compared to RAA from patients remaining in sinus rhythm. PAR4 correlated positively with expression of auto-activated caspase-1, IL-1 β and the pyroptotic pore protein gasdermin D in human RAA. In HL-1 cells, IL-1 β production was stimulated by thrombin or PAR4-AP, but not PAR1-AP. PAR4-AP additionally increased phosphorylation of CaMKII, Ryr2 and AKT/mTOR/P70S6K in HL-1 cells. Atria from PAR4^{-/-} mice expressed lower levels of activated caspase-1, IL-1 β and total and phospho-mTOR than WT atria. Sham HPx induced transient post-operative upregulation of PAR4, coinciding with elevated CaMKII, IL-1 β and total and phosphorylated mTOR.

Conclusion: Thrombin receptor PAR4 is upregulated in POAF-prone human atrial myocardium and likely contributes to the molecular POAF substrate by increasing signaling through AKT/mTOR, CaMKII and the NLRP3 inflammasome in atrial cardiomyocytes. Selective PAR4 antagonists may provide a novel therapeutic option to improve clinical management of POAF.

P080

Long non-coding RNA-mediated control of the cardiac rhythm

B. M. G. Idrissou¹, D. Esfandyari¹, S. Engelhardt¹

¹Technische Universität München, Institute of Pharmacology and Toxicology, München, Germany

Heart rhythm disorders are associated with considerable mortality, especially in an aging population. Ventricular arrhythmias are thought to cause 75-80% of cases of sudden cardiac death; a subset of patients die without prior symptoms due to inherited arrhythmia syndromes or pro-arrhythmic drugs. Since current treatment strategies have side effects and do not cure the underlying pathology, a deeper understanding of the regulatory mechanisms is required. Long non-coding RNAs (lncRNAs), defined as a class of RNAs longer than 200 nucleotides with limited coding potential and a diverse set of functions, have been reported to act as such regulatory elements. While a few lncRNAs reportedly affect the cardiac rhythm, most have been characterized in rodents. The findings have limited applicability to patients, as both the expression of lncRNAs as well as the heart rhythm show marked differences between rodents and humans.

To identify lncRNAs involved in regulating the human cardiac rhythm, we performed RNA-sequencing in human iPSC-derived cardiomyocytes and supplemented these data with transcriptomic datasets of adult human left ventricular myocardium. After determining lncRNAs with robust expression, the candidates were shortlisted according to enrichment in cardiomyocytes, conservation level and relevance to arrhythmia. We accomplished this by employing single-nuclear transcriptomic datasets, scrutinizing the genomic context and relation to known arrhythmia genes and leveraging data from genome-wide association studies with relevance to rhythm abnormalities.

To validate the seven most promising lncRNA candidates in vitro, we employed the RNA-targeting CRISPR-CasRx system. We designed a vector coding for both the CasRx enzyme as well as a sgRNA-array targeting each lncRNA, which we delivered using adeno-associated virus serotype 6 (AAV6). We were able to validate the efficiency of the knockdown in vitro via qPCR, observing robust repression of lncRNA levels of 50-90% for 6 out of 7 candidates. Optical action potential recordings via di-8-ANEPPS revealed significant effects on the action potential duration upon manipulation of 5 of the lncRNA candidates in hiPSC-CMs.

Overall, we have identified lncRNA candidates linked to the regulation of the human cardiac rhythm. After further validation and in-depth mechanistic characterization, these lncRNAs may prove to be promising novel drug targets.

P081

Effects of ergotamine, ergometrine, and LSD on mouse and human atrial preparations

H. Jacob¹, P. Braekow¹, C. Höhm¹, U. Gergs¹, B. Hofmann², L. Humphrys³, S. Pockes³, J. Neumann¹

¹Institute for Pharmacology and Toxicology, Medical Faculty, Martin Luther University Halle-Wittenberg, Halle (Saale), Germany

²Department of Cardiac Surgery, Mid-German Heart Center, University Hospital Halle, Halle (Saale), Germany

³Department of Pharmacy, University of Regensburg, Regensburg, Germany

Ergotamine, ergometrine and lysergic acid diethylamide (LSD) are known as hallucinogenic drugs. Their hallucinogenic actions are thought to be mediated by 5-HT_{2a}-receptors. We hypothesized that they might also act on cardiac serotonin receptors which are of the 5-HT₄ type in humans. To this end, we studied atrial preparations from transgenic mice with cardiomyocyte-specific overexpression of the human 5-HT₄-receptor (5-HT₄-TG) and human right atrial preparations obtained from bypass surgeries.

Ventricular function of transgenic mice was studied using isolated perfused heart preparations (Langendorff heart). In-vitro binding data for the human H₂-receptor were obtained from recombinantly expressed H₂-receptors in cell culture. We noted that ergotamine and LSD (10 μ M, each) increased force of contraction and beating rate in left or right atrial preparations from 5-HT₄-TG (n=4-5, p<0.05), respectively. However, they only act as partial agonists in 5-HT₄-TG atrial preparations. The inotropic and chronotropic effects ergotamine and LSD were antagonized by 10 μ M tropisetron in 5-HT₄-TG. Moreover, ergometrine had no effect in 5-HT₄-TG. Unexpectedly, ergotamine, ergometrine and LSD (10 μ M, each) increased force of contraction and beating rate in left or right atrial preparations, respectively, from a different transgenic mouse line, namely H₂-histamine receptor overexpressing mice (H₂-TG) as full agonists. These effects were antagonized by 10 μ M cimetidine. Moreover, the positive inotropic effects of ergotamine, ergometrine, and LSD (10 μ M, each) could be confirmed in Langendorff heart preparations from H₂-TG. Likewise, ergotamine, ergometrine and LSD (10 μ M, each) increased force of contraction and phospholamban phosphorylation in human atrial preparations (n=3-6, p<0.05). The contractile effects of ergotamine, ergometrine and LSD in human atrial preparations could be potentiated by 1 μ M cilostamide and antagonized by 10 μ M cimetidine and are, therefore, assumed to be H₂-receptor-mediated. Especially for LSD, the binding to the human H₂-receptor has been confirmed in an in-vitro assay using a recombinant expression system (pKi 4.49 \pm 0.09, n = 3). These data are of potential clinical relevance because these compounds are used for "recreative purposes" but also to treat e.g. depressions and might lead to cardiac side effects. We speculate that this knowledge might be useful in the treatment of intoxications by these hallucinogenic drugs with cimetidine.

P082

Effect of cantharidin on force and protein phosphorylation in mouse and human atrial preparations

R. Schwarz¹, B. Hofmann², U. Gergs¹, J. Neumann¹

¹Institute for Pharmacology and Toxicology, Medical Faculty, Martin Luther University Halle-Wittenberg, Halle (Saale), Germany

²Department of Cardiac Surgery, Mid-German Heart Center, University Hospital Halle, Halle (Saale), Germany

We have previously reported that cantharidin as an inhibitor of the activity of protein phosphatases 1 (PP1) and 2A (PP2A) can increase force of contraction but not beating rate in guinea pig atrial and ventricular preparations. This was accompanied by increased signals in autoradiograms on phospholamban (PLB), troponin inhibitor (TnI), C-protein and myosin light chain 20 (MLC20) in guinea pig ventricular cardiomyocytes, labeled with [³²P]-orthophosphate (J Pharmacol Exp Ther 1994, 274: 530-539). We had also shown that cantharidin increase force of contraction in human ventricular preparations (Br J Pharmacol 1996, 119: 545-550), but had not measured cantharidin-induced protein phosphorylation in humans. Therefore, we now studied those effects in isolated electrically stimulated (1 Hz) human right atrial preparations (HAP) obtained during bypass surgery and for comparison in wild type mouse left atrial (LA) and right atrial (RA) preparations. Concentration-response curves were obtained for force of contraction (LA) or beating rate (RA) in mouse (10 μ M, 30 μ M, 100 μ M cantharidin) and HAP (30 μ M, 100 μ M, 300 μ M cantharidin). Western blots with appropriate antibodies were done on freeze-clamped contracting LA, RA, or HAP to detect the phosphorylation state of PLB, TnI and MLC20. Cantharidin was more potent to increase force of contraction and protein phosphorylation in LA and RA starting at 10 μ M cantharidin with maximum effect at 100 μ M cantharidin, which started to lead in some samples to contractures (n=8). In HAP, the increase in force started at 100 μ M cantharidin. In contrast, cantharidin failed to increase beating rate in RA (n=8). The maximum effect in human atrial preparations occurred at 300 μ M leading to an increase in force of contraction (from 1.19 mN to 3.95 mN, by 332 %, p < 0.05, n = 11). Cantharidin reduced the time of relaxation (from 145 ms \pm 60 ms to 96 ms \pm 16 ms, that is by 66 %, p < 0.05, n = 11) and increased the rate of relaxation (from 25 mN/s to 88 mN/s, by 349.4 %, p < 0.05, n = 11) in HAP, respectively. Fittingly, in the very same human samples, cantharidin increased the phosphorylation state of PLB, MLC20 and TnI. We present pharmacological evidence that in the beating human atrium, PP1 and/or PP2A are able to dephosphorylate PLB, TnI and MLC20. These findings support an important role of PP in regulation of contraction and relaxation in the human heart, which may be amenable to drug therapy in patients with heart failure.

P083

Effect of dopamine-1 receptor agonists in D₁-dopamine receptor overexpressing mouse atrial preparations

L. M. Ravo Abella¹, U. Gergs¹, S. Pockes², J. Neumann¹

¹Institute for Pharmacology and Toxicology, Medical Faculty, Martin Luther University Halle-Wittenberg, Halle (Saale), Germany

²Department of Pharmacy, University of Regensburg, Regensburg, Germany

Dopamine can induce positive inotropic, chronotropic and proarrhythmic effects in the human heart but also in the wild type mouse heart via β -adrenoceptors. However, it is unclear whether D₁-dopamine receptors that are expressed on protein level in human heart, couple in principle to inotropy. Therefore, we have for the first time generated founders for transgenic mice (D₁-TG) with cardiomyocyte-specific overexpression of the human D₁-receptor. Isolated left atrial preparations of WT and D₁-TG were electrically stimulated (1 Hz) and force of contraction was measured. In isolated spontaneously beating right atrial preparations of WT and D₁-TG, the heart rate was measured. Moreover, we studied the effects of the D₁-receptor agonists SKF 38393 and fenoldopam. SKF 38393 exerted concentration-dependent (0.1 nM-1 μ M) and time-dependent positive inotropic effects only in atria of one founder (and the filial generation) of D₁-TG. The D₁-receptor antagonist SCH 29930 (1 μ M) antagonized these effects. However, no difference in chronotropic effects was observed between right atria of WT and D₁-TG. Basal force of contraction in D₁-TG was elevated and possibly therefore could not be further increased by the β -adrenoceptor agonist isoprenaline. Likewise, fenoldopam failed to increase force of contraction in D₁-TG. However, SCH 29930 alone reduced force of contraction in D₁-TG and now additionally administered fenoldopam as well as isoprenaline could augment force of contraction. We conclude that the function of the human D₁-receptor can involve inotropic effects in D₁-TG. D₁-receptors are constitutively active in D₁-TG. Conceivably,

dopamine can also act on D₁-receptors in the human heart. Conversely, the many classes of drugs that block D₁-receptors might antagonize D₁-mediated positive inotropic effects in the human heart.

P084

Clonidine is an agonist at guinea-pig cardiac H₂ receptors but not at human cardiac H₂ receptors

U. Gergs¹, B. Hofmann², U. Kirchhefer², S. Pockes⁴, L. Humphrys⁴, J. Neumann¹

¹Institute for Pharmacology and Toxicology, Medical Faculty, Martin Luther University Halle-Wittenberg, Halle (Saale), Germany

²Department of Cardiac Surgery, Mid-German Heart Center, University Hospital Halle, Halle (Saale), Germany

³Institute of Pharmacology and Toxicology, University of Münster, Münster, Germany

⁴Department of Pharmacy, University of Regensburg, Regensburg, Germany

Clinically, clonidine is sometimes used to lower blood pressure or to treat drug addiction in psychiatry. Inotropic or chronotropic effects of clonidine on the heart are not yet fully understood. There is some evidence that clonidine might act as an agonist at H₂ histamine receptors in the heart. Hence, we compared inotropic and chronotropic effects of clonidine in atrial preparations of guinea pigs and mice that overexpress the human H₂ histamine receptor in cardiomyocytes (H₂-TG) as well as inotropic effects in isolated electrically driven (1 Hz) human right atrial preparations. We noted that clonidine up to 100 µM exerted a concentration dependent positive chronotropic effect in isolated guinea pig right atrial preparations (pEC₅₀ = 5.45 ± 0.21, n = 4) that was antagonized by cimetidine and thus presumably H₂ receptor mediated. For comparison, we studied up to 100 µM clonidine in isolated left and right atrial preparations from H₂-TG. In H₂-TG, clonidine (100 µM) failed to increase force of contraction in isolated electrically driven (1 Hz) left atrial preparations and failed to augment the beating rate in isolated spontaneously beating right atrial preparations. As positive control, 10 µM histamine exerted positive inotropic and chronotropic effects in H₂-TG atrial preparations. Next, we studied isolated electrically driven (1 Hz) right atrial muscle strips from patients that underwent bypass surgery. Clonidine alone (10 µM) or in the additional presence of the phosphodiesterase III inhibitor clobutamide used to amplify signals, failed to increase force of contraction while 10 µM histamine was active to increase force of contraction. In cells, transfected with human H₂ receptors, up to 1 mM clonidine failed to bind to these receptors (n = 3). We conclude that sequence differences between the human and guinea pig H₂ receptor are sufficient that some agonists lose their ability to activate human H₂ receptors compared to guinea pig receptors. These data underscore the value of transgenic mice with the overexpressed human H₂ receptor to predict effects on human cardiac receptors. Moreover, our data would indicate that H₂ receptor stimulation is not involved in the clinical effects of clonidine.

P085

Cardiac effects of 5-methoxydimethyltryptamine and dimethyltryptamine

T. Dietrich¹, U. Gergs¹, B. Hofmann², C. Höhm¹, J. Neumann¹

¹Institute for Pharmacology and Toxicology, Medical Faculty, Martin Luther University Halle-Wittenberg, Halle (Saale), Germany

²Department of Cardiac Surgery, Mid-German Heart Center, University Hospital Halle, Halle (Saale), Germany

5-Methoxydimethyltryptamine (5MeDMT) and dimethyltryptamine (DMT) are hallucinogenic drugs and are contained in ritual drug mixtures like "ayahuasca" in South America. 5MeDMT and DMT can increase the beating rate of porcine right atrial preparations via 5-HT_{2A}-serotonin receptors. Here, we hypothesized that 5MeDMT and DMT might also act on human 5-HT₄-receptors. To this end, we studied isolated electrically driven (1 Hz) left and spontaneously beating right atrial preparations from transgenic mice with cardiomyocyte-specific overexpression of the human 5-HT₄-receptor (5-HT₄-TG) and isolated electrically driven (1 Hz) human right atrial preparations in the organ bath. Concentration response curves for 5MeDMT and DMT (1 nM - 10 µM, each) and as control for serotonin (5-HT, 1 nM - 1 µM) were performed. We noted that 5MeDMT and DMT concentration- and time-dependently increased force of contraction and beating rate in left or right atrial preparations from 5-HT₄-TG (n=8, each), respectively. 5MeDMT was more potent and effective than DMT. The inotropic effects of 5MeDMT and DMT were antagonized by 1 µM tropisetron in 5-HT₄-TG. In WT preparations, 5MeDMT, DMT, and 5-HT were ineffective. Likewise, 5MeDMT (10 µM) increased force of contraction and phospholamban phosphorylation in human atrial preparations (n=5, p<0.05). The contractile effects of 5MeDMT in human atrial preparations could be potentiated by 1 µM clobutamide and antagonized by 10 µM tropisetron. In summary, these data are of potential clinical relevance because these compounds are used for "recreative purposes" and might lead to cardiac side effects. We speculate that this knowledge might be useful in the treatment of intoxications by these hallucinogenic drugs.

P086

Human cardiac atrial effects of amphetamine and congeners

W. Hußler¹, U. Gergs¹, K. Azatsian¹, B. Hofmann², J. Neumann¹

¹Institute for Pharmacology and Toxicology, Medical Faculty, Martin Luther University Halle-Wittenberg, Halle (Saale), Germany

²Department of Cardiac Surgery, Mid-German Heart Center, University Hospital Halle, Halle (Saale), Germany

Amphetamine, pseudoephedrine, cathine and cathinone are phenylpropane derivatives and act as central stimulants. They might act as direct or indirect sympathomimetic drugs in the heart. Their effect on isolated human cardiac preparations has not been well understood. Hence, we studied amphetamine, pseudoephedrine, cathine and cathinone on isolated human right atrial preparations and for comparison on isolated atrial

preparations from wild type mice. Left atrial (LA) and right atrial (RA) preparations from mice (CD1) as well as human right atrial preparations (HAP) obtained during bypass surgery were mounted in organ baths. While RA contracted spontaneously, LA and HAP were electrically stimulated (1 Hz). Concentration-response curves were performed for force of contraction (LA, HAP) or beating rate (RA) in mouse and human preparations. Finally, samples were frozen and Western blots for phosphorylated troponin inhibitor (TnI) and calsequestrin (loading control) were performed. We noted that amphetamine, pseudoephedrine, cathine and cathinone (up to 10 µM, n=5 each) increased (p<0.05) force of contraction and beating rate in left or right atrial preparations from mice, respectively. Likewise, amphetamine, pseudoephedrine, cathine and cathinone (up to 10 µM, n=5) increased force of contraction and TnI phosphorylation in isolated human right atrial preparations. The contractile effects of amphetamine, pseudoephedrine, cathine and cathinone in human atrial preparations could be potentiated by 1 µM clobutamide and antagonized by 10 µM propranolol and abrogated by pretreatment with 10 µM cocaine. Effects in mice were much smaller than in human samples. We conclude that amphetamine, pseudoephedrine, cathine and cathinone are indirect sympathomimetic agents in the human heart and this might be of potential clinical relevance because these compounds are used for "recreational purposes" and might lead to cardiac side effects like arrhythmias and hypertension. We speculate that these side effects in patients could be treated by propranolol.

P087

Effect of temperature on contractility and phospholamban phosphorylation in isolated H₂-receptor overexpressing mouse atrial preparations

R. Hoffmann¹, U. Gergs¹, U. Kirchhefer², J. Neumann¹

¹Institute for Pharmacology and Toxicology, Medical Faculty, Martin Luther University Halle-Wittenberg, Halle (Saale), Germany

²Institute of Pharmacology and Toxicology, University of Münster, Münster, Germany

Histamine can induce positive inotropic, chronotropic and proarrhythmic effects in the human heart via H₂-receptors. These receptors are not effective in the wild type mouse (WT) heart. Therefore, we used transgenic mice (H₂-TG) with cardiomyocyte-specific overexpression of the human H₂-receptor to examine whether this receptor is influenced by temperature. Force of contraction and beating rate were measured in isolated electrically stimulated (1 Hz) left and spontaneously beating right atrial preparations of WT and H₂-TG, respectively. Hypothermia or hyperthermia was achieved by lowering or raising the temperature of the organ bath from 37°C to 23°C or 42°C. Atrial preparations were exposed to increasing concentrations of histamine (10 nM to 10 µM). Finally, samples were snap frozen, homogenized, and subjected to Western blotting to measure the phosphorylation state of phospholamban (P-PLB) at serine 16 and the expression of calsequestrin (CSQ) as loading control. Histamine induced concentration- and time-dependent positive inotropic effects only in atria of H₂-TG, but not in WT. Hypothermia and hyperthermia led to arrhythmias in WT and H₂-TG. In H₂-TG the incidence of arrhythmias was significantly higher at 42°C than at 23°C and 37°C (χ²-test, p<0.05). Moreover, we noted a longer duration of atrial arrhythmias in H₂-TG than in WT (H₂-TG: 918 ± 197 s, WT: 186 ± 91 s, n=16, p<0.05) at 42°C. The duration of arrhythmias lasted longer in both, WT and H₂-TG, at 23°C (H₂-TG: 730 ± 199 s, WT: 710 ± 222 s) than at 37°C (H₂-TG: 239 ± 92 s, WT: 149 ± 81 s, n=16 each, p<0.05). Furthermore, P-PLB/CSQ ratio was higher in H₂-TG compared to WT after addition of 10 µM histamine. The P-PLB/CSQ ratio at 23°C was lower than at 37°C in H₂-TG (1.86 ± 0.33, 2.70 ± 0.17, n=3, p<0.05). In WT the P-PLB/CSQ ratio was not temperature-dependent and lower after addition of 10 µM histamine than in H₂-TG. The time of relaxation was longer in WT than in H₂-TG at 23°C (H₂-TG: 64 ± 3.28 ms, WT: 83 ± 4.03 ms, n=16, p<0.05). The higher P-PLB/CSQ in H₂-TG can explain the faster relaxation compared to WT in presence of 10 µM histamine. Histamine was more potent to induce a positive inotropic effect in left and right atrial preparations from H₂-TG at 37 °C than at 23°C or 42°C. We conclude that the function of the human cardiac H₂-receptor is temperature-dependent, which might be of clinical relevance in fever or at lowered body temperature, e.g. during cardiac surgery.

P088

Atrial effects of psilocin and psilocybin

K. Dimov¹, U. Gergs¹, B. Hofmann², J. Neumann¹

¹Institute for Pharmacology and Toxicology, Medical Faculty, Martin Luther University Halle-Wittenberg, Halle (Saale), Germany

²Department of Cardiac Surgery, Mid-German Heart Center, University Hospital Halle, Halle (Saale), Germany

Psilocin and psilocybin are hallucinogenic drugs and are contained in ritual drug mixtures like "magic mushrooms" in South America. The hallucinogenic actions of psilocin and psilocybin are thought to be mediated by 5-HT_{2A}-serotonin receptors. Here, we hypothesized that psilocin and psilocybin might also act on the 5-HT₄ isoform, which is the predominant serotonin receptor type in the human heart. To this end, we studied isolated electrically driven (1 Hz) left and spontaneously beating right atrial preparations from transgenic mice with cardiomyocyte-specific overexpression of the human 5-HT₄-receptor (5-HT₄-TG) as well as isolated electrically driven (1 Hz) human right atrial preparations obtained from patient that underwent bypass surgery. We noted that psilocin and psilocybin (0.1 - 10 µM, each cumulatively applied) concentration- and time dependently increased force of contraction and beating rate in left or right atrial preparations from 5-HT₄-TG, respectively. Psilocin was more potent and effective than psilocybin. But both, psilocin and psilocybin, only acted as partial agonists on 5-HT₄-receptors as the additional application of serotonin (1 nM - 10 µM cumulatively applied) elicited a further increase of the force of contraction without affecting the potency of serotonin (pEC₅₀ for serotonin alone: 7.68 ± 0.25 versus pEC₅₀ for serotonin after psilocin: 7.54 ± 0.72 or after psilocybin: 7.56 ± 0.66). All above-mentioned effects, however, could not be detected in wild type (WT) mice. The inotropic and chronotropic effects of psilocin and psilocybin were antagonized by 1 µM tropisetron, a 5-HT₃ and 5-HT₄ receptor antagonist, in 5-HT₄-TG. Likewise, psilocin and psilocybin (10 µM, each) increased force of contraction and phospholamban phosphorylation in isolated human atrial preparations. The contractile effects of psilocin and psilocybin in human atrial preparations could be potentiated by 1 µM clobutamide, a phosphodiesterase III inhibitor, and antagonized by 1 µM tropisetron. These data are of potential clinical relevance because psilocin and psilocybin are used for

"recreative purposes" but also as treatment option against e.g. depression, and they might lead to cardiac side effects like arrhythmias. We speculate that tropisetron might be useful in the treatment of intoxications by psilocin and psilocybin.

P089

Cellular stress response of mouse embryonic stem cells (mESCs) to Doxorubicin and selected inhibitors of DNA repair and DNA damage response (DDR) factors

S. Federmann¹, G. Fritz¹

¹Institute of Toxikologie, Medical Faculty, Heinrich-Heine-University Düsseldorf, Düsseldorf, Germany

Background and aim: In the clinical use of the broad-range chemotherapeutic agent Doxorubicin (Doxo), a cumulative irreversible cardiotoxicity type I is dose-limiting. It is believed that both the inhibition of topoisomerase II isoforms and iron-dependent ROS formation contribute to the pathophysiology of Doxo. Endothelial cells (EC) and cardiac progenitor cells are known to be targeted by Doxo.² However, underlying molecular mechanisms are still unclear. The present studies aimed to characterize molecular determinants of Doxo sensitivity and mechanisms of the DDR of mESC and mESC-derived cardiac progenitor cells.

Methods: The *in vitro* cytotoxic effects of Doxo and two selected DDR and DNA repair modulators B02 (Rad51i) and Entinostat (HADACi), on mESCs LF2¹ were evaluated upon a 24h and 72h treatment by determining the cell viability. To further characterize the cellular response cell cycle progression, proliferation activity, apoptosis and gene expression were analyzed. Gene expression analysis of specific differentiation marker were performed using real-time quantitative PCR to examine the influence of Doxo on the differentiation potential of stem and cardiac progenitor cells.

Results: mESCs are more sensitive to Doxo compared to the two modulators. Mono-treatments impaired mESCs proliferation as reflected by reduced S-phase activity and increased apoptosis. Low dose of Doxo caused G2/M arrest (24h). Doxo cytotoxicity is increased for progenitor cells compared to mESCs. Gene expression analysis indicated that the surviving cells were able to continue differentiation into functional EC-like cells.

Conclusions and outlook: Based on the data, Doxo impairs proliferation of mESCs and promotes apoptosis but also pro-survival DDR pathways as reflected by checkpoint activation. Doxo-induced damage can either be repaired or trigger senescence in surviving cells. Similar response was already described for cardiac progenitor state cells.² In ongoing work, the formation of nuclear γ H2AX-53BP1 foci and mRNA expression of susceptibility-related factors are analyzed.

[1] J. Nichols et al., Development 1990

[2] S.K. Jahn et al., Biochim Biophys Acta Mol Cell Res 2020

P090

Post-COVID-19 alterations in platelet function of convalescent patients

C. Tolksdorf^{1,2}, E. Moritz², A. Hafkemeyer², K. Lehmann³, K. Becker³, T. Thiele⁴, M. V. Tzvetkov², S. Engel⁵, G. Jedlitschky², B. H. Rauch¹

¹Carl von Ossietzky University of Oldenburg, Department of Human Medicine, Section of Pharmacology and Toxicology, Oldenburg, Germany

²University Medicine Greifswald, Department of General Pharmacology, Greifswald, Germany

³University Medicine Greifswald, Friedrich Loeffler-Institute of Medical Microbiology, Greifswald, Germany

⁴University Medicine Greifswald, Department of Immunology and Transfusion Medicine, Greifswald, Germany

⁵University Medicine Greifswald, Department of Clinical Pharmacology, Greifswald, Germany

Introduction: Coronavirus disease-2019 (COVID-19) has been with us since the beginning of 2020. The viral respiratory illness caused by the severe acute respiratory syndrome coronavirus type 2 (SARS-CoV-2) can lead to various complications, among others to severe thrombotic complications including thrombosis.

Objectives: We have investigated alterations in platelet aggregation and activation past infection. Particularly, platelet function of recovered COVID-19 patients in comparison to individuals with no infection was examined in a longitudinal observational study.

Patients and methods: Peripheral venous blood from patients recovered for 2-15 weeks from mild SARS-CoV-2 infection (convalescents) and matched control persons (controls) was obtained after written informed consent (total n=56). The patients were invited again after 6-9 months to re-examine platelet function. Parameters of platelet aggregation were determined by light transmission aggregometry (LTA) in platelet-rich plasma (PRP). Platelet activation in washed platelets was measured by fluorescence-activated cell scanning (FACS). In addition, endogenous thrombin generation in PRP and platelet-poor plasma (PPP) was quantified by calibrated automated thrombography (CAT).

Results: No alteration in platelet aggregation was observed after stimulation of PRP-samples with various ADP (1, 2, and 10 μ M) or collagen (1 and 2.5 μ g/mL) concentrations. However, the platelet surface levels of CD62 and PAC1 measured by FACS in platelets from convalescents were markedly upregulated in comparison to samples from controls. In particular, platelets activated by ADP-concentrations of 2 μ M and by the collagen-related peptide CRP-XL at concentrations of 1 and 0.125 μ g/mL showed clear effects, especially few weeks after infection. In comparison, thrombin

formation measured by CAT was not affected in PRP or PPP from convalescents compared to control individuals.

Conclusion: While a profound, direct effect on platelet aggregation or on thrombin formation was not observed in convalescents from a mild SARS-CoV-2 infection, the expression of platelet activation markers was increased. This may indicate latent platelet hyperactivity even in a mild course of the infection, which could contribute to the development of thrombotic complications as the disease progresses.

Pharmacology – CNS / endocrine pharmacology

P091

Oxidative stress in rat brain during experimental status epilepticus: effect of antioxidants

M. Fuchs¹, H. Lau¹, J. Klein¹

¹Institute of Pharmacology and Clinical Pharmacy, College of Pharmacy, Goethe University, Frankfurt am Main, Germany

The lithium-pilocarpine model of status epilepticus is a well-known animal model of temporal lobe epilepsy. We combined this model with *in vivo* microdialysis to investigate oxidative stress and potential antioxidants during seizures. Rats were implanted with dialysis probes and pretreated with lithium chloride (127 mg/kg *i.p.*). Twenty-four hours later, they received pilocarpine (30 mg/kg *s.c.*) which initiated seizures within 30 minutes. In previous studies our group found a prominent, 20-fold increase of isoprostanes, i.e. markers of oxidative stress, in dialysates from hippocampus during seizures. In this study we investigated the effects of acute and preventive treatments with six different antioxidants (ascorbic acid, α -tocopherol, ebsele, resveratrol, *n*-tert-butyl- α -phenylnitron (PBN) and coenzyme Q10) on isoprostane levels during status epilepticus. Acute effects of antioxidants were tested by single injections of antioxidants 90 minutes after pilocarpine injection. None of the antioxidants was effective in this paradigm. In contrast, when antioxidants were given seven times every twelve hours prior to seizure induction, ascorbic acid and α -tocopherol reduced isoprostane formation by 58% and 64%, respectively. Pretreatment with the other antioxidants was again ineffective. Furthermore, we investigated the effects of antioxidants in brain homogenates prepared after 90 min of seizures. Status epilepticus decreased the ratio of reduced vs. oxidized glutathione (GSH/GSSG ratio) from 68.4 to 7.2 confirming severe oxidative stress in brain tissue during seizures. Pretreatment with ascorbic acid or α -tocopherol mitigated this effect and increased the GSH/GSSG ratio to 24.4 and 28, respectively. Additionally, we found a twofold increase of 8-hydroxy-2'-deoxyguanosine (8-OHdG) levels in brain homogenate that was prevented by pretreatment with ascorbic acid and α -tocopherol. For both parameters, GSH/GSSG ratio and 8-OHdG, the other antioxidants were not effective. Our data suggest that preventive treatment with ascorbic acid (vitamin C) or α -tocopherol (vitamin E) ameliorates oxidative damage in the brain, at least during seizures. Other antioxidants did not affect oxidative stress in brain, possibly due to poor penetration of the blood-brain barrier. Single administrations of antioxidants, e.g. during seizures were ineffective in all cases. Seizure activity was unchanged by antioxidant treatment.

P092

Inhibition of microtubule deetyrosination by parthenolide promotes CNS axon regeneration

M. Leibinger¹, C. Zeitler¹, P. Gobrecht¹, A. Andreadaki¹, A. Hilla², G. Gisselmann², D. Fischer¹

¹University of Cologne, Center of Pharmacology, Cologne, Germany

²Ruhr University of Bochum, Department of Cell Physiology, Bochum, Germany

Injured axons in the central nervous system (CNS) usually fail to regrow, causing permanent disabilities. However, viral hyper-LIL-6 (hIL-6) expression or PTEN knockout in retinal ganglion cells (RGCs) markedly promotes axon regeneration in the injured optic nerve. Moreover, intracortical injection of AAV-hIL-6 and subsequent transneuronal delivery of the cytokine to raphe nuclei enables regeneration of serotonergic axons and functional recovery after severe spinal cord injury (SCI). Here we demonstrate that besides proregenerative signaling, the full axon growth capacity of hIL-6 and PTEN knockout is limited by an induced tubulin deetyrosination in axonal growth cones. Hence, co-treatment with parthenolide, a compound blocking microtubule deetyrosination, synergistically enhances neurite growth of cultured murine primary RGCs. Systemic application of the prodrug dimethylamino-parthenolide accelerates hIL-6-mediated optic nerve and spinal cord regeneration and further improves locomotion recovery after SCI. Thus, parthenolide facilitates CNS regeneration and counteracts the adverse side effects of other pro-regenerative treatments.

Pharmacology – G-protein coupled receptors

P093

Novel real time GPER-based assays to identify substances with endocrine disrupting properties. The brominated flame retardant tetrabromobisphenol S shows significantly lower G protein-coupled receptor modifying activities compared to the widely used tetrabromobisphenol A and tetrachlorobisphenol A.

M. Frey¹, C. Stahl², R. Martens², J. Bachmann¹, F. Freiling³

¹German Environment Agency, Section IV 2.2, Dessau-Roßlau, Germany

²Steinbeis-Innovationszentrum Zellkulturtechnik, c/o Hochschule Mannheim, Mannheim, Germany

³TZW: DVGW-Technologiezentrum Wasser, Wasserchemie, Karlsruhe, Germany

Introduction: Numerous studies have measured estrogenic effects of xenobiotics. However, most in-vitro studies focused on transcriptional activation of estrogen receptors. There has been growing concern about the estrogen-disrupting activities of tetrabromobisphenol A (TBBPA) and other brominated flame retardants (BFRs). The use of TBBPA is nonregulated and TBBPA is an ubiquitous contaminant in the environment.

Objectives: The objective of the present study was to investigate the modulation of nongenomic G protein-coupled estrogen receptor (GPER) signaling. Cell based assays should be developed allowing the assessment of potential endocrine disruptors. BFRs should be evaluated for possible estrogenic or G protein modulating effects.

Material and methods: Cell lines were modified for expressing protein based Ca²⁺ and cyclic adenosine monophosphate (cAMP) sensors. Ca²⁺ mobilization and cAMP concentration changes were measured using fluorescence-based assays. For the measurement of GPER-specific effects, we compared sensor cell lines expressing endogenous GPER (SKBR3) with GPER non-expressing sensor cell lines (HSC) and HSC sensor cell lines expressing recombinant GPER.

Results: We developed Ca²⁺ and cAMP sensor cell lines with and without GPER expression for the assessment of GPER specific signaling. HSC sensor cells expressing recombinant GPER showed intracellular Ca²⁺ mobilization with β -estradiol and the known endocrine disruptor bisphenol A (BPA). Neither α -estradiol nor G1, a compound claimed to act as a selective GPER agonist, increased intracellular Ca²⁺ levels in GPER expressing HSC sensor cells. Similarly, G1 incubation of cAMP sensor GPER-expressing HSC cells resulted in no change in intracellular cAMP concentration. The BFRs TBBPA and tetrachlorobisphenol A (TCBPA) induced Ca²⁺ mobilization in both GPER expressing and GPER non-expressing sensor cell lines. TBBPA and TCBPA showed cell- and GPER dependent agonistic and antagonistic effects on cAMP signalosomes. Compared to TBBPA and TCBPA the BFR tetrabromobisphenol S (TBBPS) showed significantly lower effects in all assays.

Conclusion: GPER exhibits no G1 stimulated activity in vitro. The classification of G1 as an agonist of GPER is doubtful. The BFRs TBBPA and TCBPA modulate G protein-coupled receptor (GPCR) Gq and Gs signaling. The BFR TBBPS showing significantly lower GPCR modifying activities compared to TBBPA and TCBPA in all tests should be used as a substitute for TBBPA or TCBPA.

P094

The single nucleotide polymorphism rs7121 in the gene *GNAS* as a biomarker for tumor progression and poor survival in intrahepatic cholangiocellular carcinoma patients

B. Mählendick¹, S. Ting², K. W. Schmid², W. Siffer¹

¹University Hospital Essen, Institute of Pharmacogenetics, Essen, Germany

²University Hospital Essen, Institute of Pathology, Essen, Germany

Introduction: Gs α encoded by *GNAS* is a key player in pathways relevant for tumor progression. The synonymous germline single nucleotide polymorphism (SNP) rs7121 (c.393C>T) was shown to be associated with shorter survival in different cancer entities. Although this silent SNP seems to be a promising predictive biomarker, no experimental research was conducted to reveal the mechanisms for the effects caused by rs7121.

Objectives: In this study, we evaluated the influence of the rs7121 genotype, *GNAS* mRNA and Gs α protein expression on intrahepatic cholangiocellular carcinoma (iCC) patients' overall survival.

Patients and methods: We included formalin fixed paraffin-embedded tissue samples of 98 patients with iCC. Median follow-up period was 25.8 months. Semi-quantitative real-time PCR was performed to determine *GNAS* overall mRNA expression. Genotyping and allele-specific gene expression analysis was performed using a probe-based quantitative real-time PCR. Immunohistochemistry staining (IHC) was conducted with a monoclonal antibody against Gs α full protein.

Results: Genotypes were distributed as follows: 27.6 % CC, 43.9 % CT and 28.6 % TT. C-allele was the minor allele with a frequency of 0.49. TT genotype carriers showed a 1.4-fold increased risk ($P = 0.016$) for shorter overall survival compared to CC genotype carriers. *GNAS* mRNA expression was significantly higher in tumor tissue ($P = 0.0003$). T-allele transcript copy number was significantly higher in CT genotype carriers ($P = 0.005$). *GNAS* IHC score showed an allele dose dependent increase towards T-allele/TT genotype carriers ($P = 0.04$). iCC patients with high Gs α expression showed a 4.6-fold increased risk for a shorter overall survival ($P = 0.02$).

Conclusion: iCC patients carrying rs7121 T-allele showed a 1.4-fold increased risk for shorter overall survival. The T-allele transcript showed a significantly higher copy number and was responsible for higher gene expression and protein expression in the respective genotype carriers. A higher *GNAS* expression could be correlated to tumor growth and progression, similar as observed upon a persistent activation of Gs α signaling caused by well-known somatic missense mutations. Further analyses with other cancer entities and the correlation of rs7121 genotype and/or Gs α expression to therapy response are required to validate this synonymous germline SNP as a suitable biomarker for a more precise prognosis prediction in routine clinical diagnostics.

P095

The role of (xeno)estrogens and GPER1/GPR30 receptor for centrosome amplification and chromosomal instability *in vitro*.

J. Fahrlander¹, A. Stolz-Ertch¹, G. Schönfelder¹

¹German Federal Institute for Risk Assessment, Berlin, Germany

Introduction: Previous studies reported contradictory observations on the role of GPER1 in the development and progression of colorectal cancer (CRC). While being involved in physiological processes in the colon and mediating anti-tumorigenic effects, GPER1 has also been reported to trigger cancer related pathways. However, the molecular mechanisms underlying CRC pathophysiology and the exact role of GPER1 in numerical centrosome defects as well as in whole chromosomal instability (w-CIN) are widely unknown.

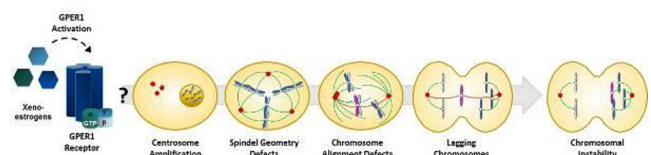
Objectives: To elucidate the link between GPER1, centrosome amplification and karyotype instability in CRC *in vitro*.

Materials and methods: Normal colon and colorectal cancer-derived cell lines were treated with GPER1-(in)activators including the GPER1-selective agonist/antagonist G1/G15 or the (xeno)estrogens 17 β -estradiol, bisphenol A and diethylstilbestrol in the presence or absence of transient or stable GPER1 repression *via* gene-specific si/shRNA. Subsequently, mitotic defects were measured by using state-of-the-art high-resolution fluorescence microscopy and live cell imaging. Karyotype instability was assessed by w-CIN-analyses using Cep-FISH and chromosome counting from metaphase spreads following karyotype analysis.

Results: Our results demonstrate a significant role of activated GPER1 in centrosome amplification potentially originating from centriole over-duplication, and leading to the formation of transient multipolar mitotic spindles that cause chromosome segregation defects during mitosis, which ultimately manifest in w-CIN and aneuploidy.

Conclusions: GPER1 promotes the development of key CRC-prone lesions like centrosome amplification and w-CIN, supporting the hypothesis of a potential pro-tumorigenic role of GPER1 during colon pathogenesis.

Fig. 1



P096

Development of FRET-based receptor conformation sensors for the opioid receptor family and analysis of opioid agonist properties

S. B. Kirchofer¹, C. Kurz¹, M. Kurz¹, M. Bünemann¹

¹Philipps-University Marburg, Department of Pharmacology and Clinical Pharmacy, Marburg, Germany

Question: The MOR is the key target for analgesia, but the application of opioids is accompanied by several issues. There is a wide range of opioid analgesics, differing in their chemical structure and their properties in receptor activation and subsequent effects. A better understanding of the differential opioid agonists regarding their effects on receptor activation and subsequent downstream effects is necessary. Here we describe the development of FRET-based receptor conformation sensors for the different opioid receptors, which enabled the direct evaluation of receptor activation and deactivation kinetics of agonists of different chemical classes. Further, we analyzed these agonists regarding downstream signaling effects.

Methods: We developed FRET-based receptor conformation sensors for the opioid receptor family. We performed FRET- and BRET-based assays in HEK293T cells in single cell and multi-well format. We analyzed effects on receptor-conformation, G-protein activation and arrestin recruitment.

Results: We were able to develop FRET-based receptor conformation sensors for MOR, KOR and NOP receptor. For these receptors, we established assays for measurements in multi-well format. We further performed single-cell measurements on a microscope. We were able to directly analyze receptor activation and deactivation kinetics for different agonists for the MOR. Here we compared the behavior of peptide agonists vs. non-peptide agonists. We further analyzed the behavior of full and partial agonists on receptor activation and subsequent effects like G-protein activation and receptor-arrestin interaction. Moreover, we could directly show on conformational level that the KOR displays a high basal activity.

Conclusion: Our work provides a new tool for the investigation of the opioid receptor family directly on receptor activation level. With these sensors, we were able to make direct statements on activation levels of receptor, like basal activity. Furthermore, we revealed diverting activation and deactivation kinetics of the various opioid agonists and raised further information on agonist properties.

Clinical pharmacology – Pharmacoepidemiology and drug safety

P097

Impact of a conventional spasmolytic on the quality of life in patients with menstrual pain - Real world evidence data from a pharmacy-based patient survey
P. Nonnenmacher¹, H. Weigmann¹, S. Landes¹, T. Weiser¹

¹Sanofi Deutschland, CHC Medical Affairs, Frankfurt am Main, Germany

Introduction: Dysmenorrhea is one of the most common gynecological dysfunctions in women of childbearing age, causing severe impairment of quality of life (QoL). Although spasmolytic drugs are commonly used for abdominal pain, little is known about their impact on QoL in menstrual disorders in a real-world setting.

Objective: Data from a pharmacy-based patient survey was analyzed to explore whether a fixed dose combination (HBB+) of 10 mg Hyoscine-N-butylbromide (HBB) and 500 mg paracetamol can improve the QoL of patients with menstrual cramps.

Patients and methods: Patients purchasing HBB+ were offered to participate in a survey to assess, among others, the impairment of QoL (Leisure, Daily Life, Sleep) before and after taking the drug. Severity of impairments caused by the complaints was assessed on a 10-point numeric rating scale, 0 representing no impairment and 10 representing very severe impairment. In addition, participants could evaluate their satisfaction with the effect of HBB+ as very satisfied, satisfied, less satisfied, or not satisfied.

Results: The survey was completed by 641 HBB+ participants, of whom 329 females used it to treat menstrual pain (mean age 32.8 ± 10.1 years) and were thus included in the analysis.

While more than 86% of the participants felt moderately to severely affected by their complaints in leisure (87.8%) and daily life (86.3%), significantly fewer felt impaired in their sleep (62.3%). Mean impairment scores were 6.6 for leisure, 6.5 for daily life and 5.0 for sleep. The simultaneous occurrence of abdominal and menstrual pain, reported by 31.6% of the respondents, does not lead to a greater QoL impairment.

After taking HBB+, >97% of participants reported no longer feeling severely impaired in their QoL due to menstrual pain (Score 8-10). On average, the impairment of leisure improved by -4.2, of everyday life by -4.3 and of sleep by -3.5 after taking HBB+ (Fig. 1).

96.6% of participants were satisfied/ very satisfied with the effect of HBB+ and 97.3% would recommend the product to others.

All changes $p < 0.05$ (paired t-test).

Conclusion: HBB+ can increase the QoL of patients with dysmenorrhea. Affected women feel less impaired in leisure, daily life and sleep and are thus better able to participate in life. This is also reflected in the high satisfaction rate of the users. HBB+ can therefore be recommended for the treatment of menstrual disorders to improve the QoL.

The study was sponsored by Sanofi.

Fig. 1

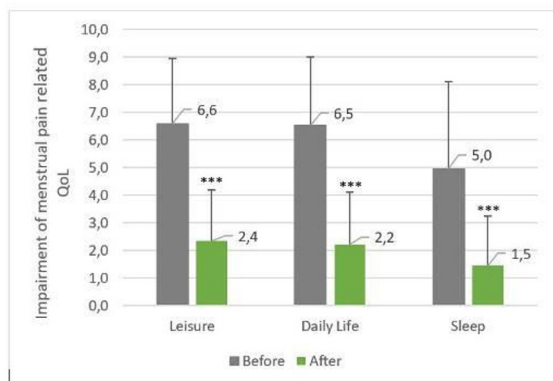


Fig. 1 Impairment of QoL due to menstrual pain before and after taking HBB+.

P098

What onset of pain relief corresponds to patients' assessment of "very fast" or "fast" in acute headache treatment? Analysis of data from an observational study on the fixed-dose combination ibuprofen+caffeine

C. Gaul¹, S. Förderreuther², W. Lehmann³, T. Weiser⁴

¹Kopfschmerzszentrum Frankfurt, Frankfurt, Germany

²Universität München, Neurologische Klinik, München, Germany

³Universität Köln, Köln, Germany

⁴Sanofi Aventis Deutschland GmbH, Medical Affairs, Frankfurt am Main, Germany

Introduction and objective: Headache patients expect fast onset of action of their pain medication. Quantitative information how onset of analgesia at a given time point relates to patient assessment is sparse. We analyzed data from a pharmacy-based observational study.

Patients and methods: A pharmacy-based exploratory survey was conducted in German community pharmacies (Gaul et al. 2022). Patients buying a fixed-dose analgesic combination product to treat their headache (400 mg ibuprofen + 100 mg caffeine) were offered a questionnaire which contained questions about time to onset of pain relief (OPR) after intake of the medication (categories: 0–5, 6–15, 16–30, 31–45, 46–60, and >60min) and assessment of time to onset of pain relief (AOPR; categories: very fast, fast, moderately fast, and slow). Spearman's rank correlation test of OPR and AOPR was performed.

Relative and cumulative relative frequencies of OPR categories stratified by AOPR categories were calculated; rate ratios (relative rates) of these cumulated relative frequencies were used to assess which AOPR category steps are able to discriminate between cumulative OPR rates (e. g. RR for OPR ≤ 15 min between AOPR for "very fast" and "fast"). RR cutoff for the discrimination between AOPR categories was set to a value of 2.

Results: Data from 827 patients could be analyzed. Correlation between OPR and AOPR was high (Spearman $r = 0.59$; $p < 0.0001$). AOPR "very fast" was given by 21.8% ("fast": 58.8%; "moderately fast": 17.5%; "slow": 1.9%). Relative frequencies of OPR by AOPR are shown in the figure, and cumulative relative frequencies in Table A. Contingency analysis showed that from OPR >15 min RR for the categories "very fast" compared to "fast" were smaller than the cutoff value of 2. For AOPR categories "fast" versus "moderately fast" RRs were smaller than 2 for OPR >30 min. For AOPR "moderately fast" vs. "slow" no statistically clear changes were observed, probably due to the small number of patients in both groups (Table B).

Conclusion: More than 80% of headache patients reported very fast or fast onset of analgesic action after intake of 400 mg ibuprofen plus 100 mg caffeine. Onset of analgesic action within 15 min can be considered "very fast", and within 30 min as "fast".

Reference: Gaul et al. 2022 Front Neurol. 2022;13:902020.

The study was sponsored by Sanofi.

Fig. 1

Figure

Relative frequencies of OPR by assessments of OPR

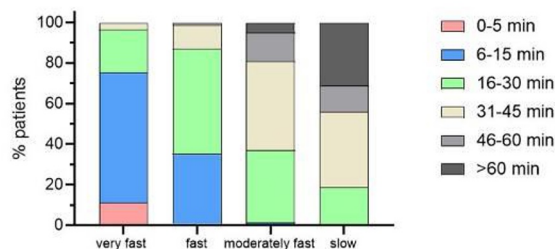


Fig. 2

Table

A)

	very fast (%)	fast (%)	moderately fast (%)	slow (%)
≤< 5 min	11.11	0.82	0	0
≤<15 min	75.55	35.39	1.38	0
≤<30 min	96.66	87.04	37.24	18.75
≤<45 min	100	98.56	80.68	56.25
≤<60 min	100	99.79	95.17	68.75
>60 min	100	100	100	100

B)

	„very fast“ vs. „fast“ (RR CI p)	„fast“ vs. „moderately fast“ (RR CI p)	„moderately fast“ vs. „slow“ (RR CI p)
≤< 5 min	13.5 4.67;38.95 <0.0001	not defined	not defined
≤<15 min	2.13 1.84;2.47 <0.0001	25.65 6.44;102.15 <0.0001	not defined
≤<30 min	1.11 1.06;1.16 <0.0001	2.33 1.88;2.89 <0.0001	1.98 0.70;5.63 0.196
≤<45 min	1.01 1.004;1.02 0.0082	1.22 1.12;1.32 <0.0001	1.43 0.92;2.22 0.108
≤<60 min	1.002 0.99;1.006 0.31	1.05 1.01;1.09 0.011	1.12 0.89;1.42 0.326
>60 min	1	1	1

(A) Cumulative relative frequencies of OPR by AOPR; (B) Ratios of cumulative relative frequencies of OPR categories (RR) with 95% confidence intervals (CI) and p-values for the comparisons of the different assessments of onset of pain relief.

P099

Which parameters affect pain reduction in acute headache treatment? Analysis of data from an observational study on the fixed-dose combination ibuprofen+caffeine

S. Förderreuther¹, C. Gaul², W. Lehmacher³, T. Weiser⁴

¹Universität München, Neurologische Klinik, München, Germany

²Kopfschmerzszentrum Frankfurt, Frankfurt, Germany

³Universität Köln, Köln, Germany

⁴Sanofi Deutschland, CHC Medical Affairs, Frankfurt am Main, Germany

Introduction and objective: Headache patients expect fast onset of action and complete pain relieve from their acute treatments. We have run a pharmacy-based observational study in patients buying a specific analgesic (400 mg ibuprofen +100 mg caffeine) and analyzed parameters of patient's perception of efficacy measures.

Patients and methods: A pharmacy-based exploratory survey was conducted in German community pharmacies (Gaul et al. 2022). Patients buying a fixed-dose analgesic combination product to treat their headache (400 mg ibuprofen+100 mg caffeine) were offered a questionnaire which contained -among others- questions about time to onset of pain relief (OPR) after intake of the medication (categories: 0–5, 6–15, 16–30, 31–45, 46–60, and >60min), assessment of time to onset of pain relief (AOPR; categories: very fast, fast, moderately fast, and slow), assessment of efficacy (categories very good, good, moderately good, bad), and pain intensity (on a 0-10 numerical pain rating scale, NRS) at baseline and 2 h after intake. Percent pain intensity difference (%PID)= 100*(NRS 2h – NRS baseline)/NRS baseline. Spearman's rank correlation tests were performed to test for statistical significance.

Results: In total data from 827 patients could be analyzed. Correlation of %PID at 2 h with assessment of efficacy was high (Spearman $r=0.487$, $p<0.0001$), and assessments corresponded well with those from a randomized controlled trial on analgesic effects of the fixed dose combination aspirin+paracetamol+caffeine for treating acute headache (Aicher, 2012). OPR corresponded well with %PID at 2h (Spearman $r=0.294$, $p<0.0001$), which was also the case for AOPR and %PID at 2 h (Spearman $r=0.319$, $p<0.0001$). I

Conclusion: This investigation showed that early onset of pain relief of an analgesic corresponds well with pain reduction at 2 h, as well as patients' assessment of overall efficacy. This further underlines the importance of fast onset of action for acute headache treatments.

References:

Aicher B, Peil H, Peil B, Diener HC.

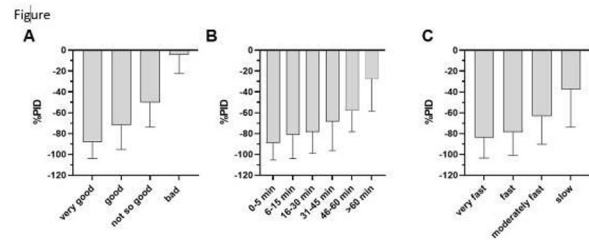
Cephalalgia. 2012;32(13):953-62. doi: 10.1177/0333102412452047

Gaul C, Gräter H, Weiser T, Michel MC, Lampert A, Plomer M, Förderreuther S.

Front Neurol. 2022;13:902020. doi: 10.3389/fneur.2022.902020.

The study was sponsored by Sanofi.

Fig. 1



(A) %PID at 2 h by assessment of efficacy; (B) %PID at 2h by onset of pain relief (OPR); (C) %PID at 2 h by assessment of time to onset of pain relief (AOPR). Data in A-C are shown as means with standard deviations.

P100

Comprehensibility and clinical relevance of absolute contraindications – the perspective of German pharmacists and physicians

W. Andrikyan¹, M. I. Then¹, P. Dürr^{1,2}, L. Jung-Poppe¹, A. K. Schuster³, L. Weisbach³, K. Farker³, M. F. Fromm¹, R. Maas¹

¹Friedrich-Alexander-Universität Erlangen-Nürnberg, Institute of Experimental and Clinical Pharmacology and Toxicology, Erlangen, Germany

²Erlangen University Hospital, Pharmacy Department, Erlangen, Germany

³Jena University Hospital, Hospital Pharmacy, University Center for Pharmacotherapy and Pharmacoconomics, Jena, Germany

Introduction: According to the European Medicines Agency (EMA), absolute contraindications in official "Summaries of Product Characteristics" (SmPCs) should be unambiguous, comprehensive and clearly outlined to ensure medication safety. However, many SmPCs might leave too much room for interpretation of contraindications, which could explain the variable clinical acceptance and implementation of official warnings in SmPCs.

Objectives: The aim of this study was to evaluate the comprehensibility and clinical relevance of contraindications in SmPCs from the perspective of physicians and pharmacists.

Materials and methods: Within the framework of the BMBF funded use case "POLAR_Mi - POLypharmacy, Drug interActions, Risks" (funding numbers 01ZZ1910C and 01ZZ1910O), an expert-based consensus team of clinical pharmacists/pharmacologists identified 24 absolute contraindications commonly missed or ignored in the clinical routine. For these contraindications, an anonymous online survey with up to two patient cases for each contraindication was constructed. Pharmacists and physicians were asked if the corresponding patient case fulfilled the contraindication as stated in the SmPC (applicable to 17 of the 24 cases) and also if the contraindication was clinically relevant in the corresponding case (applicable to 24 of the 24 cases).

Results: 27 pharmacists and 27 physicians (48.1% male, 51.9% female) completed the survey. For none of the patient cases, all experts agreed on the same answer. In 5 of 17 (29.4%) cases, no simple majority was given for an answer option by the experts regarding the fulfillment of the definition of the contraindication. For example, experts gave a broad spectrum of different answers on the definition of an "active liver disease", which is a contraindication for simvastatin according to its SmPC. With respect to clinical relevance, in 7 of 24 (29.2%) cases the experts gave diverging opinions. According to the experts, lack of alternative treatment, duration of treatment, acute/severe situations, patient or drug monitoring can have influence on the clinical relevance of a contraindicated prescription.

Conclusion: The observed disagreement of physicians and pharmacists regarding the applicability and clinical relevance of contraindications in SmPCs indicates that further efforts are needed to improve the clinical usability and relevance of contraindications in SmPCs.

P101

Analysis of drug drug interactions between somatic and psychiatric medication by application of ABDA interaction data to reports from the EudraVigilance database

R. Weber¹, D. Dubrall¹, C. Scholl¹, M. Böhme¹, M. Steffens¹, B. Sachs¹

¹Bundesinstitut für Arzneimittel und Medizinprodukte, Forschung, Bonn, Germany

Introduction: Patients with severe mental illness are at a particularly high risk for somatic comorbidities and have a high need for psychopharmacological therapy. The risk for drug drug interactions (DDI) increases with additional treatment of somatic comorbidities. In our project, we analyzed reports on adverse drug reactions (ADR) to antidepressants, neuroleptics and mood stabilizers in order to detect potential DDI with somatic medication.

Objectives: Aim of the project was to identify in ADR reports constellations of drugs for the treatment of psychiatric and somatic disorders for which an interaction potential has been described. Furthermore, we wanted to evaluate which of these combinations of drugs were most frequently associated with actual ADRs as reported in the ADR database.

Material and methods: In a first step, data from 9,677 ADR reports from the EudraVigilance database, which matched the inclusion criteria (age, country, time period, suspected drugs) were extracted. All substances mentioned in each ADR report independent whether reported as suspected/interacting or concomitant were checked for DDIs using the German ABDA-database (ABDA-Datenbank2, version as of 01.01.2022). We identified frequent interaction pairs and selected combinations of specific psychotropic and somatic substances for subsequent analysis. Therein, we investigated if the ADRs resulting from a potential interaction as identified by the interaction check matched the reported ADRs, suggesting an actual interaction. In addition, we analyzed whether the ADR(s) of the identified interaction pairs occurred more frequently than the same ADR(s) for the individual substances alone.

Results: Based on our initial analysis, we assume that the constellation of antithrombotic agents and specific antidepressants could be associated with a considerable number of hemorrhagic events. Other ADRs possibly resulting from DDI, which we investigated, include serotonin syndrome, electrolyte imbalances, and increase of pharmacological effects of betablockers.

Conclusion: Analysis of frequent DDI in ADR databases can call attention to relevant combinations possibly leading to ADRs. Research on these may help physicians to keep in mind potentially harmful combinations of drugs when treating mentally ill patients with somatic comorbidities.

P102

A descriptive analysis of medication errors reported in Vigibase for direct oral anticoagulants

C. Morgovan¹, A. Frum¹, A. Arseniu¹, A. A. Chis¹, C. M. Dobrea¹, L. L. Rus¹, A. M. Juncan¹, G. Pop¹, F. Gligor¹, S. Ghibu², L. Stoicescu³

¹"Lucian Blaga" University of Sibiu, Preclinical Department, Sibiu, Romania

²Iuliu Hatieganu University of Medicine and Pharmacy, Cluj-Napoca, Romania

³"Iuliu Hatieganu" University of Medicine and Pharmacy, Cluj-Napoca, Romania

Introduction: Compared to classic anticoagulants, direct oral anticoagulants (DOACs) have some advantages, such as: rapid onset of action, fixed doses, reduced number of drug interactions, lower risk of bleeding and a reduced need for monitoring [1]. Therefore, they can significantly improve patient adherence to treatment [2]. However, their wrong use could increase risks and mortality. Moreover, many studies reported medication errors (MEs) related to DOACs use.

The aim of the present study is to realize a descriptive analysis of MEs associated with DOACs reported in Vigibase.

Material and methods: The current study analyzed all the data from Vigibase reported until the 4th of November 2022. A descriptive analysis of adverse reactions (ADRs) included in the "Injury, poisoning and procedural complications" category was performed [3].

Results: ME reported in Vigibase were classified in 12 categories. From all reports for DOACs (dabigatran, apixaban, rivaroxaban, edoxaban, and betrixaban) in Vigibase (N=371,852), ME related to DOACs use represented 7,5% (N=28,055). Most frequent ME reports were associated with rivaroxaban (9.4%) and less frequent with dabigatran (3.2%). Regarding the type of ME reported, 30.65% were represented by off-label use, 26.63% were related to incorrect dosage, 16.60% were related to faulty administration and 12.17% were represented by wrong prescribing. Also, for dabigatran higher frequency of off-label use was observed (43% from the total of MEs), probably due to its limited indications. More than 11% of the MEs reported for apixaban were related to product issues.

Conclusions: Our study completes the clinical studies that reported MEs associated with DOAC therapy. Taking into account the positive trend of the DOAC market, pharmacists and medical staff could reduce the risks associated with the use of these drugs [4] by intervention in different stages (prescription, administration, dosage, monitoring, etc.).

References:

- McRae, H.L. et al. *Biomed.* 2021, Vol. 9, Page 262 2021, 9, 262, doi:10.3390/BIOMEDICINES9030262.
- Zirlik, A.; Bode, C. *J. Thromb. Thrombolysis* 2017, 43, 365, doi:10.1007/S11239-016-1446-0
- <https://www.vigiaccess.org/>
- Ghibu, S. et al. *Int. J. Environ. Res. Public Health* 2021, 18(18), 9776; <https://doi.org/10.3390/ijerph18189776>

P103

Development of a smartphone-application enabling personalized selection of suitable food products in consideration of drug intake, food intolerances and allergies: opportunities and limitations

D. Pemp¹, J. Wunder¹, K. Brendel², M. Bernhard-Brendel², L. Lehmann¹

¹University of Würzburg, Chair of Food Chemistry, Würzburg, Germany

²Scannel GmbH, Schwabach, Germany

Due to drug intake, food intolerances and allergies, specific foods need to be avoided by some consumers temporary or continuously. In order to implement an individual and health-maintaining choice of food, consumers must a) obtain and remember necessary health-relevant information, b) be able to read the lists of ingredients of food and c) interpret lists of ingredients and food labeling correctly.

Because of impairments, this is not easily possible for all consumers and always time-consuming. Preventable adverse health effects such as failed pharmaceutical therapies, heavy side effects and intolerance of drugs, allergic reactions as well as insufficient adherence to medical and/or dietary recommendations are possible consequences.

Thus, in a joint project by the Chair of Food Chemistry of the University of Würzburg and the medium-sized company Scannel GmbH a barrier-free, evidence-based, customizable smartphone-application enabling the identification of suitable food products was developed.

Therefore, a database was built and up to now (October 2022) 12,560 ingredients of 54,405 products were categorized and evaluated based on 169 drug interaction monographs (ABDA) and databases such as the "Bundeslebensmittelschlüssel".

Permanent or temporary medication can be directly saved in user settings by scanning the pharmaceutical registration number code. Furthermore the intolerances phenylketonuria, celiac disease and lactose, fructose and sorbitol intolerance as well as in regulation (EU) No. 1169/2011 listed food allergies - with optional consideration of cross-allergies and labelled traces of allergens - can be chosen.

By scanning a Global Trade Item Number-Code on food, user settings of individual user profiles are matched with product informations in the Scannel-database and the suitability of the product is shown for each profile using an intuitive traffic light system.

Due to challenges like obligatory vs. optional food labeling, ingredients vs. constituents of ingredients, or foods without lists of ingredients, false-positive scan results are accepted due to conservative categorization, while false negative results are avoided.

Beyond user benefits of the application, the database introduces the possibility to investigate pharmacoepidemiological and food chemistry related scientific issues, such as the amount of products in specific food groups evaluated as suitable during individual drug therapies.

P104

A descriptive study of adverse drug reactions relevant to antimicrobial resistance reported for azole antifungals

A. Arseniu¹, C. Morgovan¹, A. A. Chis¹, G. Pop¹, A. Frum¹, C. M. Dobrea¹, L. L. Rus¹, F. Gligor¹

¹"Lucian Blaga" University of Sibiu, Preclinical Department, Sibiu, Romania

Introduction: Fungal pathogens can be responsible for a wide range of diseases, ranging from mild superficial mycoses to life-threatening invasive fungal infections [1]. Although the phenomenon of antimicrobial resistance (AMR) has been demonstrated in both bacterial and fungal species, antimicrobial management has mainly focused on antibiotics [2], with antifungal resistance being underrecognized [1]. Limiting AMR requires a multidisciplinary approach, therefore recent advances in reporting and monitoring of adverse drug reactions (ADRs) related to AMR could contribute to antimicrobial stewardship.

Objectives: The aim of this study was to conduct a descriptive analysis of spontaneously reported ADRs indicating suspected resistance or inappropriate use of the following azoles: fluconazole, voriconazole, itraconazole, posaconazole and isavuconazole.

Materials and methods: Data were extracted from the World Health Organization pharmacovigilance database, VigiBase®, that was accessed through VigiAccess® [3]. Reports containing MedDRA preferred terms (PTs) that are relevant to antimicrobial resistance were included in this analysis according to a protocol published in the literature [4].

Results: Of a total of 64029 suspected ADRs involving 5 azole antifungals reported in VigiBase® up to November 8, 2022, 6252 (9.76%) were linked to AMR or inappropriate drug use. The majority of the reports were recorded for fluconazole (2297, 36.74%), followed by voriconazole (1922, 30.74%). Of a total of 446 reports registered for isavuconazole, 189 (42.38%) contained PTs relevant to AMR or improper use of the drug. Most of these reports were related to PTs such as product use in unapproved indication (74, 39.15%) and off label use (60, 31.75%).

Conclusion: Given the limited number of antifungal classes currently available for systemic use, managing patients with invasive fungal infections could be a challenge for clinicians in the setting of AMR. Thus, data collected through pharmacovigilance systems could have an important role in identifying and limiting AMR.

References:

- Fisher, M. C. et al. *Nat. Rev. Microbiol.* 20, 557–571 (2022). DOI: 10.1038/s41579-022-00720-1.
- Chiş, A. A. et al. *Biomedicines* 10, 1121 (2022). DOI: 10.3390/biomedicines10051121.
- <https://www.vigiaccess.org/>. (Accessed: November 8, 2022)
- Habarugira, J. M. V., Härmak, L. and Figueroa, A. *Antibiotics* 10, 1512 (2021). DOI: 10.3390/antibiotics10121512.

P105**Patient risk profiles in polytherapy: Patient-reported safety outcome measures, potentially inadequate medication (PIM) and drug-drug-interactions in an elderly cohort, a longitudinal investigation**

J. Radermacher¹, M. Klein¹, J. Wozniak¹, K. Just¹, T. Laurentius², C. Bollheimer², J. C. Stingl¹

¹University Hospital RWTH Aachen, Institute of Clinical Pharmacology, Aachen, Germany

²University Hospital RWTH Aachen, Department of Geriatrics, Aachen, Germany

Background: Patients at polytherapy are particularly exposed to an increased risk for adverse drug reactions.

Objectives: Assessing CYP-metabolism and pathway interactions as well as potentially inadequate medication (PIM) to find interrelationships as patient risk profiles affecting causality assessment to identify adverse drug reactions in elderly patients with polytherapy.

Methods: Patient reported side-effects are recorded within an outpatient polypharmacy consultation. For all patients at polytherapy, complete medication is assessed within a brown bag review. Patients are asked about possibly occurring adverse drug reactions, trained in their recognition, and given a booklet for their documentation. To be assessed as side effect, the WHO causality assessment is applied for every symptom reported whereas symptoms that show an association of "possible", "probable" or even more strongly related are taken into account. For all drugs taken, drug-drug-interactions are assessed based on mediq.ch. PIM are evaluated based on the PRISCUS- and will be assessed based on the "Fit FOR The Aged (FORTA)"-list as well.

Results: In this evaluation of the first fifty-one patients, mean number of drugs taken per patient was 16 (min: 5, max: 35) while average amount of diseases is 13 (min: 3, max: 33). On average 35 drug interactions per patient could be analyzed (min: 4; max: 107) with the top five addressed CYP-Pathways: 3A (46%), 2C19 (16%), 2D6 (13%), 2C9 (11%) and 1A2 (6%).

Altogether n=826 drugs are taken (mean: 16, min: 5, max: 35), 29% of the patients get at least one PIM (22 PIM in total) while top 5 of the drugs concerned are: Zopiclon (5), Oxazepam (3), Acetyldigoxin (2), Flecaïnid (2), Zolpidem (2), Lorazepam (2).

In total n=711 side-effects were reported (mean: 14, min: 0, max: 30) with causality of at least "possible". The top 5 stated side-effects were: Fatigue (40), shortness of breath (33), sleeping disorder (27), urinary incontinence (27) and dizziness (25).

Conclusion: Symptoms with causality assessment of at least possible for an adverse drug effect were frequently reported in a situation of polytherapy. The symptoms were unspecific and commonly listed side effects of many drugs. Drug-drug interactions were the most common findings in all patients that could explain the side effects, whereas the use of PIM is omnipresent. Promising data are continuously collected, but to find interrelationships will be aim of the further following investigations.

Clinical pharmacology – Pharmacogenomics and personalized medicine**P106****Gene-environment interactions and interindividual variability in xenobiotic response – a genome-wide association study in medaka**

P. Watson¹, F. Defranoux², M. Ferreira², S. Kaminsky¹, F. Loosli³, S. Stricker¹, T. Thumberger¹, B. Welz¹, S. Kullman⁴, J. Goldstone⁵, J. Wittbrodt¹

¹Uni Heidelberg, Centre for Organismal Studies, Heidelberg, Germany

²EMBL-EBI, Hinxton, United Kingdom

³Karlsruhe Institute of Technology, Institute of Biological and Chemical Systems - Biological Information Processing (IBCS-BIP), Eggenstein-Leopoldshafen, Germany

⁴North Carolina State University, Raleigh, United States

⁵Woods Hole Oceanographic Institution, Woods Hole, United States

Genetic predisposition influences susceptibility to xenobiotics and leads to different effects on individuals. In order to decipher the causative gene-environment interactions (GxE) and to gain a mechanistic understanding of the biological pathways involved in individual xenobiotic responses at the molecular level, we are conducting a large-scale genome-wide association study (GWAS). To overcome the limitations of the heterogeneity of the human genome, we make use of the high inbreeding tolerance of the teleost fish medaka (*Oryzias latipes*). This feature has led to the development of the Medaka Inbred Kiyosu Karlsruhe (MIKK) panel consisting of 80 fully sequenced and near-isogenic lines that were originally derived from the wild and therefore resemble a natural population.

The transparency of the medaka chorion and embryo enables non-invasive *in vivo* imaging. So far, we have screened about 18000 embryos of the MIKK panel with three xenobiotics (ethanol, disulfiram, caffeine) for changes in heart rate as a general physiological indicator. Significant differences in response to xenobiotics are found between the lines, ranging from absolute resistance to a substantial decrease in heart rate over time. Most lines also show different response patterns depending on the drug, indicating clear genetic effects.

F2 segregation analysis and mapping of quantitative trait loci will pave the way for the identification of contributing loci and their validation. Since medaka has many orthologous genes to humans, unravelling these will assist pharmacogenomics in the development of personalised medicine and provide a basis for the individualised assessment of environmental toxins.

P107**Influence of the single nucleotide polymorphisms rs12252 and rs34481144 in *IFITM3* on humoral immune response after vaccination against COVID-19**

I. Ciuciulkaite¹

¹Essen University Hospital, Institute of Pharmacogenetics, Essen, Germany

Introduction: Interferon-induced transmembrane protein (IFITM) 3 is a membrane-associated protein, which showed to have the ability to restrict viruses. The single nucleotide polymorphism (SNP) rs12252 in *IFITM3* has been shown to influence the susceptibility to and severity of influenza infection and the humoral immune response after vaccination against influenza. Another SNP, rs34481144, in *IFITM3* was associated with a higher risk of severe influenza infection and poor outcome. Both SNPs were also associated with SARS-CoV-2.

Objectives: The aim of this study was to measure the humoral immune response after vaccination against COVID-19 at various times points and to determine whether SNPs rs12252 and rs34481144 influence the humoral immune response after vaccination against COVID-19.

Materials and methods: 1891 participants were included in this study. All participants were vaccinated with either mRNA-1273 or/and BNT162b2. Blood samples of all participants were tested one month after first vaccination along with one and six months after the second and third vaccination. Antibody titres against SARS-CoV-2 spike protein and SARS-CoV-2 nucleocapsid protein were measured at each time point. Genotypes of the *IFITM3* rs34481144 and rs12252 polymorphisms were determined for all participants.

Results: The humoral immune response significantly increased at one month and decreased at six months after the second and third vaccination against COVID-19 ($P < 0.0001$). The humoral immune response one month after the first and second vaccination as well as six months after the second vaccination was higher in participants vaccinated with mRNA-1273 ($P < 0.0001$). By the third vaccination, participants vaccinated three times with BNT162b2 had a lower immune response one and six months after the third vaccination than participants vaccinated homogeneously or heterogeneously with mRNA-1273 ($P < 0.0001$). rs12252 were not associated with antibody titres after vaccination against COVID-19. rs34481144 A-Allele carriers had higher antibody titres one month after the first vaccination with BNT162b2 ($P < 0.04$).

Conclusion: Although, both SNPs rs12252 and rs34481144 were promising candidates, just rs34481144 could be associated with the humoral immune response after the vaccination against COVID-19.

P108**Characterization of the EMPAR cohort – Health care claims data and CYP2D6 profiles**

T. Huebner¹, M. Steffens¹, S. Heß², D. Langner³, U. Schneider³, F. Falkenberg³, R. Linder³, J. Stingl⁴, B. Haenisch^{1,5,6}, C. Scholl¹

¹Federal Institute for Drugs and Medical Devices, Research Department, Bonn, Germany

²Federal Institute for Drugs and Medical Devices, Health Research Data Center, Bonn, Germany

³Techniker Krankenkasse, Hamburg, Germany

⁴RWTH Aachen University, Institute for Clinical Pharmacology, Aachen, Germany

⁵German Center for Neurodegenerative Diseases, Bonn, Germany

⁶University of Bonn, Center for Translational Medicine, Bonn, Germany

Introduction: Drug prescriptions in routine care in Germany are not accompanied by pharmacogenetic testing for optimal drug selection and dosing. Thus, the impact of pharmacogenetic profiles on the safety of drug therapy and the use of statutory health insurance services was evaluated in the study EMPAR. This cooperation project of the Federal Institute for Drugs and Medical Devices, the German Center for Neurodegenerative Diseases and the German health insurance provider Techniker Krankenkasse (TK) was executed to identify necessities for the utilization of genetic testing in routine care to improve drug therapy.

Objectives: Evaluation of the impact of selected pharmacogenes, drug therapy, adverse drug reactions (ADRs) and the use of statutory health insurance services.

Patients and methods: Anonymized healthcare claims and pharmacogenetic data of 10748 adult TK insureds of the EMPAR population were assessed. Analysis was performed to characterize the study population with regard to e.g. CYP2D6 phenotypes, CYP2D6 substrate and inhibitor prescriptions, saturation scores and the occurrence of adverse drug reactions. CYP2D6 phenotypes were derived from genotyping with the Agena Bioscience iPLEX® PGx 74 and the VeriDose® CYP2D6 CNV panel.

Results: First evaluations focused on general population characteristics such as long-term prescriptions and actionable variants of CYP2C9, CYP2C19, VKORC1 and SLC01B1. Thereby, a majority of participants were carrier of ≥ 1 actionable variant that can affect the safety of drug therapy of associated drugs. In a subcohort with prescriptions of anticoagulants and antithrombotic agents, extreme phenotypes of CYP2C9, CYP2C19 or VKORC1 relevant for drug metabolism of the according drug collective was detected in $>25\%$ of the cohort. Furthermore, 21 % of participants received ≥ 2 and 2.3 % even ≥ 5 prescriptions in each quarter of the baseline year which indicated a long-term use of several drugs in parallel and thus a risk of interactions. In current evaluations, analyses were extended to CYP2D6 related population characteristics. Here, we also present first data on CYP2D6 inhibition and saturation (54.8% of participants affected) according to prescription data and the risk of phenoconversion and ADRs in a German population.

Conclusions: EMPAR provides analyses of pharmacogenetic data matched with health care claims data and thus contributes to the assessment of the clinical utility of pharmacogenetic testing in routine care.

P109

A comparison of pharmacogenomic raw genotyping data from DTC-GT services and third-party interpretation websites with conventional laboratory testing

J. Bonzon¹, E. S. M. Ermanni¹, M. Moser¹, G. A. Kullak-Ublick¹

¹Universitätsspital Zürich, Klinische Pharmakologie & Toxikologie, Zürich, Switzerland

Introduction: In the last years, there was a development of affordable direct-to-consumer genetic testing (DTC-GT) services and of online tools to interpret single nucleotide polymorphisms (SNP) in individual patients. In this context, an increasing number of patients has been found to exhibit modified drug metabolism due to genetic variations.

Objectives: The aim of this case study is to investigate how precise such genotyping results are, compared to standard laboratory testing, and how to manage and inform patients who commission their own pharmacogenetic testing and present these at their next consultation.

Patients and methods: A 32 year-old man with burn-out experienced numerous adverse drug reactions under trimipramine and vortioxetine, both substrates of the cytochrome P450-enzyme (CYP) 2D6, as well as almost no antidepressant effect under escitalopram, a substrate of CYP2C19. After reading online about pharmacogenomics, the patient ordered a DNA test at MyHeritage® (MH), and uploaded the file with the detected SNPs on Codegen®. He found out that he probably has an altered metabolism for CYP2D6 and CYP2C19, both relevant for the metabolism of his medication. The attending psychiatrist asked for an assessment of these findings in our outpatient service for pharmacogenetics.

Results: The laboratory approach (pharmacogenetic testing in the hospital) showed a homozygous genotype for a non-functional allele of CYP2D6 (*4/*4, poor metabolizer) and a heterozygous genotype for a variant with increased activity for CYP2C19 (*1/*17, rapid metabolizer), consistent with the patient's findings. A deeper look at the SNPs analysed in the assay of MH showed that only a part of the possible defining (sub-) alleles of CYP2D6*4 were investigated. In addition, as some of the analysed alleles overlapped with other alleles of CYP2D6, the identification of the exact genotype using only the data of MH was not possible. The same limitations applied to CYP2C19.

Conclusion: In this case, the SNPs delivered an estimation of the metabolizer status of CYP2D6 and 2C19 which was consistent with the laboratory findings. However, as not every known mutation was analysed, and as no information was available about the reliability of the database of Codegen®, the self-diagnosis using online tools for CYP450 genotyping can be useful to obtain a first idea about possible variants of metabolizer status, but an exact identification of the genotype requires conventional laboratory testing.

P110

Detection of bladder cancer specific mutations in human tissue and urine samples by mass spectrometry

N. Reichelt¹, C. Köhler¹, T. Brüning¹, H. U. Käfferlein¹

¹Institute for Prevention and Occupational Medicine of the German Social Accident Insurance, Ruhr University Bochum (IPA), Bochum, Germany

Urothelial cancer (UCa) is a common type of cancer in Germany and the Robert-Koch-Institute predicted around 30,000 new cases for 2022. Since UCa is often multifocal, it has a high recurrence rate requiring regular follow-up investigations. The current diagnostic gold standard is cystoscopy of the (upper) urinary tract. However, cystoscopy is invasive and painful, often prompting patients to evade surveillance check-ups. Therefore, diagnosis of recurrent cancers is prolonged and risk of tumor progression increases. Consequently, the interest in non-invasive diagnostic methods is great. The aim of this study was the development of a multiplex-assay for the detection of 40 bladder cancer specific mutations and the evaluation of their potential as biomarkers for UCa.

253 tissue samples (202 with UCa, 51 without) and 214 urine samples (142 with UCa, 72 without) were tested for the presence of mutations at 40 sites on 13 different genes that have been previously associated with UCa (*ARID1A*, *ATM*, *EP300*, *ERBB2*, *FGFR3*, *HRAS*, *KDM6A*, *KMT2D*, *KRAS*, *PIK3CA*, *RB1*, *TP53*, *TSC1*). The analysis was performed using the MassArray iPLEX Pro system (AgenaBioscience) allowing the simultaneous detection of up to 15 mutations in one assay. In short, a multiplex PCR is followed by allele-specific primer-extension and the extension products are analysed by MALDI-TOF-MS.

In samples from patients with UCa, at least one mutation was detected in 48.5% of the tissue samples and 52.8% of the urine samples. A comparison of the mutational fingerprint in tissue and urine specimen of the same individual showed matching results for 104 of 139 samples (74.8%). For 19 patients, the mutational load was higher in urine. 70% of the detected mutations were either located on *PIK3CA* or *FGFR3* with *PIK3CA* c.1633G>A p.E545K being the most common (tissue: 21/202 and urine: 19/142). In samples without UCa, mutation frequency was <3% in both tissue and urine.

Overall, our multiplex assay achieved a sensitivity of 52.8% at a specificity of 97.2% for the non-invasive detection of UCa in urine. The sensitivity could be improved by adding more mutation sites or using a more sensitive approach since the applied iPLEX Pro method cannot detect allele frequencies lower than 5-10%.

P111

Targeted investigation of prenyltransferase promoters shows no aberrant DNA methylation in cancer cells, but reveals evidence for differential, CpG-site-specific maximum proportion of DNA methylation independent of cell line, chromatin state and methylation mechanism.

D. Jung¹, H. S. Bachmann¹

¹Witten/Herdecke University, Institute of Pharmacology and Toxicology, Centre for Biomedical Education and Research (ZBAF), School of Medicine, Faculty of Health, Witten, Germany

Introduction: Proteinprenyltransferases (PTases) are a group of four enzymes conserved in all eukaryotes. They transfer lipophilic prenyl moieties to the C-terminus of hundreds of proteins, including the γ -subunit of G proteins and the majority of small GTPases, which rely on prenylation for proper function and localization. Pharmacological inhibitors of PTases (PTIs) are tested in cancer treatment, but are also considered as a novel treatment option for infectious diseases. Aberrant protein prenylation and expression of PTases is associated with a number of diseases, especially cancer. Response to PTIs in clinical studies is determined by PTase expression, as well. We've shown previously that genetic variation can explain part, but not all of the variability in the response to PTIs. We therefore aim to assess the influence of epigenetic factors on PTase expression and PTI response.

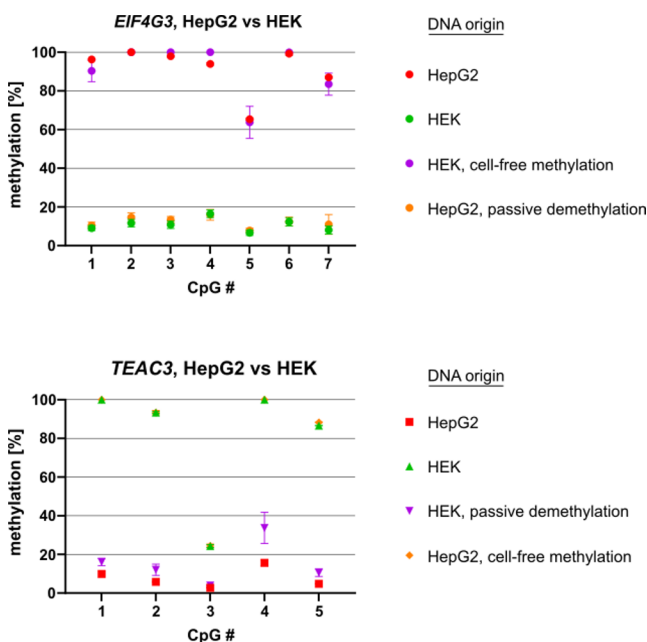
Objective: We investigated whether PTase gene expression is dysregulated epigenetically in cancer cell lines by DNA methylation of promoter-associated CpG islands.

Materials and methods: The methylation status of promoter-associated CpG islands of PTase genes was determined in a panel of cancer cell lines in a targeted approach by pyrosequencing. As negative and positive controls, we used passive reduction of methylation via dilution/amplification, and cell-free methylation using M. SssI methyltransferase, respectively, as well as loci that were annotated as predominantly unmethylated or methylated in public databases.

Results: We found no evidence for aberrant DNA methylation within the studied regions of PTase gene promoters in any of the investigated cancer cell lines, including carcinomas of the kidney, leukaemic T cells, osteosarcoma and neuroblastoma cells. Surprisingly however, we observed that CpG sites exhibited the same distinct maximum DNA methylation proportions, both *in vivo* and after cell-free methylation of unmethylated DNA (Fig. 1).

Conclusion: Our results indicate that aberrant PTase expression and protein prenylation in cancer cells – and consequently, the variable response to PTIs in cancer trials – is not caused by aberrant DNA methylation of PTase promoters. Additionally, using a targeted approach, we found evidence for a site-specific limit to the maximum proportion of DNA methylation caused by a yet unknown mechanism. To our knowledge, this is the first report of a site-specific apparent limit that applies for both *in vivo* and cell-free DNA methylation.

Fig. 1



P112**PharmFreq: a comprehensive database of worldwide allelic frequencies in clinically important pharmacogenes**

R. Tremmel^{1,2}, Y. Zhou³, L. Nevasadova⁴, S. Laari², E. Eliasson³, V. M. Lauschke^{1,4,2}

¹Dr. Margarete Fischer-Bosch-Institute of Clinical Pharmacology, Stuttgart, Germany

²University of Tuebingen, Tuebingen, Germany

³Department of Laboratory Medicine, Karolinska Institutet, Stockholm, Sweden

⁴Department of Physiology and Pharmacology, Karolinska Institutet, Stockholm, Germany

Introduction: Drug metabolism and drug transport are inter-individually variable. Genetic variants significantly explain a large fraction of expression and activity of transporters and enzymes of CYP, UGT or SULT families. Evidence-based pharmacogenetics (PGx) guidelines have been established to recommend drugs and dosage in personalized medicine approaches. For worldwide clinical implementation, it is of importance to have access on information about the occurrence and frequency of PGx variants in specific populations and ethnics. The aim of this study was to collect worldwide frequency data on the most important pharmacogenes to create a population pharmacogenomics database and to provide this information to the community.

Methods: Data on allele frequencies of pharmacogenes such as *CYP2B6*, *CYP2C19*, *CYP2C9*, *CYP2D6*, *CYP3A5*, *DPYD*, *TPMT* and *UGT1A1* with available clinical guidelines was collected from PharmGKB. Furthermore, a comprehensive PubMed literature search was carried out. Allele frequency information, cohort size, and ethnical background (e.g. population, ancestry) were documented. A R-Shiny web application was applied to visualize and share the data.

Results and conclusion: Currently, allele frequency data of more than 1000 studies was collected covering 130 countries and populations, 14 genes and almost 180 alleles. Most of the studies have been performed in subjects with East Asian and European ancestry. African and South American populations and particularly studies analyzing populations from Oceania were underrepresented. As expected, most alleles have been investigated for *CYP2D6* and *DPYD*, the genes with the highest genetic variability among those included in the database. In total, 43% of all analysed alleles have absent or decreased function (43%) in contrast to 3% with increased function according to CPIC. Well known differences between geographical groups with respect to allele frequencies and genetic complexity (e.g. *DPYD*, *CYP2D6*, *CYP2C19* or *HLA-B*) can be illustrated in the database. To facilitate the search and download for country specific allele frequencies we developed a web-based interactive dashboard. Users can download all information and are invited to contribute their own data.

This work was supported by the Robert Bosch Stiftung (Stuttgart, Germany)

P113**Assessment of circulating metabolites reveals isobutyrate and propionate associated with lean NAFLD: consequences on steatosis prediction and lipid accumulation**

M. Haag^{1,2}, S. Winter^{1,2}, A. M. Kemas³, J. Tevini⁴, A. Feldman^{5,6}, S. Eder^{5,6}, T. K. Felder⁴, C. Datz^{6,7}, G. Liebisch⁸, O. Burk^{1,2}, B. Paulweber^{5,6}, V. M. Lauschke^{1,3}, M. Schwab^{1,9,2}, E. Aigner^{5,6}

¹Dr. Margarete Fischer-Bosch Institute of Clinical Pharmacology, Stuttgart, Germany

²University of Tübingen, Tübingen, Germany

³Karolinska Institutet, Department of Physiology and Pharmacology, Stockholm, Sweden

⁴Paracelsus Medical University, Department of Laboratory Medicine, Salzburg, Austria

⁵Paracelsus Medical University, First Department of Medicine, Salzburg, Austria

⁶Paracelsus Medical University, Obesity Research Unit, Salzburg, Austria

⁷Hospital Oberndorf, Department of Internal Medicine, Oberndorf, Austria

⁸Regensburg University Hospital, Institute of Clinical Chemistry and Laboratory Medicine, Regensburg, Germany

⁹University Hospital Tübingen, Department of Clinical Pharmacology, Institute of Experimental and Clinical Pharmacology and Toxicology, Tübingen, Germany

Introduction: As NAFLD is considered a metabolic disorder, metabolomics analysis in serum/plasma can provide novel diagnostic markers of disease and guide functional *in vitro* investigations to broaden mechanistic insight. While alterations in circulating metabolites have been described for obese NAFLD knowledge about changes related to body weight and a potential contribution of microbial metabolites is limited.

Objectives: Investigation of serum metabolites, including microbial bile acids (BAs) and short-chain fatty acids (SCFAs) and their association with lean NAFLD.

Patients and methods: 204 subjects were allocated to four groups: lean healthy (n=61), lean NAFLD (n=49), obese healthy (n=47) and obese NAFLD (n=47). BAs and SCFAs were quantified by mass spectrometry followed by linear modelling in subgroups (all, lean and obese) alongside metabolomics data acquired by the Biocrates p180 Kit. NAFLD prediction was assessed based on a random forest approach. Functional effects of significantly altered molecules were confirmed in organotypic 3D primary human liver cultures.

Results: Analysis of the complete cohort revealed that NAFLD subjects had elevated amino acids and isobutyrate accompanied by reduced amounts of lysophosphatidylcholines and hydroxylated sphingomyelins. Lean NAFLD group exhibited a 2.6-fold increase of isobutyrate together with elevated methionine sulfoxide, propionate and phosphatidylcholines. Within obese NAFLD subjects, higher circulating amounts of sarcosine were evident alongside reduced lysine and asymmetric dimethylarginine. Using a subset of metabolites (including microbial SCFAs) resulted in a median area under the curve of 0.86 for NAFLD prediction considering gender and BMI. *In vitro* experiments in 3D human liver spheroids demonstrated that propionate and isobutyrate induced lipid accumulation and altered expression of genes involved in lipid and glucose metabolism.

These findings provide strong evidence for a potential relationship between circulating SCFAs and alterations in hepatic lipid homeostasis.

Conclusion: Lean NAFLD is characterized by a distinct metabolite pattern related to amino acid metabolism, lipids and microbial SCFAs. These observations suggest metabolic differences between etiologies of fatty liver disease possibly related to alterations in transmethylation processes and/or gut microbial activity that should be considered for a non-invasive diagnosis and/or staging of NAFLD including fibrosis.

P114**Multi-dimensional omics profiling of a biobank reveals the interindividual variability of ADME gene expression in human liver**

K. Klein^{1,2}, A. T. Nies^{1,2,3}, M. Haag^{1,2}, U. Hofmann^{1,2}, P. Artursson⁴, N. Handin⁴, O. Burk^{1,2}, R. Tremmel^{1,2}, S. Winter^{1,2}, Y. Zhou⁵, E. Schaeffeler^{1,2,3}, U. M. Zanger¹, V. M. Lauschke^{1,6}, M. Schwab^{1,2,3,7}

¹Dr. Margarete Fischer-Bosch Institut für Klinische Pharmakologie, Stuttgart, Germany

²University of Tuebingen, Tuebingen, Germany

³University of Tuebingen, iFIT Cluster of Excellence (EXC2180), Tuebingen, Germany

⁴Uppsala University, Departments of Pharmacy, Uppsala, Sweden

⁵Karolinska Institutet, Department of Laboratory Medicine, Stockholm, Sweden

⁶Karolinska Institutet, Department of Physiology and Pharmacology, Stockholm, Sweden

⁷University of Tuebingen, Departments of Clinical Pharmacology, and of Pharmacy and Biochemistry, Tuebingen, Germany

Introduction: Drug metabolism and drug transport are known to be interindividually variable in human liver. Hepatic expression variation of genes involved in absorption, distribution, metabolism, and excretion (ADME) processes is a general problem impacting drug treatment, efficacy, and safety. Personalized medicine aims to optimize treatment efficacy by leveraging the individual's genetic makeup as well as additional environmental, epigenomic and metabolomic factors.

Objectives: However, even in the postgenomic era, there is still limited knowledge with regard to biochemical, physiological, and pathophysiological factors that contribute to the interindividual variability of expression and function of ADME genes in human liver. Variability of some transporters only <50% can be explained by genetic and nongenetic determinants. Cytochrome P450 star-allele variants contribute 50% for CYP2D6, and 10% for CYP2B6 to protein and activity expression variability.

Methods: To comprehensively elucidate factors impacting expression and function (mRNA levels, protein, enzyme activity) of 340 ADME genes grouped in six gene families we used a liver tissue collection (n=150), for which extensive patient and clinical documentation is available. We integrated multi-dimensional comprehensive omics profiling (genomics, transcriptomics, metabolomics), and targeted analyses (immunoquantified protein contents, mass-spectrometric determined transporter and cytochrome P450 data as well as enzyme activities), and applied univariate and multivariate regression statistics. Computational prediction of SNV function considered coding, epigenetic, non-coding, and regulatory effects in human liver.

Results and conclusion: Variability of ADME gene expression was quantified and co-regulatory modules were identified. Furthermore, expression quantitative trait analyses for phase I, II, transporter or nuclear receptor family members, considering nongenetic factors will estimate explained and unexplained variability. Novel factors impacting expression and function can be identified and functionally tested in 3D spheroid culture models with primary hepatocytes. New hypotheses, signatures or biomarkers, could be derived that may be of interest for prediction of drug efficacy and toxicity.

This work was supported by the Deutsche Forschungsgemeinschaft (DFG, German Research Foundation) under Germany's Excellence Strategy - EXC 2180 - 390900677, and the Robert Bosch Stiftung (Stuttgart, Germany)

Clinical pharmacology – Pharmacokinetics and PK/PD modelling**P115****"RNA-Analytics via Microscale Thermophoresis (MST) - A tool to study molecular interactions in solution"**

M. Herkt¹

¹Fraunhofer Institute for Toxicology and Experimental Medicine ITEM, Cardiovascular Research (CVR), Hannover, Germany

Abstract: Thermophoresis describes a process in which molecules undergo directional movement due to a temperature gradient, of which Microscale Thermophoresis (MST) takes advantage of. It can be utilized for highly sensitive interaction studies of fluorescently labeled RNA-based therapeutics at a microliter scale, regardless of their size or chemical composition. Thus, MST is significantly superior to ITC and SPR in terms of sample volume consumption or experimental setup, as it also does not require immobilization of an interaction partner. MST can be used to investigate various RNA/DNA/proteins for their binding capacity towards potential target structures in a pre-clinical setting. In this way, binary and ternary interactions can be assessed and analyzed for future RNA-drug candidates being identified early on and in a cost-efficient manner.

Motivation: The 8th German Pharm-Tox Summit is a perfect opportunity to raise the awareness for this novel and innovative technique, which gained more track in pre-clinical

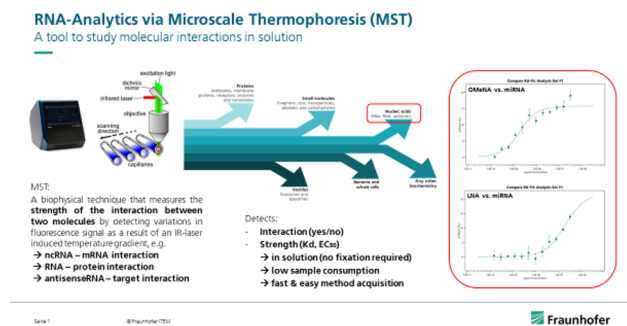
drug-development in recent years. Molecular interactions are at the fundament of all biological processes, while RNA/RNA, RNA/DNA and RNA/protein interactions play a major role at all levels of gene regulation, extra/intracellular communication and also in today's health crisis challenges. This technique allows for studying mechanisms of cell-adhesion and -entry of all kinds of exogenous entities *in vitro* and could be a straight forward tool to gain better understanding of infection mechanisms and intracellular signaling.

References: Name: Dr. Markus Herkt, MSc, BSc, CHKA

Affiliation(s): Fraunhofer Institute for Toxicology and Experimental Medicine ITEM, Nikolai-Fuchs-Str. 1, 30625 Hannover

Field of expertise: RNA-(Bio)Analytics / RNA Therapeutics

Fig. 1



P116

Workflow proposal for setting upper concentrations in *in vitro* toxicity testing
*R. Landsiedel*¹, *E. Fabian*¹, *B. Birk*², *S. Melching-Kollmuss*³, *C. Wiemann*³, *D. Fink-Weyer*¹

¹BASF, Experimental Toxicology and Ecology, Ludwigshafen, Germany

²BASF SE, Experimental Toxicology and Ecology, Ludwigshafen, Germany

³MatTek In Vitro Life Science Laboratories, Bratislava, Slovakia

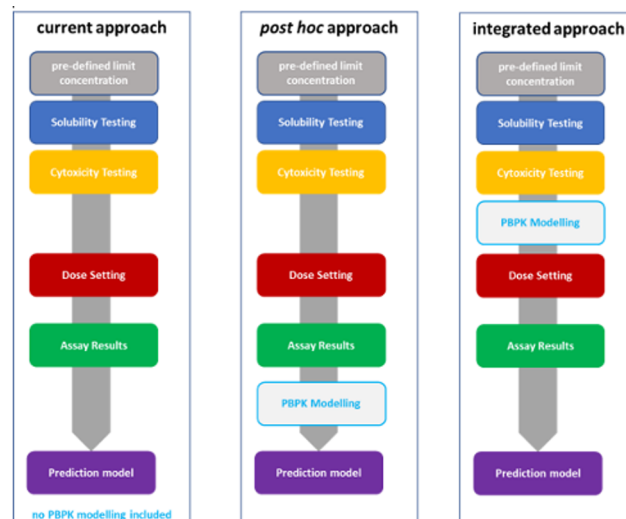
Introduction: *In vitro* assays are increasingly used in regulatory testing and are intended to provide data applicable to hazard classification and risk assessment. While classical *in vivo* test methods define the highest tested dose, which is either limited by general toxicity (e.g. maximum tolerated dose (MTD) defined by body weight gain) or by consequential classification limits (e.g. limit dose 2000 mg/kg b.w.), *in vitro* studies often do not.

Objectives: Routinely, solubility and cytotoxicity of a test substance drive the highest concentrations tested in an *in vitro* study. Those concentrations may, however, cause unspecific effects. Moreover, those test results may not be relevant to subsequent classification and risk assessment, since they exceed *in vivo* achievable doses. We propose setting upper concentrations *in vitro* considering the corresponding *in vivo* doses.

Materials and methods: We introduce a workstream to set upper *in vivo* concentrations using pharmacokinetic (PBPK) models, considering *c_{max}* in plasma of a test substance applied *in vivo* at the highest dose used in an animal study i.e., limit dose or the MTD. The concept also considers the unbound fraction of the test substance, as well as adjustment factors for uncertainty.

Results and conclusion: Currently any result of an *in vitro* assay is used in a prediction model (PM) to draw toxicological conclusions (left column in the figure, current approach). An upper *in vitro* concentration derived from relevant *in vivo* doses could be used to either filter those assay results which originate from exceedingly high concentrations (middle column in the figure, *post-hoc* approach) from entering the PM or – even more efficiently – set the upper concentration based on *in vivo* doses (right column in the figure, integrated approach).

Fig. 1



P117

Effect of aging on the pharmacokinetics of metformin, penicillin, sumatriptan, and metoprolol in rats

*M. J. Meyer-Tönies*¹, *A. Wind*¹, *D. Karaica*², *V. Micek*², *I. Vrhovac Madunic*², *D. Brejčak*², *J. C. Stingl*³, *J. Brockmöller*⁴, *I. Sabolic*², *M. V. Tzvetkov*¹

¹University Medicine Greifswald, Institute of Pharmacology, Greifswald, Germany

²Institute for Medical Research and Occupational Health, Molecular Toxicology Unit, Zagreb, Croatia

³University Hospital of the RWTH Aachen, Institute of Clinical Pharmacology, Aachen, Germany

⁴University Medical Center Göttingen, Institute of Clinical Pharmacology, Göttingen, Germany

Drug pharmacokinetic studies are usually performed in young and healthy individuals. However, the drugs analyzed are often taken by elderly individuals. Except for a known decline in kidney function, it is unclear whether and how drug pharmacokinetics change in elderly. The aim of this study was to analyze how strongly ageing affects drug pharmacokinetics and whether we can predict pharmacokinetics in elderly based on data from young and healthy individuals.

To this end, we performed a pharmacokinetic study using elderly (2 years old) and young (2 months) Wistar rats. Due to known sex-differences in the expression of drug-metabolizing enzymes and drug transporters, this set up additionally enabled analyzing sex effects. Rats were fasted overnight and received a cocktail containing 100 mg/kg metformin, 100 mg/kg penicillin V, 5 mg/kg sumatriptan, and 20 mg/kg metoprolol p.o. Six blood samples and total urine excreted were collected over 12 h and drug concentrations were measured using LC-MS/MS and drug pharmacokinetic parameter were calculated. The drugs were chosen, on the one hand, to be commonly used in elderly and on the other hand, to may serve as probe drugs for drug-metabolizing enzymes and drug transporters.

We observed age-dependent differences in the drug pharmacokinetics in rats. Both metformin and penicillin V had a 1.6-fold reduction in renal clearance in elderly compared with adult rats. Metoprolol had a 1.8-fold reduction in extrarenal clearance with age. In addition, the pharmacokinetics of most of the drugs showed sex differences, as may have been expected from the known differences in drug-metabolizing enzyme and transporter expression. We observed differences in the metabolism of metoprolol between rats and humans. While the dominant metabolite in rat was α -hydroxy metoprolol, in human it was O-desmethyl metoprolol. These species differences warrant attention when transferring pharmacokinetic data obtained in rats to humans.

To summarize, we observed both age and sex-dependent differences in the pharmacokinetics of metformin, penicillin V, sumatriptan, and metformin in rats.

P118

Determination of Respiratory Pharmacokinetic Parameters using a Combination of Physiologically Based Pharmacokinetic Modelling and an Isolated Perfused Lung Model

*N. Nowak*¹, *S. Escher*², *K. Bluemlein*³, *K. Schwarz*¹

¹Fraunhofer Institute for Toxicology and Experimental Medicine, Aerosol Technology and Aerosol Biophysics, Hannover, Germany

²Fraunhofer Institute for Toxicology and Experimental Medicine, In-silico Toxicology, Hannover, Germany

³Fraunhofer Institute for Toxicology and Experimental Medicine, Bio- and Environmental Analytics, Hannover, Germany

Introduction: Information on systemic available substance concentration is an important element for both pharmacology and toxicology in the pre-clinical development of new

drugs or the risk assessment of chemicals. In recent years, uptake via the inhalational route has gained particular interest.

Objectives: To investigate pharmacokinetics of inhaled substances in an *in vivo* relevant model, the applicability of Isolated Perfused Rat Lungs (IPLs) in combination with computational modelling for pulmonary absorption studies was explored.

Materials and methods: The IPL, providing a fully intact organ system with cellular, structural and functional integrity, that is ventilated and perfused, was established. For investigations into mass transfer processes through the lung, IPLs are exposed to aerosols and the concentration profile of the substance is analyzed in the perfusate. For the translation of the data into a permeability coefficient, a physiological multi-compartment-model (lung lining fluid, tissue, blood per lung generation) lung was developed, simulating the systemic uptake of aerosols as well as further uptake and clearance processes (mucociliary and macrophage clearance, dissolution) in the IPL.

Results: The computational model was used to calculate an effective transfer velocity through the lung, using the experimentally determined concentration profiles in the IPLs. For ciprofloxacin, the apparent permeability coefficient (Papp) was determined to be 4 x 10⁻⁷ cm/s. As expected, a significantly higher apparent permeability coefficient of about 1.5 x 10⁻⁵ cm/s was found for a smaller and more lipophilic substance, while a much lower value was observed for a larger molecule (MW >> 1000 Da). The obtained Papp values were used to model the venous concentration-time profile using an inhalation-focused human PBPK model developed by Fraunhofer ITEM. The comparison of the modelled venous concentration-time profile corresponded well to experimental human data.

Conclusion: These first results demonstrate that the use of the whole organ model of the isolated perfused lung in combination with PBK modelling is suitable for studying the pulmonary absorption kinetics of inhaled substances. This contributes well to the development of new inhalable drugs and risk assessment of chemicals as well as to the 3R principles by reduction of animal experiments. Further work will aim to extend the applicability domain of the model and define tiered testing strategies.

P119

Gene Expression and Protein abundance of minor drug metabolizing enzymes in human intestine and liver: an inter- and intra-subject analysis

C. Wenzel¹, J. Lapczuk-Romanska², M. Ostrowski², M. Drozdzik², S. Oswald³

¹University Medicine Greifswald, Pharmacology, Greifswald, Germany

²Pomeranian Medical University, Pharmacology, Szczecin, Germany

³University Medical Center Rostock, Pharmacology, Rostock, Germany

Drug metabolism by phase I and phase II-enzymes is a major determinant of oral bioavailability. There is convincing evidence that several drugs undergo extensive first pass metabolism already in intestinal epithelia. In this regard, the protein abundance of several intestinal drug-metabolizing enzymes (DMEs) such as CYP3A4 and UGT1A1 were found to be comparable to that in the liver. However, contrary to available data on major DMEs there is so far only little known about the expression of several other enzymes involved in drug metabolism, which were so far beyond the main focus, i.e. "minor" DMEs. Thus, it was the aim of this study to characterize the gene expression and protein abundance of these minor DMEs in human intestine and liver. Accordingly, we successfully developed and validated a mass spectrometry-based targeted proteomics method for the quantification of 11 clinically relevant minor carboxylesterases (CES), UDP-glucuronosyltransferases (UGT) and cytochrome P450 (CYP)-enzymes (CES1, CES2, CYP1A1, CYP2A6, CYP2C18, CYP2J2, CYP3A7, CYP4F2, CYP4F12, CYP4A11 and UGT2B17). We applied our method to jejunal and liver tissue specimens of 11 healthy organ donors (8 males, 3 females, age: 19-60 years). Our analysis was performed in whole tissue lysate subjected to the filter aided sample preparation procedure (FASP) including a tryptic digest. In addition, the respective mRNA levels of the encoding genes were determined by quantitative real-time RT-PCR. All studied proteins, with the exception of CYP1A1 and CYP4A11, could be detected in human livers. Most of the studied enzymes were also detected in the jejunum. Here, we found several enzymes to be of higher (e.g. CES2, UGT2B17, CYP2J2) or similar (e.g. CYP2C18) protein abundance compared to the liver. On the contrary, the protein abundance of most of the investigated enzymes were higher in liver tissue (i.e. CES1, CYP2A6, CYP2J2). While significant correlations between gene expression and protein data could be detected in intestinal or liver tissue for some enzymes (e.g. CES1, CES2), significant correlations between intestinal and hepatic protein abundance could only be observed for UGT2B17. Moreover, our results demonstrated a high variability between the individuals. Precise data on protein abundance as generated in our study may be useful for PBPK-based modelling and prediction. This approach can be used for estimating optimized dosing, which in turn may improve efficacy and safety of drug therapy.

Pharmacological – pharmacological education

P120

Information and teaching materials for conscious environmental handling of pharmaceuticals for human use

J. S. Strehse¹, G. Maack², A. Hein², E. Maser¹

¹Institute of Toxicology and Pharmacology for Natural Scientists, University Medical School Schleswig-Holstein Campus Kiel, Kiel, Germany

²German Environment Agency, Dessau, Germany

Question: Our environment is polluted with a multitude of trace substances. Active substances of pharmaceuticals represent a special group of these pollutants. Even if they are taken as intended, they cannot be prevented from entering the environment

completely, since consumers excrete pharmaceuticals and their metabolites, which can enter the environment via wastewater. However, it is possible to minimise the entries. To achieve this, consumers as well as allied health professionals must be informed in a comprehensive and comprehensible manner about their options to minimise the input of pharmaceuticals in the environment. Appropriate information materials are being produced for this purpose in a two-year project in cooperation with the German Environment Agency.

Methods: Raising awareness of the issue of pharmaceutical residues in the environment among allied health professionals has to take place at three levels: First, the possibilities should be explored to firmly anchor the topic in the licensing and training regulations of medical and pharmacy professionals. Secondly, freely available teaching materials are to be created to make it easier for lecturers to get to grips with the topic. Thirdly, materials for the further training of medical doctors and pharmacists are to be created. These should then be made freely available to further training institutions. In order to take the needs of the later users of the teaching materials sufficiently into account, several workshops will be organised during the project period.

Results and conclusion: Previous studies have shown that allied health professionals are important as multipliers to raise the awareness of the environmental problems of pharmaceutical residues among consumers. Therefore, the topic needs inclusion in their training and study regulations. But the implementation is not simple in all possible regulations. However, it is always possible for lecturers to include the topic of pharmaceutical residues in the environment in their teaching. The workshops also showed that there is great interest on the part of both teachers and students. The previous ideas for designing the teaching materials, which for instance are to consist of freely available PowerPoint slides, were also very positively received. Furthermore, constructive suggestions for improvement were made and possibilities for successful dissemination of the materials were discussed with the participants.

P121

Desorption/ionization mass spectrometric methods for drug quantification in biological matrices and their validation following regulatory guidance.

M. Fresnais¹, W. E. Haefeli¹, R. Longuespée¹

¹University Hospital Heidelberg, Department of Clinical Pharmacology and Pharmacoepidemiology, Heidelberg, Germany

Mass spectrometry (MS) is currently the gold standard for quantification of small-molecule drugs in liquid or liquefied biological matrices for pharmacokinetic (PK) and pharmacodynamic (PD) applications. Especially, liquid chromatography (LC) coupled to electrospray ionization (ESI)-MS plays a pivotal role in the practice of clinical pharmacology and dedicated guidelines exist for the validation of developed bioanalytical assays¹. Today, additional approaches for surface analyses of samples, namely desorption/ionization (DI)-MS methods, emerged in the toolbox of the clinical pharmacologist for drug quantification in solid or solidified biological matrices. Among these, matrix-assisted laser (MAL)DI and desorption electrospray ionization (DESI) were proven robust for rapid and/or spatially resolved absolute quantification of drugs in tissue sections and plasma. Recently, major efforts have been focused on the validation of newly developed DI-MS assays according to the regulatory guidelines from the Food and Drug Administration (FDA), European Medicine Agency (EMA) and the International Conference for Homogenization (ICH), and the elaboration of new recommendations specific to on-surface studies².

DI-MS will be introduced based on developments of dedicated assays and experience from our group. The assets and drawbacks of DI-MS compared to LC-MS will be discussed, as well as analytical workarounds to compensate the lack of chromatographic separation prior to MS analysis, such as the use of ion-mobility (IM). For this, the development and full validation of rapid and sensitive MALDI-IM-MS/MS for the quantification of the tyrosine kinase inhibitor osimertinib will be used to demonstrate how IM-MS/MS can improve sensitive and specificity of drug quantification assays in selected regions of interest of tissue sections³. Finally, recent hardware enhancements for DESI-IM-MS/MS will be presented for the quantification of the ERK1/2 inhibitor ulixertinib⁴.

In conclusion, DI-MS represents an original extension of the analytical portfolio for the clinical pharmacologist. This presentation aims at introducing its value to the DGPT community.

1. EMA. ICH M10 on bioanalytical method validation.
2. Fresnais et al. *Anal Chem* 2021, 93 (19), 7152-7163.
3. Fresnais et al. *Cancers (Basel)* 2020, 12 (7).
4. Fresnais et al. *Pharmaceuticals (Basel)* 2022, 15 (6).

P122

PubPharm's tools for advanced searches: Generating structured drug overviews from literature

C. Draheim¹, H. Kroll², P. Sackhoff², S. Wulle¹

¹Technische Universität Braunschweig, Universitätsbibliothek, Braunschweig, Germany

²Technische Universität Braunschweig, Institut für Informationssysteme, Braunschweig, Germany

The Specialised Information Service Pharmacy (SIS, in German "Fachinformationsdienst Pharmazie") develops novel and innovative tools to ease the literature access for academic pharmaceutical scientists (1). Its central service PubPharm (www.pubpharm.de) is a drug-centred platform that offers a traditional keyword-based search for literature, a structure search for bioactive substances, and novel services to ease the exploration of literature (2,3). The latest development is the so-called Drug Overview Service

(www.narrative.pubpharm.de/drug_overview). This service automatically generates overviews about drugs by utilizing information from the latest research publications and curated databases like ChEMBL. For example, the molecular formula, structure, and mass as well as pKa and logP values are shown. In addition, the service visualises associations to other pharmaceutical and pharmacological relevant concepts such as known indications, target interactions, further drug associations, administration routes or dosage forms, and investigated methods for the searched drug. At each time, a click on the corresponding concept invokes a literature search for the association between the clicked concept and the searched drug to provide helpful evidence.

PubPharm comprises more than 55 million pharmacology-, toxicology- and pharmacy-specific publications, including the complete Medline/PubMed and additional life science resources: Journal articles, preprints, information on clinical trials, patents, books, e-books and international dissertations. PubPharm and all its tools are freely available. The SIS is a cooperation between the University Library and the Institute for Information Systems of TU Braunschweig and is funded by the DFG – Deutsche Forschungsgemeinschaft (German Research Foundation).

References:

1. Draheim C, Kefler K, Wulle S. PubPharm – die Rechercheplattform. PZ Prisma 2019; 26(2):68-74.
2. Kroll H, Plötzky F, Pirklbauer J, Balke W-T. What a Publication Tells You — Benefits of Narrative Information Access in Digital Libraries. In Proceedings of the 22nd ACM/IEEE Joint Conference on Digital Libraries (JCDL '22). ACM 2022; Article 9, 1-8. <https://doi.org/10.1145/3529372.3530928>
3. Kroll H, Draheim C. Narrative Information Access for a Precise and Structured Literature Search. O-Bib. Das Offene Bibliotheksjournal 2021; 8(4):1-13. <https://doi.org/10.5282/o-bib/5730>

P123

Alpha-adrenergic receptors in clinical practice – Present and future

P. Lechsner¹, E. G. Ban¹

¹UMFST Targu Mures, Targu Mures, Romania

Introduction: Adrenergic receptors were first discovered in 1948 and since then continuous research is targeting each type of these receptors. The use of α -adrenergic receptors in cardiovascular pharmacology has its well-established place but recent studies also revealed therapeutic possibilities in the neuromodulator pathways as well as in immune responses.

Objectives: The aim of this short review is to give an insight into the vast array of pharmacotherapeutic targets in α -adrenergic pathways and to draw students' attention on recent research possibilities.

Materials and methods: We carried out a state-of-the-art review on the topic of α -adrenergic receptors including studies from medical databases: PubMed, Ovid MEDLINE, EMBASE, Web of Science, Google Scholar, Cochrane Library during a 2-month period. Keywords used were alpha adrenergic receptors, molecular target, immunity, noradrenaline, and pharmacotherapy. To ensure good quality, data presented in an article was cross checked until clear results were obtained. In the review we included articles with well defined data and ongoing research.

Results: According to the results revealed by our state-of-the-art review we observed that $\alpha 1$ -adrenergic receptors show future possibilities in immune-response modulation in which, when activated, receptors located on the surface of immune cells will modulate development, proliferation and circulation of immune cells. The therapeutic possibilities regarding $\alpha 2$ -adrenergic receptors are even more versatile. Studies included in our research reveal future usage of $\alpha 2$ -adrenergic receptors in treating the pain caused by gastrointestinal inflammation. Other points of interests are observed in therapy of autoimmune diseases, fibromyalgia and chronic fatigue – all of these being of special interest in today's medical practice.

Conclusion: Based on the data gained during this review we can conclude that research continues into lots of different areas of clinical practice and seems promising. Today's students and tomorrow's doctors should observe the hidden possibilities of the adrenergic system.

This work was supported by the George Emil Palade University of Medicine, Pharmacy, Science, and Technology of Targu Mures, Research Grant number NR. 224/4.

Toxicology – Toxicological education

P124

Innovative online toxicology teaching: ToxLearn4EU, an Erasmus international project

H. Stopper¹, E. E. Bankoglu¹

¹University of Wuerzburg, Institute of Pharmacology and Toxicology, Wuerzburg, Germany

The European Green Deal calls for a better monitoring, reporting and prevention of the pollution of air, water, soil and consumer products. Emerging pollutants such as microplastics or nanoparticles, but also complex mixtures require innovative methods to

evaluate their toxicity, and to monitor our environment. Consequently, the global toxicology testing market is expected to grow. Thus, the next decade will see an increasing demand for highly qualified toxicologists, especially in Europe.

With this background, the Erasmus project ToxLearn4EU aims to develop freely available online toxicology lectures. As a consortium of 10 partners from 9 European countries, and lead by Toulouse University, various formats of innovative teaching will be implemented, such as interactive online courses and problem-based learning (PBL). Additionally, summer schools will provide advanced courses for students as in person events. The Würzburg University project group as the German partner will oversee the organization of 10 online lectures in the field of "priority and emerging pollutants", organize one transnational meeting and contribute lectures to all topics and activities.

Altogether, ToxLearn4EU will develop a total of 300h (equivalent to 10 ECTS) of student workload in the form of 10 interactive courses (1 ECTS each). These contents are intended to be used directly by teachers or to serve as a model to develop their own online resource. Accessibility by other audiences working in the specific domain (e.g. advisors, etc.) is possible as lifelong learning course.

P125

Updates in legislation and advice for read-across in REACH

D. Bell¹, A. A. Anastasi¹, N. Andersson¹, J. Ballester Casals¹, G. Cartledge¹, R. Cesnaitis¹, A. Gissi¹, J. Honkanen¹, J. Laitinen¹, A. Piranova¹, A. Richarz¹, E. Stiglbauer¹, F. Temussi¹, J. vom Brocke¹

¹ECHA, Helsinki, Finland

The European Commission (EC) concluded in its second report on the operation of REACH that REACH was fully operational and delivering results towards its objectives. Despite steady progress, there are however key issues that hamper progress, notably the non-compliance of registration dossiers. Subsequently the EC and ECHA prepared a Joint Action Plan to improve compliance of registration dossiers. Improving the clarity of certain legal provisions was highlighted and a corresponding amendment to the REACH regulation, which amends Annex XI, 1.5 Grouping and read-across, applies from the 08 January 2023. ECHA has published advice to accompany the legal text. This presentation summarises the changes to the legal text and sets out advice for the changes to the legal text for grouping and read-across.

Toxicology – Toxicological methods and in vitro toxicology

P126

Assessment of metabolic perturbation by Novaluron in the context of endocrine disruption

A. Schmitt¹, J. Choi¹, M. de-Lourdes Marzo Solano¹, P. Marx-Stöbling¹, L. Niemann¹, C. Kneuer¹

¹Federal Institute for Risk Assessment, Department of Pesticides Safety, Berlin, Germany

Introduction: In 2018, EFSA and ECHA published a guidance document (GD) on the identification of endocrine disruptors (ED) with criteria focusing exclusively on oestrogen-, androgen-, thyroid- and steroidogenesis (EATS)-mediated mechanisms¹. Up to now, there is no guidance on how to assess ED properties with non-EATS-mediated mechanisms.

Objectives: The case of Novaluron is presented to discuss regulatory needs for an assessment of potential ED properties via non-EATS-mediated mechanisms.

Materials and methods: As part of a regulatory process, the full toxicological data package of Novaluron, a non-approved pesticide in the EU, was reviewed to be able to perform an ED assessment.

Results: It was concluded that the criteria for T-mediated adversity are not met. For the EAS-related modalities, no conclusion could be drawn due to missing data². On the other hand, in short- and long-term toxicity studies in mice, rats and dogs, an increase in body weight gain in the absence of increased food consumption was seen in the treated groups. This was accompanied by an increase in cholesterol, triglyceride and/or glucose levels. Given that these changes may be possibly linked to an endocrine mode of action (MoA), they would be considered "sensitive to, but not indicative of" endocrine-mediated effects according to the GD, thus calling for further investigation. However, due to a lack of testing strategies, the ED assessment for a non-EATS-mediated MoA for Novaluron remains inconclusive². Nevertheless, suitable follow-up investigations to elucidate the mechanism responsible for the metabolic changes should be initiated, e.g. studies on the glucagon/insulin balance and fatty acid metabolism (for details, see poster by Sreejita Das "Investigating the effect of Novaluron on HepaRG cells").

Conclusion: Novaluron is one of the first substances reviewed in line with the ECHA/EFSA (2018) GD, for which a potential non-EATS-mediated endocrine MoA leading to metabolic perturbation cannot be excluded. Based on the available data, it is not possible to postulate a robust MoA. In analogy to the testing strategy for EATS modalities, additional mechanistic data (similar to Levels 1 and 2 of the OECD Conceptual Framework for Testing and Assessment of ED³) should be initiated if *in vivo* studies demonstrate non-EATS-related endocrine adversity.

¹EFSA Journal 2018;16(6):5311

²EFSA Journal 2022;20(1):7041

³10.1787/9789264304741-en

P127

Assessment of the performance of a New Approach Method (NAM) testing DIO1 inhibition using a human microsome based, colorimetric assay

A. Weber¹, B. Birk¹, V. Gini¹, S. Hoffmann², K. Renko³, N. Hambruch¹, S. Coecke⁴, S. Schneider¹, D. Funk-Weyer¹, R. Landsiedel^{1,5}

¹BASF SE, Experimental Toxicology and Ecology, Ludwigshafen am Rhein, Germany
²seh consulting + services, Paderborn, Germany

³Bundesinstitut für Risikobewertung (BfR), Berlin, Germany

⁴European Commission, Joint Research Centre (JRC), Ispra, Italy

⁵Freie Universität Berlin, Institute of Pharmacy, Pharmacology and Toxicology, Berlin, Germany

Introduction: The interference of chemicals with thyroid homeostasis can lead to adverse effects in humans. Exogenous chemicals that alter functions of the endocrine system and consequently causes adverse health effects are termed "endocrine disruptors". So far *in vitro* testing of the interference with thyroid homeostasis has been limited and without regulatory acceptance. EURL ECVAM in cooperation with a network of EU laboratories (EU-NETVAL), is coordinating the validation of multiple *in vitro* methods to address different key events potentially affecting thyroid homeostasis. One such method is the DIO1-SK assay. Deiodinases (DIO) are important, local regulators of TH action. DIO1, one of three isoforms and mainly expressed in thyroid, liver, and kidney, serves as one main source of the active hormone T3 via deiodination of T4 and plays a role in recycling of iodide via deiodination of inactive TH metabolites.

Objectives: The reproducibility of the method has previously been established (Weber et al. 2022; DOI: 10.1089/aivt.2022.0010). Here, we report on the predictivity assessment, where the predictivity of the method is investigated by testing a blinded set of substance and developing a prediction.

Materials and methods: A set of 22 test substances consisting of known DIO *in vitro* inhibitors as well as inactive substances and substances otherwise interfering with the thyroid axis were tested in the standardized DIO1-SK assay. The released iodide was quantified via the Sandell-Kolthoff (SK) reaction. Experiments were performed on blinded substances that were later unblinded; results were statistically evaluated and compared to literature data. Finally, an *in vitro* prediction model was generated.

Results: Seven test substances produced a maximum DIO1 inhibition greater than 90% and eleven test substances below 20%; they were regarded as inhibitors and non-inhibiting substances, respectively. Two test substances, Ketoconazole and Silicristin, were found to be not applicable based on assay interferences. Inhibition data were consistent with results of relevant *in vitro* and computational models.

Conclusion: Using the variation of control data, an *in vitro* prediction model was defined categorizing test substances (i) by efficacy using the maximum inhibition data into three different categories. The test substances that produced a maximum DIO1 inhibition greater 90% where further categorized based on potency using the IC50 data of the test substance.

P128

Development of novel techniques advanced by bioinformatics methods for the characterization of biogenic toxins

D. Käser¹, F. Ramm¹, M. Stech¹, A. Zemella¹

¹Fraunhofer-Institut für Zelltherapie und Immunologie, Institutsteil Bioanalytik und Bioprozesse IZI-BB, Zellfreie und Zellbasierte Bioproduktion, Potsdam, Germany

Food and environmental toxins are important to characterize as we are exposed to them during our everyday life. In addition to known environmental hazards, toxin-producing species expand into new habitats and pharmaceuticals such as Aspirin, Acetaminophen or antihistamines accumulate in our environment. Therefore, it is important to analyze and characterize toxins and their effects as fast as possible. This study aims to develop a platform for the characterization of biogenic proteinaceous and non-proteinaceous toxins.

Experimental set ups will be extended by bioinformatic methods such as specified "Design of Experiments" and data evaluation scripts. Selected toxins and pharmaceuticals will be analyzed. Due to the difficult production of proteinaceous toxins using cell-based systems, proteinaceous toxins are synthesized using cell-free protein synthesis. Subsequently, toxins and pharmaceuticals are functionally characterized. These data will be used as a foundation to establish bioinformatic systems.

Therefore, three steps are established.

1) A database for toxins that have been synthesized and analyzed in cell-free systems is set up. A "Design of Experiments" approach will be applied in order to enhance the synthesis and functional characterization of novel environmental toxins as well as mutants from well-characterized toxins.

2) Various assays will be set up and enhanced by bioinformatic algorithms. One example will be the quantitative optical hemolysis assay enhanced by a Python analysis script. This

assay will rapidly analyze hemolytic toxins such as pore-forming bacterial proteins. This assay will allow to demonstrate the different hemolytic activities between different proteins as well as between wild type proteins and mutants.

3) A precise characterization of toxins and toxic compounds will be performed. Therefore, cell-based assays, in particular using liver cells, will allow establishing disease score parameters as well as identifying toxicological risk parameters.

This study will enhance analytical procedures for biogenic toxins. The methods developed here will reduce experimental set ups and provide a cost and time efficient alternative.

P129

AI tools and methods for screening, extracting and evaluating NAM data for chemical risk assessment

T. Blümmel¹, J. Rehn¹, C. Mereu¹, F. Graf¹, C. Kneuer², P. Wittkowski², A. Sonnenburg², F. Padberg², K. Bech², B. van der Lugt³, H. Bouwmeester³, N. Kramer³, T. Dobrikov¹

¹d-fine GmbH, Chemical Industry Services, Frankfurt am Main, Germany

²German Federal Institute for Risk Assessment, Pesticides Safety- Toxicology of Active Substances and their Metabolites, Berlin, Germany

³University, Toxicology, Wageningen, Netherlands

Introduction: EFSA's Science Studies and Project Identification & Development Office (SPIDO) and other strategic initiatives have identified Artificial Intelligence (AI) as key technology for implementation of New Approach Methodologies (NAMs) in chemical risk assessments.

Objectives: The project AI4NAMs was initiated to explore AI-supported applications in searching, extracting, and integrating NAM-based data into chemical risk assessment for selected chemicals or endpoints relevant to EFSA and finally for their integration in 'AOP-like knowledge networks' (AOP – Adverse Outcome Pathway).

Materials and methods: A structured evaluation framework was applied for review of candidate tools and software gathered in a long list through a survey. The application process was broken down in seven workflow steps with specific subtasks, from 'initial data collection' to 'data integration'. For each of the seven workflow steps, specific selection criteria, reflecting the respective requirements and challenges, and standardised evaluation options were developed. All tools and software were assessed against a set of general criteria, assigned to process workflow steps they could support and finally evaluated based on specific criteria for the assigned workflow step.

Results: The survey identified several promising tools. While only few support several workflow steps at once, most tools focus on rather specific tasks within a particular workflow step. Thus, combinations of multiple tools (henceforth referred to as toolchain), tailored to six specific case studies, most likely provide the best end-to-end support for the process. To facilitate the identification of suitable tool combinations for specific applications, the present work provides a framework for the assessment of tools on different aggregation levels, specifically criterion categories and workflow steps.

Conclusion: This survey serves as tool catalogue / picklist and provides an adjustable quantitative evaluation framework for tools and software to support systematic data review related to NAMs in chemical risk assessment. This framework allows to provide a quick overview of the tools' overall performance for the specified tasks and to derive shortlists of the most suitable tools.

P130

hiPSCs and hiPSCs-derived renal proximal tubular cells showed different response to nephrotoxic compounds

L.M. Mboni Johnston¹, N. Schupp¹

¹Institute of Toxicology, Heinrich Heine University of Düsseldorf, Düsseldorf, Germany

Introduction: Given that many drug candidates fail in clinical trials due to nephrotoxicity, better models are needed to identify potential toxicity early in the developing process. Human-induced pluripotent stem cells (hiPSCs) differentiating into proximal tubular epithelial cells (PTEC) could provide a 3R-conform alternative model to test and identify potential nephrotoxins.

Objectives: Therefore, the present study investigates the vulnerability of PTEC-like cells generated from hiPSCs towards well-known nephrotoxins.

Materials and methods: hiPSCs were differentiated into PTEC-like cells for 9 days by cultivating them in renal epithelial cell growth medium supplemented with bone BMP 2/7. The progression of the hiPSCs to PTEC-like cells was analyzed using qPCR and protein expression. Functional assays were also used to check functionality after differentiation. In addition, compound screening was performed for 24 h.

Results: Currently, we have shown that hiPSCs exhibited PTEC-like morphology after the applied differentiation protocol. Moreover, the cells showed increased expression of prototypical PTEC markers and transporters, while stem cell markers were downregulated. Furthermore, the PTEC-like cells were capable of megalin-dependent cubilin-mediated endocytosis of fluorescently labeled albumin, proving their functionality. hiPSCs and differentiating cells were more sensitive to the nephrotoxin cisplatin than the fully differentiated cells, which was not observed for another nephrotoxin, cyclosporin A.

Differentiating cells were more susceptible to oxidative stress than hiPSCs and PTEC-like cells. Consistent with these data, these cells expressed low levels of genes involved in the regulation of oxidative stress responses. In addition, hiPSCs showed increased expression of genes involved in DNA repair pathways, which decreases as the differentiation process progresses.

Conclusion: Already this small selection of compounds used shows the diverse reaction of cells in various differentiation states to substances with a different mode of action. While it is obvious that a DNA-damaging substance like cisplatin has the highest impact on fast-growing proliferating cells, the deleterious effect of oxidants on differentiating cells was unexpected. Overall, the hiPSC-derived *in vitro* kidney model is useful for investigating the nephrotoxic potential of several selected compounds and the effects of these toxins on the differentiation process.

P131

Stem cell-derived alveolar epithelial cells as promising lung cell source for preclinical drug testing and toxicity screening

M. Müller¹, Y. Kohl¹, A. Gemmann¹, S. Wagner¹, H. von Briesen¹, H. Zimmermann¹
¹Fraunhofer Institute for Biomedical Engineering, Bioprocesses and Bioanalytics, Sulzbach, Germany

Besides an exposure pathway for pathogens and toxicants, the lung is a potential entry route for pharmaceuticals. Lung diseases such as COPD or COVID-19 are widely spread in society and need to be further investigated. Therefore, the lung is an organ of interest in research and there is a great need for a reliable lung cell source for *in vitro* applications [1]. To date, human induced pluripotent stem cells (hiPSC) can be differentiated into several lung cell types. Protocols are difficult to establish and mostly contain 3D steps, such as organoid formation [2–3]. 3D approaches and organoids are usually complex and their properties strongly influence the outcome of the differentiation process. To date, they are not yet applicable to high throughput approaches, such as preclinical testing of promising drug candidates. In this presentation, a reproducible method for a 3D-hiPSC-differentiation of a distal lung cell type, alveolar epithelial cells type 2 (AEC2) will be presented. This bioreactor-based process, includes few working steps and enables to produce high amounts of cells under shear stress and homogenous nutrient supply. This is a promising method, which combines the advantages of 3D and high throughput, when it comes to the practical implementation of hiPSC-derived cell types in drug development and toxicity testing. Since it could be proved, that AEC2 generated in this study, express the SARS-CoV-2 receptors ACE2 and TMPRSS2, they could serve as an ideal model to investigate pathomechanisms and identify effective drug candidates. Experiments with pseudotyped SARS-CoV-2 were performed to proof the suitability of this model for the intended application.

1. Moreira, A.; Müller, M.; Costa, P.F.; Kohl, Y. Advanced *In Vitro* Lung Models for Drug and Toxicity Screening: The Promising Role of Induced Pluripotent Stem Cells. *Adv. Biol.* **2021**, doi:10.1002/adbi.202101139.
2. Yamamoto, Y.; Korogi, Y.; Hirai, T.; Gotoh, S. A method of generating alveolar organoids using human pluripotent stem cells. *Methods Cell Biol.* **2020**, *159*, 115–141, doi:10.1016/BS.MCB.2020.02.004.
3. Jacob, A.; Vedaie, M.; Roberts, D.A.; Thomas, D.C.; Villacorta-Martin, C.; Alysandratos, K.D.; Hawkins, F.; Kotton, D.N. Derivation of self-renewing lung alveolar epithelial type II cells from human pluripotent stem cells. *Nat. Protoc.* **2019**, *14*, 3303–3332, doi:10.1038/s41596-019-0220-0

P132

Suffocation through strong agglomeration of particles in the nose of test animals – new approaches for acute high dose inhalation studies that only consider animal survival

G. Brue¹, N. Krueger², K. Weber³, N. Warfving³, A. Vitali³, J. Nolde⁴, T. Schuster², O. Creutzenberg¹, P. Janssen¹, B. Wessely², M. Stintz⁵

¹Fraunhofer Institute for Toxicology and Experimental Medicine (ITEM), Department of Inhalation Toxicology, Hannover, Germany

²Evonik Operations GmbH, Hanau-Wolfgang, Germany

³AnaPath Services GmbH, Oberbuchsitzen, Germany

⁴Grace Europe Holding GmbH, Worms, Germany

⁵Technische Universität Dresden, Dresden, Germany

In case of lethality, the OECD technical guideline 436 only requires the count of dead animals and a rough macroscopic examination of the outer surfaces of the organs in the abdominal and thoracic cavity. High concentrations of low-density particles, such as hydrophobic SAS, can cause in an acute inhalation test lethality at concentrations in the range of 100–1000 mg/m³. Seven of this kind of particle types were chosen at concentrations in the range of 500 mg/m³ for acute inhalation studies with an expanded endpoint pattern. For the acute nose-only inhalation studies three male and female rats were exposed for 4 hours according to OECD TG 436. By adding additional parameters the expanded experimental design was used to assure the scientific validity of older results. Moreover a thorough histopathological examination of the respiratory tract, especially the upper respiratory tract (nasal cavities) was done. For one of seven substances animals died spontaneously or were sacrificed due to moribund conditions during or shortly after cessation of exposure ahead of schedule. Prior to death, the animals showed signs of anemia and a decreased respiratory rate. The histopathology screening confirmed the cause of morbidity/death in all animals by asphyxia and mechanical blockage of the upper respiratory tract. Partial blockages were also shown for other of the 7 substances. This impaired respiration up to total airway obstruction, which can be misdiagnosed as a toxic effect, suggests that acute high dose inhalation studies are not suitable for certain substances.

P133

Suitability of precision cut kidney slices for the detection of nephrotoxic effects

F. Roofs¹, C. Spruck¹, N. Schupp¹

¹Heinrich-Heine-University, Institute of Toxicology, Medical Faculty, Düsseldorf, Germany

Background and objectives: The *ex vivo* cultivation of precision cut tissue slices is hypothesized as a promising option for the investigation of organ toxicity under the 3R principle, since they may represent a link between the classical *in vitro* and *in vivo* systems. They reflect the complex organ anatomy and the interplay of different cell types. This allows kinetic analyses while lowering the animal numbers. Here we show the *ex vivo* cultivation of precision cut kidney slices (PCKS) which we evaluated for their suitability to detect acute nephrotoxic effects.

Materials and methods: The state of mouse PCKS was evaluated using different viability assays and by histopathology. Treatment with different concentrations of known nephrotoxins and non-nephrotoxins was conducted for 4 h and 24 h and afterwards the viability of the slices was assessed.

Results: The viability of untreated kidney slices was ~70 % after 24 h and ~50 % after 72 h incubation. First changes of the morphology of the tissue became already apparent after 4 h. Treatment of kidney slices with the known nephrotoxins cisplatin and cyclosporin for 4 h already showed a tendency of a dose dependent decrease in viability. After 24 h incubation a clear reduction of viability was observed as compared to the untreated control. The treatment with non-nephrotoxic acarbose showed no cytotoxic effects.

Discussion and Conclusion: In conclusion, PCKS seem to be suitable for a specific detection of acute nephrotoxic effects. Additional substances and toxicity-related read-outs have to be used to further assess the potential of this 3R-conform model.

P134

Precision cut liver slices for 3R-conform assessment of hepatotoxicity

A. Erbay¹, G. Fritz¹, N. Schupp¹

¹University of Düsseldorf, Institute of Toxicology, Medical Faculty, Düsseldorf, Germany

Background and objectives: For the investigation of organ toxicity under 3R principles cell culture, co-cultures or even organoids are not sufficient to seize the high complexity of whole organs. *Ex vivo* cultivation of precision cut tissue slices could act as a link between the classical *in vitro* and *in vivo* systems, reflecting the complex organ anatomy and the interplay of different cell types and allowing kinetic analyses while lowering the animal numbers. Our aim was to establish an *ex vivo* model of mouse precision cut liver slices (PCLS) for use in substance-oriented biomedical research.

Materials and methods: For this goal, among other parameters, different slice thicknesses, medium and buffer gassed with carbogen, various medium supplements and culture duration of the PCLS were systematically modified to optimize the incubation conditions. Viability assays and histological evaluations were performed to compare the effects of the different conditions. Under optimized conditions the slices were treated with toxic and control substances.

Results: The viability of the liver slices was over 70 % after 24 h and over 50 % after 48 h incubation. Treatment with the known hepatotoxin acetaminophen for 4 h and 24 h resulted in a dose-dependent loss of viability. The same was observed after 24 h treatment with cisplatin. Isoniazid, known to trigger drug-induced liver injury, was not toxic on the liver slices. This can be explained by the lack of immune response in the liver slices which is crucial for the hepatotoxic mechanism of isoniazid. The substance intended as negative control, melatonin, caused a loss of viability only in the highest concentration after the 24 h treatment period.

Discussion and conclusion: In conclusion, PCLS accurately showed toxicity of directly hepatotoxic substances while none was observed with an indirect hepatotoxin. Therefore, our preliminary studies underline the usefulness of PCLS for hepatotoxicity studies.

P136

Opportunities and challenges of an imaging-based cell-cycle assay (CCA) for screening approach of chemicals

C. Oberfrank¹, N. Roth¹, B. Birk¹, B. Ellinger², D. Funk-Weyer¹, R. Landsiedel¹

¹BASF SE, Experimental Toxicology and Ecology, Ludwigshafen, Germany

²Fraunhofer Institute, Fraunhofer-Institut für Translationale Medizin und Pharmakologie ITMP, Hamburg, Germany

Introduction: The European Chemical Strategy for Sustainability strives for products that are "safe and sustainable by design". For this, screening methods are needed which give early indication of toxic effects to guide product development is crucial to achieve this. Naturally, these screening methods should be efficient and should not use animals. Such a New Approach Method (NAM) is the "cell cycle assay" (CCA). Disturbance of the cell cycle (CC) is associated with impaired cell proliferation, carcinogenesis, and developmental toxicity. The CCA is used in BASF screening strategies for many years. The standard approach measures the proliferation of a suspension cell line (Mouse Lymphoma Cells, L5178Y/TK) by flow cytometry. Significant shifts ($\geq 10\%$ or $\geq 20\%$, respectively) of cell populations in G0/G1-phase and S-phase, and/or G2/M-phase are assessed as "positive" effects on the CC.

Objectives: Here, we present an alternative CCA using live cell imaging technology (IncuCyte S3, Sartorius, Germany) allowing to use a wider range of cell types (adherent/suspension cells).

Materials and methods: A549 cells were transduced (Sartorius Kit: Cat. 4779) with a fluorochrome to allow separation of the different CC phases (red: G1; green: S/G2/M; yellow: G1/S, colorless: M/G1). The aim of the study was to compare the data of 14 chemicals with the BASF standard flow cytometry approach and to learn more about the strength and weaknesses of the method.

Results: A549 cells showed sufficient labelling after transduction and robust doubling time (17.8 ± 1.3 hours). The advantage of the imaging-based method is the observation of the cell cycle activity over time to identify also potential transient effects. However, overlapping fluorescence is limiting the precise assessment of "negative" and "positive" substances. Moreover, the S3 IncuCyte does not allow fluorescence based cytotoxicity testing simultaneously. An additional cytotoxicity test must be included to distinguish between specific and unspecific effects.

Conclusions: Compared to the traditional flow-cytometric CCA, the live cell imaging-based CCA offers information on potential transient effects but does not provide sufficient precise results. The imaging-based CCA can be used as add-on to the flow-cytometric methods to obtain mechanical, dose and time-related information.

P137

Comparison of grouping of phenoxy herbicides with metabolomics *in vitro* and *in vivo*

F. Zickgraf¹, V. Giri¹, V. Haake², B. Birk¹, S. Sperber¹, H. A. Huener¹, A. Verlohner¹, P. Driemert², T. Walk², H. Kamp², D. Funk-Weyer¹

¹BASF SE, Ludwigshafen am Rhein, Germany

²BASF Metabolome Solutions, Berlin, Germany

Metabolomics can address grouping/read-across from a biological perspective. Recently, it has been shown that grouping/read-across based on metabolomics *in vivo* data could waive animal studies (van Ravenzwaay, 2016). Further, *in vitro* metabolomics allows grouping and identification of mode of actions of different liver and nephrotoxicants in HepG2 cells (Ramirez, 2018).

Analyzing the metabolic profiles of the phenoxy herbicides MCPA, MCPP and 2,4 DP from 28-day rat *in vivo* and 48 h HepG2 *in vitro* studies, we show that with metabolomics *in vitro* we can obtain a similar grouping as with metabolomics *in vivo* - although 2 different test systems are applied.

In addition, principal component analyses show that phenoxy herbicides cluster with peroxisome proliferators but separate from liver enzyme inducers both *in vivo* and *in vitro*.

Metabolomics *in vitro* might be a promising tool for grouping/read-across of substances based on a biological perspective. However, future analyses are necessary to investigate whether metabolomics *in vitro* in HepG2 cells can also be used for different toxicants with various target organs.

B. van Ravenzwaay, S. Sperber, O. Lemke, E. Fabian, F. Faulhammer, H. Kamp, W. Meilert, V. Strauss, A. Strigun, E. Peter, M. Spitzer, T. Walk (2016) Metabolomics as read-across tool: A case study with phenoxy herbicides. *Regulatory Toxicology and Pharmacology* 81, 288-304

T. Ramirez, A. Strigun, A. Verlohner, H-A. Huener, E. Peter, M. Herold, N. Bordag, W. Meilert, T. Walk, M. Spitzer, X. Jiang, S. Sperber, T. Hofmann, T. Hartung, H. Kamp, B. van Ravenzwaay (2018) Prediction of liver toxicity and mode of action using metabolomics *in vitro* in HepG2 cells. *Archives of Toxicology* 92:893-906.

P138

A novel primary cell airway model from the porcine trachea for the development and screening of inhalative drugs and their formulations

R. Rittersberger¹, J. N. Martin¹, A. Dabbars¹, G. Koslowski¹, K. Schindowski¹

¹University of Applied Sciences Biberach, Institute of Applied Biotechnology, Biberach an der Riß, Germany

Introduction: Inhalative drug delivery has gained attention by the Covid19 pandemic. Translatable preclinical *in vitro* models are essential to develop drugs for the respiratory tract. Most current cell lines are derived from cancer cells and are limited to reflect the physiological conditions in the airways. Here, we describe the development and characterization of an *in vitro* primary epithelial cell model from porcine trachea. The use of such model to screen toxicity of aerosolized proteins and of excipients for protein formulations is demonstrated.

Objectives:

- Establish suitable extraction and seeding method of trachea epithelial cells (TECs)
- Characterization of the TEC primary model
- Use of TECs for toxicity studies and excipient screen

Materials and methods: Isolation and cultivation procedures were established for TEC based on earlier research. RPMI2650 cells were used for comparison. TEC were cultivated at air-liquid interface (ALI) in transwells and characterized by their trans-epithelial electrical resistance (TEER) and for protein expression by RT-PCR and immunofluorescence (IF). Toxicity was determined by Alamar Blue conversion.

Results: A direct seed method for the TECs was established and the cells displayed high TEER values as an indication for a tight cellular layer. IF staining revealed Mucin producing and ciliated cells. TECs are suitable for toxicity screening of aerosolized proteins as they are robust but with a sufficient sensitivity against toxic substances. Cytotoxic concentrations for the stabilizers HP- β -Cyclodextrin, Tween 20/ 80 and Poloxamer 188 were determined and will be discussed.

Conclusion: The characterization of the TEC primary model demonstrated the shortcomings of the permanent airway cell model RPMI 2650. TECs have a 10 – 40x higher TEER value, grow in organized monolayers instead of cancer-like multilayers and differentiate in ALI to a typical airway epithelial cell. The toxicity testing of various proteins showed no toxic effect, even at high concentrations. A further development of the model is needed to include immune cells to test for immunotoxicity, especially of the aggregated products.

P139

Ferroptosis after sulfur mustard exposure

T. Demel¹, D. Steinritz¹, F. Worek¹, S. Rothmiller¹

¹Institut für Pharmakologie und Toxikologie der Bundeswehr, München, Germany

Introduction: Even though the blistering agent sulfur mustard (SM) is known for over 200 years, the exact mechanism of cellular damage is unknown. Thus, a specific therapy is missing. Since SM induces the production of reactive oxygen species and overloads anti-oxidative systems, oxidative stress is discussed as main driver of toxicity. Initiated by failed antioxidant defense, the non-apoptotic and iron-dependent regulated cell death ferroptosis could be a new, until now not identified pathway in the molecular toxicology of SM. Targeting ferroptosis could represent a novel therapeutic option after SM exposition.

Question: Investigation of ferroptosis after SM exposure as novel pathomechanism.

Materials and methods: HaCaT or A549 cells were exposed to SM or ferroptosis inducers Erastin and RSL-3. Intensity changes of lipid droplets, glutathione peroxidase-4 (GPX4), system Xc- (xCT) and apoptosis inducing factor mitochondria associated 2 (AIFM2) were determined using flow cytometry. Effects of pretreatment and treatment with deferoxamine (DFO), ciclopirox (CPX), α -tocopherol (α -TOC) and ferrostatin-1 (FER-1) on cell viability were measured with Alamar Blue assay. Oxidized and reduced glutathione were measured with a luminescence-based assay.

Results: GPX4 signal decreased after Erastin and RSL-3 but not SM exposure. Levels of xCT and AIFM2 were increased in both RSL-3 and SM exposed cells. Lipid droplet staining showed higher intensity after RSL-3 and SM exposure but was lowered after Erastin. Treatment of SM exposed cells with DFO and α -TOC reduced this effect. Total glutathione was reduced for RSL-3 and SM in a dose-dependent manner, while both Erastin concentrations tested had no influence on RSL-3. Cell viability at 300 μ M SM exposure improved with 6.26 μ M DFO and 10.23 μ M α -TOC treatment. However, this effect was not significant for treatment and pretreatment in SM dose-response curves.

Conclusion: RSL-3, a GPX4-inhibitor, and SM seem to have overlapping effects on A549 and HaCaT cells. Erastin interfering with xCT might induce ferroptosis differently. Treatment with the literature-known ferroptosis inhibitors DFO, CPX, α -TOC and FER-1 did not show significant effects on cell viability after SM exposure. More research in the context of SM and ferroptosis is needed to understand the underlying mechanisms.

P140

Development of RNA-based risk assessments for cardiotoxicity in rat cardiomyoblasts and living myocardial slices

A. L. K. Heim¹, M. Otto^{1,2}, L. Elenschneider¹, M. Fuchs^{1,2}, M. Bentele^{1,3}, N. Abbas^{1,3}, J.

Weusthoff^{1,3}, A. Just³, A. Stucki-Koch¹, S. Escher¹, T. Thum^{1,3,2,4}, J. Fiedler^{1,3,2}

¹Fraunhofer Institut für Toxikologie und Experimentelle Medizin ITEM, Kardiologische

Forschung, Hannover, Germany

²Fraunhofer Cluster of Excellence Immune-Mediated Diseases (CIMD), Hannover, Germany

³Hannover Medical School, Institute of Molecular and Translational Therapeutic Strategies (IMTTS), Hannover, Germany

⁴Hannover Medical School, REBIRTH Center for Translational Regenerative Medicine, Hannover, Germany

Introduction: *In-silico*-based adverse outcome pathways (AOPs) have been proposed as a valuable tool in toxicology to screen for molecular interactions with biological targets, known as molecular initiating events (MIEs). AOPs include measurable key events (KEs) linking MIEs with adverse outcomes (AOs), building a KE network enabling to predict the likelihood of AOs. Alternatives to *in-vivo* studies are highly requested for human safety assessments during drug development.

Objectives: We aimed to increase the precision of predicting AOs and minimize the risk of AO onset during heart failure drug development. Therefore our goal was to integrate a dose-dependent RNA-based mechanistic risk assessment evaluating transcriptome changes *in-vitro* to obtain pathways and benchmark concentrations potentially affecting cardiac fibrosis.

Materials and methods: *In-silico*, AOP network database was used to redefine early events leading to cardiac fibrosis. Rat cardiomyoblasts (H9C2) and living myocardial slices (LMS) were treated with TAA, MSDH and CQD or in combination with TGF β for 24h. Viability and cytotoxicity were determined using LDH and WST1 assay. NF κ B-dependent reporter assay detected inflammatory response. H9C2 cells were used for whole transcriptome TempO-Seq analysis. Parallel to *in-vitro* and *ex-vivo* assays, clinical data of human heart failure (hHF) patients was screened underlining key characteristics of myocardial failure *in-vivo*.

Results: We identified LD20 concentrations for selected compounds in H9C2 cells. TAA and MSDH reduced NF κ B signaling in a pro-inflammatory setup implying a possible anti-fibrotic therapy in early inflammatory stages whereas CQD increased NF κ B signaling indicating an endogenous activation of inflammatory response. Whole transcriptome analysis identified deregulated target genes that were compared to hHF gene networks underlining the value of our selected model system. Translation of experimental approaches to an *ex-vivo* system of LMS revealed first functional data supporting the prediction of cardiotoxicity.

Conclusion: We here emphasize that the multimodal combination of RNA-based risk assessment is an upcoming technology to detect small molecule-induced changes and contribute to toxicological profiling. Our results also demonstrate the resilience of AOPs using cardiac fibrosis as an exemplary setup. Collectively, we suggest that AOPs might ameliorate drug-safety during drug development in the context of e.g. heart, lung and liver biology.

P141

Different geometry of diffusion cells and its impact on cutaneous penetration of Caffeine *in vitro*

N. Schmieder¹, C. Rieken¹, E. Fabian¹, D. Funk-Weyer¹, R. Landsiedel¹
¹BASF, Experimental Toxicology and Ecology, Ludwigshafen, Germany

Introduction: For risk assessment of substances, it is of great interest to examine their dermal uptake. The Dermal absorption studies *in vitro* according to OECD test guideline no. 428, enable measurement of the penetration of a substance in and through the skin.

Objectives: Different experimental settings are used in dermal penetration studies. It is, however, not well understood, how variations of these settings influence the overall result. We investigated potential differences in the penetration of Caffeine as a function of the geometry of the diffusion cells.

Materials and methods: Diffusion cells with a diameter of 11.28 mm, 9 mm and 5 mm were used with an application area of 1 cm², 0.65 cm² and 0.20 cm², respectively. Experimental parameters, such as the flow rate and the application volume were adapted to the respective cell geometry. The exposure time for all experiments was 8 hours with a total experimental duration of 24 hours. The flow rate was 2.3 mL/h for the diffusion cells with an application area of 1 cm², and 1.5 and 0.46 mL/h for the diffusion cells with an area of 0.65 cm² and 0.20 cm², respectively. Caffeine was radioactively labeled and was applied in ethanol/tap water 1/1 (v/v). The target concentration was 50 mg/mL and the radioactive target dose was 50 kBq/cm².

Results: The measured penetration of Caffeine depended on the geometry of the diffusion cells: The absorbed dose was 9.28%, 7.68% and 5.95% of applied dose for cells with application areas of 1 cm², 0.65 cm² and 0.20 cm², respectively. The determined permeability constants (Kp) were 19.13 x 10⁻⁵, 16.22 x 10⁻⁵ and 12.02 x 10⁻⁵ cm/h for the different application areas, respectively.

Conclusion: The penetration of Caffeine depended on the dosed skin surface areas in Franz-like diffusion cells, although the methods were adapted to the cell geometry in respect of application volume and receptor flow. Therewith, the results of the current study demonstrate that dermal absorption *in vitro* is modified also by the defined experimental setup.

P142

Influence of drug candidates on sulfur mustard induced senescence in human mesenchymal stem cells

A. Neu¹, T. Bertsche², F. Worek¹, A. Schmidt³, S. Rothmiller¹
¹Bundeswehr Institute of Pharmacology and Toxicology, Munich, Germany
²Leipzig University, Institute of Pharmacy, Leipzig, Germany
³University of the Federal Armed Forces, Institute of Sports Science, Neuburg, Germany

Introduction: The bifunctional alkylating agent sulfur mustard (SM) is a chemical warfare agent that is primarily harmful to the skin. Chronic wound healing disorders often result from SM exposure. A possible contributor could be the recently described SM induced senescence in human mesenchymal stem cells (hMSC). Senescence impairs their regenerative function in wound healing, as they persist in the damaged tissue for long periods and maintain a proinflammatory microenvironment.

Objectives: In this initial study, we investigated whether SM induced senescence in hMSC can be reduced by the addition of drug candidates, such as the PARP inhibitor Olaparib, the vitamin niacin or the growth factor FGF-2.

Materials and methods: The hMSC were isolated from the bone marrow of femoral heads. For quality assurance, analysis of surface antigens was performed by flow cytometry, as well as differentiation potential and morphology. The cells were treated with the drug candidates 23 hours before (\pm prophylaxis) and 24 hours after (\pm therapy) SM exposure (40 μ M). The proportion of senescent cells was detected by senescence-associated β -galactosidase staining. Cell culture supernatants were analysed for secreted cytokines and chemokines. Further investigations were performed by NAD and ATP quantification assays and expression profiling by qPCR.

Results: Niacin and FGF-2 were able to reduce SM induced senescence when administered prophylactically. An increased downregulation of FGF-5 by FGF-2 pretreatment as well as an increased expression of TIMP1 by FGF-2 pre- and posttreatment was observed. The prophylactic administration of niacin in SM treated cells showed a reduced secretion of IL-6. In addition, niacin pretreatment was shown to increase intracellular NAD⁺ and ATP levels. Olaparib induced senescence under both therapy and prophylaxis conditions and was therefore not further investigated.

Conclusion: In summary, a reduction in senescence was shown after prophylactic administration of niacin and FGF-2. Further investigation should clarify molecular mechanism of action of the two drug candidates in the context of SM induced senescence in hMSC. FGF-2 and niacin individually or in combination could be used in the future as an innovative prophylaxis for SM exposure.

P143

Melanin Nanoparticles as Novel Approach in Malignant Melanoma Treatment – An *In Vitro* Assessment

I. Marcovici^{1,2}, I. Pinzaru^{1,2}, D. Coricovac^{1,2}, I. Macasoși^{1,2}, C. Dehelean^{1,2}

¹Faculty of Pharmacy, "Victor Babes" University of Medicine and Pharmacy, Timisoara, Romania

²Research Center for Pharmaco-Toxicological Evaluations, Faculty of Pharmacy, "Victor Babes" University of Medicine and Pharmacy, Timisoara, Romania

Introduction: Malignant melanoma (MM) remains one of the most aggressive cancer types with a narrow therapeutic arsenal in advanced disease stages. Melanin (MEL) is a polymeric pigment widely spread among many living organisms and the first-line defense mechanism of the skin against MM development. The interest in melanin research has gained considerable momentum lately, especially as nanosized carrier for various therapeutics in cancer treatment. However, the use of MEL in the form of nanoparticles for MM therapy lacks an extensive investigation so far.

Objectives: Based on the above considerations, the current research aimed at exploring the efficiency of MEL nanoparticles (MEL-NPs) in the treatment of MM via *in vitro* evaluations.

Materials and methods: This study was conducted on two human MM cell lines: RPMI-7951 and A375. MEL-NPs were synthesized through the polymerization of dopamine hydrochloride in NaOH media and dispersed in ultrapure water for further experiments. The impact on cell viability was determined by applying the CellTiter-Glo Luminescent Assay. Cell morphology and the intracellular distribution of MEL-NPs were illustrated using bright-field microscopy. The impact of MEL-NPs on RPMI-7951 and A375 cells' nuclei and cytoskeleton was evaluated using immunofluorescence staining. Relative fold expression of pro-apoptotic markers (Bax, Bid, Bad, Bak) was determined using the real-time polymerase chain reaction (PCR) method.

Results: The 24 h treatment of RPMI-7951 and A375 cells with MEL-NPs (10, 25, 50, 75, and 100 μ g/mL) significantly lowered their viability in a dose-dependent manner. Bright-field microscopy highlighted a successful cytoplasmic internalization of MEL-NPs in both MM cells leading to cell pigmentation. MEL-NPs generated morphological changes in RPMI-7951 and A375 cells such as cell rounding accompanied by a significant loss of cell confluence, as well as nuclear apoptotic-like features such as dysmorphology, fragmentation, and chromatin condensation. MEL-NPs induced apoptosis-specific rearrangements in the cytoskeletal tubulin and actin filaments and elevated the expression of the pro-apoptotic markers in RPMI-7951 and A375 cells.

Conclusion: These results revealed that MEL-NPs exerted a potent anti-melanoma activity *in vitro* against RPMI-7951 and A375 cells by inducing apoptosis.

P144**Investigating the effect of Novaluron on HepaRG cells**

S. Das¹, P. Marx-Störling¹, M. L.M. Solano¹, K. Jochum¹, A. Schmitt¹, C. Kneuer¹
¹Bundesinstitut für Risikobewertung (BfR), Pesticides Safety, BERLIN, Germany

Introduction: Novaluron is an insect growth regulator, which works by inhibiting chitin synthesis. It acts by ingestion and contact, and causes abnormal endocuticular deposition and abortive moulting. In today's world, obesity is a rising concern. *In vivo* studies with high doses of Novaluron have revealed a significant body weight increase in all species (rats, mice and dogs), all sexes, at different time points of development as well as slight changes in triglycerides, cholesterol and glucose level. In a 90-day study in rats (Ammannati 1993), body weight effects and increase in triglycerides were noted from 50 ppm (approx. 3.5 mg/kg bw/d). The human liver is the main organ for fatty acid metabolism and maintaining energy homeostasis. Hence, the investigation of hepatic mechanisms potentially involved in the observed effect was selected as a starting point. Several molecular initiating events (MIE) on the level of receptor activation, and key events (KE) on the gene expression level may lead to intracellular triglyceride accumulation that can be measured *in vitro* and finally lead to hepatic steatosis. It is well known that obesity is associated with hepatic steatosis.

Objectives: The present study aimed to investigate whether the increase in body weight as an adverse outcome observed *in vivo* with high doses of Novaluron may be initiated by hepatic triglyceride accumulation.

Materials and Methods: Differentiated HepaRG cells were used as a model of the human liver and incubated with 20, 40, 60, 80, 100, 120, 140, 160 mg/l of Novaluron for 72 hours. Cell viability was assessed by WST-1 and neutral red uptake assays. AdipoRed assay was conducted for quantifying intracellular triglycerides.

Results: Cytotoxicity was not observed in the assays in the tested concentration range. With the increasing concentration of Novaluron from 20 mg/L to 160 mg/L, there is a significant increase in triglyceride accumulation with respect to the negative control. The effect of Novaluron on target genes responsible for fatty acid metabolism using qRT-PCR and PCR array is currently ongoing with selected concentrations of 20, 100, and 160 mg/l.

Conclusion: Novaluron induces triglyceride accumulation *in vitro*. The molecular analysis will help us to understand the mechanism involved in the increase in body weight and biochemical changes observed *in vivo*.

Keywords: Molecular Initiating event, key events, adverse outcome, Novaluron, body weight, triglyceride.

P145**Characteristics of dusts from recycling of carbon fiber reinforced thermoplastics (CFRP) and their toxic potential**

G. Westphal¹, L. Tölle², C. Monsé¹, N. Rosenkranz¹, D. Walter³, N. Haibel³, M. Hopp², J. Bünger¹

¹Ruhr-Universität Bochum, Institut für Prävention und Arbeitsmedizin der DGUV Institut der Ruhr-Universität Bochum (IPA), Bochum, Germany

²Universität Paderborn, Kunststofftechnik Paderborn, Paderborn, Germany

³Justus-Liebig-Universität Gießen, Institut für Arbeits- und Sozialmedizin, Gießen, Germany

Introduction: CFRP are increasingly used for lightweight construction due to excellent specific strength and rigidity. The recycling of these materials may produce fiber-containing dust and thus health hazards to workers.

Objectives: The aim of this project was to achieve basic knowledge about the characteristics of generated dusts by comminution of CFRP as well as their toxic and inflammatory potential.

Methods: Preliminary laboratory-scale tests were done in a cutting mill, using different feedstock sizes and rotational speeds. The ground material was sieved and size distribution analyzed using a scanner. Based on these data, investigations under conditions of real use were done with a single screw shredder. All materials were provided by Bond Laminates GmbH (Lanxess, Germany). Inhalable dust was measured using a Scanning Mobility Particle Sizer, an Aerodynamic Particle Sizer, and by REM analysis according to the VDI Guideline 3492. Particle induced chemotaxis was investigated to assess the inflammatory potential of the generated dusts: NR8383 rat macrophages were challenged with the CFRP-particles and the cell supernatants were applied in a Boyden chamber assay with differentiated HL-60 cells. Cytotoxicity was analyzed using the alamarBlue Assay.

Results: The preliminary investigations and the tests under real conditions led to comparable results. High total fiber concentrations occurred under all conditions, increasing speed led to an increase in fiber mass and concentration. The proportion of relatively short, non-respirable fibers initially increased with accelerating speed, but a further increase did not lead to a further shortening (short fibers are disadvantageous for further use). Respirable fibers occurred under all conditions, but in contrast to the total fiber dust, their proportion remained similar under all test conditions. Accordingly, cytotoxicity and induction of cell migration were unaffected by the study conditions. The CFRP dusts showed low cytotoxicity and very small induction of cell migration, compared to the silica positive control and historical data on granular and fibrous particles.

Conclusions: The number of respirable fibers of the generated CFRP dusts was small and the observed biological effects were weak. However, the optimization of the

processes should focus on the reduction of fibers with hazardous dimensions. Special safety precautions should be taken, since a pronounced bio-persistence of CFRP dust must be assumed.

P146**Assessing the direct effect of antibiotics on mitochondrial respiration**

J. Sailer¹, S. Schmitt², H. Zischka^{1,3}, E. Gnaiger²

¹Technical University Munich, Institute of Toxicology and Environmental Hygiene, München, Germany

²Oroboros Instruments, Innsbruck, Austria

³Helmholtz Center Munich, Institute of Molecular Pharmacology and Toxicology, München, Germany

Introduction: Antibiotics may cause severe adverse effects, e.g. damaging the gut microbiome or causing nephron- and hepatotoxicity, and are the most common cause of drug-induced liver injury [1]. Due to bacterial origin, mitochondria might be primary targets of antibiotics related to these severe outcomes. While several studies have reported midterm effects of antibiotics on mitochondrial respiration and protein synthesis, hardly any study examined the direct effects of antibiotics on mitochondrial function in detail [2,3].

Material and methods: Respiration of intact/permeabilized HEK293 cells was measured with Oroboros Oxygraph-2k oxygen electrode following a SUIT protocol from Oroboros SUIT-008-D025 in DatLab 7.4. Mitochondrial membrane potential was measured in the same device, using fluorescence sensors simultaneously. Antibiotics were titrated in LEAK; OXPHOS N, OXPHOS NS or ET, with the following concentrations: Gentamicin 0.1 mg/ml up to 4 mg/ml; Ciprofloxacin and Amoxicillin 10 µg/ml up to 2 mg/ml. Of note, especially the applied lower doses of Gentamicin are clinically relevant doses, while the higher ones may reflect its kidney accumulation.

Results: Gentamicin and Ciprofloxacin, but not Amoxicillin, have a direct toxic effect on mitochondria in HEK293 cells by increasing LEAK respiration and by inhibiting the ET system. While oxidative phosphorylation inhibition is substrate dependent for Gentamicin, this is not seen for Ciprofloxacin. In addition, both antibiotics reduce the maximal capacity in the ET state. Solely Gentamicin inhibits complex IV activity in a time-dependent manner. The increase in LEAK caused by Gentamicin is found to be accompanied by a mitochondrial membrane potential loss.

Conclusion: This study shows direct toxic effects of Gentamicin and Ciprofloxacin on mitochondria. Given the frequent use of antibiotics in the treatment of bacterial infections, awareness of their toxicity should be raised. The mitochondrio-toxic effects may significantly contribute thereto, which should be considered in pre-clinical and clinical testing.

[1] Tarantino G. et al. (2017): *Hepato Res.* 37:410-415

[2] O'Reilly M. et al. (2019): *Front Cell Neurosci.* 13:13:416. doi: 10.3389/fncel.2019.00416.

[3] Oyebo OT. et al. (2018) *Toxicology Mechanisms and Methods*, 1–31. doi:10.1080/15376516.2018.1528651

P147**An LC-MS method to study displacement of thyroid hormones from serum proteins by test substances.**

L. Jedermann¹, A. G. Weber^{1,2}, L. H. Köppl¹, M. Weissenfeld¹, B. Birk³, E. Fabian¹, B. Wareing¹, S. Melching-Kolmuss³, D. Funk-Weyer¹, R. Landsiedel^{1,2}

¹BASF SE, Experimental Toxicology and Ecology, Ludwigshafen am Rhein, Germany

²FU Berlin, Pharmacology and Toxicology, Berlin, Germany

³BASF SE, Agricultural Solutions, Limburgerhof, Germany

Introduction: Thyroid hormones (TH) affect and regulate a variety of functions in the body, for instance the basal metabolic rate, and neuronal development. In the human bloodstream >99 % of THs are bound to proteins, such as thyroxine binding globulin (TBG), transthyretin (TTR) and albumin (ALB). The displacement of thyroxine (3,5,3',5'-tetraiodothyronine, T4) from its protein binding site by substances is one mode of action (MoA) disturbing the TH homeostasis.

Objectives: Develop a method to assess the displacement of T4 from the thyroid hormone binding proteins, TTR.

Materials and methods: As an initial step the protein, T4 and test substance are incubated for one hour at room temperature. Then, protein loaded with T4 and test substance was separated from unbound T4 and unbound test substance by size exclusion chromatography. The protein-bound T4 and test substance are then dissociated from the protein via ethanol extraction. The concentration of T4 (and test substance) in the extract is then quantified by LC-MS analysis. Protein-bound T4 was plotted as function of T4 and test substance-concentrations to derive IC50 of the test substance.

Results: For the known T4-inhibitors Tetrabromobisphenol A and Pentachlorophenol, IC50-values of 366 nM and 82 nM were determined. 4-Hydroxy-3,5-dichlorobiphenyl is less known to have T4-displacement properties, but was found to be a potent inhibitor with an IC50 of 172 nM.

Conclusion: The presented *in vitro* assay could reproducibly determine the displacement of T4 from TTR by test substances. The assay can be used to identify substances potentially disturbing the thyroid homeostasis by this MoA. As future perspective, testing of additional TH binding proteins, ALB and TBG, different combinations of the proteins as well as serum from rats and humans will be addressed.

P148

Cyp activities in a monolayer culture of primary mouse hepatocytes cultivated for five days

M. Scherer¹, E. Fabian¹, S. Betzer^{2,3}, B. Wareing¹, J. Leidner^{1,2}, D. Funk-Weyer¹, R. LANDSIEDEL^{1,2}

¹BASF SE, Experimental Toxicology and Ecology, Ludwigshafen am Rhein, Germany

²FU Berlin, Pharmacology and Toxicology, Berlin, Germany

³BASF SE, Agricultural Solutions, Limburgerhof, Germany

Introduction: Hepatocytes play a major role in the metabolism of xenobiotics due to the expression of Cytochrome P450 (Cyp) and other xenobiotic metabolizing enzymes (XMEs). Cyps are a superfamily of monooxygenases, which are inducible by xenobiotic substances. Induction of Cyps can profoundly change the clearance and metabolic activation of the respective substances (<https://doi.org/10.1007/s00204-020-02777-4>). Additionally, altered gene expressions which lead to Cyp-induction can also induce cell proliferation and hamper apoptosis pathways. To study these effects, prolonged cultivation of hepatocytes is required. Here, we established and characterized a primary mouse hepatocyte culture for five days and characterized the Cyp activities.

Objectives: The aim of this study was to establish a monolayer culture of primary mouse hepatocyte over five days and to characterize the cells for their viability and basal activities of defined Cyps and XMEs over the time course of the experiment.

Materials and methods: Primary hepatocytes were isolated by a two-step perfusion procedure of C57BL/6 J-mice. The cells were seeded in 96 well plates and cultivated for five days. The viability of the culture over the cultivation period was evaluated via visual assessment using a microscope and by the MTT-Assay. The activities of Cyps were determined by the AROD-Assay, using EROD for the specific activity of Cyp1A, PROD for Cyp2B and BROD for Cyp3A, respectively. Additionally, Cyp enzyme activities were measured with a cocktail of specific Cyp-substrates; formed metabolites were quantified by LC-MS. The results were statistically evaluated and compared to literature data.

Results: The basal activity without induction for Cyp2b was 2.32 pmol min⁻¹ 106 cells⁻¹ and for Cyp3a 2.71 pmol min⁻¹ 106 cells⁻¹, measured by respective AROD activities. Regarding Cyp1a, the measured fluorescence signal was below the LOD of 1.0 pmol. During the incubation time of five days, viability decreased by about 30%. The activity of Cyp2b and Cyp3a enzymes increased 4.8-fold between 24 hours and 72 hours after perfusion, and remained relatively constant until the end of the experiment after 96 hours.

Conclusion: A monolayer culture of primary mouse hepatocytes sustained sufficient viability and Cyp2b as well as Cyp3a activity for five days. This could make the primary hepatocyte culture applicable for enzyme induction studies *in vitro*.

P149

Frequencies and TCR repertoires of human metal-specific CD4+ T cells

F. Riedel¹, M. Aparicio Soto¹, C. Curato¹, L. Münch¹, A. Abbas¹, H. J. Thierse¹, W. K. Peitsch², A. Luch¹, K. Siewert¹

¹The German Federal Institute for Risk Assessment (BfR), Department 7: Chemicals and Product Safety, Berlin, Germany

²Klinik für Dermatologie und Phlebologie, Vivantes Klinikum im Friedrichshain, Berlin, Germany

Contact allergies to metal ions are common in industrialized countries. The current diagnostic standard is patch testing, which mimics allergic contact dermatitis (ACD). The inflammatory ACD reaction is mediated by allergen-specific CD4+ and CD8+ T cells. To date, no reliable blood-based test is available.

We developed a novel activation-induced marker (AIM) T cell assay to quantify metal-specific CD4+ T cells *ex vivo*. We characterized their T cell receptors (TCR) to understand metal ion binding and cross-reactivity.

Human peripheral blood mononuclear cells were incubated with metal salts and anti-CD40 blocking antibodies for 5 h. CD154 (CD40L) cell surface expression on metal-specific CD4+ T cells was detected by multi-parameter flow cytometry. High-throughput sequencing with an RNA and unique molecular identifier-based protocol allowed a full-length and error-corrected analysis of metal-specific TCR α - and β -chains.

Stimulation with nickel, cobalt, palladium, copper, platinum, and gold salts (Ni²⁺, Co²⁺, Pd²⁺, Cu²⁺, Pt²⁺, Au³⁺) induced concentration-dependent CD154 expression on human naïve (CCR7+, CD45RA+) and memory (non-naïve) CD4+ T cells. *In vitro* expanded clones were specifically restimulated, confirming TCR-mediated activation. At a metal ion concentration of 200-400 μ M, only a few allergic individuals topped the high background frequencies of metal-specific CD4+ memory T cells.

High-throughput sequencing revealed distinct overrepresentations of gene segments, i.e. TRAV9-2 for Ni²⁺-specific TCR (28% of TCR), TRAV2 for Co²⁺-specific TCR (8%), and the TRBV4 gene segment family for Pd²⁺-specific TCR (21%). As a second independent

mechanism of metal ion recognition, metal-specific TCR showed a common overrepresentation of one histidine in the complementarity determining region 3 (CDR3; 15% of α -chains, 34% of β -chains). We observed extensive cross-reactivity among metal-specific TCR that included the identified features.

The CD154 upregulation assay constitutes a comprehensive, fast, sensitive, and quantitative approach to analyze metal-specific CD4+ T cells. TCR repertoire analysis revealed distinct metal ion binding points underlying the high percentages of Ni²⁺-, Co²⁺-, and Pd²⁺-specific CD4+ T cells. The TCR repertoire characteristics impede blood-based allergy detection. Our approach opens new possibilities for chemical-specific T cell detection for diagnostic tests, sensitizer prediction and cross-reactivity assessment.

P150

Phenotypic anchoring for OMICS-guided assessment of liver toxicity in zebrafish

G. Hayot¹, C. Cramer von Clausbruch¹, R. Martinez Lopez², S. Scholz³, J. Colbourne⁴, U. Strähle¹, C. Weiss¹, R. Peravali¹, T. Dickmeis¹

¹Karlsruher Institut für Technologie, IBCS-BIP, Eggenstein-Leopoldshafen, Germany

²LEITAT, Barcelona, Spain

³Helmholtz-Centre for Environmental Research - UFZ, Department Bioanalytical Ecotoxicology, Leipzig, Germany

⁴University of Birmingham, School of Biosciences, Birmingham, United Kingdom

The zebrafish (*Danio rerio*) has become a popular model organism for studying embryonic development, genetics, and toxicology. As vertebrates sharing 70 % of their coding genes with humans, zebrafish are also widely used for modelling human diseases. Their small size, external development, transparent embryos, easy husbandry and breeding, and the large number of eggs they lay make them a valuable model for drug and toxicity screening. Already the older embryos possess a functional liver, allowing to assess compound effects on this organ *in vivo*.

In the context of PrecisionTox (www.precisiontox.org), a large-scale EU project aiming at OMICS based toxicity prediction using invertebrate and early life stage vertebrate model organisms, we wish to establish a workflow for identifying compounds with adverse effects on the zebrafish embryonic liver.

The selected test compounds are known or suspected liver toxicants. To assess overall toxicity, we used the vibration/startle response of zebrafish embryos as a phenotypic read-out, employing a custom-built system. Embryos were exposed to different concentrations of the compounds for 48 h, and benchmark doses (BMD) were determined using a customized KNIME workflow. Liver integrity was specifically examined by Oil Red O staining. Compound effects on glucocorticoid signalling activity were measured with the Glucocorticoid Responsive *In vivo* Zebrafish Luciferase activity (GRIZLY) assay previously developed by our laboratory [1].

Within the PrecisionTox consortium, transcriptome and metabolome data will be acquired for all tested compounds at BMD10 and 25 as determined by the vibration/startle assay. To anchor these OMICS data with respect to adverse liver phenotypes, we measured the size of the embryonic liver and assessed its lipid content by Oil Red O staining after 48 h of exposure. Furthermore, the GRIZLY assay examined whether glucocorticoid signalling, one important regulator of liver function, was altered by the compounds.

Our workflow aims at enabling rapid assessment of liver toxicity in zebrafish embryos, providing phenotypic data that complement the OMICS data generated by the PrecisionTox consortium. With this phenotypic anchoring, we hope to be able to identify novel transcriptomic and metabolic marker patterns that are predictive for liver toxicity.

1. Weger et al., ACS Chem. Biol. 7, 1178–1183 (2012)

P151

Quantitative and qualitative assessment of cytotoxicity by automated fluorescence microscopy in human hepatocytes

C. A. Cramer von Clausbruch¹, C. Weiss¹, T. Dickmeis¹, R. Peravali¹, U. Strähle¹, J. Colbourne², G. Hayot¹, S. Scholz³, R. Martinez Lopez⁴

¹Karlsruhe Institute of Technology, Institute of Biological and Chemical Systems - Biological Information Processing, Eggenstein-Leopoldshafen, Germany

²The University of Birmingham, School of Biosciences, Birmingham, United Kingdom

³Helmholtz Centre for Environmental Research GmbH - UFZ, Department of Bioanalytical Ecotoxicology, Leipzig, Germany

⁴LEITAT Technological Center, Human & Environmental Health & Safety Materials Safety Unit, Barcelona, Spain

Human and environmental health alike rely on the safety of chemicals introduced to the global market and everyday life. Fast, low-cost screening systems able to provide reliable toxicity data have become increasingly relevant with the significant rise of compounds to be assessed in the industrial and pharmaceutical domains. In the context of the 3 R approach to reduce, refine and replace animal experiments for chemical risk assessment, the demand for new approach methodologies (NAMs) including cell-based *in vitro* assays is increasing [1].

In the context of PrecisionTox (www.precisiontox.org), a large-scale EU project aiming at prediction of human toxicity based on OMICS using invertebrate and early life stage vertebrate model organisms, we wish to establish a workflow for identifying compounds with adverse effects in human liver cells.

For our experiments, we chose the epithelial-like human hepatocyte cell line HepG2, an established model to predict drug induced liver injury and to study metabolism, cytotoxicity and genotoxicity [2]. Cells were incubated for 48 hours with a diverse suite of industrial chemicals and pharmaceuticals. Plates were imaged using an automated high-throughput fluorescence microscopy assay, which provides information on diverse cellular endpoints, such as morphological phenotypes, altered cell proliferation, cell viability and mode of cell death [3].

Within the PrecisionTox consortium, transcriptome and metabolome data will be acquired for all tested compounds at BMD10 and 25 as determined by the inhibition of proliferation. To anchor these OMICS data with respect to adverse liver phenotypes, we assessed different morphological phenotypes in HepG2 cells. Quantitative structure-activity relationships are presented for some case studies of structurally similar compounds. As reference compounds, known or suspected hepatotoxicants were also included and effects are compared to *in vivo* data obtained in zebrafish embryos.

Our findings validate the use of cell-based high-throughput microscopy assays as a reliable tool for rapid toxicity screening. Employing zebrafish embryos for *in vitro/ in vivo* comparison allows hazard assessment of chemicals specifically addressing target organ toxicity as illustrated here for hepatotoxicants.

- [1] Colbourne et al. (2022) Environmental Advances, Volume 9,100287
 [2] O'Brien et al. (2006) Arch Toxicol.;80(9):580-604
 [3] Hansjosten et al. (2018) Arch Toxicol, 92 (2): 633-649.

P152

Study on the contribution of adjuvants on the sensitising potential of plant protection products using *in vitro* experiments

S. Seifert¹, S. Katherina¹, A. Sonnenburg¹, J. Grottker¹, S. Martin¹, B. Denise¹

¹German Federal Institute for Risk Assessment, Department 6- Pesticides Safety, Berlin, Germany

Introduction: In the authorisation of plant protection products (PPPs) the local lymph node assay (LLNA) is one of the accepted *in vivo* tests for the classification of mixtures for the endpoint skin sensitisation. Alternatively, concentration thresholds of single components are assessed for the classification of mixtures according to Regulation (EC) No 1272/2008 (CLP). However, there is a concern for misclassification and the underestimation of PPP sensitisation by this approach (e.g. Kurth et al., 2019).

Objectives: Our main objectives are the investigation of the following hypotheses:

- Non-sensitising co-formulants contribute to the potential of sensitisers contained in mixtures below their assigned effect levels, e.g. by enhancing uptake
- The combination of sensitisers below their individual effect level leads to observable mixture effects

Materials and methods: In the current project, we present data of a PPP investigated with the human cell line activation test (hCLAT) using THP-1 cells. We tested the product, different co-formulants and combinations of co-formulants. We measured IL-8 with an enzyme-linked immunosorbent assay in the supernatant of the cells after treatment. Additionally, we present data from a T-cell activation assay and QSAR predictions generated with Derek Nexus and the OECD toolbox.

Results: Here we present *in vitro*- and *in silico* data on a selected PPP that is positive in an *in vivo* test, but contains only known sensitisers underneath the concentration limits for sensitisation. The sensitising outcome of the *in vivo* test was confirmed by hCLAT and IL-8 measurements. A potential additional sensitiser was identified with hCLAT, IL-8 measurements, QSAR predictions and a T-cell assay. The combination of co-formulants containing known and the tentatively identified sensitiser did not fully explain the observed potency of the PPP.

Conclusion: Combination effects of low dose sensitisers did not fully explain the potency of the PPP. Possible explanations include the kinetic influence of sensitisers by other co-formulants or the formation of sensitisers by degradation processes in the PPP.

P153

Label-free quantitative proteomics on human bronchial epithelial cell proteome after cadmium exposure

M. Link¹, A. Hartwig¹

¹Karlsruhe Institute of Technology, Institute of Applied Biosciences; Department of Food Chemistry and Toxicology, Karlsruhe, Germany

Cadmium compounds are toxic and carcinogenic and occur ubiquitously in the environment. Possible sources of exposure include industrial pollution, smoking, or food. Especially inhalation exposure at workplaces has been associated with elevated risks of lung cancer. Cultured lung cells exposed to cadmium compounds react with specific changes in gene expression related to the oxidative stress response, and metal homeostasis [1]. Since gene expression does not completely reflect the protein status of the cell, a detailed examination of the proteome is of high relevance. In this work, we have

used a proteomics approach to determine the impact of cadmium on the global BEAS-2B cell proteome.

A bottom-up workflow followed by nanoLC-MS/MS measurement and data-dependent acquisition was applied as a proteomics method. The data were then processed using a label-free quantitative approach. The BEAS-2B cells were treated with cadmium for 24 hours. After cell lysis and protein denaturation, the proteomics workflow was then performed employing the Filter Aided Sample Preparation (FASP) method in which cell protein samples are processed chemically and digested with trypsin for further analysis. Due to regular buffer exchange via ultra-centrifugation, FASP is a very efficient sample preparation method.

Concerning the ATP content, a low cytotoxic effect of cadmium started at a concentration of 5 µM. Therefore, 1-5 µM cadmium were used for further experiments. The proteomics data showed a dose-dependent increase in the relative protein intensity of oxidative stress markers like heme oxygenase 1 and heat shock 70 kDa proteins. Furthermore, the protein level of metal-binding proteins like Metallothionein 2A was increased after cadmium exposure as well as the pro-apoptotic protein BAG family molecular chaperone regulator. In contrast, the expression of for example the enzyme Ribonuclease H1 was decreased in a dose-dependent matter.

These data reflect the oxidative potential of cadmium in BEAS-2B cells. Interestingly, we detected a decrease in RNase H1 protein levels, which have not been studied yet. Overall, these results confirm in principle observations revealed by gene expression studies [1]. The proteomics method applied in this study is suitable to gain a comprehensive insight into global proteome changes and possible mechanisms and pathways of cadmium toxicity.

- [1] Fischer, B; Neumann, D; Piberger, AL; Risnes, SF; Köberle, B; Hartwig, A; Arch Toxicol. 2016, 90(11)

P154

New approach methods for the identification of skin allergens

K. Egele¹, B. Blömeke²

¹Universität Trier, Sekretariat der Arbeitsgruppe "Allergie" der Ständigen Senatskommission zur Prüfung gesundheitsschädlicher Arbeitsstoffe der DFG, Trier, Germany

²Universität Trier, Trier, Germany

Today, several new approach methods (NAMs) and validated protocols are published for identification of skin sensitizing small (≤ 1000 Da) organic compounds (OECD guideline 442B-E). It is generally assumed that only a combination of results from methods addressing different key events in the adverse outcome pathway is sufficient to predict skin sensitization potential. Subsequently, defined approaches were introduced (OECD guideline 497) on how to combine data obtained to determine whether or not a chemical will cause skin sensitization and, if possible, classification of the contact allergen according to potency. We compiled data of the widely tested benzoyl peroxide and demonstrate the application of available tools to predict skin sensitization. Overall, the prediction of the potential of benzoyl peroxide was comparable between *in vivo* LLNA data and the use of NAMs. This promising data will enhance the confidence in the "Next Generation Risk Assessment".

P155

The *in vitro* biological activity of probiotics combination on human colorectal carcinoma cells

A. Anton^{1,2}, I. Pinzaru², C. A. Dehelean²

¹University of Medicine and Pharmacy Victor Babes Timisoara, Toxicology, Drug Industry, Management and Legislation, Timisoara, Romania

²University of Medicine and Pharmacy Victor Babes Timisoara, Toxicology, Drug Industry, Management and Legislation, Timisoara, Romania

Background: The human microbiotic system plays a vital role in maintaining optimal health. Colon diseases, from simple dysfunctions to colorectal cancer (CRC), are often associated with microbiota imbalances [1]. According to GLOBOCAN statistics, the incidence of CRC among women ranks second globally (16.2/100,000), respectively third in terms of the male sex (23.4/100,000) [2]. Current therapeutic protocols, especially those for advanced stages, are accompanied by multiple adverse effects and a low survival rate despite the progress of recent years. Therefore, in-depth studies are needed in terms of finding new specific and targeted protocols. A viable therapeutic alternative is represented by the use of probiotics, which have proven to be beneficial for the immune and intestinal systems, while being intensively studied in recent years for their anticancer, antidiabetic, antioxidant and antibacterial properties [3].

Aim: The current study was purposed to assess the *in vitro* biological activity of a combination of probiotics (*Lactobacillus sporogenes*, *Streptococcus faecalis* T-110, *Clostridium butyricum* TO-A and *Bacillus mesentericus* TO-A) on human carcinoma colorectal cells (HCT 116).

Methods: HCT-116 cells were cultivated in 96-well plates and when reaching a confluence of 80% were treated with various concentrations (0.5, 5, 10, 50 and 100 million CFU per mL) of combination of probiotic strains (*L. sporogenes*/*S. faecalis* T-110/*C. butyricum* TO-A/*B. mesentericus* TO-A in a ratio of 1/ 0.6/ 0.04/ 0.02). The MTT (3-(4,5-dimethylthiazol-2-yl)-2,5-diphenyltetrazolium bromide) assay was applied to assess cell viability following the protocol described in the literature [3]. In order to evaluate the changes at the nucleus level, Hoechst 33342 reagent was used [3]. Both the cell

morphology and the changes at the nucleus level were analyzed with the Cytation 1 instrument (BioTek Instruments Inc., Winooski, VT, USA) and the analysis and image processing was performed using the dedicated software Gen5™ (BioTek Instruments Inc., Winooski, VT, USA).

Results: The obtained results highlighted an impairment of viability depending on the exposure time and the dose, at the highest concentration, the most pronounced alterations were observed, both in terms of cell morphology and viability. After nuclear staining, apoptotic changes were observed - fragmentation and chromatin condensation.

P156

Cytotoxicity assessment of *Galium verum* extracts on human melanoma cells

A. D. Semencescu¹, I. Pinzaru¹, C. Dehelean¹

¹"Victor Babes" University of Medicine and Pharmacy Timisoara, Toxicology, Drug Industry, Management and Legislation, Timisoara, Romania

Introduction: Since ancient times, the therapeutic properties of plant species have been highlighted, knowing their role in the treatment of various pathologies, especially based on their chemical composition. *Galium verum*, belonging to the *Rubiaceae* family, is recognized for its antimicrobial, antioxidant activity and for beneficial effects on gastrointestinal and renal systems. Despite the traditional use of *Galium* species, there are still limited studies on the pharmacological activity and involvement in cancer alternative treatment, particularly melanoma.

Objectives: The aim of the current study was to evaluate the cytotoxic effect of two *Galium verum* extracts (total ethanolic extract - TEGv and ethyl acetate fraction - TEAGv) on the human melanoma cell line RPM1-7951.

Materials and methods: The extracts were characterized in terms of chemical composition by HPLC-MS and in terms of antioxidant activity by the DPPH method. Subsequently, cell viability was performed using the MTT assay, followed by microscopic evaluation of cell morphology 24 h after stimulation with different concentrations (15 - 100 µg/mL). The Hoechst 33342 staining assay was conducted to highlight the cytotoxic effects of extracts at the level of cell nuclei.

Results: The results indicated that both extracts possessed a significant antioxidant activity, compared to that of ascorbic acid, used as a positive control. At 24 h post-stimulation, TEGv and TEAGv induced a dose-dependent decrease in the viability of skin cancer cells. At the lowest concentration, no major changes in cell morphology were observed. The highest concentration produced a significant decrease in the number of cells and the confluence, especially in the case of TEGv, with signs of cell death, the cells becoming round and detaching from the plate.

Conclusion: The data obtained showed that *Galium verum* extracts have a dose-dependent cytotoxic effect on skin cancer cells and can be effective against melanoma cells, but further studies are needed to identify the mechanism of action.

P157

Oleanolic acid encapsulated in liposomes as a potential therapeutic approach for hepatocellular carcinoma

L. Macasoj^{1,2}, I. Pinzaru^{1,2}, C. Dorina^{1,2}, M. Cabuta¹, I. Marcovici^{1,2}, O. M. Cretu¹, C. A. Dehelean^{1,2}

¹"Victor Babes" University of Medicine and Pharmacy, Timisoara, Romania

²Research Center for Pharmacotoxicological Evaluations, Faculty of Pharmacy, "Victor Babes" University of Medicine and Pharmacy Timisoara, Eftimie Murgu Square No. 2, 300041 Timisoara, Romania, Timisoara, Romania

Introduction: Despite the advancements in treatment and diagnosis, cancer remains a major threat to human health. Current antitumor therapy raises some negative aspects: non-selective action, occurrence of toxic reactions, possibility of tumor cell resistance. Oleanolic acid (OA) has a wide distribution in plants and has many biological properties, including antitumor properties. Despite this, the main disadvantage of this compound is its low solubility. Liposomes are efficient delivery systems and a suitable solution which can serve as a therapeutic target for mitochondria.

Objectives: The current study focused on: i) encapsulation of oleanolic acid in liposomes (OA-Lip); ii) evaluation of the cytotoxic effect of OA-Lip on hepatic cells (HepG2 - hepatocellular carcinoma cells, HepaRG - healthy hepatocytes); iii) assessment of the impact of OA-Lip on cell morphology and on cellular organelles with a role in apoptosis (nuclei, actin filaments); iv) sample influence on pro-apoptotic gene expression and v) cellular respiration assessment.

Materials and methods: MTT assay was used to evaluate the potential selective cytotoxic effect of OA-Lip (concentrations between 1-75 µM) on hepatocellular carcinoma cells and healthy hepatocytes. Also, immunofluorescence techniques were applied to highlight the impact of the compound on the structure of the actin filaments and the nuclei. Finally, by determining the expression of pro-apoptotic genes, and the evaluation of cellular respiration by carrying out high-resolution respiration studies, the potential type of cell death involved in the cytotoxic effect was determined.

Results: The obtained liposomes meet the quality standards in terms of particle size (<200 nm) as well as encapsulation capacity (>65%). OA-Lip showed a selective cytotoxic profile, causing a dose and time-dependent decrease in the viability of HepG2 cells while not affecting HepaRG cells significantly. Further, the effects of OA-Lip were accompanied by the appearance of signs of cell apoptosis, as well as an increase in pro-apoptotic genes expression in HepG2 cells. In addition, the cellular respiration of HepG2 cells was drastically affected.

Conclusion: The preliminary results suggest OA-Lip may exert therapeutic effects on hepatocellular carcinoma cells, providing a basis for future studies in this field.

This research was funded by "Victor Babes" University of Medicine and Pharmacy, postdoctoral grant, OA-LIP-MIT.

P158

Development of an Allergy Test for Tropomyosin in Novel Foods

V. Feng¹, A. Koellner², K. I. Hirsch-Ernst², M. Peiser²

¹Institute for Biochemistry, FU Berlin, Thielallee 63, 14195 Berlin, Germany

²German Federal Institute for Risk Assessment (BfR), Unit Food Risks, Allergies and Novel Foods Department Food Safety, Berlin, Germany

Introduction: A number of novel foods based on insects such as yellow mealworm, migratory locust or house cricket, have recently undergone authorisation within the EU. However, consumption of insect protein may cause allergic reactions in certain individuals. Data provided by Broekman et al. (2016) suggest a high (87 %) probability for an allergic history to shrimp to be associated with allergic cross-reactivity to protein from mealworm. The assessment of allergy-related risks plays a crucial role towards protecting consumers from allergic (anaphylactic) reactions; however, a predictive non-clinical assay for assessment of the allergic potency of insect-based foods has hitherto not been available.

Objectives: The goal was to develop a predictive assay for food allergy from foods based on complete or processed insects as ingredients. Tropomyosins from shrimp and house dust mite were tested as model allergens.

Materials and methods: Peripheral blood mononuclear cells were isolated from non-allergic donors by density gradient centrifugation. Monocyte-derived dendritic cells (MoDCs) were generated by adherence (Gramlich et al., 2019), followed by 5-day cell culture in RPMI 1640/10% FCS with GM-CSF (100 ng/mL) and IL-4 (10 ng/mL). 48 h after stimulation, costimulatory CD86, adhesion molecule CD54 and MHC-II molecule HLA-DR were stained using corresponding fluorochrome-coupled monoclonal antibodies and analysed by FACS. Release of IL-8 was detected in culture supernatants by ELISA.

Results: Expression of CD86, CD54 and HLA-DR were dose-dependently increased on MoDCs by stimulation with 0.1, 1 and 10 µg/ml natural shrimp or house dust mite (Der p10) tropomyosin. Results were calculated as RFI (rel. fluorescence intensity). RFI values for CD86 reached 759-900 % and 1088-1321 % after stimulation by 10 µg/ml of natural shrimp or house dust mite tropomyosin, respectively. Considering that a RFI value ≥ 150 % for CD86 would be regarded as a positive result in the dermal sensitisation assay h-CLAT (OECD TG442E), the new assay proposed here would suggest tropomyosin to be a strong allergen. In addition, natural shrimp and dust mite tropomyosin induced high release of IL-8 into the supernatants of MoDCs.

Conclusion: The present food allergy test dose-dependently detected tropomyosin from different arthropod species and may contribute to animal-free testing for specific key events within the AOP259 Food Allergy. (Internal funding by BfR-LMS-08-1322-803)

Toxicology – Toxins

P159

Mutational analyses of proteinaceous toxins using cell-free systems

F. Rammler¹, D. Kaser¹, M. Stech¹, A. Zemella¹

¹Fraunhofer-Institut für Zelltherapie und Immunologie, Institutsteil Bioanalytik und Bioproduktion IZI-BB, Zellfreie und Zellbasierte Bioproduktion, Potsdam, Germany

Toxic proteins comprise a variety of different substances with diverse mechanisms of action. In various cases, mutations occur and the functionality of the toxin changes and detection assays might not be suitable any more. The characterization of such toxins and their mutants is essential for a better understanding of their mode of action and the development of novel therapeutics. Toxic moieties and toxins themselves are difficult to express in adequate amounts in living cells. Thus, cell-free systems have emerged as a versatile technology for studying toxic proteins. As a cell-lysate rather than viable cells is used, toxic effects on the host organism can be circumvented. Cell-free systems are open systems allowing to adapt the reaction to the individual protein's need. Radioactively and fluorescently labeled amino acids can be added for quantitative and qualitative analysis.

Here we present the use of cell-free protein synthesis to analyze proteinaceous toxins and their mutants. First, bacterial pore-forming toxins and their mutants are synthesized and functionally characterized. The model protein Cytotoxin K and different mutants were analyzed in order to detect the influence of mutations in the protein. Secondly, AB5 toxin subunits were modified and fluorescently labeled. The catalytic subunit of the Cholera toxin was mutated within the catalytic center and therefore silenced.

The data presented show the versatility of CFPS to synthesize, modify and investigate proteinaceous toxins. These data further facilitate cell-free systems for studying intracellular trafficking of toxins as well as vaccine development as non-toxic variants can be synthesized.

P160

Revising sulfated glucosaminoglycans as receptors for *C. difficile* TcdA reveals a minor role in uptake of toxin

R. Gerhard¹, D. Henkel¹, H. Tatge¹

¹Medizinische Hochschule Hannover, Hannover, Germany

CRISPR/Cas9-mediated functional gene knockout led to the identification of several specific receptors for *Clostridioides difficile* TcdA and TcdB as well as for other large clostridial glycosyltransferase of *Paenoclostridium sordellii* and *Clostridium novyi*. Obviously, these glycosyltransferases use redundant receptor binding epitopes for cell entry via different receptors, thus enabling entry into majority of cells from different tissue and species. Recently, sulfated glucosaminoglycans (sGAG) were identified as binding structures for *C. difficile* TcdA (Tao et al., 2019, Nat Microbiol. 4:1760-1769; DOI 10.1038/s41564-019-0464-z). The search for further TcdA specific receptors prompted us to generate a sGAG deficient HeLa cell line (HeLa SLC35B2^{-/-}) for sGAG independent toxin uptake. SLC35B2^{-/-} cells were devoid of sulfate transporter, which are essential for sulfation of structures within the endoplasmic reticulum. Revising previously published data showed that sGAG seem to play a minor role in uptake of TcdA. Besides HeLa SLC35B2^{-/-} cells we further generated SLC35B9 deficient clones of HT29 cells by means of CRISPR/Cas9-mediated GFP-insertion into the specific gene. Modification of genes were checked by specific PCR, insertion of GFP coding sequence by fluorescence microscopy and absence of sGAG by FACS analysis using antibody against heparansulfate. In addition, established CHO delta XylT cell line that lacks functional xylose transporter was included into the study for testing SLC35B2 independent loss of sGAG. We found that HeLa SLC35B2^{-/-}, HT29 SLC35B2^{-/-} and CHO delta XylT showed no significant changes in sensitivity towards TcdA compared to the respective wildtype cells. Our data implicate secondary role of sGAG in abundance or endocytosis of functional yet still unknown receptor. Furthermore, CRISPR/Cas9 modified cells might differentially compensate specific gene knockdown that could bias results.

P161

Human Peptides α -Defensin-1 and -5 Inhibit Pertussis Toxin in different ways

C. Kling¹, K. Ernst¹, H. Barth¹, A. Pulliainen²

¹Universitätsklinikum Ulm, Ulm, Germany

²University of Turku, Turku, Finland

Whooping cough is a severe childhood disease, caused by the bacterium *B. pertussis*, releasing Pertussis toxin (PT) as a major virulence factor. PT is a protein AB₅-type toxin, with the enzymatically active A-subunit PTS1 and five B-subunits, responsible for binding and transport of PTS1 into the cytosol. In the cytosol, PTS1 ADP-ribosylates Gai, leading to disturbed cAMP signaling [1]. Since PT plays a pivotal role in causing severe courses of disease [2], we aim to identify and characterize new inhibitors against PT to provide starting points for novel therapeutic strategies. Recently, we identified the human antimicrobial peptides α -defensin-1 and -5 as inhibitors of PT in several cell-based assays as well as an *in vitro* enzyme activity assay [3].

To further elucidate the underlying mechanism of inhibition of PT by α -defensin-1 and -5, we incubated CHO and A549 cells with fluorescently labeled PT on ice, to allow binding but no uptake of PT. Subsequently, the amount of PT bound to cells was measured by flow cytometry. As a result, the presence of α -defensin-5 strongly reduced the amount of PT bound to cells, whereas α -defensin-1 caused only a mild reduction. With immunocytochemistry, we analyzed PT location within cells after 4h of incubation. In the presence of α -defensin-1, the signal of PT was stronger compared to cells treated only with PT. In the presence of α -defensin-5, the signal of PT was clearly altered from a diffuse intracellular to a more focal and dot-like signal suggesting that α -defensin-5 might interfere with cellular uptake of PT. Employing specific antibodies, we also examined the location of α -defensin-1 and -5 in CHO and A549 cells. α -defensin-1 distributed evenly in the cytosol whereas α -defensin-5 distributed unevenly around the cells.

Taken together, these data suggest that α -defensin-1 inhibits PT mainly by entering cells and inhibiting enzyme activity of PTS1, whereas α -defensin-5 mainly inhibits uptake of PT into the cells. These findings, as well as experiments with the closely related α -defensin-2, -3, -4, and -6 contribute to elucidating the structure-activity relationships of α -defensins for inhibiting PT, thus paving the way for optimization of α -defensins as inhibitors of PT as potential novel therapeutic strategies against the life-threatening disease whooping cough.

1. Loch et al. *FEBS J.* 2011
2. Scanlon et al. *Toxins* 2019
3. Kling et al. *Toxins* 2021

P162

Chlamydia muridarum TC0438 - a new DxD-motif harbouring chlamydial cytotoxin

H. Genth¹, M. Kühnel¹, C. Lanfermann¹, I. Schelle¹, C. Rheinheimer¹, A. Klos¹

¹Medizinische Hochschule Hannover, Hannover, Germany

In humans, *Chlamydia trachomatis* causes urogenital diseases including infertility in women, and trachoma, the world's leading cause of preventable blindness. Sharing a high degree of similarity of the genetic content, *Chlamydia muridarum* (Cmu) is a related mouse-adapted species that is frequently used as model organism in animal studies. As intracellular bacteria, Chlamydiae modify their host cells by translocated effector proteins to permit long-term survival. In Cmu, most plasticity zone ORFs are transcribed in the early to middle phase of the developmental cycle, among them TC0437, TC0438, and TC0439. Within their N-terminal domains, each TC0437, TC0438, and TC0439 harbors the aspartate-X-aspartate (DXD) motif that is generally regarded to be involved in binding and coordination of nucleotide sugars and divalent metal ions. This observation has led the hypothesis that each TC0437, TC0438, and TC0439 is a putative cytotoxin sharing a domain structure and an enzymatic/biological activity comparable to that of the *C. difficile* toxin A and toxin B (TcdB). Ectopic expression of the N-terminal domains of each N-TC0437, N-TC0438, and N-TC0439 in HeLa cells induced cytotoxicity comparable to the activity of TcdB. Mutation of the DXD motif reduced N-TC0438-induced cytotoxicity. Activation of Rho-GTPases by the cytotoxic necrotizing factor 1 (CNF1) preserved cell from N-TC0438-induced cytotoxicity. In their activated GTP-bound state, Rho-GTPases seemed to be protected from the putative covalent modification catalyzed by N-TC0438. Finally, N-TC0438 inhibits the activation of the ERK pathway. In this regard, the capability of TC0438 of limiting ERK activation during chlamydial infection might be useful in order to prevent cell death and to promote intracellular survival of Cmu.

P163

Simultaneous Detection, Differentiation and Quantification of Eight Staphylococcal Enterotoxins in a Multiplex Suspension Assay

P. Dettmann¹, M. Skiba¹, T. C. Meyer¹, D. Stern¹, A. Rummel², M. B. Dörner¹, H. W. Mages¹, S. Maurischat³, S. Schaarschmidt³, B. Strommenger⁴, M. Avondet⁵, B. G. Dörner¹

¹Robert Koch Institute, Centre for Biological Threats and Special Pathogens (ZBS), Biological Toxins (ZBS3), Berlin, Germany

²Hannover Medical School, Institute for Toxicology, Hannover, Germany

³German Federal Institute for Risk Assessment, Department Biological Safety, Berlin, Germany

⁴Robert Koch Institute, Department of Infectious Diseases, National Reference Centre (NRC) for Staphylococci and Enterococci, Division of Nosocomial Pathogens and Antibiotic Resistances, Wernigerode, Germany

⁵Federal Department of Defence, Civil Protection and Sports, Spiez Laboratory, Spiez, Switzerland

⁶Robert Koch Institute, Department of Infectious Diseases, National Reference Centre (NRC) for Staphylococci and Enterococci, Division of Nosocomial Pathogens and Antibiotic Resistances, Wernigerode, Germany

⁷Federal Department of Defence, Civil Protection and Sports, Spiez Laboratory, Spiez, Switzerland

Staphylococcus aureus (*S. aureus*) is a well-known ubiquitous bacterium expressing a plethora of virulence factors. Here we focus on the detection of a group of bacterial toxins causing one of the most common food-borne intoxications: staphylococcal enterotoxins (SEs). More than 20 different SEs and SE-like molecules have been described with 30-86% sequence homology on amino acid level. Detection of SEs is crucial under the aspects of consumer health, food safety and outbreak investigation. Commercial detection methods for the five classical SEs (SEA-SEE) exist with limited sensitivity and specificity. Recent work indicates the involvement of further enterotoxins in food poisoning, which are currently undetectable on the protein level by commercial assays.

While *se* gene detection based on nucleic acids has its merits, this approach displays only the potential for toxin production on the genetic level, but explicitly not the expression of SEs and their quantity. Furthermore, preheated food usually only contains the heat-resistant toxins, not the heat-sensitive bacterial agent limiting the usability of genetic detection methods in an outbreak situation.

The aim of this work is therefore to establish a highly sensitive and specific multiplex suspension array that recognizes a broader range of SEs including their variants. For this purpose, monoclonal antibodies (mAbs) against eight SEs, namely SEA to SEI, have been newly generated by classical hybridoma fusion and recombinant techniques. The mAbs were comprehensively characterized for their SE specificity and binding affinity and detect their specific antigens down to the low pg/mL-levels in classical sandwich-ELISAs.

Finally, the novel SE-antibodies have been implemented in a suspension array based on the Luminex® technology, which allows for the first time the simultaneous detection, differentiation and quantification of multiple SEs from minimal sample volumes. To ensure broad detection coverage of known SE variants, both the classical sandwich-ELISA targeting individual SEs and the suspension array detecting SEA to SEI have been evaluated on supernatants of 140 selected and whole genome sequenced (WGS) *S. aureus* strains.

In summary, we here present the development and validation of a highly sensitive and specific detection method for an extended group of SEs relevant in food poisoning outbreaks.

P164**Multifunctional peptide nanocarrier for targeted pharmacological modulation of metastatic breast cancer cell proliferation and osteolysis in the bone microenvironment**N. Stadler¹, B. Gao², S. L. Kuan², T. Weip², H. Barth¹¹University of Ulm, medical centre, Institute of experimental and clinical pharmacology, toxicology and pharmacology of natural products, Ulm, Germany²Max-Planck institute, Max-Planck-Institut für Polymerforschung, Mainz, Germany

Bone is a common site for metastasis of cancers including breast carcinoma (BC) [1]. BC cells lead to an alteration of the bone microenvironment by promoting osteoclastogenesis and in turn, osteoclasts stimulate tumour progression [2, 3]. To overcome this vicious cycle and due to the resistance of metastatic BC to common therapies, a novel supra-molecular transport system was developed based on avidin/biotin technology to down-modulate growth and proliferation of BC cells as well as the activity of osteoclasts. In this approach, the biotinylated *Clostridium botulinum* C3 protein was coupled to the central binding platform avidin. C3 is only internalized into the cytosol of monocytic cells including osteoclasts [4], but not into other cell types and leads to mono-ADP ribosylation of the GTPases Rho A, -B and -C, thereby inhibiting Rho-mediated signal transduction and actin-dependent cell functions such as proliferation and migration [5]. To also target the BC cells in the bone niche, three biotinylated entities of the EPI-X4-derived peptide JM173 [6, 7] were coupled to the avidin-C3 complex. JM173 binds to the CXCR4 receptor [6], which is overexpressed in BC and should enable the selective delivery of therapeutic cargo molecules (e.g. C3) into the cytosol of BC. We demonstrated that the resulting nanocarrier (JM173)-BDPAvi-C3 binds to CXCR4 expressing A431 cells and HeLa cells. It drastically enhanced the uptake of C3 enzyme into non-monocytic cells and lead to characteristic C3-induced morphological changes in both cell types. Since C3 is also taken up by osteoclasts and down-modulates their bone resorption activity [4], (JM173)-BDPAvi-C3 targets both, bone-degrading osteoclasts as well as metastatic BC cells in the bone niche.

[1] Coniglio, Front. Endocrinol. 9, 2018, p. 313

[2] Wang et al., Bone Res. 8, 2020, p. 30

[3] Zarrer et al., Biomolecules 10, 2020, p. 337

[4] Tautzenberger et al., PLOS ONE 8(12): e85695, 2013

[5] Barth et al., Front. Immunol. 6:339, 2015

[6] Zirafi et al., Cell Rep. 11, 2015, pp. 737–747

[7] Harms et al., Acta Pharmaceutica Sinica B, 11(9), 2020, pp. 2694-2708

P165**Evaluation of the *in vitro* neutralizing capacity of anti-ricin antibodies**A. El Houari¹, S. Worbs¹, D. Stern¹, L. Lequesne², M. L. Orsini Delgado², S. Simon², B. G. Dornier¹¹Robert Koch-Institut, ZBS3 Biologische Toxine, Berlin, Germany²Commissariat à l'énergie atomique et aux énergies alternatives, Gif-sur-Yvette, France

Ricin is a protein toxin produced by the plant *Ricinus communis*. It is known for its highly toxic and potentially lethal properties with no approved antidote available to date. A number of research groups worldwide are evaluating specific anti-ricin antibodies (Abs) for their neutralizing abilities to make an antidote available in medium term. At RKI and CEA we were able to develop a panel of neutralizing monoclonal Abs (mAbs). In the context of the current French-German ANR/BMBF project PLANT, individual mAbs as well as mAb combinations are now comprehensively characterized and tested for their neutralizing activity. A focus is laid on identifying combinations of up to three mAbs targeting different epitopes that provide a synergistic neutralizing effect against ricin intoxication.

Determining different epitope groups by using epitope binning methods via surface plasmon resonance (SPR) spectroscopy helped us choosing the best mAb-combinations with the potentially highest synergy. At RKI, the neutralizing capacity of the different mAbs was measured individually or in combinations of two or three mAbs using a real-time cytotoxicity assay. The results obtained were evaluated and found to be in congruence with those obtained at CEA using an end-point cytotoxicity assay based on a different experimental setup.

Along with cytotoxicity assays, the specificity of the mAbs to bind the A or B chain of the toxin as well as their capability to bind ricin isolectins D and E and the related *R. communis* Agglutinin (RCA120) was determined by ELISA and SPR. When comparing results from neutralization assays with SPR data a correlation between inhibition capacity and mAb affinity was identified. Hence, for the Abs exhibiting a high neutralizing capacity, a high affinity was observed (KD ~ 10⁻¹⁰-10⁻¹¹ M).

In preparation for the analysis of future *in vivo* experiments, the capability of the mAbs to specifically detect ricin bound in tissue cells after fixation was evaluated by immunofluorescence staining and flow cytometry. A panel of mAbs turned out to be useful for staining of the toxin in cells after fixation.

Based on the results obtained by the different approaches combinations of two or three Abs presented the best neutralizing capacities *in vitro*. In the framework of the PLANT project the best mAb combinations will be evaluated in a mouse model of ricin intoxication.

Pharmacology – G-protein coupled receptors**P166****Characterization of GPR4 antagonists using FRET-based GPR4 reporter cell lines**F. Wunder¹, A. Woermann¹, M. Karlstetter², H. Meier¹, M. Koch¹¹Bayer AG, Drug Discovery Sciences, Wuppertal, Germany²Bayer AG, Therapeutic Area 2, Wuppertal, Germany

GPR4 is a proton sensing G protein-coupled receptor (GPCR) belonging to a family of three closely related receptors including GPR4, GPR65 (OGR1), and GPR68 (TDAG8). GPR4 is activated by extracellular acidification and activation is coupled to the Gαs/cAMP-signaling pathway.

Here we report the generation and characterization of recombinant human, rat and mouse GPR4 reporter cell lines. In these GPR4 reporter cells, cAMP generation stimulated by reduction of extracellular pH can be monitored in real-time using a FRET-based intracellular cAMP biosensor. Measurements were performed on 384-well and 1536-well microtiter plates. Acidification of the extracellular solution stimulated an immediate FRET ratio reduction of the EPAC-based biosensor in the GPR4 reporter cells, which reflects an increase of the intracellular cAMP concentration. In contrast, extracellular acidification of the parental EPAC reporter cell line did not induce any changes of biosensor-mediated FRET signals. Half-maximal activation of GPR4 was observed at ~ pH 7.4.

GPR4 reporter cells were used to characterize available small molecule GPR4 antagonists. To our surprise, we could show that the antagonist potencies are largely dependent on the extracellular pH. At more acidic pH values antagonist potencies were found to be strongly reduced. In addition, in contrast to previous reports we could show that GPR4 antagonists possess similar pH-dependent potencies on human, rat and mouse GPR4. Our findings have large implications on the suitability of these GPR4 antagonists for *in vitro* and especially for *in vivo* studies.

P167**The Membrane Palmitoylated Protein 1 (MPP1) Induces Angiotensin II AT1 Receptor (AGTR1) Sensitization *In Vitro* and Features of Heart Failure *In Vivo***J. Abd Alla¹, E. Negerer¹, A. Langer¹, U. Quatterer¹¹ETH Zurich, Molecular Pharmacology, Zurich, Switzerland

Cardiovascular diseases and heart failure are still major causes of morbidity and mortality in the elderly as pathomechanisms are incompletely understood, and pharmacological targets for new treatments are lacking. In order to elucidate pathomechanisms and to identify potential new targets, we searched for up-regulated transcripts in different models of heart failure. We found the consistent up-regulation of MPP1 (Membrane Palmitoylated Protein 1) in our whole genome gene expression data of different heart failure models, i.e., (i) heart failure induced by long-term chronic pressure overload, (ii) heart failure induced by long-term atherosclerosis of aged Apoe^{-/-} mice, and (iii) heart failure induced by overexpression of the Raf kinase inhibitor protein, RKIP. The Membrane Palmitoylated Protein 1 (MPP1) belongs to the family of membrane-associated guanylate kinase (MAGUK) scaffolding proteins. However, the function of MPP1 in the heart or in heart failure is not known. To investigate the impact of an increased MPP1 level in the heart, we generated transgenic mice with myocardium-specific expression of MPP1 under control of the alpha-MHC (alpha-myosin heavy chain) promoter. At an age of 8 months, Tg-MPP1 mice with 2-fold increased MPP1 protein levels showed cardiac dysfunction with a significantly reduced left ventricular ejection fraction of 39.0 ± 6.9 % compared to 55.2 ± 3.7 % in non-transgenic B6 controls (p = 0.0005, ± s.d., n=6). Echocardiography also detected the left ventricular enlargement of Tg-MPP1 mice, which was confirmed by histopathological analysis. Concomitantly, transgenic Tg-MPP1 mice showed an increased number of the cardiac hypertrophy-promoting and heart failure-enhancing angiotensin II AT1 receptor, AGTR1. Up-regulation of the AGTR1 protein was mediated by MPP1 also in non-cardiomyocyte HEK (human embryonic kidney) cells because MPP1 expression led to increased AGTR1-eYFP protein levels, which were quantitated in HEK cells by fluorescence spectroscopy. Taken together, we identified MPP1 as a previously unrecognized heart failure-induced protein, which sensitizes the heart failure-stimulating angiotensin II AT1 receptor, AGTR1.

P168**Metabolic and cellular factors determining the therapeutic effect of dimethyl fumarate**J. Kosinska¹¹Institut für Klinische und Experimentelle Pharmakologie und Toxikologie, Lübeck, Germany

Multiple sclerosis (MS) is an autoimmune disease of the central nervous system, in which the interaction between a variety of immunopathological and neuropathological mechanisms leads to inflammation, demyelination, axonal loss and gliosis. Dimethyl fumarate (Tecfidera) has been approved for the treatment of relapsing-remitting multiple sclerosis (MS) and has been shown to improve neurological symptoms but unfortunately, not all patients respond to the drug. *In vivo* DMF is rapidly metabolized to monomethyl fumarate (MMF), which is an agonist of the hydroxycarboxylic acid receptor 2 (HCA2) along with butyrate, a short chain fatty acid (SCFA) produced by the microbiome. We hypothesized that the response to DMF may depend on the endogenous production of butyrate. Using an animal model of MS, experimental autoimmune encephalomyelitis (EAE), mice were fed with high-fiber diet (HFD), lauric-acid-rich diet (LAD), or with normal chow (NC), in order to modulate butyrate production. Interestingly, DMF had the biggest therapeutic effect on neurological deficits when mice were fed with HFD but it had no effect on LAD-fed animals. Plasma levels of MMF were not affected by any diet. In accordance with previous work, when mice were fed with HFD, the DMF effect depended

on HCA2. HFD induced the expression of HCA2 in Ly6C^{intermediate} monocytes and in microglia, whereas neutrophils expressed HCA2 at a high level irrespective of the diet. By the conditional knockout in brain endothelial cells and in neutrophils, we further investigate the function of HCA2. In *Ly6G-Cre; Hca2^{fl/fl}* mice, HCA2 was deleted in neutrophils and the therapeutic effect of DMF was lost suggesting that DMF exerts its therapeutic effect by activating HCA2 in neutrophils. Current work tries to elucidate how HFD modulates the sensitivity of neutrophils to MMF stimulation. At the clinical level, our data suggest a strategy to increase the response rate to DMF.

P169

Signature of cannabinoid receptor phosphorylation in vitro and in vivo

V. Stammer¹, S. Schulz¹, A. Kliever¹

¹Jena University Hospital, Pharmacology and Toxicology, Jena, Germany

Cannabis belongs to one of the oldest cultivated plants for medical use in human history. Since more than 8000 years different parts of the *Cannabis sativa* plant were used for treatment of different disorders like pain or nausea. After a short period of aversion against Cannabis and its ingredients modern medicine is rediscovering cannabinoids as therapeutics for more and more diseases. Development of new drugs acting on cannabinoid receptors is challenged by the lack of precise understanding of the molecular mechanisms of drug effects. This results in a current lack of novel therapies for novel neuropsychiatric drugs.

Recently we developed phosphorylation-specific antibodies for the carboxy-terminal serin and threonine residues for the CB1R and CB2R. For the first time, this approach allows us to investigate and compare the agonist-induced phosphorylation pattern of synthetic CBR ligands WIN55,212-2 and CP55,940 compared to the herbal CBR agonists Δ^9 -tetrahydrocannabinol (THC) and Cannabidiol (CBD) from *C. sativa*.

CB1R and CB2R stably expressed in human embryonic kidney cells 293 (HEK293) exhibited a strong multi-site phosphorylation of the cannabinoids WIN55,212-2 and CP-55940, which is time and dose dependent. A slight basal phosphorylation could be detected in both receptors which could be blocked by treatment with lambda-phosphatase. Pretreatment with the antagonist AM251 inhibited the agonist-induced phosphorylation pattern.

Incubation with the PKC activator PMA and the PKA activator Forskolin revealed evidence of a heterologous phosphorylation process. Preincubation with the GRK2/3 inhibitor compound 101 revealed evidence for a GRK 5/6-dependent second messenger cascade. This assumption was confirmed after using GRK inhibitors.

CB1R immunoprecipitation from brain lysates also confirmed the agonist-induced phosphorylation pattern in vivo.

Finally, our results will help forecasting the effects of new drugs and thereby help identifying compounds with improved pharmacological profiles.

P170

Relaxin receptor RXFP1 is targeted by novel interaction partners CTRP1, CTRP6 and CTRP8 in corneal wound healing

H. F. Nicolaus^{1,2}, T. Klönisch³, A. Ludwig¹, F. Paulsen², F. Garreis²

¹Friedrich-Alexander-Universität Erlangen-Nürnberg, Institute of Experimental and Clinical Pharmacology and Toxicology, Erlangen, Germany

²Friedrich-Alexander-Universität Erlangen-Nürnberg, Institute of Functional and Clinical Anatomy, Erlangen, Germany

³University of Manitoba, Department of Human Anatomy and Cell Science, Winnipeg, Canada

Introduction: G-protein coupled receptor relaxin/insulin-like family peptide receptor 1 (RXFP1) signaling plays an important role in various physiologic as well as pathophysiologic processes, including cardiovascular diseases, fibrosis, and cancer. In addition, binding of relaxin to RXFP1 has been demonstrated to promote corneal wound healing through increased cell migration and modulation of extracellular matrix formation. Recently, C1q/tumor necrosis factor related proteins (CTRP) 1, 6 and 8 have been identified as novel interaction partners of RXFP1.

Objectives: In this study, we aimed to investigate the effect of CTRP1, CTRP6 and CTRP8 on ocular surface wound healing and its dependence on the RXFP1 receptor pathway.

Materials and methods: CTRP1, CTRP6 and CTRP8 expression was analyzed by RT-PCR and immunohistochemistry in human tissues and cell lines derived from the ocular surface and lacrimal apparatus. In vitro ocular surface wound modeling was performed using a scratch assay. We analyzed the effects of different concentrations of recombinant CTRP1, CTRP6 and CTRP8 on cell proliferation and migration in human corneal and conjunctival epithelial cell lines. To determine the dependence of on RXFP1 signaling, ligand binding to RXFP1 was inhibited by a specific anti RXFP1 antibody.

Results: We detected CTRP1, CTRP6 and CTRP8 expression human cornea, conjunctiva, meibomian gland, nasolacrimal duct, lacrimal gland, and all investigated cell lines. Stimulation with CTRP1, CTRP6 and CTRP8 resulted in an increased surface defect healing rate in human corneal epithelial cells in a dose dependent manner, but not in conjunctival epithelial cells. Inhibition of RXFP1 lead to complete suppression of CTRP6

and CTRP8 effects on the surface defect healing rate in HCE while CTRP1 effects were not fully suppressed.

Conclusion: Our findings demonstrate a novel role for CTRP1, CTRP6 and CTRP8 in corneal wound healing by targeting the relaxin receptor RXFP1. This may provide future opportunities for drug discovery in the treatment of corneal wounds.

P171

Role of Ubiquitination for co-internalization of arrestin3 with G protein coupled receptors

S. Ernst¹, N. Mößlein¹, M. Bünemann¹, C. Krasel¹

¹Philipps-Universität Marburg, FB Pharmazie, Institut für Pharmakologie und klinische Pharmazie, Marburg, Germany

Introduction: Arrestins are a small family of four proteins known for their ability to bind phosphorylated G-protein-coupled receptors leading to their desensitization and internalization. Some GPCRs like the β_2 -adrenergic receptor interact only transiently with arrestins leading to internalization of the receptor without arrestin (class A), while other GPCRs like the parathyroid hormone receptor form stable complexes with arrestins causing co-internalization of the receptor with arrestin to endosomes (class B).

Objectives: It was suggested before that the binding of other proteins to arrestins may influence their co-trafficking with receptors. Here we focused on the binding of two different proteins to arrestins: first we wanted to investigate the effect of arrestin ubiquitination by mutation of two specific lysine residues to arginine. Second, we mutated four residues at the C-terminal end of the finger loop region to alanine which were previously implicated in interaction of arrestin2 with the ESCRT0 protein STAM1.

Materials and methods: Co-internalization was assessed by confocal microscopy and quantified by a bystander BRET assay between arrestin3 fused to Renilla luciferase and a Renilla GFP-labelled FYVE-domain as an endosomal marker. To determine the affinity of the arrestins for the receptors we used dual-colour FRAP-measurements.

Results: Mutation of two specific lysine residues reduced the agonist-dependent ubiquitination of the arrestin. This mutant also did not co-internalize with a number of different class B GPCRs while its affinity to agonist-bound GPCRs was unchanged. When the putative STAM1 binding site was mutated, the resulting arrestin3 also did not co-internalize with several different class B GPCRs. We are currently characterizing this mutant further. To assess the role of ubiquitination we treated cells with the E1 inhibitor TAK243 (10 μ M). This reduced whole-cell ubiquitination by about 90% but had only a modest effect on arrestin3 co-internalization with class B receptors.

Conclusion: Co-trafficking of arrestins to endosomes with class B GPCRs depends on two specific lysine residues and on a binding site at the base of the finger loop region suggested to be important for binding of the adaptor-protein STAM1. It is currently unclear in which order these two sites are engaged. Our results with TAK243 suggest that arrestin ubiquitination may not be as important as previously thought.

P172

FRET-based neurotensin 1 receptor conformation sensor to study on- and off-kinetics in intact cells and under cell-free conditions

U. Hochban¹, P. Dahlhaus², M. Kurz¹, D. Higer², M. Bünemann¹

¹Philipps-Universität Marburg, Institut für Pharmakologie und klinische Pharmazie, Marburg, Germany

²Philipps-Universität Marburg, Institut für pharmazeutische Chemie, Marburg, Germany

G protein-coupled receptors (GPCRs) constitute the largest family of membrane receptors and play a key role in signal transduction of extracellular stimuli into intracellular signaling pathways. They play an important role regarding the pharmacotherapy of many diseases. The neurotensin 1 receptor (NTSR1) is involved in many physiological functions such as analgesia, hypothermia and hypotension and therefore is an interesting target for drug development. We aim to study and compare ligand-induced conformational changes of this receptor both in intact cells and under cell-free conditions. Therefore, we generated a NTSR1 conformation sensor, which reports receptor activation in intact cells by means of Foerster resonance energy transfer (FRET). In order to test the suitability of this sensor to detect conformational changes of the NTSR1 *in vitro*, we compared signal strength and ligand concentration dependency in intact cells and in permeabilized cells. No major difference was observed, proving the general suitability of our approach. Next, we are aiming to use this NTSR1 receptor conformation sensor in the context of purified receptors, which will be immobilized on glass coverslips suitable for TIRF imaging. This method will be further developed to allow for drug screening in the plate reader format.

In conclusion, we could show that our NTSR1 based FRET sensor is still functional and gives robust signals to its endogenous ligand under permeable and cell-free conditions. This method widens the possibility of studying GPCRs and could be helpful in ligand screening for finding new drugs.

P173

Agonist affinity of prostanoid receptor sensors decreases in non-intact cells
M. Kurz¹, I. Wallenstein¹, M. Ulrich¹, U. Hochban¹, S. Kirchofer¹, H. Lemoine^{2,3}, M. Bünemann¹

¹Philipps Universität, Institut für Pharmakologie und klinische Pharmazie, Marburg, Germany

²Heinrich Heine University, Düsseldorf, Germany

³LWL lab, Düsseldorf, Germany

G protein-coupled receptors (GPCRs) are highly relevant in human physiology and pharmacology. To monitor the direct drug effects on receptor activity, Förster resonance energy transfer (FRET) based GPCR conformation sensors are valuable tools. These sensors are commonly measured in living cells. Therefore we investigated in this study whether the cell intactness of the hosting cell affects the ligand-induced sensor activation.

HEK cells carrying the respective receptor sensor construct were investigated by means of FRET. Cells either where measured intact, permeabilized using saponin or as membrane fragments. The measurements where either performed using single cells at a fluorescent microscope or multiple cells at a plate reader.

We observed a right shift in the EC50 value for prostaglandin E2 (PGE2) at EP4 receptor sensor of about one order of magnitude in both membrane fragments and permeabilized cells and four times faster wash out kinetics of the PGE2 effect at EP4 receptor sensor in permeabilized cells. The prostanoid receptor sensors for EP2 receptor activated with PGE2, TP receptor activated with U46619 and IP receptor activated with Iloprost showed a similar right shift in EC50 in non intact cells. The non prostanoid lipid receptor FFAR3 activated with propionic acid did not show an apparent difference in EC50 value upon permeabilization, but 2.4 faster wash out kinetics. The tested non lipid GPCR sensors, the peptide μ -opioid receptor activated with DAMGO and the alpha-2A adrenergic receptor activated with noradrenaline, did neither show an observable right shift in EC50 value nor faster kinetics. Using the EP4 receptor as a model system, we studied the effects of ion composition as well as ATP and GTP and the nature of the activating ligand. The affinity loss in permeabilized cells was not affected by any of these factors in our experiments.

Taken together we observed a similar loss in affinity for all tested prostanoid receptor sensors upon disruption of the cell intactness, while we did not find an example for non lipid GPCR sensors. The underlying mechanism is still elusive. A major contribution of the electrolyte composition, ATP, GTP, the nature of the activating ligand or, based on a steric hindrance, influences of G protein binding on the observed effect seem unlikely. We speculate that the entrance to the orthosteric binding pocket, which faces the plasma membrane in most lipid GPCRs, could possibly be related to the affinity loss.

P174

Human DP2 receptor based FRET conformation sensor gives new insights into pharmacology and reveals arachidonic acid to be a partial agonist DP2 receptor
M. Ulrich¹, M. Kurz¹, A. Bittner¹, H. Strenger¹, M. Bünemann¹

¹Philipps-University of Marburg, Department of Pharmacology and Clinical Pharmacy, Marburg, Germany

The DP2 receptor is a member of the G-protein coupled receptor class. It plays important physiological roles e.g. in the regulation of the immune response and is target for ramatroban which is licensed for the treatment of allergic rhinitis and currently under investigation for the treatment of COVID. DP2 receptor is activated by the arachidonic acid (AA) product prostaglandin (PG) D2. PGD2 is enzymatically formed by cyclooxygenase (COX) in a twostep process from AA via PGH2. We constructed a Fluorescence Resonance Energy Transfer (FRET) based conformation sensor of the human DP2 receptor to further investigate the pharmacology and dynamics of this important prostanoid receptor.

Single living HEK cells transient or stably expressing the DP2 receptor sensor were investigated by means of FRET at an inverted fluorescent microscope. Furthermore, FRET measurements of multiple cells carrying the construct, were performed at a plate reader.

The FRET conformation sensor based on the human DP2 receptor showed a concentration dependent decrease in emission ratio upon stimulation with different agonists. We observed a robust signal to noise ratio and were able to measure concentration response curves both in single cell as well as in multi-cell FRET recordings. The DP2 receptor was activated by a number of substances besides PGD2 such as PGF2 α and Indometacin, which reflects the wt-receptor properties. We compared the agonistic effect of the substances to the one of PGD2 and thereby classified the efficacy of the tested compounds. The licensed drug ramatroban showed a concentration dependent inhibition of PGD2 induced receptor activity in a competitive manner. Surprisingly AA showed a direct partial agonistic effect at the DP2 receptor sensor, while the EC50 was right shifted about three orders of magnitude compared to PGD2. AA led to DP2 receptor induced GIRK channel currents indicating DP2 receptor activation by AA.

The human DP2 receptor FRET sensor is therefore well suited to study and potentially screen novel drug candidates, to directly determine their efficacy and to gain direct insights into their binding kinetics as well as DP2 receptor conformational dynamics. The direct AA effect on DP2 receptor raises the question if DP2 receptor could act as an AA sensor, which would require a high local arachidonic acid concentration.

P175

Mode and sites of action of ligands activating the human GPR84-receptor
S. Pannervelam¹, L. Casimir¹, I. von Kügelegen¹

¹University of Bonn, Department of Pharmacology, Bonn, Germany

Introduction: The G protein-coupled receptor 84 (GPR84) is a poorly characterized, proinflammatory orphan receptor with its pathophysiological roles not yet been completely clarified. The receptor can be activated by medium-chain free fatty acids (MCFAs). In a previous study it has been demonstrated that 2- or 3-hydroxylated MCFAs were effective at activating GPR84. In the present study we investigated the site and the agonistic mode of action of 2-hydroxydodecanoic acid and analogues at the wild type and mutant human GPR84 (hGPR84)-receptors.

Methods: Recombinant wild type and mutant hGPR84-receptors were stably expressed in CHO-Fip-In cells with the expression vector pcDNA5. The receptor expression was visualized using a FITC-coupled antibody directed against the V5-epitope and analysed by laser scanning microscopy. Effects of agonists on forskolin-induced cellular cAMP formation were also analysed in these cells.

Results: Laser scanning microscopy showed a reduced expression of the C3.25A mutant receptor when compared to wild type receptors or R3.26A or H7.35A mutant receptors. 2-Hydroxydodecanoic acid and 2-hydroxytetradecanoic acid induced marked concentration-dependent decreases in forskolin-induced cAMP production in cells expressing wild type receptors (halfmaximal concentrations 2.7 and 0.4 μ M, respectively). Tetradecanoic acid was less potent when compared to 2-hydroxytetradecanoic acid. In cells expressing the C3.25A mutant receptor inhibitory effects of 2-hydroxydodecanoic acid and 2-hydroxytetradecanoic acid were almost lost. A reduction of the responses to 2-hydroxydodecanoic acid and 2-hydroxytetradecanoic was observed in cells expressing R3.26A mutant receptors. The same was true when 2-hydroxydodecanoic acid was tested in cells expressing the H7.35A mutant receptor.

Conclusions: The results confirm potent agonistic actions of 2-hydroxylated fatty acids at the hGPR84. The data indicate a crucial role of the cysteine residue C3.25 for the structure and the expression of the receptor protein. Moreover, the residues R3.26 and H7.35 are likely to be involved in ligand recognition of the receptor.

Pharmacology – Immunopharmacology / inflammation / anti-infectives

P176

A novel CDK12 degrader time and dose-dependently suppresses NF- κ B signaling
J. Priester¹, M. Kracht¹

¹Justus Liebig University Giessen, Rudolf Buchheim Institute for Pharmacology, Giessen, Germany

Introduction: CDK12 and its close homolog CDK13 are elongation-associated CDKs phosphorylating serine 2 of the C-terminal domain of RNA-Polymerase II during transcriptional elongation. CDK12 plays an essential role in the maintenance of genome stability as loss of CDK12 causes a transcriptional defect that affects genes involved in DNA-damage repair and replication. This has led to the concept that CDK12 functions primarily as a tumor suppressor. However, we found that the pro-inflammatory cytokine interleukin-1 (IL-1) triggers the phosphorylation of CDK12 and CDK13 in HeLa cells as revealed by unpublished mass spectrometry analysis of the phospho-proteome. This raises the question, if CDK12 is mechanistically and functionally connected to the IL-1-NF- κ B pathway.

Objectives: We aim to study the impact of rapid CDK12 degradation on the IL-1 signaling pathway, including IL-1 driven gene expression and protein secretion.

Material and methods: HCT116 cells were treated with the novel, cell-permeable PROTAC inhibitor BSJ-4-116, which combines a small molecule that binds to CDK12 with a proteasome targeting domain to promote rapid CDK12 degradation. In parallel, an auxin-inducible degron system was established allowing rapid and transient depletion of CDK12. The influence on the IL-1 signaling pathway was investigated using Western Blot analysis, RT-qPCR and ELISA.

Results: The treatment with the BSJ-4-116 results in almost complete degradation of both, CDK12 and CDK13. BSJ-4-116 time and dose-dependently suppresses IL-1 signaling and the subsequent inducible gene expression and protein secretion. In contrast, the auxin-inducible degron system promotes highly specific degradation of CDK12, but not CDK13, and did not affect IL-1 upstream signal transduction.

Conclusion: The suppression of NF- κ B signaling by the new pharmacological PROTAC approach appears to cause substantial off-target effects (on other protein kinases such as IKKs) or indirect effects (resulting from global transcriptional inhibition by loss of CDK12/13), raising doubts on the specificity of BSJ-4-116. The precise role of CDK12 in relation to CDK13 will therefore be further studied by combining the auxin-inducible degron system with other genetic approaches (e.g. RNAi) in order to unravel the specific contribution of CDK12 and CDK13 to the IL-1-NF- κ B system as well as to inflammatory gene expression in general.

P177**The role of autophagy and the related ER-phagy in coronavirus infected cells**F. M. Dort¹, D. Heylmann¹, M. Kracht¹¹Rudolf Buchheim Institute of Pharmacology, Justus Liebig University, Gießen, Germany

Introduction: The replication of coronaviruses (CoV) is functionally and structurally closely linked to the endoplasmic reticulum (ER). It is therefore not surprising that the infection causes profound activation of ER stress and the unfolded protein response (UPR). Our own published proteome analyses identified a number of CoV-regulated components involved in autophagy (including ER-phagy), ER quality control and ER-associated protein degradation (ERAD). ER-phagy is an autophagy-related process with the capacity to target parts of the ER for lysosomal degradation to maintain ER homeostasis or to terminate (patho)physiological ER expansion.

Objectives: The central aim of this study is to clarify the roles of autophagy, in particular ER-phagy, in the CoV replication cycle. This requires the establishment of methods that facilitate the quantitative measurement of various types of autophagic flux in living cells.

Materials and methods: For this purpose we established a fluorescent tandem reporter system consisting of in frame fusions of ER- (RAMP4) or autophagosome (LC3)-associated proteins with GFP-mCherry proteins. These tandem reporters allow the visualization of activated ER-phagy or autophagy pathways, respectively, based on the rapid loss of GFP fluorescence as soon as the reporter localizes to the lysosome. Using lentiviral transduction, the reporter proteins were transduced into different cancer cell lines (Huh7, HeLa). Successful transduction was validated by Western blot and fluorescence microscopy analyses. Flow cytometry was utilized to measure changes in fluorescence upon starvation and treatment with bafilomycin A1.

Results: Starvation led to the activation of autophagy and ER-phagy in selected parts of the ER, whilst the addition of the lysosomal inhibitor bafilomycin A1 inhibited these processes. Western blot analyses of the canonical autophagy marker proteins (LC3B and p62 / SQSTM1) confirmed the observed changes in autophagic flux.

Conclusion: The combination of the tandem reporter systems with flow cytometry facilitates the quantitative assessment of the proportion of cells that undergo autophagy or ER-phagy during a given period of time. The assay will now be used to monitor the dynamic changes in ER-phagy resulting from coronavirus infection.

P178**CRISPR/Cas9-based activation and depletion of individual cytokine genes**H. Peppler¹, J. Meier-Soelch¹, M. Kracht¹¹Justus-Liebig-Universität, Rudolf Buchheim Institute of Pharmacology, Giessen, Germany

Introduction: Cytokines mediate cell-cell communication during infection and inflammation. Ultimately, the combined activities of all activated cytokine genes and their corresponding proteins precisely regulate the recruitment, activation and differentiation of infiltrating immune cells as well as their communication with local cells in the inflamed tissue environment. Until today, it is still impossible to control the local cytokine environment in a targeted manner.

Objectives: An interesting question, therefore, is if cytokine-associated disease states can be therapeutically targeted at the level of mRNA transcription by repressing or activating specific genes alone or in combination.

Materials and methods: To address this issue, we established clustered regularly interspaced short palindromic repeats (CRISPR)-based activation (using dead Cas9 enzymes and transcriptional activator domains) and knockout systems (using inducible Cas9 wt versions) with the final goal to manipulate individual or specific groups of cytokine genes. An initial focus was to selectively express or suppress the NF- κ B-driven cytokines IL-8 and IL-6 as well as their intracellular negative regulators (*NFKBIA*, *TNFAIP3*).

Results: So far, a variety of lentiviral transduction vectors have been designed and molecularly cloned in order to efficiently transduce epithelial and liver cancer cell lines with the CRISPR activation and depletion systems. In preliminary experiments, the functionality of the vectors has been assessed in tumor cell lines at the mRNA and protein level by combining RT-qPCR, ELISA, and Westernblot analysis. Next, these systems will be used to alter human macrophage phenotypes in co-culture assays by means of the genome-edited tumor cell lines.

Conclusion: Altogether, these CRISPR/Cas9-based systems will be further optimized to modulate key (host-) factors during infection and inflammation with the aim to provide a new mode to control cell-cell communication in innate immune responses.

P179**Analysis of global RNA and protein biosynthesis in response to interleukin-1 by a metabolic labelling approach**S. Hanel¹, J. Maier-Soelch¹, M. Kracht¹¹Justus-Liebig-Universität, Rudolf-Buchheim-Institut für Pharmakologie, Giessen, Germany

Introduction: Members of the interleukin-1 (IL-1) family activate multiple cell types by inducing a rapid, but transient transcriptional activation and secretion of a number of other interleukins and chemokines such as IL-6 and IL-8 (CXCL8). The IL-1-specific gene signature is key to a diverse range of chronic or acute inflammatory conditions, but it is not well understood to which extent IL-1 also affects basic or general cellular processes.

Objectives: During attempts to establish assays to monitor nascent transcription, we coincidentally observed that IL-1 temporarily reduces the global rate of gene transcription in HCT116 and HeLa cancer cells. We therefore investigated this phenomenon in a broader range of cell lines, including diploid, non-transformed cells such as hTERT-RPE-1 epithelial cells or MRC-5 fibroblasts and to correlate it with global protein biosynthesis rates.

Materials and methods: To investigate the basal or inducible kinetics of global transcription rates, we metabolically labelled nascent RNA with the uridine analogue 5-Ethynyluridine (5-EU) in living cells. After fixation of the cells, the alkyne group of 5-EU was covalently coupled to the azide group of a fluorescent dye by means of a copper-catalysed CLICK reaction. In parallel, the puromycin analogue OPP (O-propargyl-puromycin) was used to label newly synthesized polypeptides by the same strategy. We applied fluorescence microscopy to quantify metabolically labelled newly synthesized RNAs and proteins in single cells using the software "CellProfiler".

Results: In five cell lines, treatment with IL-1 for 1 hour downregulated global RNA synthesis by about 10-25% compared to non-treated cells. This effect was inhibited by 5Z-7-Oxozeanol, an inhibitor of transforming growth factor β -activated kinase 1 (TAK1), which is an upstream activator of IL-1 signalling. Inhibition of RNA synthesis occurred transiently at the peak of IL-1-inducible gene expression and ceased thereafter. In contrast, the global synthesis of polypeptides remained unaffected. [1]

Conclusion: These data suggest that cells activated by IL-1 can only provide the rapid and massive supply of further inflammatory mediators at the expense of reducing overall biosynthesis of nucleic acids. The molecular mechanisms behind this observation and its possible implications in the inflammatory process require further investigation.

Pharmacology – Nuclear receptors, enzymes and other targets**P180****Glycolytic flux control by drugging phosphoglycolate phosphatase**E. Jeanclos¹, J. Schloetzer², K. Hadamek¹, N. Yuan-Chen³, M. Alwahsh⁴, R. Hollmann⁴, S. Fratz¹, D. Yesilyurt-Gerhards¹, T. Frankenbach¹, D. Engelmann¹, A. Keller¹, A. Kaestner¹, W. Schmitz⁵, M. Neuschwander⁶, R. Hergenroder⁴, C. Sotriffer³, J. P. von Kries⁶, H. Schindelin², A. Gohla¹¹University of Würzburg, Pharmacology and Toxicology, Würzburg, Germany²University of Würzburg, Rudolf Virchow Center, Würzburg, Germany³University of Würzburg, Pharmacy, Würzburg, Germany⁴Leibniz Institute for Analytical Sciences-ISA, Dortmund, Germany⁵University of Würzburg, Physiological Chemistry, Würzburg, Germany⁶Leibniz Institute for Molecular Pharmacology-FMP, Berlin, Germany

Targeting the intrinsic metabolism of immune or tumor cells is a therapeutic strategy in autoimmunity, chronic inflammation or cancer. Metabolite repair enzymes may represent an alternative target class for selective metabolic inhibition, but pharmacological tools to test this concept are needed. Here, we demonstrate that phosphoglycolate phosphatase (PGP), a prototypical metabolite repair enzyme in glycolysis, is a pharmacologically actionable target. Using a combination of small molecule screening, protein crystallography, molecular dynamics simulations and NMR metabolomics, we discover and analyze a compound (CP1) that inhibits PGP with high selectivity and submicromolar potency. CP1 locks the phosphatase in a catalytically inactive conformation, dampens glycolytic flux, and phenocopies effects of cellular PGP-deficiency. This study provides key insights into effective and precise PGP targeting, at the same time validating an allosteric approach to control glycolysis that could advance discoveries of innovative therapeutic candidates.

P181**ANG – a critical factor in pathological aging and Alzheimer's disease?**M. Joerg¹, J. E. Plehn¹, V. T. T. Nguyen², L. Besseri¹, K. Endres², M. Helm¹, K. Friedland¹¹Institute of Pharmaceutical and Biomedical Sciences, Pharmacology and Toxicology, Mainz, Germany²University Medical Center, Psychiatry and Psychotherapy, Mainz, Germany

Introduction: Alzheimer's disease (AD) is the most common neurodegenerative disease, characterized by gradual cognitive decline and later dementia. Human angiogenin (ANG) is a protein playing a crucial role in stress response and protecting cells. ANG cleaves cytoplasmic tRNAs leading to the inhibition of the proapoptotic signal pathway. In addition

to that, RNA modifications play a critical role in RNA function and stability. The tRNA modification m⁵C plays a crucial role in stress-induced tRNA cleavage [1,2].

Objectives: RNA modifications have already emerged as new and important targets for research and therapy in other neurodegenerative diseases. Neither the pathophysiological role of tRNA functions nor of tRNA modifications is characterized in pathological aging or AD. We aim to characterize tRNA modifications, which have a crucial impact on translation and various other cellular processes, which will contribute significantly to the pathophysiological understanding of AD.

Materials and methods: For determining ANG protein expression, wildtype (wt) C57BL/6J and transgenic (tg) 5x FAD animals were used. All human brain samples were received from the Netherlands Brain Bank (NBB). For mRNA expression levels, RNAseq data from the *Adult Changes in Thought (ACT)* study were analyzed. ANG expression levels were determined using Western Blot. Analysis of tRNA modifications were performed by LC-MS/MS.

Results: We revealed that ANG expression is impaired in animal models and human brain samples in aging and AD. Altered ANG expression, may result in: enhanced apoptosis and increased neurodegeneration. We were able to detect gender-specific effects in AD, which is interesting given the epidemiology of AD, which states that significantly more women are affected in old age. First results of LC-MS/MS revealed changes for m⁵C in aging and AD.

Conclusion: In summary, we revealed that ANG expression is partially altered during aging and AD. This line of research could be a new road to defining early biomarkers for AD and represent an important step toward developing new therapeutic strategies.

[1] Prehn, J. H. M. & Jirstrom, E. Angiogenin and tRNA fragments in Parkinson's disease and neurodegeneration. *Acta Pharmacologica Sinica* (2020).

[2] Fagan, S. G., Helm, M. & Prehn, J. H. M. tRNA-derived fragments: A new class of non-coding RNA with key roles in nervous system function and dysfunction. *Prog. Neurobiol.* 205, 102118 (2021).

P182

The role of RNA modification m¹A in Alzheimer's Disease.

M. Joerg¹, C. Lietz¹, M. Kristen¹, F. Pichot¹, N. Kreim², N. Ruffini³, S. Gerber³, Y. Motorin^{4,5}, M. Helm¹, K. Friedland¹

¹Institute of Pharmaceutical and Biomedical Sciences, Pharmacology and Toxicology, Mainz, Germany

²Institute of Molecular Biology (IMB), Bioinformatic Core Facility, Mainz, Germany

³Institute for Human Genetics, Mainz, Germany

⁴Université de Lorraine-INSERM, Epitranscriptomics and RNA Sequencing (EpiRNA-Seq) Core Facility, Nancy, France

⁵Université de Lorraine, IMoPA, UMR7365 CNRS, Nancy, France

Introduction: Messenger-RNA, transfer-RNA, RNA-derived fragments and RNA modifications offer a new and potential field of cellular regulation and signaling pathways. One mechanism of particular interest to regulate mRNA fate post-transcriptionally is mRNA modification. Especially m¹A mRNA methylation is highly discussed due to methodological differences. However, one single m¹A site in mitochondrial ND5 mRNA was unanimously reported by different groups. ND5 is one subunit of complex I of the respiratory chain. It is considered essential for the coupling of oxidation and proton transport. This m¹A site might be involved in the pathophysiology of Alzheimer's disease (AD). Formation of this m¹A methylation is catalyzed by higher TRMT10C protein levels, leading to translation repression of ND5 [1-3].

Objectives: We aim to examine the function of m¹A in different models ranging from cell models to human brain samples in order to understand the role of m¹A in mitochondrial protein biosynthesis and mitochondrial dysfunction.

Material and methods: Wildtype (wt) C57BL/6J and transgenic (tg) 5x FAD animals were used. All human brain samples were received from the Netherlands Brain Bank (NBB). For mRNA expression levels, RNAseq data from the Adult Changes in Thought (ACT) study were analyzed. TRMT10C expression levels were determined using Western Blot. Analysis of m¹A was performed using an Illumina® sequencing approach.

Results: We found enhanced m¹A methylation of ND5 mRNA in an AD cell model as well as in AD patients. Our findings suggest that this newly identified mechanism might be involved in Aβ-induced mitochondrial dysfunction. We also found altered TRMT10C expression as well as m¹A misincorporation in cell and animal AD models. For the first time, we demonstrated TRMT10C induced m¹A methylation of ND5 mRNA leads to mitochondrial dysfunction.

Conclusion: We hypothesize, that m¹A on mRNA of complex I subunit ND5, is the cause of complex I impairment and mitochondrial dysfunction in aged people and late-onset AD (LOAD).

[1] Rousakis, A. et al. Diverse functions of mRNA metabolism factors in stress defense and aging of *Caenorhabditis elegans*. *PLoS One* (2014).

[2] Safra, M. et al. The m¹A landscape on cytosolic and mitochondrial mRNA at single-base resolution. *Nature* (2017).

[3] Li, X. et al. Base-Resolution Mapping Reveals Distinct m¹A Methylome in Nuclear- and Mitochondrial-Encoded Transcripts. *Mol. Cell* 68, 993-1005.e9 (2017).

P183

Effects of farnesyltransferase inhibitors on matrix-vesicle mediated mineralization in osteosarcoma cells

T. Bürgel¹, D. Diehl¹, H. S. Bachmann¹

¹Centre for Biomedical Education and Research (ZBAF), School of Medicine, Faculty of Health, Witten/Herdecke University, Pharmacology & Toxicology, Witten, Germany

Introduction: Farnesylation describes an important post-translational modification. During this farnesylation process, the heterodimeric enzyme farnesyltransferase (FTase) catalyzes the irreversible covalent binding of a 15-carbon isoprenoid group to proteins containing a C-terminal CAAX-motif. Farnesylation of approximately 200 CAAX-proteins is crucial for their function and ensures to anchor with lipid membranes. These CAAX-proteins play pivotal roles in different cellular processes. Despite its physiological role, farnesylation is also involved in different diseases like cancer or Progeria. After studies with high-throughput screenings, a class of drugs targeting the FTase were developed, the FTase inhibitors (FTI).

Osteosarcoma is one of the most common malignant primary bone tumors mainly occurring in children and young adults. Standard therapy includes a multidrug chemotherapy combined with radiation and resection.

Objectives: Patient survival did not evolve for the last decade, which suggests the need for new specific treatments. The goal is to gain information about the role of farnesylation in osteosarcoma.

Materials and methods: To test the influence of different FTIs SaOS2 cells were mineralization-stimulated and stained with Alizarin Red S. Protein expression was analysed by SDS-PAGE and the characteristic band was sent to nano-LC-ESI MS/MS. To prove the hits, qPCR was performed. A fluorescent assay with a dansylated peptide (GCVLS) was used to measure intracellular FPP levels.

Results: FTI treatment of osteosarcoma cells (SaOS2) resulted in decreased mineral deposition. However, a self-implemented continuous fluorescent enzyme assay measuring intracellular farnesyl pyrophosphate (FPP) accumulation could not prove the theory of an inhibitory effect through accumulation of FPP yet. Furthermore, exogenous FPP and GGPP have no impact on the mineralization. A nano-LC-ESI MS/MS proteome analysis of a characteristic SDS band appearing in treatment groups showed upregulation of Lamin B1, a farnesylated protein of the nuclear envelope and marker for cell senescence in cancer.

Conclusion: This project may lead to a better understanding of farnesylation in osteosarcoma as well as for the impact of the nuclear Lamin network in cell physiologies. Furthermore, FTIs might be an interesting therapeutic option for Osteosarcoma in the future.

P184

Pharmacological characterization of the interaction between human farnesyltransferase variants with the proto-oncogene Ras

J. J. Schott¹, S. Hinz², H. Bachmann¹

¹Institute of Pharmacology and Toxicology, Center for Biomedical Education and Research (ZBAF), School of Medicine, Faculty of Health, Witten/Herdecke University, Pharmacology and Toxicology, Witten, Germany

²PharmaCenter Bonn, Pharmaceutical Institute, Pharmaceutical & Medicinal Chemistry, Rheinische Friedrich-Wilhelms-Universität Bonn, Bonn, Germany

Introduction Farnesylation is a post-translational modification in eukaryotic cells that is essential for the functionality and signal transduction of several proteins, particularly Ras, which is very important for cell growth and differentiation. In this process, the heterodimeric enzyme farnesyltransferase (FTase) attaches a 15-carbon isoprenoid group to a C-terminal CAAX motif of the target proteins. In addition to the already known FTase F1, our research group recently discovered four new variants of FTase that share the same α-subunit (FT-α) but differ in their β-subunit (FT-β). Farnesylation is essential for the localization of Ras to the cell membrane, its activation and therefore its correct function. In order to inhibit its activity in cancer, farnesyltransferase inhibitors (FTIs) such as Tipifarnib and Lonafarnib have been developed. The failure of these FTIs in oncogenic therapy might be related to the tissue-specific expression of the different FTase variants and tumor-type-dependent mutations of Ras isoforms.

Objectives We aim to characterize the interaction between the FTase variants with their physiological partner FT-α and their substrate Ras. Furthermore, we will also investigate a possible inhibitory effect of FTIs on the FTase variants.

Methods NanoBit assays were performed in order to detect real-time protein-protein interaction of the FTase variants with Ras as well as to examine the influence of the FTIs Tipifarnib and Lonafarnib on the mentioned interactions.

Results Our results indicate strong interaction of F1 with both FT-α and the tested Ras proteins, whereas the new FTase variants show a reduced interaction with its partner FT-α in comparison to F1. Furthermore, the interaction between FTase variants with H-Ras and KRas4B is significantly higher than with FT-α. By adding the FTIs Lonafarnib and Tipifarnib, we can observe a significant decrease in protein interaction for the different variants proportional to the FTI concentrations.

Conclusion Our results are promising and show that the NanoBit assay is a powerful tool to detect the efficacy of various new FTIs in the future and may lead to a more detailed elucidation of Ras farnesylation. Furthermore, characterization of the new variants is

important, as there is little knowledge about their detailed function, capabilities, and inhibitability by FTIs.

P185

Metabolic effects of *Cimicifuga racemosa* extract Ze 450 on mitochondria and implications for the resistance against oxidative cell death

M. Günther¹, M. Rabenau², J. Drewe², G. Boonen², V. Butterweck², C. Culmsee¹

¹Philipps-Universität Marburg, Klinische Pharmazie, Marburg, Germany

²Max Zeller Söhne AG, Romanshorn, Switzerland

Cimicifuga racemosa extract is a well-established herbal medication widely prescribed to treat menopausal symptoms that has gained interest as a metabolic regulator. Recent work suggests that *Cimicifuga racemosa* extract Ze 450 directly regulates mitochondrial energy turnover through its actions on complex I of the mitochondrial electron transport chain (ETC) [1-4]. However, the mechanisms by which *Cimicifuga extract* Ze 450 affect the formation of mitochondrial energy metabolites, representing a key role for the ETC activity, remain poorly defined.

To gain a comprehensive insight into the signaling effects of the extract on the mitochondrial proteome and metabolome, neuronal HT22 cells were treated with Ze 450 and analyzed by mass spectrometry. Real-time measurements of mitochondrial and glycolytic respiration were performed to detect acute effects of the *Cimicifuga* extract on the mitochondrial energy release. MitoPlates® were used to understand how substrate utilization and metabolic activity can be reprogrammed upon treatment.

Here we demonstrate that Ze 450 inhibits glucose and glutamine utilization in mitochondria leading to a suppressed mitochondrial-dependent biosynthetic activity. Rather, *Cimicifuga racemosa* extract Ze 450 decreases the flow of glucose- and glutamine-derived metabolic intermediates into the Tricarboxylic Acid (TCA) cycle, leading to reduced citrate production and de novo lipid biosynthesis. In models of oxidative stress, it was also shown that reprogramming of mitochondrial metabolism by Ze 450 is largely dependent on glutamine depletion, as inhibition of glutaminolysis – but not the depletion of glucose entry into the TCA cycle, resulted in protection against ferroptosis.

Our data indicate that the metabolic effects of *Cimicifuga racemosa* extract Ze 450 are due to restriction of important anaplerotic substrates required for TCA cycle-dependent biosynthesis. These observations provide both new insight into the mechanism of Ze 450 action on metabolic adaptations but also highlight its role for the resilience against age-related processes engaged by impaired mitochondria and the loss of antioxidative capacities.

References:

1. Moser C et al., *Phytomedicine* 2014; 21: 1382-1389.
2. Friederichsen et al., *Arch Gynecol Obstet* 2020; 301: 517-523.
3. Rabenau et al., *Phytomedicine* 2019; 52: 107-116.
4. Rabenau et al., *Antioxidants* 2021; 10: 1432.

Pharmacology – Signal transduction and second messengers

P186

Relevance of Rac1 in doxorubicin-induced cytotoxicity in different primary cardiac cell types

P. Kucuk¹, G. Fritz¹

¹Heinrich Heine University Düsseldorf, Institute of Toxicology, Düsseldorf, Germany

Introduction: Irreversible cardiotoxicity limits the clinical use of doxorubicin (DOX) in cancer therapy. Lipid lowering drugs (statins) and small-molecule Rac1 inhibitors have been shown to mitigate the DOX-induced cardiotoxicity. However, cardiomyocyte-specific Rac1 knockout mouse models failed to fully reflect the benefit of the pharmacological inhibition of Rac1.

Objectives: In this study we aimed to investigate the relevance of Rac1 and other Rho GTPases in DOX-induced cytotoxicity in different primary cardiac cell types.

Materials and methods: Primary cardiomyocytes, cardiac endothelial cells and cardiac fibroblasts isolated from the hearts of C57BL/6 mice were used to investigate the cytotoxic effects of DOX, in the presence or absence of Rac/Rho inhibitors. DNA double-strand break (DSB) formation and repair were analysed by detection of nuclear γH2AX foci. Expression of selected genes was determined by real-time RT-qPCR. Cell viability and apoptosis were evaluated using the Alamar Blue and TUNEL assays, respectively.

Results: DOX-induced DSB levels varied markedly between the cardiac cell types. In cardiomyocytes, relatively low levels of DSB were induced and remained persistent after DOX treatment. Efficient repair of DOX-induced DSB was observed only in cardiac endothelial cells and cardiac fibroblasts. In all of the cell types, pharmacological inhibition of Rac1 and/or Cdc42 attenuated DOX-induced DSB formation. DOX reduced the viability of all primary cardiac cell types in a dose dependent manner. Yet, a substantial induction of apoptosis following DOX treatment was not observed in cardiomyocytes. Despite the marked reduction in the formation of DSB, pharmacological inhibition of Rac1 only mildly ameliorated DOX-induced cytotoxicity in a dose and cell type dependent manner.

Conclusion: Our findings suggest that (i) cardiac cell types other than cardiomyocytes are also of substantial importance in the pathophysiology of DOX-induced cardiotoxicity and (ii) both Rac1 and Cdc42 impact the DOX-induced DNA damage response in other cardiac cell types than cardiomyocytes.

P187

PP2A-PR72 improves contractile function of cardiomyocytes

J. R. Herting¹, J. H. König¹, U. Kirchhefer¹

¹University of Münster (WWU), Pharmacology and Toxicology, Münster, Germany

Question: PP2A-PR72 is a cytosolic, Ca²⁺-binding protein, mainly expressed in myocardium. As a regulatory subunit of protein phosphatase 2A (PP2A), PR72 forms a heterotrimeric complex together with a catalytic C and structural A subunit. It has been hypothesized that PR72 regulates activity and targeting of PP2A. But only few is known about cardiac function of PR72-PP2A.

Methods: Therefore, we overexpressed PP2A-PR72 in transgenic mouse hearts under control of the αMHC promoter (TG). We measured protein expression levels by Western blotting, PP2A activity, and sarcomere length (SL) shortening and Ca²⁺ transients in isolated ventricular cardiomyocytes, electrically stimulated at 0.5 Hz, under basal conditions, maximum β-adrenergic stimulation by 1 μM isoprenaline, and PP2A-inhibiting conditions using 3 nM okadaic acid (OA).

Results: The total protein content of PP2A-PR72 was elevated by 2.5-fold in TG hearts while expression of the catalytic PP2A subunit and global PP2A activity were unchanged between groups.

Under basal conditions, TG vs. wild type (WT) cells showed increased SL shortening (amplitude: 0.08±0.06 vs. 0.04±0.04 μm, respectively, n=120, P<0.05) and hastened SL relengthening (τ: 0.22±0.15 vs. 0.33±0.23 s, respectively, n=120, P<0.05). In addition, TG vs. WT cells had increased Ca²⁺ transient amplitudes (0.11±0.04 vs. 0.09±0.04 r.U., respectively, n=120, P<0.05) and faster Ca²⁺ decay (τ: 0.36±0.14 vs. 0.47±0.17 s, respectively, n=120, P<0.05).

Maximum β-adrenergic stimulation enhanced contractile function and Ca²⁺ cycling in TG and WT cells. TG vs. WT cells exhibited increased SL shortening (amplitude: 0.26±0.08 vs. 0.23±0.09 μm, respectively, n=60, P<0.05) and faster Ca²⁺ decay (τ: 0.12±0.03 vs. 0.15±0.04 s, respectively, n=60, P<0.05).

PP2A inhibition by OA accelerated SL relengthening by 39 % (τ, n=60, P<0.05 vs. basal) and Ca²⁺ decay by 17 % (τ, n=60, P<0.05 vs. basal) only in TG cells while WT cells were not affected. In contrast, OA treatment increased Ca²⁺ transient amplitudes only in WT cells while TG cells remained unchanged.

Conclusion: Taken together, PP2A-PR72 overexpression improved contractile function and Ca²⁺ cycling of cardiomyocytes under basal conditions and under β-adrenergic stimulation. Since PP2A activity was unchanged in whole-heart homogenates and PP2A led to different functional phenotypes in TG vs. WT cells, PR72 might promote local targeting of PP2A to contractile and Ca²⁺ regulating effectors of the myocardium.

P188

Enhanced cAMP level and cAMP-dependent transcription in human induced pluripotent stem cell derived atrial cardiomyocytes with Annexin A4 knockout

J. Schmidt¹, M. Seidl¹, F. U. Müller¹, U. Kirchhefer¹, E. Fehrmann¹

¹Institute of Pharmacology and Toxicology - University of Münster, Münster, Germany

Annexin A4 (AnxA4), a member of the Ca²⁺ and phospholipid-binding annexin protein family, is associated to atrial fibrillation (AF). In previous studies, we identified AnxA4 as a specific inhibitor of adenylyl cyclase type 5 (AC5) in HEK293 cells. AC5 catalyses cAMP production and AC-cAMP signalling dysregulation plays a role in AF development. Thus, we investigated whether AnxA4 is involved in the cAMP-dependent regulation of gene transcription in human induced pluripotent stem cell-derived atrial cardiomyocytes (iPSC-aCM).

Therefore, we generated an AnxA4 knockout (KO) in an iPSC wildtype (WT) line using CRISPR/Cas9. The AnxA4-KO iPSC line showed typical iPSC morphology, normal 46, XY karyotype and loss of AnxA4 protein detected by western blot. To promote atrial cell fate, small molecule based 2D differentiation to iPSC-aCM was induced via retinoic acid treatment (0.5 μM). Four weeks after differentiation and maturation, KO iPSC-aCM showed increased intracellular cAMP levels vs. WT (fmol cAMP mean±SEM: WT 2147±264, KO 3224±129*, WT/KO n=5 cell lysates from independent differentiations each, *p<0.05 vs. WT) under acute AC stimulation using forskolin derivative NKH477 (NKH, 50 μM for 1 h), while no differences under basal conditions were detected. Further, increased cAMP levels were associated with mRNA upregulation of cAMP-dependent target genes like proapoptotic transcription factor inducible cAMP early repressor (ICER) and gluconeogenesis involved phosphoenolpyruvate-carboxykinase 1 (PCK1) under direct AC stimulation with NKH. By RT-qPCR we then analysed if the observed transcriptional changes correlate to NKH stimulation in a time- and/or concentration-dependent manner. The concentration series (0.03-3 μM, each for 1 h) showed that lower NKH concentrations were sufficient for the induction of ICER (0.03 vs. 0.06 μM) and PCK1 (0.3 vs. 3 μM) in KO vs. WT. Time series (15-150 min, each 1 μM NKH) revealed an earlier ICER (30 vs. 45 min) induction in KO vs. WT. While PCK1 mRNA induction was observed in KO (45 min), no induction was detected in WT.

In conclusion, AnxA4 KO iPSC-aCM showed increased cAMP levels after direct AC stimulation with NKH, most likely caused by abolished AC5 inhibition due to deletion of AnxA4. Moreover, cAMP elevation in AnxA4 KO iPSC-aCM was accompanied by an upregulation of cAMP-target genes. These findings demonstrate AnxA4 as a main regulator of cAMP production and transcription in human iPSC-derived atrial cardiomyocytes.

P189

cNMPs as potential therapeutics for various human carcinoma cell lines

S. Wolter¹, M. Postels¹, L. A. Giller¹, R. Seifert¹

¹Hannover Medical School, Institute of Pharmacology, Hanover, Germany

Introduction: Breast cancer has overtaken lung cancer as the most commonly diagnosed malignant neoplasias in women. Ovarian cancer is also a common neoplasia in women (1). Therefore, the development of new therapeutic approaches is necessary. Previously, we demonstrated the apoptosis-inducing potential of cCMP and cUMP in S49 mouse lymphoma cells and in a human erythroleukemia cell line (2).

Methods: We analysed the anti-proliferative effects of the second messengers cAMP, cGMP, cCMP and cUMP, using the membrane-permeable acetoxymethyl ester analogues (cNMP-AMs). We used the alamarBlue assay to analyse proliferation of the human estrogen (ER) and progesterone (PR) receptors-positive MCF-7 and the ER- and PR-negative MDA-MB-231 (MDA) breast cancer cell lines. Furthermore, we analysed the effects of cNMP-AMs on proliferation of the ovary cancer cell lines PA-1, SK-OV-3, SW 626 and Caov-3. qRT-PCR analysis was performed for expression of MDR4, MDR5 and PDE-isoforms. Transporters were inhibited by probenecid and PDEs with IBMX or PDE-isoform specific inhibitors.

Results: We found a cell type-specific expression pattern for MDR4 and MDR5. All cNMP-AMs showed a time- and concentration-dependent anti-proliferative effects in MCF-7 and MDA cells, whereas the control substance PO4-AM3 had no effect. cCMP-AM was the most potent compound in both cell lines. Combination of cNMP-AMs with a MRP inhibitor augmented the anti-proliferative effects. Ovarian cancer cells responded to cNMP-AMs in a cell-line-specific manner. The proliferation of SW 626 cells was unaffected, but combination with probenecid slightly reduced proliferation. Otherwise, all cNMP-AMs reduced proliferation in PA-1 cells. SK-OV-3 and Caov-3 cells shows a nucleobase-specific reaction.

Conclusion: Our data show an anti-proliferative activity of cCMP-AM in MCF-7 and MDA cells and different effects in ovarian cancer cell lines. The results for the MDA cells are particularly important because this cell line has been used as a model for the currently difficult-to-treat form of breast cancer. We thus plan to perform further studies in other cancer cell lines with cNMP-AMs and other membrane-permeable analogues in combination with PDE- and MRP-inhibitors to analyse the mechanisms. Further, comparative expression-studies could help to understand the different responsiveness of the cell lines to cNMP-AMs.

References:

[1] Siegel, RL *et al.*, *J. Clin. Oncol.* 7:209-249 (2021)

[2] Dittmar, F *et al.*, *Biochem Pharmacol.* 112:13-23 (2016)

P190

Identification of constituents conveying signals from MYD88L265P and CXCR4 or CXCR4-WHIM mutants leading to enhanced malignancy of Waldenstrom macroglobulinemia

L. Abdella¹, M. Wist¹, P. Gierschik¹, B. Moepps¹

¹Universitätsklinikum Ulm, Institut für Experimentelle und Klinische Pharmakologie, Toxikologie und Naturheilkunde, Ulm, Germany

Introduction: Waldenstrom macroglobulinemia (WM) is an indolent B-cell lymphoproliferative disorder characterized by bone marrow infiltration by IgM-secreting lymphoplasmacytic cells. A somatic mutation in MYD88L265P is described in 90% of WM patients, while CXCR4-WHIM mutations are present in 30-40% of the cases. CXCR4-WHIM mutations are associated with lower response rates to the Bruton's tyrosine kinase (Btk) inhibitor ibrutinib.

Objective: The identification of potential constituents conveying signals from MYD88L265P and CXCR4 or CXCR4-WHIM mutants, thus leading to enhanced malignancy of WM.

Materials and methods: Cellular signaling (inositol phosphate production, changes in protein kinase phosphorylation and NFκB-regulated transcriptional activation) and protein-protein interactions (*NanoBRET*[™] Technology) were addressed in cells exogenously and/or endogenously expressing MYD88L265P and CXCR4-WHIM mutants.

Results and conclusion: Co-expression of MYD88L265P with wild type Btk or constitutively active BtkE41K resulted in increased inositol phosphate formation, which was synergistically enhanced in the presence of PLCγ2. As shown by BRET studies interaction of Btk and PLCγ2 is increased by co-expression of the Btk activator Syk and further enhanced by the B cell linker protein SLP65. These findings imply that MYD88 acts to amplify BCR-induced, Btk-regulated, and PLCγ2-mediated cellular signaling. In contrast to the widely accepted assumption that CXCR4 regulates phospholipase activity, no CXCR4- or CXCR4-WHIM mutants-induced Btk-mediated PLCγ2 activation was observed in cells exogenously or endogenously expressing CXCR4 and PLCγ2. Since the activation

of hematopoietic cell kinase (Hck) has been reported to confer ibrutinib resistance, we set out to analyze Hck activation as potential converging signal of MYD88L265P and CXCR4-WHIM mutant-induced signaling. BRET experiments show that expression of Hck increases Btk/PLCγ2 interaction, which is enhanced in the presence of MYD88L265P. Similarly, BRET studies show a direct interaction of Hck with Syk which is augmented in presence of MYD88L265P. Interestingly, a ligand-independent interaction of Hck with CXCR4 and CXCR4 WHIM mutants was also observed. In view of the reports indicating the important pro-survival role of Akt activation in WM cells with CXCR4 WHIM mutations, the role of Akt as a downstream target of Btk and Hck is currently investigated.

P191

Plexins are required for epithelial regeneration

D. Zhao¹, I. Matkovic¹, D. Brandt¹, T. Worzfeld¹

¹Marburg University, Institute of Pharmacology, Biochemical-Pharmacological Center (BPC), Marburg, Germany

The intestinal epithelium is the fastest self-renewing tissue in mammals. Under homeostatic conditions, this self-renewal is driven by intestinal stem cells and rapidly proliferating cells in the so-called transit amplifying zone. Plexins comprise a family of transmembrane receptors for semaphorins. The semaphorin-plexin system plays important roles in cell-cell communication in different biological contexts, e.g., nervous system development and immune responses. However, the functional significance of semaphorin-plexin signaling in epithelial cells is incompletely understood. Here, we show that plexins are expressed in the intestinal epithelium. Gene deletion studies in mice *in vivo* and in intestinal organoids *in vitro* indicate that, under physiological conditions, plexins are dispensable for intestinal form and function. In contrast, our data demonstrate a critical requirement of plexins for intestinal regeneration after irradiation injury. Moreover, we show that plexins mediate this regenerative effect via the modulation of the activity of small GTPases. In summary, our findings reveal an important function of plexins in intestinal regeneration.

P192

Development of a cUMP-specific BRET sensor

T. Dolgner¹, D. Neumann¹, R. Seifert¹, B. Schirmer¹

¹Medizinische Hochschule Hannover, Institut für Pharmakologie, Hannover, Germany

In contrast to the 3',5'-cyclic nucleotides cAMP and cGMP, little is known about the analogous pyrimidine nucleotides. First indications of a functional relevance in eukaryotic cells came from the fact that several bacterial toxins, originally classified as pure adenylyl cyclases or guanylyl cyclases, turned out to be promiscuous nucleotidyl cyclases instead¹. In a mouse lung infection model, it was shown that cUMP in particular correlated with the severity of the disease². While the quantification of cyclic pyrimidine nucleotides is now possible in a highly specific and sensitive manner using HPLC-MS/MS analysis, there is still no way to determine cellular cCMP and cUMP concentrations in intact cells in real time. Based on the recently identified effector proteins PycTM (cCMP-specific) and PycTIR (cUMP-specific), which are highly conserved in bacteria³, we want to develop sensor proteins that are tagged using nanoluciferase (NLuc) and the fluorescent protein mVenus in such a way that a change in the BRET (*bioluminescence resonance energy transfer*) ratio occurs after ligand binding. First, we generated a PycTIR-based cUMP sensor for this purpose, since this protein is a cytosolic protein for which the design of a sensor is presumably more straightforward than for transmembrane proteins such as PycTM. Starting with the complete NLuc-PycTIR-mVenus sensor protein, in which both cUMP binding and the functionality of the BRET interaction partners could be shown, the efficiency of the sensor is further optimised by targeted truncation of the native protein.

¹Voigt, Ulrike *et al.* (2011) The effector protein ExoY secreted by *Pseudomonas aeruginosa* is a nucleotidyl cyclase with preference for GTP. *BMC Pharmacol* 11 (Suppl 1), P74

²Kloth, Christina *et al.* (2018) The Role of *Pseudomonas aeruginosa* ExoY in an Acute Mouse Lung Infection Model. *Toxins* 10(5):185.

³Tal, Nitzan *et al.* (2021) Cyclic CMP and cyclic UMP mediate bacterial immunity against phages. *Cell* 184 (23):5728 - 5739.e16

Author index

A

Abbas, A. P149
 Abbas, N. P140
 Abd Alla, J. P167
 Abdella, L. P190
 Abdollahi, A. 20
 Abel-Beckmann, M. P053
 Abraham, K. 1, P063, P032, 3
 Abu-Taha, I. P079
 Achner, L. 60
 Ackermann, G. P035
 Adjaye, J. P135
 Agarwal, N. 65
 Aherrahrou, Z. 60, 61
 Ahmadreza, D. 20
 Aigner, A. P075
 Aigner, E. P113
 Algharably, E. 51, P074
 Alsaleh, R. P039, 33, 72
 Alt, P. P059
 Altenbuchner, A. 48
 Alwahsh, M. P180
 Amézaga Solé, N. 37
 Anastasi, A. A. P125
 Andersson, N. P125
 Andreadaki, A. P092
 Andresen, K. J. P065
 Andrikyan, W. P100, 48
 Anger, L. T. P061
 Anliker, M. 17
 Annibale, P. 43
 Anton, A. P155
 Aparicio Soto, M. P149
 Apel, P. P038
 Arnold, C. 57
 Arseniu, A. P102, P104
 Artursson, P. P114
 Avondet, M.-A. 27, P163
 Avramopoulos, P. 83
 Azatsian, K. P086
 Aßfalg, K. 81

B

Babaei Khorzoughi, R. 83
 Bachmann, H. S. P007, P111, P183, P184
 Bachmann, J. P093
 Bader, M. 60
 Bakchoul, T. 76
 Ballester Casals, J. P125
 Bals, R. 18
 Ban, E.-G. P123
 Banerjee, K. P011
 Bankoglu, E. E. P124
 Baranyai, T. 85
 Bartel, K. 64
 Barth, H. P161, 26, P164, 29
 Bartsch, R. P060
 Batke, M. P031, P050
 Bauer, B. P041
 Baumgarten, B. T. 11
 Bebe, E. 63
 Bech, K. P129
 Becher, F. 27
 Beck, A. P018
 Beck, C. 82, 9
 Becker, K. P090
 Becker, W. P002
 Beckschulte, M. P037
 Bedke, J. 22
 Beer-Hammer, S. 76, 19
 Beisswenger, C. 18
 Bell, D. P125
 Bellmann-Weiler, R. 17
 Below, M. 46
 Beneke, V. 84
 Bentele, M. P140
 Bergau, N. 1
 Berlin, M. 65
 Bernhard-Brendel, M. P103
 Bernhard, M. 37, P073
 Bertermann, R. 71
 Bertsche, T. P142
 Besser, M. P007
 Bessler, L. P181
 Betzer, S. P148
 Birk, B. P127, P136, P137, P116, P147
 Birkenfeld, L. P024
 Birnbaumer, L. 65
 Bischof, H. P023, P024
 Bitsch, A. 52
 Bittner, A. P174
 Blank, A. 25, P008
 Bleich, S. 50
 Bloch, D. 75
 Bluemlein, K. P118

Blömeke, B. P154
 Blümmel, T. P129
 Boden, P. P033
 Bodi, D. 6
 Boehm, U. 65
 Boengler, K. 57
 Bohlen, D. 68
 Boivin-Jahns, V. 41
 Bolduan, V. 38
 Bollheimer, C. P105
 Bomhard, A. 82
 Bonzon, J. P109
 Boonen, G. P185
 Boran, B. 27
 Borchers, J. 5
 Borho, J. 29
 Bouwmeester, H. P129
 Braekow, P. P081
 Braeuning, A. 2, 7, 53
 Brand, T. 11
 Brandes, R. 60, 61
 Brandt, D. P191
 Brandt, M. 18
 Brandt, S. 3
 Brauch, H. P023
 Braun, A. 84
 Bredeck, G. 28
 Breljak, D. P117
 Brendel, K. P103
 Brenner, H. 3
 Brenner, M. P065
 Brinkmann, B. P060
 Brinkmeier, H. 39
 Brock, W. 71
 Brockmeyer, H. 52
 Brockmüller, J. P019, P117
 Brode, J. 5
 Bros, M. 38
 Bruckmüller, H. P071, 56
 Brueckner, J. P022
 Bruening, T. 69
 Bruer, G. P132
 Brunner, T. 57
 Bruns, D. 65
 Bröker-Lai, J. 65
 Brüning, T. 34, P110
 Buchmüller, J. P037
 Burczyk, M. 81
 Burghardt, R. 4
 Burhenne, J. 25
 Burk, O. P113, P114
 Burkhalter, M. 81, 79
 Burns, L. 27
 Bury, D. 34, 69
 Busch, M. 28
 Busschots, K. 27
 Butterweck, V. P185
 Bánki, Z. 17
 Böhme, M. P101
 Büch, T. P075
 Büchter, C. P010
 Bünemann, M. P096, 40, P171, P172, P173, P174
 Bünger, J. P145
 Büning, T. H. P064, P065
 Bürgel, T. P183
 Bürkle, A. 74, P046, 31, P048

C

Cabuta, M. P157
 Campbell, K. 27
 Camunas-Soler, J. 63
 Capellacci, S. 6
 Carlsson, M. J. 8, P053
 Cartledge, G. P125
 Cascorbi, I. P071, 56, P072
 Casimir, L. P175
 Cebo, M. 76
 Cesnaitis, R. P125
 Chao, Y.-K. 64
 Chatterjee, A. P006
 Chatterjee, M. 76
 Chaves-Olarte, E. 26
 Cheng, C.-C. 82
 Chis, A. A. P102, P104
 Cho, H. P028
 Choi, J. P126
 Chovolou, Y. P038
 Christ, B. 84
 Christ, P. 46, 47
 Christmann, M. P040, 57, 8
 Ciuciulkaite, I. 15, P107, 23
 Coecke, S. P127
 Colbourne, J. P150, P151
 Conerney, C. P029
 Coricovac, D. P143
 Corley, R. P054
 Cramer von Clausbruch, C. A. 87, P150, P151
 Cretu, O.-M. P157
 Creutzenberg, O. P132
 Cruz Santos, M. P024

Culmsee, C. P005, 62, P185
 Curato, C. P149

D

Dabbars, A. P138
 Dahlhaus, P. P172
 Dahling, V. 50
 Dai, X.-Q. 63
 Damme, K. 22
 Daniel, H. 22
 Das, A. 72
 Das, S. P144
 Datz, C. P113
 de-Lourdes Marzo Solano, M. P126
 Defranoux, F. P106
 Degen, G. H. 4
 Dehelean, C. A. P143, P156, P155, P157
 Deißler, A. 19
 Dejban, P. 20
 Dekant, R. 71, 35
 Dekant, W. 71
 Delaval, M. N. 72
 Dell'Aversano, C. 6
 Dembski, S. 84
 Demel, T. P139
 Demuth, P. 57, P036
 Denise, B. P152
 Denzinger, S. 11
 De Rijcke, M. P065
 Dettmann, P. P163
 Di Buccchianico, S. 72
 Dickmeis, T. 87, P150, P151
 Diehl, D. P183
 Dietrich, A. P059
 Dietrich, T. P085
 Dimov, K. P088
 Dinkel, K. 65
 Dittmer, U. 15
 Dittrich, K. 76
 Dittrich-Breiholz, O. 10
 Djuari, M. P052
 Dobrea, C. M. P102, P104
 Dobrev, D. P079
 Dobreva, G. P011
 Dobrikov, T. P129
 Dolga, A. 77
 Dolgner, T. P192
 Doll, T. 52
 Dony, E. P045
 Dopler, A. 17
 Dorina, C. P157
 Dormann, H. 48
 Dörner, B. G. 27, P163, P165
 Dörner, M. B. P163
 Dort, F. M. P177
 dos Santos, T. 63
 Draheim, C. P122
 Drees, A. P050
 Drees, D. 17
 Drewe, J. P185
 Drexler, H. 73, P066
 Driemert, P. P137
 Drozdzik, M. P119
 Dubrall, D. 46, 47, P101
 Dumke, R. 49
 Duong Phu, D. M. 81
 Duran Fernandez, I. 9
 Dürr, P. P100

E

Ebert, K. E. 69
 Eble, F. 31
 Ebner, I. P067
 Ebner, T. 21
 Eckstein, D. P055
 Eder, S. P113
 Egele, K. P154
 Ehrhardt, A. P007
 Eichel, L. 68
 El-Armouche, A. 14, 49
 Elenscheider, L. P140, P052
 El Houari, A. P165
 Eliasson, E. P112
 Ellinger, B. P136
 Elsner, C. 15
 Endig, L. P046
 Endres, K. P181
 Endres, S. 58
 Engelhardt, J. 16
 Engelhardt, S. 82, 83, P080, 9
 Engeli, S. P090
 Engelke, M. 52, P052
 Engelmann, D. P180
 Engelmann, J. 4
 Erbay, A. P134
 Erhard, F. P073
 Ermanni, E. S. M. P109
 Ernst, K. P161
 Ernst, S. P171
 Escher, S. E. P050, P140, P118

- Esfandiyari, D. 83, P080
 Eshwaran, R. P006
 Eskici, G. 42
 Esselen, M. P034, P068
- F**
 Fabian, E. P141, P116, P147, P148
 Fabricius Pedersen, M. 42
 Fahrer, J. 57, 8, P033, P035, P053, P036
 Fahrländer, J. P095
 Falkenberg, F. P108
 Faragó, N. 85
 Farker, K. P100
 Federmann, S. P089
 Fehrmann, E. P188
 Feiertag, K. 75
 Felder, T. K. P113
 Feldman, A. P113
 Fellermann, M. 29
 Fels, B. 60
 Felske, C. P053
 Fender, A. P079
 Fender, J. 41
 Feng, V. P158
 Feng, Y. P006
 Ferdinandy, P. 85
 Ferreira, M. P106
 Feuerherd, M. 82
 Fiedler, J. P078, P003, 84, P140
 Fischer, B. C. 75, 54, P043, P047
 Fischer, D. P004, P092
 Fischer, F. P051
 FitzGerald, R. P031
 Foerster, K. 25
 Foil, D. P043
 Fomba, K. W. 28
 Foth, H. P055
 Frankenbach, T. P180
 Fratz, S. P180
 Freeling, F. P093
 Freichel, M. 65
 Frericks, M. P045
 Fresnais, M. P121, 59
 Frey, M. P093
 Friedland, K. P181, P182
 Frischmuth, T. 82
 Fritz, G. P186, P134, P089, P044
 Fromknecht, S. P022
 Fromm, M. F. 22, 48, P100
 Fromme, H. 4
 Frum, A. P102, P104
 Fu, X. 76
 Fuchs, M. P091
 Fuchs, M. P078, P003, 84, P140
 Funk, F. 11
 Funk-Weyer, D. P127, P136, P137, P141, P116, P147, P148
 Funk Weyer, D. P045
 Fux, V. 17
 Förderreuther, S. P098, P099
 Förtsch, S. P036
 Füchtbauer, A. 12
 Füchtbauer, E.-M. 12
- G**
 Gahn, J. P011
 Gao, B. P164
 Garreis, F. P170
 Gaul, C. P098, P099
 Gaulton, K. J. 63
 Gawaz, M. 76
 Gayen, S. P069
 Gebauer, L. P019
 Gebel, J. P004
 Gedik, N. 11
 Geisler, R. 87
 Geisler, T. 76
 Geisslinger, F. 64
 Genth, H. P162
 Genuneit, J. 3
 Gerber, S. P182
 Gergs, U. P081, P082, P083, P084, P085, P086, P087, P088
 Gerhard, R. P160
 Germann, A. P131
 Gerull, F. 4
 Ghibu, S. P102
 Giehm, L. 42
 Gierschik, P. P190, 58
 Giesen, J. 12
 Giller, L. A. P189
 Giri, V. P127, P137
 Giricz, Z. 85
 Gisselmann, G. P004, P092
 Gissi, A. P125
 Glahn, F. P055
 Gleiss, K. 32
 Gligor, F. P102, P104
 Gnaiger, E. P146
 Gobrecht, P. P004, P092
 Gohla, A. P180
 Goldstone, J. P106
 Graf, F. P129
- Graumann, J. P076
 Graupera, M. P011
 Greiner, B. 13
 Greiner, T. 50
 Greweling-Pils, M. C. 86
 Griem, P. 69
 Griesmacher, A. 17
 Grimm, C. 64
 Grohmann, R. 50
 Grottker, J. P152
 Groß, D. P023
 Groß, S. P078
 Grube, M. P014
 Gräter, H. P026
 Gröne, H. J. P009
 Gründemann, D. P017
 Guan, K. 14
 Gudermann, T. P059, P018
 Guedes, M. 18
 Gundert-Remy, U. P031
 Gupta, P. P011
 Gursky, E. 87
 Guver, E. P046
 Gyöngyösi, M. 85
 Göen, T. 73, P066
 Göllitz, F. P057
 Görbe, A. 85
 Gümüs, K. S. P008
 Günther, M. P185
- H**
 Haag, M. 22, P113, P114
 Haake, V. P137
 Haarmann-Stemmann, T. 55
 Haberkorn, U. 65
 Habrian, C. 42
 Hadamek, K. P180
 Haefeli, W. E. 21, 25, 59, P008, P121,
 Haenisch, B. P108
 Hafkemeyer, A. 39, P090
 Hafner, S. 17
 Hagemann, A. P007
 Haibel, N. P145
 Hainke, B. P077
 Halawa, M. P006
 Hambruch, N. P127
 Hammer, H. 53
 Han, J. Y. 63
 Hancke, K. 3
 Handgretlinger, R. 19
 Handin, N. P114
 Hanel, S. P179
 Hang, Y. 63
 Hansen, F. K. P075
 Haralambiev, L. 39
 Harter, P. 51
 Hartl, D. 19
 Hartung, F. 55
 Hartwig, A. P060, P051, P153, 32
 Hasanvand, A. 20
 Hasselgren, C. P061
 Hayen, H. 34, 69
 Hayot, G. 87, P150, P151
 Heber, S. 29
 Heidenreich, E. 65
 Heim, A.-L. K. P140
 Hein, A. P120
 Heinze, M. 50
 Heise, T. 75, 54
 Hell, R. 65
 Hellmann, A. P042
 Helm, B. 49
 Helm, M. P181, P182
 Hempel, G. P028
 Hengstler, J. G. 4
 Henkel, D. P160
 Hennekinne, J.-A. 27
 Henninger, C. P044
 Herbel, J. N. 37, P073
 Hergenröder, R. P180
 Herkt, M. P115
 Hermann, J. 65
 Hernandez Torres, L. D. 61
 Herrmann, H. 28
 Herrmann, K. P043, P047
 Herrmann, S. 67
 Herting, J. R. P187
 Hessel-Pras, S. P037, P047
 Heylmann, D. P177, 8, P036
 Hef, S. P108
 Hefßlinger, M. 79
 Hilger, D. P172, 42
 Hilla, A. P004, P092
 Hintzsche, H. P041
 Hinz, S. P184
 Hirn-Derksen, B. P028
 Hirsch-Ernst, K.-I. P158
 Hochban, U. P172, P173
 Hoermann, G. 17
 Hoevener, J.-B. 61
 Hoffman, T. 8
 Hoffmann, H. 82
 Hoffmann, M. P070
- Hoffmann, R. P087
 Hoffmann, S. P127
 Hofmann, B. P081, P082, P084, P085, P086, P088
 Hofmann, U. P114
 Hohlfeld, T. P077
 Hollmann, R. P180
 Honarvar, N. P045
 Honkanen, J. P125
 Hopp, M. P145
 Horn, G. P056, 74
 Hu, H. 42
 Huber, M. 57
 Huebner, T. P108
 Huener, H.-A. P137
 Hulme, C. P002
 Humphrys, L. P081, P084
 Hund, N. P060
 Hußler, W. P086
 Häussler, S. 86
 Höchsmann, B. 17
 Höhm, C. P081, P085
 Hörtnagl, P. 17
- I**
 I., T. 51
 Idrissou, B. M. G. P080
 Inoue, A. 42
 Inui, K.-i. 22
 Isakoff, E. 42
- J**
 Jacob, H. P081
 Jahnke, G. P060
 Janssen, P. P132
 Jansson, D. 27
 Jeanclos, E. P180
 Jebens, H. P007
 Jedermann, L. P147
 Jedlitschky, G. 39, P090
 Jejenywa, V. O. P050
 Jenke, R. P075
 Jennings, C. 42
 Jochum, K. P144, 53
 Jochum, T. P030
 Joerg, M. P181, P182
 John, H. P056
 Jordan, M. P003
 Joshua, C. 63
 Josuran, R. 27
 Juncan, A. M. P102
 Jung, D. P111
 Jung-Poppe, L. P100, 48
 Junk, H. P063
 Jurida, L. 10
 Just, A. P078, 84, P140
 Just, K. S. 46, P105, P013, P015
 Jäck, N. 31
 Jäger, N. 74
- K**
 Kadakia, N. 63
 Kadic, A. 54
 Kaestner, A. P180
 Kaina, B. P036
 Kalisch, C. 35
 Kaminsky, S. P106
 Kamler, M. P079
 Kamp, H. P137
 Kampa, B. 27
 Kandeel, F. R. 63
 Kappenstein, O. 6
 Kappert, K. 13
 Karaca, M. 75
 Karaica, D. P117
 Karamifard, K. 20
 Karlstetter, M. P166
 Kaschina, E. 13
 Kaser, D. P159, P128
 Katherina, S. P152
 Katnahji, N. P020
 Keller, A. P180
 Kellner, R. 52
 Kemas, A. M. P113
 Kersch, C. P039, 33, 72
 Keyl, C. P077
 Khajavi, N. P018
 Khatun, S. P069
 Khobta, A. 8, 30
 Kiesewetter, F. 73
 Kilo, S. 73, P066
 Kim, S. K. 63
 Kim, Y. J. P028
 Kimpel, J. 17
 Kintscher, U. 13
 Kirchhefer, U. P084, P087, P187, 36, P188
 Kirchhofer, S. B. P096, P173
 Kirsch, V. 70
 Kirsten, M. 45
 Kiss, B. 85
 Kitzinger, R. P040
 Klapproth, E. 14
 Klawonn, A. 16
 Klebl, B. 65

Kleider, C. P049
 Klein, J. P091
 Klein, K. P114
 Klein, M. P105
 Kleinbongard, P. 11
 Kleindl, M. 11
 Klersy, T. 60
 Klews, J. 51
 Kliewer, A. P169
 Kling, C. P161
 Klonisch, T. P170
 Klos, A. P162
 Klose, P. 14
 Klotz, C. 5
 Knapp, F. 10
 Kneuer, C. P126, P129, P043, P144, 75, P047
 Kobilka, B. 42
 Koch, H. M. 34, 69
 Koch, M. P166
 Koczera, P. P017
 Koellner, A. P158
 Koesling, D. 12, 78
 Kohl, Y. P131
 Kolahian, S. 19
 Kolossa-Gehring, M. P038
 Konopa, A. 44
 Kopaliani, I. 14
 Kopf, S. 65
 Koschorreck, J. P064
 Kosinska, J. P168
 Koslitz, S. 34
 Koslowski, G. P138
 Kostka, T. P033
 Kouidrat, N. M. Z. P135
 Kracht, M. 10, P176, P177, P178, P179
 Kraft, M. 4
 Kramer, N. P129
 Kranawetvogl, T. P056
 Krasel, C. 40, P171
 Kratzmann, M. P008
 Krefl, P. P022
 Kreim, N. P182
 Kreuz, R. 51, P074
 Krieger, M. 35
 Krings, O. P055
 Krisna Kumar, K. 42
 Kristen, M. P182
 Kroll, H. P122
 Kruck, S. 22
 Krueger, N. P132
 Kuan, S.-L. P164
 Kubot, M. P068
 Kucuk, P. P186
 Kudiabor, F. 7
 Kullak-Ublick, G. A. P109
 Kullman, S. P106
 Kuner, R. 65
 Kurz, C. P096
 Kurz, D. 3
 Kurz, M. P096, P172, P173, P174
 Kusche-Vihrog, K. 60, 61
 Käfferlein, H. U. 34, P110
 Kähler, M. 56, P072
 Köhler, C. P110
 König, J. P043, P047
 König, J. H. P187
 König, J. 22
 Köppl, L.-H. P147
 Körper, S. 17
 Kühne, F. P067
 Kühnel, M. P162
 Künitzer, A. P064
 Künzel, S. 14
 Küpper, J.-H. P037, P035

L

L.M. Solano, M. P144
 Laarif, S. P112
 Laitinen, J. P125
 Lakus, J. 38
 Landes, S. P027, P097
 Landsiedel, R. P127, P136, P141, P148, P116, P045, P147
 Lanfermann, C. P162
 Lange, J. 39
 Langer, A. 80, P167
 Langmia, I. M. 24
 Langner, D. P108
 Lapczuk-Romanska, J. P119
 Latorraca, N. 42
 Lau, H. P091
 Laurentius, T. P105
 Lauschke, V. M. P112, P113, P114
 Lechsner, P. P123
 Lee, M. 51
 Leggewie, S. P077
 Lehane, C. P077
 Lehmacher, W. P098, P099
 Lehmann, K. P090
 Lehmann, L. P049, P103
 Lehner, J. 3
 Leibinger, M. P092
 Leidner, J. P148

Leinders-Zufall, T. 65
 Lemichez, E. 27
 Lemoine, H. P173
 Lenich, A.-K. P001
 Leonhardt, D. P049
 Lequesne, L. P165
 Lerch, M. 42
 Leuthold, P. 22
 Lezoualc'h, F. 77
 Li, L. P021
 Liebisch, G. P113
 Liebl, M. E. 51
 Lietz, C. P182
 Lin, Y. P011
 Linder, R. P108
 Link, M. P153
 Linnebacher, M. 57
 Liqi Tan, L. 65
 Litterst, M. 56, P072
 Loacker, L. 17
 Loeffler, C. 6
 Lohrmann, R. 51
 Lohse, M. J. 43
 Longuespée, R. P121, 59
 Loosli, F. P106
 Lorenz, K. 11, 14, 67, 37, 41
 Lorenz, L. P075
 Lott, J. P042
 Luch, A. P062, P149, P067
 Ludwig, A. P170
 Ludwig, J. 83
 Luginbühl, W. 27
 Lukowski, R. P022, P023, P024
 Lump, T. 32
 Lutz, L. 5
 Lämmerhofer, M. 76

M

Ma-Hock, L. P054
 Maack, G. P120
 Maas, R. P100, 48
 Macaçoil, I. P143, P157
 MacDonald, P. E. 63
 Madden, S. P023
 Mages, H. W. P163
 Maier, S. P023
 Maier-Soelch, J. P179
 Makkos, A. 85
 Malek, S. P071
 Mallick, M. 63
 Mally, A. 71, 35, 5
 Mangerich, A. P046, 31, P048
 Manke, M. 76
 Maqusee, S. 42
 Marcovici, I. P143, P157
 Martens, R. P093
 Martin, J. N. P012, P138
 Martin, S. P152
 Martinez Lopez, R. P150, P151
 Marx-Hofmann, A. 17
 Marx-Stoelting, P. 75, 53, 54, P126, P144
 Marzo Solano, M. d. L. 54
 Maser, E. P120, P064, P065
 Masquelier, J. 27
 Masuda, S. 22
 Masutin, V. 33
 Mathar, I. 65
 Matkovic, I. P191
 Matt, L. P022
 Matta, I. 63
 Matthes, J. P020
 Matysik, S. 81
 Matzner, J. P010
 Maurischat, S. P163
 Mayer, R. 49
 Mboni Johnston, I. M. P130
 Meabed, M. 8, 30
 Medina, E. 86
 Meid, A. 25
 Meier, H. P166
 Meier, M. A. 44
 Meier-Soelch, J. P178
 Meinert, F. P074, 51
 Melching-Kollmuss, S. P116, P147
 Melnikov, Y. P061
 Menges, L. 12
 Menzel, J. P032
 Mereu, C. P129
 Mergia, E. 78
 Merkel, M. P005
 Merkel, S. P062, P067
 Meyer, T. C. P163
 Meyer-Tönnies, M. J. P117
 Miccoli, A. 53
 Micek, V. P117
 Michaelis, J. 29
 Miele, V. 6
 Mierzala, A.-S. 27
 Mikus, G. 21, 25
 Mikut, R. 87
 Miller, M. 63
 Mini Vijayan, S. 73, P066
 Mirtschink, P. 14

Mittendorff, C. P079
 Moepps, B. P190
 Mohamed, I. P011
 Mohsen, C. 20
 Monien, B. 1, P063, P032
 Monsé, C. P145
 Montabana, E. 42
 Monti, M. 6
 Moreno-Pérez, A. 65
 Morgovan, C. P102, P104
 Moritz, E. P090
 Morof, F. 39
 Morosawa, Y. 71
 Moser, M. P109
 Mosloff Mathiesen, J. 42
 Motorin, Y. P182
 Muehlich, S. 44
 Muhareb, A. 25
 Muschiol, E. P068
 Musengi, Y. P047
 Möhlendick, B. P094, 15
 Mörbt, N. P058
 Mösslein, N. 40, P171
 Müller, A. P058
 Müller, F. U. 36, P188
 Müller, I. P059
 Müller, J. P017, P070, 24
 Müller, J. P. P015
 Müller, M. 64
 Müller, M. P008
 Müller, M. P131
 Müller, O. 60, 61
 Müller, P. P065
 Müller, R. 18
 Müller, T. P018
 Münch, L. P149

N

Nagel, I. 56
 Nagy, R. N. 85
 Nawroth, P. 65
 Nerger, E. P167
 Neu, A. 74, P142
 Neuenschwander, M. P180
 Neumann, D. P192, 45
 Neumann, J. P081, P082, P083, P084, P085, P086, P087, P088
 Nevosadova, L. P112
 Ngyen, V. T. T. P181
 Nia, Y. 27
 Nicolaus, H. F. P170, 48
 Niebergall-Joos, E. P077
 Niemann, L. P126
 Nienhaus, A. 26
 Nies, A. T. 22, P114
 Nilles, J. 21
 Nolde, J. P132
 Nonnenmacher, P. P027, P097
 Nordbeck, P. 67
 Nowak, N. P118
 Nuray, E. P048
 Nussbaumer, P. 65
 Nürnberg, B. 76, 19

O

O'Brien, E. 42
 Oberfrank, C. P136
 Oertel, R. 49
 Okamoto, H. 71
 Okino, M.-L. 63
 Ola, R. P011
 Oles, P. 54
 Opialla, T. 75
 Orsini Delgado, M. L. P165
 ORTNER, N. J. 66
 Ostrowski, M. P119
 Oswald, S. P119
 Ottenheim, R. 65
 Otto, M. 84, P140

P

Pabel, U. P038
 Padberg, F. P129
 Palzer, K.-A. 38
 Pannervselvam, S. P175
 Pantzke, J. 72
 Papatheodorou, P. 26
 Papatheodorou, Y. 31
 Paul, M. 2
 Paulsen, F. P170
 Paulweber, B. P113
 Pautz, A. 38
 Peil, M. P035
 Peiser, M. P158
 Peitsch, W. K. P149
 Pemp, D. P103
 Penczynski, K. 3
 Penna, A. 6
 Peppler, H. P178
 Peravali, R. 87, P150, P151
 Perhal, A. 80
 Peter, R. 3
 Peter-Ventura, A. P005

- Peters, A. P037
 Peters, M. 78
 Pfaff, T. P016
 Pfanne, A. P078, 84
 Pfistermeister, B. 48
 Philipp, M. 81, 79
 Pich, A. P078
 Pichot, F. P182
 Pinzaru, I. P155, P156, P157
 Piranova, A. P125
 Plehn, J. E. P181
 Plomer, M. P026
 Pockes, S. P081, P083, P084
 Poetz, O. 53
 Pohlmann, G. 84
 Pop, G. P102, P104
 Popoff, M. 27
 Poschet, G. 65
 Postels, M. P189
 Pott, C. 56, P072
 Preissl, S. 63
 Priester, J. P176
 Protzer, U. 82
 Pulliainen, A. P161
 Puskás, L. G. 85
 Puustinen, A. 27
 Pylatiuk, C. 87
 Pätzold, N. 8
 Pinzaru, I. P143
 Pöschmann, A. P040
- Q**
 Quarz, C. 8
 Quitterer, U. 80, P167
- R**
 Raasch, W. 60, 61
 Rabenau, M. P185
 Rad, R. 82
 Radermacher, J.-C. P013, P105
 Rafahi, M. P019
 Rajendra Kumar, A. 87
 Ramanujam, D. P. 82, 83, 9
 Ramin, T. 50
 Ramm, F. P159, P128
 Rasenberger, B. 57, 8
 Rasetti-Escargueil, C. 27
 Rashidian, A. 20
 Rauch, B. H. P090
 Rauen, U. P056
 Rayo Abella, L. M. P083
 Reamon-Buettner, S. M. 52
 Rech, A. P073
 Reetz, A. E. 54
 Rego Terol, J. 65
 Rehn, J. P129
 Reichelt, N. P110
 Reiffert, K. P044
 Reinartz, S. P076
 Reinders, J. 4
 Reinders, Y. 11
 Reinhardt, J. P. 36
 Reischl, M. 87
 Reiter, M. 35
 Renko, K. P127, 54
 Renner, B. 49
 Renz, H. 19
 Rezende, F. 60, 61
 Rheinheimer, C. P162
 Richarz, A. P125
 Richling, E. P030, 68, 70, 8
 Richter, C. 65
 Riedel, F. P149
 Rieken, C. P141
 Rittersberger, R. P012, P138
 Ritz, V. 54
 Rockenfeller, P. P007
 Rodríguez, C. 26
 Rohrbach, S. 10
 Rooffs, F. P133
 Rosencrantz, S. 84
 Rosenkranz, N. P145
 Roslan, A. P024
 Rossi, A. 28
 Rossi, H. P041
 Roth, N. P136
 Rothenbacher, D. 3
 Rothmiller, S. 74, P139, P142, 31
 Rox, K. 86
 Ruez, S. 21, P001
 Ruffini, N. P182
 Rummel, A. 27, P163
 Runge, D. P014
 Rus, L. L. P102, P104
 Russwurm, M. 12
 Ruszkiewicz, J. P046, 31, P048
 Ruth, P. P023
 Ryu, C. P028
 Röhl, C. P038
 Rönnpagel, V. P014, 39
- S**
 Sabolic, I. P117
- Sachs, B. 46, 47, P101
 Sachse, B. P037, P047
 Sackhoff, P. P122
 Safi, S. 82
 Saffig, P. 14
 Saier, C. P010
 Sailer, J. P146
 Sailer, S.-A. 79
 Sander, M. 63
 Sarmini, L. 30
 Sassi, Y. 83
 Schaarschmidt, S. P163
 Schaeffeler, E. 22, P114
 Schanbacher, C. 67
 Schanz, S. P024
 Schelle, I. P162
 Schennach, H. 17
 Scherer, M. P148
 Scherf-Clavel, O. 35
 Schettgen, T. P038
 Schilling, B. P073
 Schindelin, H. P180
 Schindowski, K. P012, P138
 Schins, R. 28
 Schirmer, B. P192, 45
 Schlitzer, M. P005
 Schlobach, J. P007
 Schloetzer, J. P180
 Schlosser, A. P073
 Schmalzing, G. P021
 Schmid, K. W. P094
 Schmid, M. 46, 47
 Schmidt, A. 74, P142
 Schmidt, A. P040
 Schmidt, A. P078
 Schmidt, C. Q. 17
 Schmidt, J. P188
 Schmidt, K. P078, P003
 Schmidt, L. S. 56, P072
 Schmidt, M. 77
 Schmidt, S. 17
 Schmieder, N. P141
 Schmitt, A. P126, P144
 Schmitt, J. P. 11
 Schmitt, S. P146
 Schmitz, W. P180
 Schmitz-Spanke, S. P039, 33, 72
 Schneider, M. 50
 Schneider, S. 51, P127
 Schneider, U. P108
 Schnura, E. 51
 Schober, A. P055
 Schofield, K. P002
 Scholl, C. P108, P101, 24
 Scholz, S. P150, P151
 Schorb, S. P051
 Schott, J. J. P184
 Schreiber, U. P034
 Schrenk, D. P035
 Schrezenmeier, H. 17
 Schriever-Schwemmer, G. P060
 Schroth, W. P023
 Schrör, K. P077
 Schubert, S. 49
 Schulte, J. S. 36
 Schulz, R. 85
 Schulz, S. P169
 Schulz, T. P062
 Schulze, F. P049
 Schumacher, J. 26
 Schumacher, P. P051, 32
 Schumann, B. P055
 Schupp, N. P130, P133, P134, P135
 Schuster, A. K. P100
 Schuster, T. P132
 Schwab, M. 22, P023, P113, P114
 Schwartz, M. A. P011
 Schwarz, K. P118
 Schwarz, R. P082
 Schwarz, Y. 65
 Schweizer, S. P062
 Schwerdtle, T. P063
 Schädler, J. 82
 Schäfer, B. P037
 Schäfers, C. 74
 Schönfelder, G. P095
 Schütte, A. P050
 Sehner, C. P025
 Sehouli, J. 51
 Seidl, M. D. 36, P188
 Seifert, J. 50
 Seifert, R. P189, P192, 45
 Seifert, S. P152
 Seiser, T. P045
 Seiwert, N. 57, P036
 Semenescu, A. D. P156
 Serban, J. 71
 Sergeev, M. 44
 Setemes, O. M. P071
 Sewald, K. 84
 Sharma, S. 71
 Shigano, M. P045
 Shinkevich, V. P076
- Shinohara, M. 71
 Sickmann, A. 11
 Sieg, H. 2, 7
 Siepe, M. P077
 Sievering, S. 4
 Siewert, K. P149
 Siffert, W. P094, 15
 Simon, S. 27, P165
 Sirbu, A. 43
 Skiba, M. 27, P163
 Skiniotis, G. 42
 Sklorz, M. 72
 Sommerfeld, L. P076
 Sommerfeld, M. 13
 Sonnenburg, A. P129, P152
 Sotriffer, C. P180
 Spaehn, D. P022
 Spanier, B. 22
 Sperber, S. P137
 Sperhake, J. P. 82
 Spielmeier, A. 6
 Spruck, C. P133
 Staab-Weijnitz, C. 82, P059
 Stadler, N. P164, 29
 Stahl, C. P093
 Stahlmecke, B. 28
 Stammer, V. P169
 Stech, M. P159, P128
 Steffens, M. P108, P101
 Stegmaier, J. 87
 Stegmüller, S. P030, 68, 70, 8
 Steinke, J. 84
 Steinmetz, F. P029
 Steinritz, D. 74, P139
 Stern, D. P163, P165
 Stilgenbauer, E. P125
 Stingl, J. C. 24, 46, P017, P013, P070, P117, P015, P108, P105
 Stintz, M. P132
 Stintzing, F. C. P058
 Stoicescu, L. P102
 Stojkov, D. P023
 Stolz-Ertych, A. P095
 Stopper, H. P124
 Stratemann, H. P054
 Strehse, J. S. P120, P064, P065
 Strenger, H. P174
 Stricker, S. P106
 Striessnig, J. 66
 Strommenger, B. P163
 Strähle, U. 87, P150, P151
 Stucki-Koch, A. P140
 Stöber, S. 32
 Stürmer, E. P007
 Sudman, J. 76
 Szymanski, W. P076
 Sänger, B. 35
 Sündermann, J. 52
- T**
 Tang, S. 62
 Tardio, L. B. 36
 Tartaglione, L. 6
 Tatge, H. P160
 Temussi, F. P125
 Tevini, J. P113
 Theile, D. 21
 Then, M. I. P100
 Thiele, T. P090
 Thierse, H.-J. P149
 Thum, T. P078, P003, 84, P140
 Thumberger, T. P106
 Tiedemann, L. 56, P072
 Tietz, T. P062, P067
 Ting, S. P094
 Tolksdorf, C. P090
 Tolstik, E. 11
 Tomićić, M. T. P040
 Torres Pereiro, M. P009
 Toto, S. 50
 Tralau, T. 75, 53
 Tremmel, R. P112, P114
 Trenk, D. P077
 Tsvilovskyy, V. 65
 Tuckermann, J. P001
 Tuneew, I. 42
 Turek, C. P058
 Twarock, S. P077
 Tzvetkov, M. V. P117, 39, P090
 TÖRÖK, F. 66
 Tölle, L. P145
- U**
 Ullrich, A. P014
 Ulrich, M. P173, P174
 Unger, T. 13
- V**
 Vaccarello, P. 82, 9
 van der Lugt, B. P129
 van Geffen, C. 19
 Van Haelst, S. P065
 Vanninen, P. 27

Varga, Z. V. 85
 Varone, A. 6
 Varra, M. 6
 Varriale, F. 6
 Veen, M. 77
 Veh, E. P049, P051
 Verheyen, M. 78
 Verlohner, A. P137
 Vetter, W. P062
 Vitali, A. P132
 Vogel, M. P053
 Volland, H. 27
 Vollmar, A. 64
 Vollmer, A. S. 8
 vom Brocke, J. P050, P125
 von Briesen, H. P131
 von Kries, J. P. P180
 von Kugelgen, I. P175
 Vrhovac Madunic, I. P117
 Vögele, P. P058
 Volkel, W. 4, P032

W

Wabitsch, M. 3
 Wagner, B. 15
 Wagner, S. P131
 Wakefield, J. P029
 Walk, T. P137
 Wallenstein, I. P173
 Walter, D. P145
 Walther, U. P016
 Wang, G. 63
 Wang, H. 42
 Wang, Y. 87
 Wang, Y. P006
 Wareing, B. P147, P148
 Warfving, N. P132
 Wartenberg, P. 65
 Watson, P. P106
 Weber, A. G. P127, P135, P147
 Weber, K. P132
 Weber, L. P007
 Weber, R. P101
 Weber, S. 14
 Weber, S. P042
 Weickert, C. 3
 Weidemann, F. 67
 Weigel, C. P056
 Weigel, T. 84
 Weigmann, H. P027, P097
 Weikert, C. 1, P032
 Weil, T. P164
 Weindl, G. 16
 Weinmann, C. 80
 Weisbach, L. P100
 Weisemann, J. 27
 Weiser, T. P026, P027, P097, P098, P099
 Weiss, C. 87, P150, P151
 Weiss, G. 17
 Weiss, J. 21
 Weiss, T. 69
 Weissenfeld, M. P147
 Welz, B. P106
 Wenzel, C. P119
 Werfel, S. 83
 Werner, S. 10
 Wessely, B. P132
 Westphal, G. P145
 Weusthoff, J. P140
 Wichert, U. P065
 Widenmeyer, F. 82
 Wiedemann, J. 14
 Wiederanders, P. L. 85
 Wieland, T. P006
 Wiemann, C. P116
 Wille, T. P056, P057
 Williamson Riffle, B. P045
 Wilms, G. P002
 Wind, A. P117
 Winter, S. 22, P113, P114
 Wirth, A. 65
 Wist, M. 58, P190
 Witt, A. 14
 Wittbrodt, J. P106
 Wittkowski, P. P129
 Wittman, S. 57
 Wittmann, S. P036
 Wittwer, M. 27
 Woermann, A. P166
 Wolf, L. P022
 Wollin, K.-M. P038
 Wolter, S. P189
 Wondany, F. 29
 Worbs, S. 27, P165
 Worek, F. P056, P057, 74, P139, P142
 Worzfeld, T. P191, P076, P009
 Wozniak, J. P105, P013
 Wrobel, S. A. 34
 Wu, K. C. P061
 Wulle, S. P122
 Wunder, F. P166
 Wunder, J. P103
 Wätjen, W. P010

Würger, L. 7
 Wüst, L. 35

Y

Yamoune, S. P070, 24
 Yan, H. 77
 Yang, J. P024
 Yesilyurt-Gerhards, D. P180
 Yildiz née Dreymueller, D. 18
 Yilmaz, K. 12
 Yuan-Chen, N. P180

Z

Zaborosch, C. 27
 Zaloga, J. P039
 Zander, A. P045
 Zanger, U. M. P114
 Zeitler, C. P092
 Zeleny, R. 27
 Zellmer, S. P062, P067
 Zemella, A. P159, P128
 Zeng, C. 63
 Zenz, T. P075
 Zernecke-Madsen, A. 37
 Zhao, D. P191
 Zhou, L. P009
 Zhou, Y. P112, P114
 Zickgraf, F. P137
 Ziegler, P. P015
 Ziemann, C. 52, P052
 Zierler, S. P018
 Zimmermann, H. P131
 Zimmermann, R. 72
 Zindel, D. 40
 Zischka, H. P146
 Zolk, O. 50
 Zorn, M. 65
 Zufall, F. 65
 Zwanzleitner, L. 51